UNIVERSITY OF OKLAHOMA

GRADUATE COLLEGE

EVALUATION OF LONG-TERM PERFORMANCE OF IN-STREAM CHANNEL STABILITY STRUCTURES FOR PROTECTING OKLAHOMA BRIDGES AND ROADS

A THESIS

SUBMITTED TO THE GRADUATE FACULTY

in partial fulfillment of the requirements for the

Degree of

MASTER OF SCIENCE IN ENVIRONMENTAL ENGINEERING

By

ADELLA KUSTER

Norman, Oklahoma

2021

EVALUATION OF LONG-TERM PERFORMANCE OF IN-STREAM CHANNEL STABILITY STRUCTURES FOR PROTECTING OKLAHOMA BRIDGES AND ROADS

A THESIS APPROVED FOR THE

SCHOOL OF CIVIL ENGINEERING AND ENVIRONMENTAL SCIENCE

BY THE COMMITTEE CONSISTING OF

Dr. Jason Vogel, Chair

Dr. Keith Strevett

Dr. Jeffery Volz

Acknowledgements

First, I would like to thank my advisor Dr. Vogel for giving me this opportunity and supporting me along the way. I started working at the Oklahoma Water Survey when I was 19 years old, and I would not trade the experiences I have gained over the past three years for the world. I would also like to thank my other committee members, Dr. Strevett and Dr. Volz for their expertise and guidance.

Next I want to thank the other students at the Oklahoma Water Survey who assisted me on this project. There were many long (both hot and cold) days in the field where I had an amazing team of students helping me collect this data. Special thanks to Brett, Paul, and Jake for being the go-to guys in the field. Whether it was kayaking or wading across the river, carrying the heavy equipment, or simply taking pictures, their help was crucial to this project. I am extremely grateful to have had this team behind me.

Finally, I want to thank my family and friends for their love and support. I would not have completed this project if not for my mom's love and advice. She is the person I always call when I don't know what else to do, and she always has words of encouragement. I am extremely thankful to have my support network, including my boyfriend, Matt, who provided constant support and dinner on busy days. Thank you all for everything you have done for me over the past year.

Table of Contents

List of Figures

List of Tables

Abstract

Streambank erosion can damage bridges, hydraulic structures, and private property. In-stream structures may be installed to control river migration and limit bank erosion during large precipitation events. Historically, the structures most widely used by the Oklahoma Department of Transportation include Kellner jetties, rip rap, pile diversions, and bendway weirs. These structures each use different methods to decrease erosion and stream migration; therefore, their effectiveness may differ based on a variety of variables including stream geomorphology, site and watershed characteristics, and occurrence of extreme precipitation events. Many of these structures have been installed on Oklahoma rivers but have not been consistently evaluated.

Previously, two studies completed by the Oklahoma Department of Transportation and the University of Oklahoma in 1971 and 1989 have qualitatively evaluated the effectiveness of over 20 in-stream structures near transportation infrastructure. In this project, remote evaluations of the characteristics of the streams and watersheds, along with on-site stream surveys and geomorphological studies, were completed. This project augments and enhances the previous studies through quantitative analyses of the durability of the structures, stream characteristics, and stream geomorphology. Logistic regressions indicated that soil type and structure design impact the success of different structures. Pile diversions were more likely to fail on rivers with more sand, potentially due to the mobility of a sandy river bed. Kellner jetties failed more frequently with smaller angles between the stream flow line and the Kellner jetty lines. Overall, structures were more successful in streams with higher silt content in their bank material. This data can be used in the future for making decisions surrounding streambank stabilization projects in Oklahoma. The results of this study provide a unique opportunity to optimize the likelihood of successful implementation of in-stream structures in rivers with varying characteristics.

Chapter 1: Introduction and Literature Review

Streambank erosion can cause damage to bridges, hydraulic structures, and private property, resulting in high repair costs and even lost lives (Lagasse et al. 1995). Approximately 82% of bridges in the United States transverse alluvial streams (Lagasse et al. 2016). Bank scour has been shown to be the leading cause of bridge failure in the United States, causing 53% of recorded bridge failures between 1989 and 2000 (Wardhana and Hadipriono 2003). Damage to bridges by streams costs an estimated 50 million dollars per year (Lagasse et al. 1995). An average of one billion dollars is annually spent on streambank stabilization and restoration efforts within the continental United States (Bernhardt et al. 2005), but despite the cost, an estimated 50% of these stabilization efforts did not result in the intended outcome (O'Neil and Fitch 1992). The use of instream structures is a common solution to streambank erosion, but the understanding of factors that affect their success is lacking. Knowledge of these factors a could reduce the rate of failure and improve cost-effectiveness.

Previous studies have been completed to investigate streambank stabilization methods, such as jetties, pile diversions, and rip rap at bridge sites in Oklahoma (Keeley 1971; Harp and Thomas, 1989). These studies evaluated in-stream structures near bridge-stream crossings around Oklahoma. The first study evaluated 20 sites, while the second evaluated those same 20 sites, plus five additional sites (Keeley 1971; Harp and Thomas, 1989). This project will evaluate those 25 sites, with the exception of a few, and several new bridge crossing sites with instream structures across Oklahoma. The Keeley (1971) and Harp and Thomas (1989) studies were qualitative analyses of the sites, including photos, sketches, and narrative descriptions.
Over recent decades, advancements in geomorphological characterization of streams have been developed that have the potential to provide guidance in predicting the erosion potential at a

particular site and the likelihood that different bank stabilization methods will be successful for certain situations. This study includes quantitative data that has been compiled and analyzed to determine factors that may cause different structure types to succeed or fail.

Although many of the in-stream stabilization practices are not utilized as often as they were in the past, this project will provide a unique opportunity to investigate their effectiveness and structural integrity past the time that was thought to be their useful life. A long-term quantitative evaluation of different in-stream structures and the factors that impact their success will help inform future streambank stabilization projects.

1.1 Literature Review

There are many different types of in-stream streambank stabilization methods. Some work by diverting the energy of the stream away from the bank while others work by covering the bank material and protecting it from erosion (revetments). The bank stabilization methods most commonly found at sites in Oklahoma are Kellner jetties, pile diversions, rip rap, bendway weirs, and spur dikes.

1.1.1 Kellner Jetties

Kellner jetties are permeable structures built to slow the flow of water. They are constructed on streambanks and protrude into the stream to decrease the energy of the water along the streambank and direct it towards to the middle of the stream. The velocity of water is reduced in the Kellner jetty field, allowing sediment to settle out and build up the bank. Thus, Kellner jetties are often used in streams with high sediment loads and relatively low bank slopes. This streambank stabilization method was discovered in the 1920's and was very common in the 1950's and early 1960's (Army Corps of Engineers 1963). Kellner jetties were successful in silty streams with substantial channel scour in New Mexico and Arkansas in the 1950's. They have

been found to result in a two-thirds reduction in stream velocity in the jetty field, allowing for the deposition of sediment (Army Corps of Engineers 1963). An example of a Kellner jetty field is shown in Figure 1.

Figure 1. Example of a Kellner jetty field on the Washita River in Oklahoma, taken in 1950 (Lewis 2020).

The design of Kellner jetties has been standardized by the Army Corps of Engineers (1963). A Kellner jetty field is made up of Kellner jacks tied together with two cables (Figure 2). The jacks can be made of various materials: wood, steel, or concrete, but ODOT and the Army Corps of Engineers (1963) primarily used steel jacks. A design diagram for Kellner jetties is shown in Figure 2.

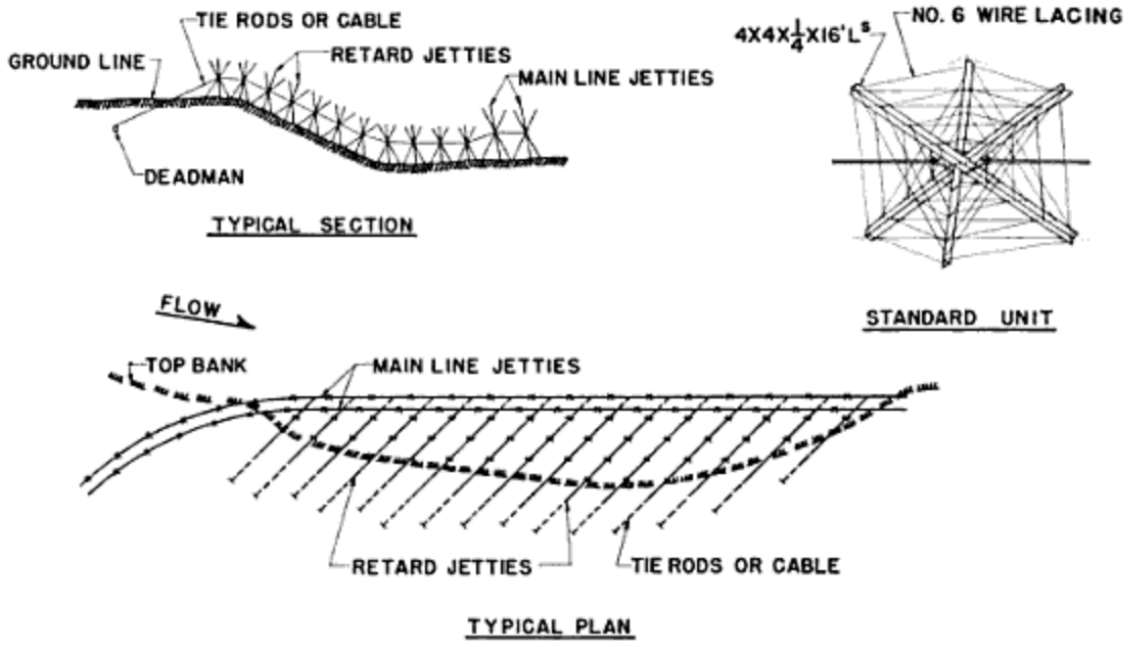

Figure 2: Diagram of a steel Kellner jetty, showing main lines, retard lines, and the design of an individual unit (Army Corps of Engineers 1963).

There are typically two diversion (main) lines placed along the desired channel length with retard lines jetting from the top of the bank, where they are secured, to the main lines (Army Corps of Engineers 1963). The retard lines are placed at an angle of 45 to 70 degrees from the diversion line along the bank (Army Corps of Engineers 1963; Harp and Thomas 1989). The retard lines are typically spaced 125 to 250 ft at critical curves in the channel but can be spaced up to 500 ft apart at less critical parts along the bank (Army Corps of Engineers 1963). This is summarized in the table below.

Table 1: Standard Kellner jetties design criteria (Army Corps of Engineers 1963).

Parameter	**Criteria**
Number of Diversion Lines	2
Angle of Retard Lines to Diversion Lines	45-70^{o}
Spacing between Retard Lines	125-250ft

Harp and Thomas (1989) reported that Kellner jetties did not function in streams with sandy soils because the structures would settle into the streambed during high flows. The Army Corps of Engineers (1963) recommended the use of Kellner jetties in wide, shallow rivers with high sediment content in the southwest United States, which applies to many streams in Oklahoma. The expected lifetime of a Kellner jetty field is 50 years, so with the peak of Kellner jetty use in the 1950's and early 1960's, many are now past their intended lifetime (Army Corps of Engineers 1963; Cochran 1963).

1.1.2 Pile Diversions

Pile diversions divert the flow of the water away from the bank to encourage bank stabilization. These structures, while effective in redirecting the flow, are less effective at encouraging sediment deposition on the streambanks. In successful cases, sandbars are created between pile diversions, meaning the velocity slowed enough to allow for deposition of sand in those regions; however sediment does not deposit around these structures as it does with Kellner jetties (Keeley 1971). Many of the remaining pile diversions in Oklahoma are made of treated timber, as untreated wood deteriorates more quickly (Harp and Thomas 1989). Harp and Thomas (1989) noted that damage to a pile diversion does not necessarily constitute failure because the diversion pile protects the bank by taking the impact of the high flow event. In Oklahoma, they have been successful at diverting flow, but were easily worn by the elements and are expensive to construct and install, leading to their decline in popularity. Though the use of pile diversions in Oklahoma became less common over time, they once were a popular practice and are present at many sites in this study (Harp and Thomas 1989). Figure 3, below, shows a pile diversion in the Arkansas River, north of Bixby, Oklahoma.

Figure 3. Image of pile diversion on the Arkansas River north of Bixby, Oklahoma, taken in 1988 (Harp and Thomas 1989).

1.1.3 Rip Rap

Unlike previously mentioned techniques, rip rap is a revetment, which works by protecting the bank material from erosion rather than diverting the stream's energy away from the bank. Rip-rapping consists of placing adequately sized rocks, capable of withstanding stream energy, to absorb the energy of water on the banks and prevent erosion. Before the rip rap is installed, the bank is typically graded to have a consistent slope that is less than 1:2 vertical to horizontal (Keown et al. 1977). The layer of stones should have an under layer of a fabric or geotextile to increase bank stability, and it must allow for seepage while preventing bank erosion. The rip rap is effective if it prevents bank erosion and resists undercutting during high flow conditions (Keown et al. 1977). There are many empirical relationships used to determine optimum stone size for the potential hydraulic conditions the rip rap will have to withstand. This optimum stone size is then typically the median stone size in the rip rap blanket (Keown et al. 1977). Sharp edges on stones increase stability, and length-to-width ratios of the stones should be under 3:1. The rip rap layer should be at least as thick as the maximum stone diameter or twice the average

stone diameter (Keown et al. 1977). There are many different design methods, including those from Army Corps of Engineers, California Highway Department, and Bureau of Reclamation (Walters 1982). Lindsey et al. (1982) found that the longevity of rip rap blankets depends on the physical and chemical composition of the rocks used and the weathering agents they are exposed to over time, so results may vary greatly depending on location and environmental circumstances.

Figure 4: Rip rap along bridge abutment in good condition, taken near Laverne, Oklahoma, in 2020.

1.1.4 Bendway Weirs

Bendway weirs are transverse, rip-rapped in-stream structures that point inward and slightly upstream (Thornton et al. 2007; Khosronejad et al. 2017). For the purposes of this study, bendway weirs are placed on the outer bank of meanders in a stream and are always placed as multiple weirs in sequence. Their purpose is to deflect high-velocity, near-bed flow away from the outer bank and increase flow resistance near the base of the outer bank (Thornton et al. 2007; Khosronejad et al. 2017). An example of bendway weirs is shown in Figure 5.

Figure 5: Image of bendway weirs (Thornton et al. 2007).

Bendway weirs are typically designed to be one quarter to one third of the stream width and at a 50-80 degree angle with the bank. The design of bendway weirs is summarized by Khosronejad et al. (2017).

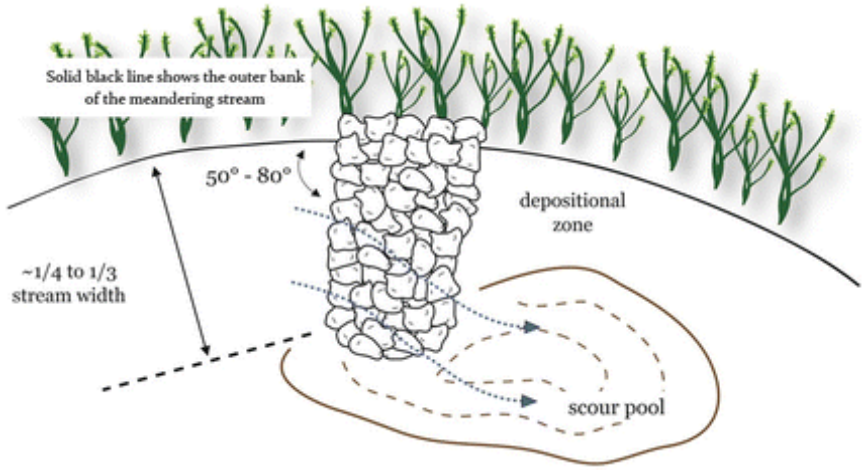

Figure 6: Standard bendway weir design (Khosronejad et al. 2017).

Abad et al. (2008) found that the installation of bendway weirs creates stagnant or recirculating flow between the weirs, which if the river is carrying high levels of sediment, would allow for deposition of sediment between the weirs. This result was confirmed by

Scurlock (2014), illustrated in Figure 7. Additionally, the stream thalweg and energy shifts to the tip of the bendway weirs (Abad et al. 2008). Water velocities between bendway weirs has been found to be 40% of the maximum centerline velocity prior to the weir installation. Centerline and inner bank velocities both significantly increased with the installation of bendway weirs on the outer bank (Thornton et al. 2007). The distance between the bendway weirs is an important consideration in the design because they must be close enough to allow for stagnant or recirculating flow, but if they are too close, they may become uneconomical (Scurlock 2014).

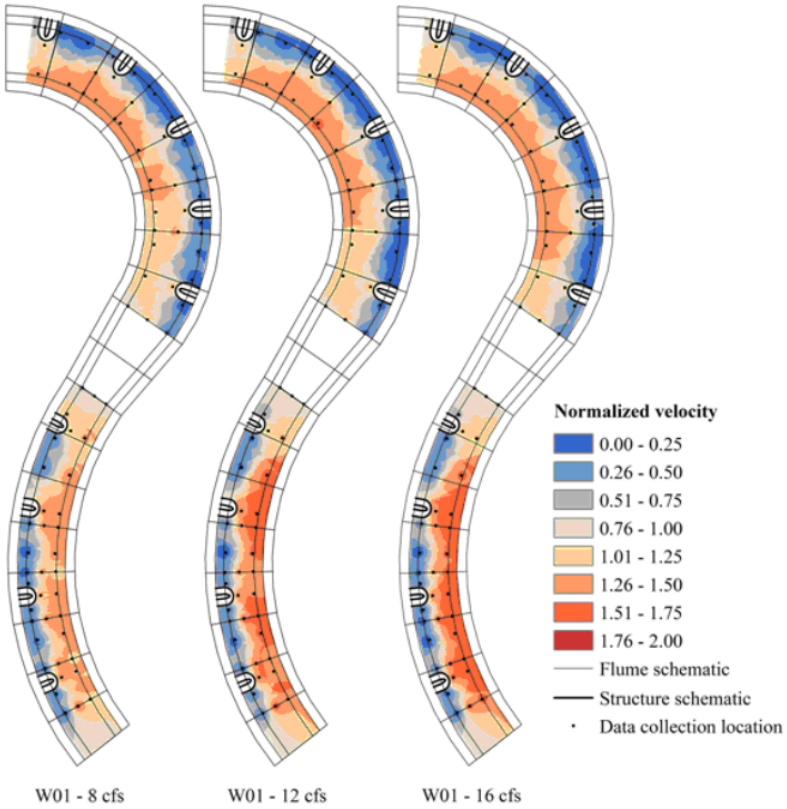

Figure 7: Normalized water velocities in stream meanders with bendway weirs (Scurlock 2014).

Bendway weirs work similarly to pile diversions, but they are impermeable, and less susceptible to damage, resulting in lower repair costs and a longer lifetime.

1.1.5 Spur Dikes

Bendway weirs and spur dikes are both rip-rapped structures that work by diverting the flow away from the bank of concern. Some studies claim these terms are synonymous (Thornton et al. 2007) while other differentiate between them based on design crest elevation (Scurlock 2014). For the purposes of this study, bendway weirs are placed on meanders in a stream, and spur dikes are placed immediately upstream of a bridge embankment. Bendway weirs protrude into the stream while spur dikes, in this study, travel along the streambank and curve slightly away from the stream to protect the bridge abutment. Because of their role in guiding the stream under the bridge, spur dikes are also often called guide banks (Lagasse et al. 1995). Bendway weirs are also always placed as multiple weirs in sequence while spur dikes are a singular structure. Spur dikes have been found to be consistently effective at protecting bridge abutments from scour, but geomorphic factors and bridge abutment design impact their effectiveness (Karaki 1960; Harp and Thomas 1989). Spur dikes should be designed so that water at high flows does not top the dike, which could cause scour around the dike and bridge abutment (Karaki 1960). An example of the design of a spur dike is shown in Figure 8.

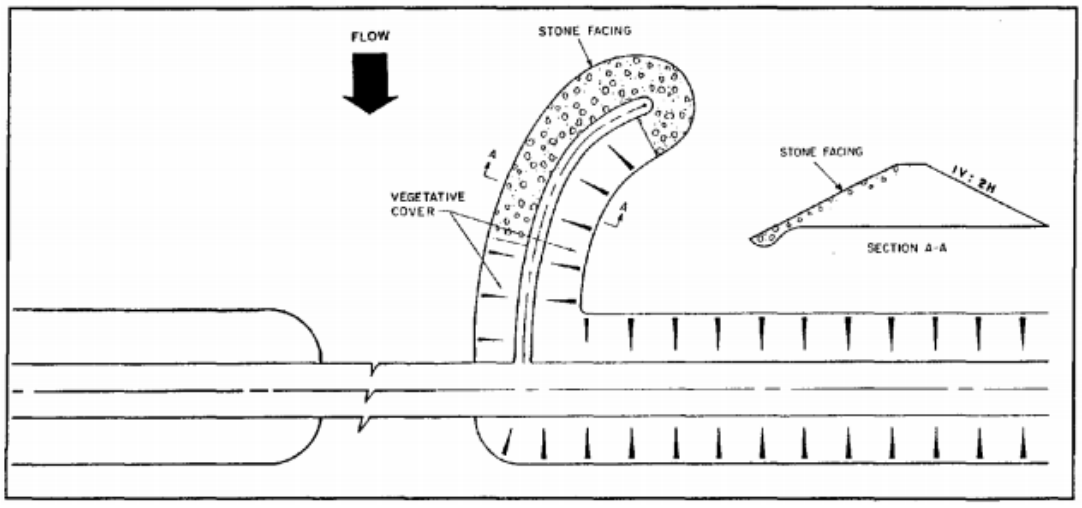

Figure 8: Diagram of spur dike (Lagasse et al. 1995).

Unlike other in-stream structures included in this study, spur dikes are only placed immediately upstream of a bridge abutment to redirect the stream's energy under the bridge.

1.1.6 Gabion Baskets

Gabion baskets are similar to rip rap in that they are revetments made of loose rock material. The rocks in gabion baskets are held together in wire structures, as shown in Figure 9.

Figure 9: Photo of gabion baskets near Hydro, OK.

Gabion baskets are some of the most expensive streambank protection methods, but they are sometimes preferred for aesthetic reasons. There are many factors that may cause gabion baskets to fail, including foundation stability, scour around the baskets, damage to the wire mesh, and high sheer stress. If the foundation material is silt or sand, there is a risk of the gabions settling into the ground. High velocity and sheer stress in combination with non-cohesive bank material can lead to scour around or under the gabion baskets (Freeman and Fischenich 2000). Because of the high cost of these structures, it is important that the site and design are thoroughly evaluated prior to installation.

1.1.7 Rock Vanes

Unlike jetties, pile diversions, and bendway weirs, rock vanes run nearly parallel to the flow of the stream. They allow the stream to flow over the rock structure during higher flows, which makes them less prone to damage from debris in the stream. Because of these factors, rock vanes do not increase the channel roughness and will cause less degradation downstream of the structure (Odgaard and Kennedy 1983). Odgaard and Lee (1984) have developed design criteria based on stream characteristics, hydraulic factors, and stream curvature. Odgaard and Lee (1984) recommend that the ratio of vane height to water depth is between 0.2 and 0.5 at all "erosion-causing flow rates" and that the vanes form an angle of 10-15 degrees with the flow line.

Figure 10: Aerial photo of rock vane in the Illinois River near Tahlequah, OK (GoogleEarth 2020).

Rock vanes are a less intrusive form of streambank stabilization, so they may be preferred in more minor cases of stream-bank erosion, when downstream conditions are important, or when aesthetics are a consideration.

1.1.8 Other Bank Stabilization Methods

Other bank stabilization methods found at sites around Oklahoma include piles of automobile bodies or used tires, gabion baskets, rock vanes, and plantings. Automobile bodies and used tires will not be included in this study because they are antiquated methods of streambank stabilization that are no longer used (Harp and Thomas 1989). Bioengineering techniques are becoming more common methods of streambank stabilization, including live siltation, live stakes, and vegetated mechanically stabilized earth (VMSE). Studies have found these methods to be more effective than rip rap and concrete because they do not restrict the channel as traditional revetments do (Lagasse et al. 2016; Li 2006).

1.1.9 Previous Oklahoma Site Evaluations

This study will be a follow-up to two previous studies that have evaluated the effectiveness of bank stabilization techniques at sites in Oklahoma (Keeley 1971; Harp and Thomas 1989). Keeley (1971) completed an initial evaluation of 20 bridge sites in Oklahoma from 1968 to 1970. The report provides documentation of the conditions at these sites during the first couple decades of installation of these structures. The same sites, plus five more, were evaluated again from 1988 to 1989 (Harp and Thomas 1989). Both of these reports concluded that bank erosion is a complex process that was not well understood at the time the structures were implemented. They also concluded that methods such as rip rap, Kellner jetties, pile diversions, and spur dikes demonstrated results of varying effectiveness, and there is no permanent solution to streambank erosion. Harp and Thomas hypothesized that bank material impacted the effectiveness of Kellner jetties, but they had no quantitative data to test this hypothesis (1989). A typical field data sheet from Harp and Thomas (1989) included the date, site identifiers, qualitative streamflow description, qualitative weather description, construction history, embankment description

(slope, protection, special notes), river bank soil type, riverbank vegetation type, as well as the structure type, description, and present condition. Both reports contained detailed sketches of each site, marking any eroding banks and locations of all structures (Keeley 1971; Harp and Thomas 1989). The evaluations in these two studies would be considered qualitative by scientific standards.

1.1.10 Geomorphology

Geomorphic analysis in the context of engineering and implementation is used to quantify river channel morphological parameters. In general, stream-reach equilibrium is dominated by the hydrology, hydraulics, and sediment load. Geomorphic factors that affect streambank and, thus, bridge stability include watershed land use, historical hydrologic data, stream slope, sinuosity, bank slope, channel shape, riffle-pool spacing, and the location and design of any streambank stabilization structures (Smith and Patrick 1979; Keefer et al. 1990; Lagasse et al. 1995). Watershed land use and historical hydrologic data can provide information on the amount of runoff entering a stream, which produces streambank erosion and sediment transport. Stream slope is directly proportional, and sinuosity is inversely proportional to the mass flux of sediment in a stream (Smith and Patrick 1979). Bank slope, channel shape, and riffle-pool spacing are all factors that help characterize a stream and, thus, understand its susceptibility to erosion and instability (Keefer et al. 1990; Lagasse e al. 1995).

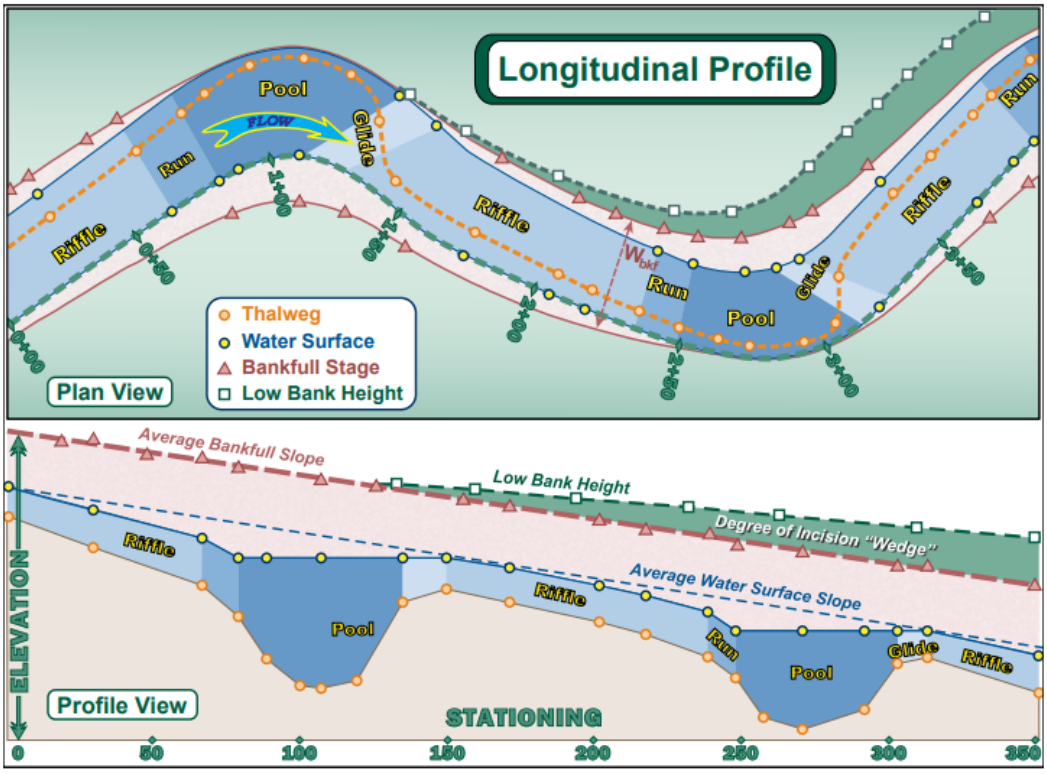

Figure 11: Riffle-pool pattern in longitudinal profile (Rosgen 2014).

By incorporating geomorphic stream characteristics into previous evaluation procedures of Keeley (1971) and Harp and Thomas (1989), improved evaluation procedures can be developed, and improved recommendations on when and where to implement specific streambank stabilization and protection measures in Oklahoma can be made.

1.2 Objectives

The objectives of this study are:

1. To complete remote data collection for each site, including stream sinuosity, watershed land use, and historical hydrologic data.
2. To complete a long-term study with field visits to many sites with different in-stream structures around Oklahoma.
3. To add more quantitative data to the study of the structures, including velocity profiles and stream geomorphology.

4. To determine any patterns of stream or watershed characteristics causing different structures to fail.
5. To establish a standard methodology for evaluating the effectiveness of in-stream structures.

Chapter 2: Methodology

This project involved three major components: remotely collected data, site surveys, and statistical analysis. The remotely collected data provides a general characterization of the stream and watershed, including some geomorphological characteristics and hydrologic data. The remote data collection included modern and historical data to understand how each site has changed since the installation of the structures. Site visits provide a snapshot in time of the site, including the evaluation of the integrity of the in-stream structures, velocity profiles, cross sections, a longitudinal profile, and streambank soil classification. Regression analyses were completed using both remote and field data to determine what variable(s) impact the failure or success of different in-stream structures. Due to the limited number of sites with some in-stream structures, a full statistical analysis was only completed on some structure types.

2.1 Site Descriptions

The sites studied are located in many different regions of Oklahoma on a variety of rivers and streams. The major Oklahoma rivers with two or more sites are the Washita, North Canadian, Canadian, Cimarron, and Red rivers. There are eight sites on the Washita River, five on the North Canadian, three on the Canadian, four on the Cimarron, and two on the Red River. There are also singular sites on the Arkansas and Illinois rivers, and smaller rivers and streams with

sites as well. A map of the locations of these sites around the state of Oklahoma is shown in Figure 12.

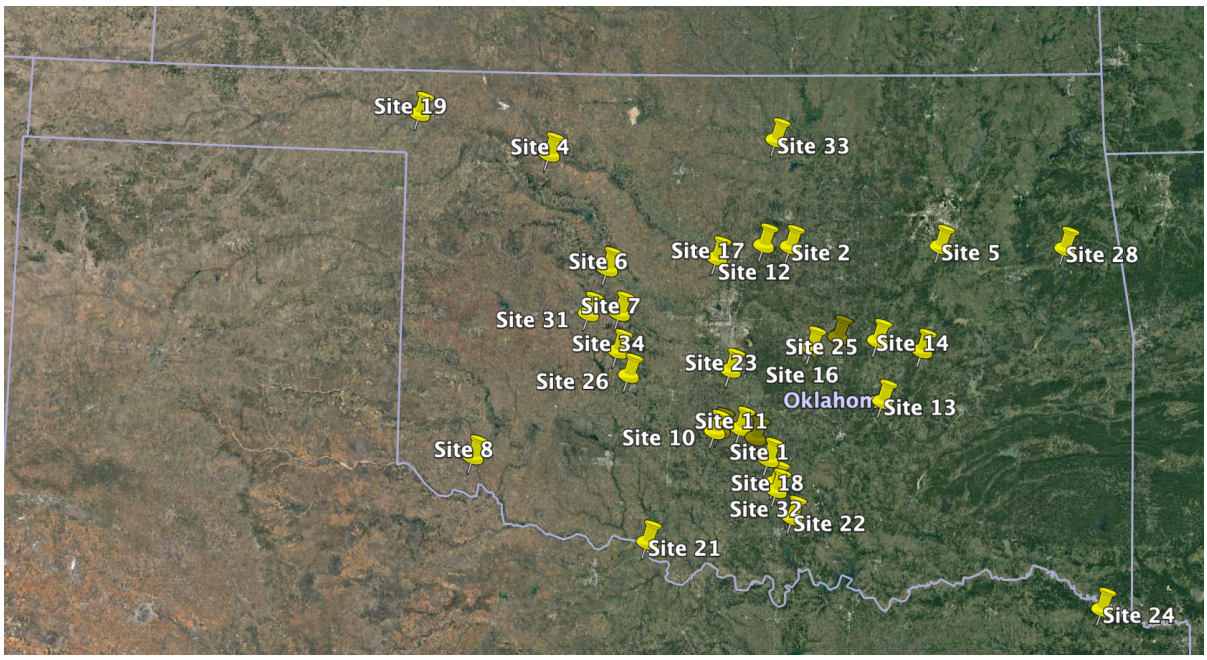

Figure 12: Map of study sites (GoogleEarth 2020).

Information about the sites, including river, road, structure type, and indication of whether they were studied in 1971 or 1989 is summarized in Table 2 (Keeley 1971; Harp and Thomas 1989).

*Table 2: Site information summarized, including indication of whether they were studied in 1971 or 1989 (Keeley 1971; Harp and Thomas 1989). *Not included in current study*

Site No.	Highway	River Name	Type of Structure (Year Built)	1971	1989
1	U.S. 77	Washita River	Kellner Jetty (1949), pile diversions (1959); rip-rapped dikes (1959	X	X
2	U.S. 177	Cimarron River	Kellner jetties (unknown), pile diversions (1950, 1963); rip-rapped dikes (1953); rip rap (1957, 1965),	X	X
3*	S.H. 51	Cimarron River	Rock dike (1934); Kellner jetties (1938); pile diversions (1957); rip-rapped dike (1957)	X	X
4	U.S. 281	Cimarron River	Kellner jetty (1940-52?), pile diversions (1955), rip rap (1958)	X	X
5	U.S. 64	Arkansas River	Kellner jetty (1938, 1948); rip rap (1950?); rock spur dike (1959); pile diversions (1959)	X	X
6	U.S. 281	North Canadian River	Kellner jetty (1927)	X	X
7	U.S. 281	Canadian River	Kellner jetties (1937, 1939, 1949, 1951); pile diversions (1958); rock spur (1960-64?)	X	X
8	U.S. 62	Salt Fork of the Red River	Kellner jetties (1936, 1939); rip rap (1957); pile diversions (1957)	X	X
9*	S.H. 5	North Fork of the Red River	Kellner jetties (between 1942 and 1954)	X	X
10	S.H. 76	Washita River	Pile diversions (1953)	X	X
11	S.H. 74	Washita River	Kellner jetties (1949); ScourStop	X	X
12	S.H. 33	Cimarron River	Rip rap (1944, 1957); Spur dike (1957); pile diversions (1957); Bendway weirs	X	X
13	S.H. 48	Canadian River	Pile diversions (1951, 1959); rip rap (1957, 1959, 1960)	X	X
14	S.H. 84	North Canadian River	Kellner jetties (1949); rip rap (1949, 1958); pile diversions (1958)	X	X
15*	S.H. 2	Canadian River	Rip-rap (1947); pile diversions (1948); “bank retards” (1948)	X	X
16	S.H. 3	North Canadian River	Kellner jetty (1949);	X	X
17	S.H. 74	Cimarron River	Rayfield jetty (1937); rip rap (1937, 1956, 1957, 1967); dikes (1956, 1957); Kellner jetty (1968)	X	X
18	I-35	Washita River	Rip rap (1967); Kellner jetty (1968)	X	X
19	U.S. 283	Beaver River	Kellner jetties (1938, 1949); dike (1949)	X	X
20	I-35	Washita River	Pile diversion (1968-69);	X	X
21	S.H. 79	Red River	Rip rap (unknown); trilock block (1983); Kellner jetty (unknown); Henson type fence (unknown)		X
22	S.H. 53	Washita River	Spur dike (1972); rip rap (1972); Kellner jetty (1981)		X
23	I-35	Canadian River	Kellner jetty (1989); rip rap (1989)		X
24	U.S. 259	Red River	Kellner jetties (about 1960)		X
25	S.H. 48	North Canadian River	Kellner jetty (1985); rip rap (1985)		X
26	U.S. 281	Sugar Creek	Rock Drop Structure (2001)		
27	S.H. 99	North Canadian River	Bendway Weirs (2001)		
28	S.H. 10	Illinois River	Plantings and Rock Vanes (2016)		
29	S.H. 19	Washita River	Kellner jetty (1999)		
30*	S.H. 19	Washita River	Kellner jetties (1980s)		
31	I-40	Deer Creek Trib	Gabion Baskets (2000)		
32	S.H. 7	Washita River	Kellner jetty (2004)		
33	S.H. 156	Salt Fork of Arkansas River	Directional Spurs and Rip rap (1990s)		
34	U.S. 281	Sugar Creek	Rock Drop Structure (2004)		

2.2 Remote Data Collection

Data was collected from many different online databases to provide background on the stream and watershed's characteristics and hydrologic history.

2.2.1 Streamflow and Watershed Data

To gather general information about the site and contributing watershed, the watershed for each site was delimited using USGS StreamStats (U.S. Geological Survey 2020). Average streamflow, storm flow rates. and watershed area were collected for each site.

2.2.2 Watershed Land Use

After each site's contributing watershed was delimited, it was downloaded as a shapefile and used for further analysis. Each site's watershed shapefile was uploaded into ArcMap and overlayed on top of the National Land Cover Database (NLCD) 2016 land use map (NLCD Data 2016). From this data, the percent of the watershed that is developed is the most important factor because of its impacts on the stream hydrology (Smith and Patrick 1979).

2.2.3 Historic Photos

Historic aerial photos were downloaded from the Oklahoma Aerial Photo Inventory (2019) and georeferenced in ArcMap software by Esri. The photos were georeferenced using at least three points that link the old aerial pictures to a current base map, including roads, buildings, or historical landmarks. An example of georeferenced historical photos is shown in Figure 13.

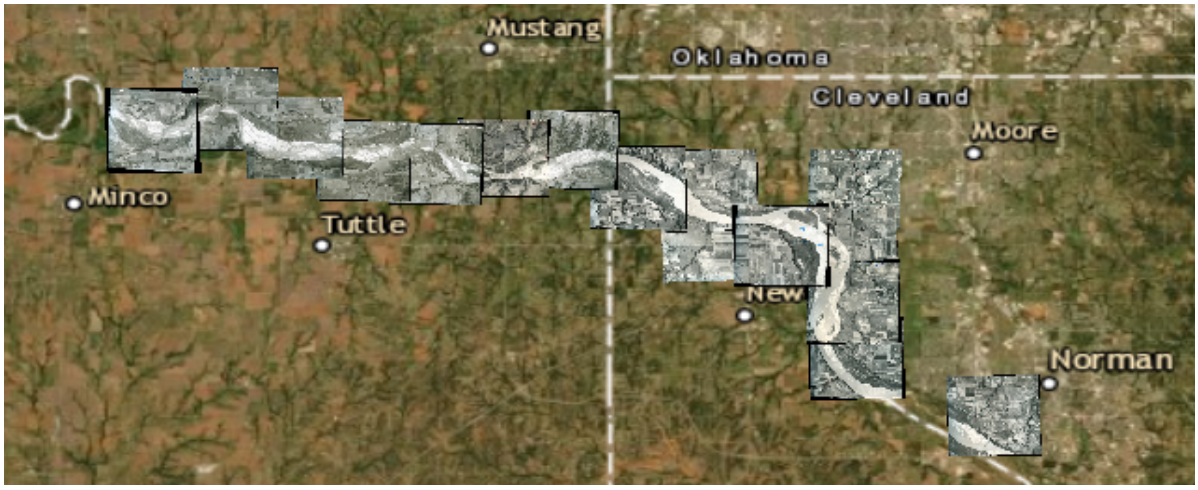

Figure 13: Georeferenced historical images from 1957 of the Canadian River from Minco to Norman (Oklahoma Aerial Photo Inventory 2019).

These photos were used for objective evaluation of the progress of the sites, for measuring historic sinuosity, and for measuring the distance the thalweg has moved over time.

2.2.4 Stream Sinuosity

Stream sinuosity contributes to the geomorphic characterization of a stream and impacts sediment transport (Smith and Patrick 1979). Sinuosity was found from the previously georeferenced aerial images, both historic (if available) and current (GoogleEarth 2020). The sinuosity of a stream is equal to the length of the stream channel divided by the straight line distance of the chosen stream reach. The sinuosity was calculated for a one-mile straight line reach upstream of each bridge site.

2.2.5 Kellner Jetty Angles

The angles between the Kellner jetties and the stream flowline is of concern because it may impact the hydraulics in the Kellner jetty field. Because the location of the stream flowline changes over time, the angles were found at various points in time: at installation, in 1971, in 1989, and current. The angle at the time of installation was found from ODOT streambank protection plans or historic aerial images and may be limited by plan and image availability

(Lewis 2020). The angles in 1971 and 1989 was measured from the detailed sketches of the stream reaches and Kellner jetty fields in the previous reports (Keeley 1971; Harp and Thomas 1989). Current Kellner jetty angles were measured from aerial images if the Kellner jetties are still visible on the site (GoogleEarth 2020). The angles over times were combined into two variables (oldest Kellner jetty angle and most recent Kellner jetty angle) to maximize the sample size for regression analysis.

2.2.6 Depth to Bedrock

The depth to bedrock was collected from borings in ODOT bridge plans for each site, separated by bank (Lewis 2020). Each bank has multiple borings, so the minimum, arithmetic mean, and coefficient of variation for depth to bedrock were used in the statistical analyses. Measurements from borings in the main stream channel were not used.

2.2.7 Historical Precipitation Data

Using the National Oceanic and Atmospheric Administration's (NOAA) archive of historical precipitation data, the hydrologic conditions surrounding the installation of structures at each site can be quantified (NCEI 2021). Precipitation data was gathered for the first five years following the installation of each structure at each site. To consider impacts of large precipitation events that occur upstream in a site's watershed, historical precipitation data was collected from three stations per site: one close to the site, one in the middle of the watershed, and one upstream in the watershed. The selection of these stations depended on data availability in the relevant time period for each site. The statistical analyses evaluated the impact of precipitation at the site in addition to precipitation throughout the watershed as separate variables. The variables considered were the total number of precipitation events greater than 0.5in per day within one, three, and five years of installation, both at all three stations throughout

the watershed and at the one closest to the site. The threshold of 0.5in is based on United States Department of Agriculture findings that daily precipitation below 0.5in produced insignificant amounts of soil erosion (Wischmeier and Smith 1978; Renard 1997).

The maximum return period of a 24-hr storm was another variable considered from the precipitation data, which was calculated based on the NOAA precipitation frequency data server (2005). The maximum return period within one, three, and five years of installation was found at each of the three stations throughout the site's watershed. Variables included in the statistical analyses were the maximum return period at the site closest to the site, the overall maximum return period at all three sites in the watershed, and the arithmetic and geometric means of the maximums at each of the three sites in the watershed, all within one, three, and five years of installation.

2.2.8 Lateral Movement of Thalweg

The lateral movement of a stream at a bridge location over time provides information on how at-risk the bridge abutments may be. It also shows how stable the stream channel is and contributes to the understanding of the stream's geomorphology (Lagasse et al. 1995). The lateral movement of the thalweg was measured at the bridge crossing and is the distance the thalweg has moved away from the bank of concern. A positive distance is movement away from the bank of concern while a negative distance is movement towards the bank of concern. The thalweg location at the time of the installation of the structures was compared to the thalweg location at the time of the field survey. The thalweg location at the time of installation was measured to a reference point on ODOT bridge or streambank protection plans (Lewis 2020) or landmarks on historic photos and compared to field survey data.

2.3 Site Surveys

In the field, many different quantitative and qualitative methods were used to gather information about the properties of the river. Qualitative methods include a sketch of each site with the location of the bridge crossing, meanders, eroding banks, and different structures that are found. Photos were taken of the bridge, river (upstream and downstream of the bridge), structures, eroding banks, and banks where structures were or are located.

2.3.1 Longitudinal Profile

A longitudinal profile of the stream was collected by surveying along the thalweg, or deepest part of the stream, with a Topcon ES Total Station. The longitudinal profiles started upstream of the structures and continued until the bridge crossing. Data points were taken every 20-40 feet along the thalweg. Water depths were collected with every data point along the longitudinal profile if accessible. The longitudinal profile shows riffle-pool patterns along the length of the river as well as the stream slope along the top of the water (Rosgen 2014). The stream slope was determined by a best-fit line along the surface of the water in the longitudinal profiles.

2.3.2 Cross Sections

Cross sections were collected at the location of stabilization structures as well as at a local riffle, if accessible, and immediately downstream of the bridge. The exact locations of each cross section was chosen so they were representative of the river and banks in each location of interest (Rosgen 2014). The cross sections were taken to the top of the bank, if accessible, and as far up the bank as possible if the top was not accessible, using the Topcon ES Total Station. Points were taken every 2-20 feet along the cross section, depending on the topography of the bank, and points were further apart if the bank topography has little variability. If accessible, the water

depth was measured by a survey rod along with every point taken across the width of the stream. If water depth measurements by hand are not possible, the Sontek S5 acoustic Doppler current profiler (ADCP) was used to collect water depths across the width of the stream for the cross section.

2.3.3 Velocity Profiles and Near-Bank Stress

Velocity profiles were collected at each cross section, using an ADCP. Velocity profiles show the stream velocity perpendicular to the cross sectional plane (Rosgen 2014). The ADCP used was a SonTek S5 ADCP, which collects a data point every second as it crosses the stream and contains velocity measurements along the depth of each data point. ADCP data collection methods varied depending on the accessibility of the river. In wadable rivers, a rope was attached to either side of the ADCP, extending bank-to-bank along the cross section of concern, and the ADCP was dragged across the river. In non-wadable streams, the ADCP was attached to the back of a kayak and floated across the cross-section from one bank to the other. A photo of this is shown in Figure 14.

Figure 14: ADCP attached to back of kayak for cross sections in non-wadable rivers.

The ADCP does not collect velocity data in water less than one foot deep, so in small streams, a second site visit was made to get a velocity profile during higher flow.

The velocity profiles were used to calculate near-bank stress (NBS). There are seven different factors that can be used to rate NBS, and a velocity gradient is the preferred factor (Rosgen 2014). The velocity gradient was calculated by finding the change in velocity over the distance from the bank of concern from the velocity profiles in RiverSurveyor Live, Sontek's data visualization program. The faster the velocity increases, moving away from the bank of concern, the higher the velocity gradient and higher rating of NBS. Based on the calculated gradient, the NBS is categorized into one of six ratings. The ratings and their velocity gradient ranges are listed in Table 3 (Rosgen 2014).

Table 3: Near-bank stress (NBS) ratings based on velocity gradient (Rosgen 2014).

Rating	**Very Low**	**Low**	**Moderate**	**High**	**Very High**	**Extreme**
Velocity Gradient (ft/sec/ft)	<0.50	0.50-1.00	1.01-1.60	1.61-2.00	2.01-2.40	>2.40

2.3.4 Bank Erosion Hazard Index Survey and Sediment Analysis

The bank erosion hazard index (BEHI) is a measure of streambank erosion potential, based on many different factors. For the purposes of this study, a modified version of the BEHI developed by Rosgen (2014) was used, which omits bankfull measurements, shown in Table 4. The BEHI was calculated by assigning a score for each category according to the range the bank of concern falls in and summing the score for all the categories and any adjustments.

Table 4: Modified BEHI scoring system, including the ratio of root depth to bank height, root density, surface protection, bank angle, and adjustments for bank material and stratification (Rosgen 2014).

`BEHI Category	Score	Root depth/bank height (%)	Root Density (%)	Surface Protection (%)	Bank Angle (degrees)	Total
Very low	1	90-100	80-100	80-100	0-20	<6
Low	3	50-89	55-79	55-79	21-60	6-12
Moderate	5	30-49	30-54	30-54	61-80	13-20
High	7	15-29	15-29	15-29	81-90	21-28
Very High	8.5	5-14	5-14	10-14	91-119	29-34
Extreme	10	<5	<5	<10	>119	>34

Material Adjustment		**Stratification Adjustment**	
Bedrock	Automatically very low	**No Layer**	0
Boulder	Automatically low	**Single Layer**	5
Cobble	-10	**Multiple Layers**	10
Gravel	5		
Sand	10		
Silt/Loam	0		
Clay	-20		

Root depth, root density, and surface protection were all estimated using the procedures described in Rosgen (2014), and a visual inspection for stratification was completed on site. Bank height and bank angle were taken from cross sections. Samples of bank material were taken on banks of concern for the sediment adjustment. Particle size distribution analyses were completed by both sieve and hydrometer methods according to ASTM standards D6913 and D7928, respectively (2017). Duplicates were performed on 10% of samples for quality assurance. Data from the particle size distributions was also included in the statistical analyses as well. The variables extracted from the particle size distributions included the percent sand, percent silt, and percent clay based on the Unified Soil Classification System (USCS), as shown in Table 5 (U.S Department of Agriculture 2012).

Table 5: Unified Soil Classification System by particle size (U.S. Department of Agriculture 2012).

USCS Particle Classification	**Clay**	**Silt**	**Sand**	**Gravel**
Particle Size (mm)	<0.002	0.002-0.05	0.05-2.0	>2.0

Other sediment variables found were effective particle size (d_{10}), uniformity coefficient, and coefficient of curvature. The effective particle size (d_{10}) is the particle size at which 10% of the sample, by weight, is smaller in diameter. The same logic applies for the variables of d_{30} and d_{60}. The equations for uniformity coefficient (C_u) and coefficient of curvature (C_c) are shown in equations 1 and 2, respectively.

$$C_u = d_{60}/d_{10} \quad (1)$$

$$C_c = d_{30}^2/(d_{10} * d_{60}) \quad (2)$$

The uniformity coefficient represents the variability in the particle sizes in the sediment sample. Little variability corresponds to high uniformity and a high uniformity coefficient. These sediments are considered poorly graded in geotechnical engineering. High variability corresponds to a low uniformity coefficient and a well-graded soil. The coefficient of curvature also identifies a poorly or well-graded soil. Well-graded soils have a coefficient of curvature between one and three. A well-graded soil can be condensed more than a poorly-graded soil, which makes it stronger (Budhu 2011).

2.4 Determination of Failure or Success

After the site visits, each structure was deemed either a failure or a success. In general, the structures were successful if they fulfilled their intended purpose, but the purpose of each structure is slightly different. Explanations of successes and failures for the most common structures in this project are listed in Table 6.

Table 6: Explanation of success and failure of Kellner jetties, pile diversions, rip rap, and spur dikes

Structure Type	Explanation of Success	Explanation of Failure
Kellner Jetties	- Slows down stream velocity along bank of concern - Builds up bank - Encourages vegetation growth	- Washed away by stream - Sunk into streambed - Stream eroded through Kellner jetty field
Pile Diversions	- Diverts stream energy away from bank of concern - Develops sand bar - Encourages vegetation growth	- Stream eroded past initial installation of pile diversions - Sunk into streambed
Rip Rap	- Remains on bank of concern - Covers native sediment	- Washed away by the stream
Spur Dikes	- Protects bridge abutment from erosion - Prevents erosion upstream of bridge abutment	- Stream eroded around spur dike - Scour occurred behind spur dike

Based on site visits, historical aerial images, and previous reports (Keeley 1971; Harp and Thomas 1989), each structure studied could be fully evaluated.

2.5 Statistical Analyses

Remote data and field data were combined in statistical analyses to find any patterns in the data that could determine the likelihood of a structure to fail. After each site was visited, the structures on the site were deemed a failure if the bank has eroded around them, they were washed away, or they have not contributed to the stabilization of the bank, and a success otherwise. The data collected was combined into a spreadsheet for statistical analysis, including the failure or success of each structure, represented by a zero or a one, respectively. Variables included in the spreadsheet are listed in Table 7.

Table 7: Complete list of variables included in statistical analysis. (LPE = large precipitation events, >0.5in in 24 hr; BEHI = Bank Erosion Hazard Index.)

Other structures present on bank (binary)
% gravel, % sand, % silt, % clay in bank material
Sediment factors: d_{10}, d_{40} uniformity coefficient (C_u), gradation coefficient (C_c)
Depth to bedrock: arithmetic mean, minimum, coefficient of variation
Angle of Kellner jetties: at installation, in 1971, in 1989, current, oldest, most recent
Number of LPE: total at three stations throughout watershed and at one station closest to site within one, three, and five years of structure installation
Maximum return period at station closest to site within one, three, and five years of installation
Maximum of all return periods at three stations throughout watershed within one, three, and five years of installation
Geometric and arithmetic means of maximum return period at each station in watershed within one, three, and five years of installation
Sinuosity
Stream slope
% watershed developed
Average streamflow
BEHI rating
% root density
Watershed area
Lateral movement of thalweg at bridge crossing
Location of structures (1=meander, 0=straightaway)

First, a correlation matrix was used to determine what variables individually correlate with failure and success. This narrowed down the variables to be used in the regressions. Linear regressions were run in Excel, using individual and multiple variables chosen based on the correlation matrix, but no significant regressions were found. Because of the categorical nature of the dependent variable (success and failure) in this study, logistic regressions are more appropriate for the data analysis (Dowdy et al. 2004). Logistic regressions use the log odds of the proportion (p) of positive outcomes, successes in the case of this study, as the dependent variable. This is called a logit, and equation 3 is its calculation. If the proportion is zero, the logit is negative infinity, and if the proportion is one, the logit is positive infinity (Dowdy et al. 2004).

$$logit(p) = log_e(\frac{p}{1-p}) \quad (3)$$

Logistic regression analyses were completed in R, using one or multiple variables to determine what variables or combination thereof can best predict the failure or success of a structure. To analyze the data in a logistic regression, it was modeled as binomial. When the data was analyzed to develop a logistic regression model, the program determined coefficients (C_n) for each input variable (x_n) and an intercept (a). These were then used to calculate the logit, using equation 4 (Dowdy et al. 2004).

$$logit(p) = a + C_1x_1 + C_2x_2 \ldots + C_nx_n \quad (4)$$

The modeled proportion was then back-calculated, using equation 3, which was plotted to show the estimated probability of a success based on the input variables.

Variables with the strongest correlations with the binary success or failure variable were chosen to run logistic regressions. If these variables described the same concept (historical precipitation, sediment), the one with the strongest correlation was used in the regressions. The variables are clustered by concept in Table 7. A combination of a conceptual understanding of the variables' interaction with each other in the streambank erosion process and statistical analyses were used to determine what variables to run in the logistic regressions for each structure. Variables were then eliminated based on p values, which were also retrieved from R for each variable and the intercept. Regressions were completed on Kellner jetties, pile diversions, and all of the structures together. A significance threshold of $p < 0.1$ was used because of the limited number of data points for pile diversions and Kellner jetties. With the higher number of data points for the regression with all of the structures, a significance threshold of $p < 0.05$ was used.

Chapter 3: Results and Discussion

Examples of results from the major rivers represented in this study and logistic regressions analyzing the data by structure type are presented in this section. Complete results are shown in Appendices A-G. Additionally, a summary table with all variables used in the analysis is presented in Appendix H.

3.1 Longitudinal Profiles

The longitudinal profiles show the riffle-pool patterns, stream slope, and lateral location of the thalweg at each site. Maps of the lateral thalweg location at each site are in Appendix C, and all longitudinal profiles are in Appendix D. The longitudinal profiles differed between the major rivers in Oklahoma, so an example from each major river with multiple sites studied is shown. The first major river is the Washita River, which is located in southwestern Oklahoma. Figure 15 is a map of the Washita River in Oklahoma (MapSof 2021).

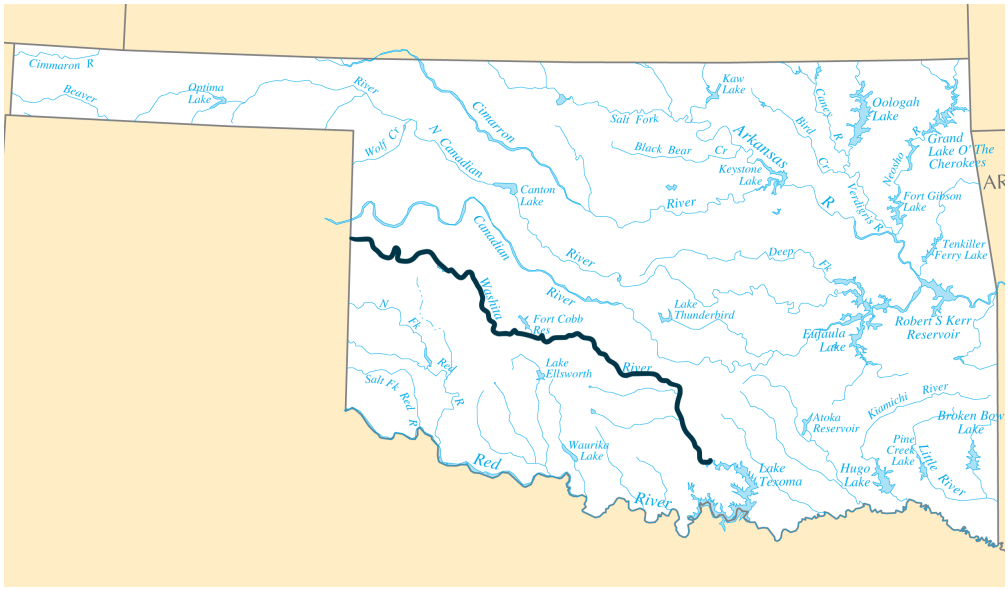

Figure 15: Map of Washita River in Oklahoma (MapSof 2021).

Figure 16 is an example of a longitudinal profile on the Washita River, from site 18 near Davis, Oklahoma.

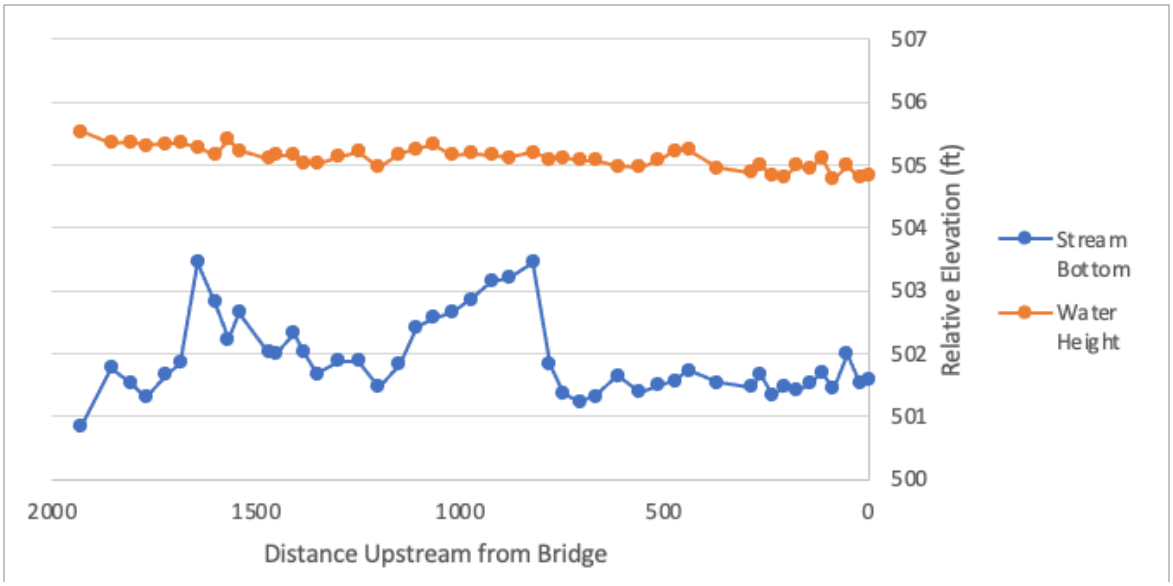

Figure 16: Site 18, Washita River and U.S 77 South of Davis in Murray county, longitudinal profile.

A riffle is located around 1000 feet upstream from the bridge with pools around 1250 and 500 feet upstream from the bridge. There is little variability in the stream slope but drastic changes in water depths along this reach of the river. The data points taken along the thalweg of the river can show where the thalweg is laterally in the stream. The lateral location of the thalweg at site 18 is shown in Figure 16.

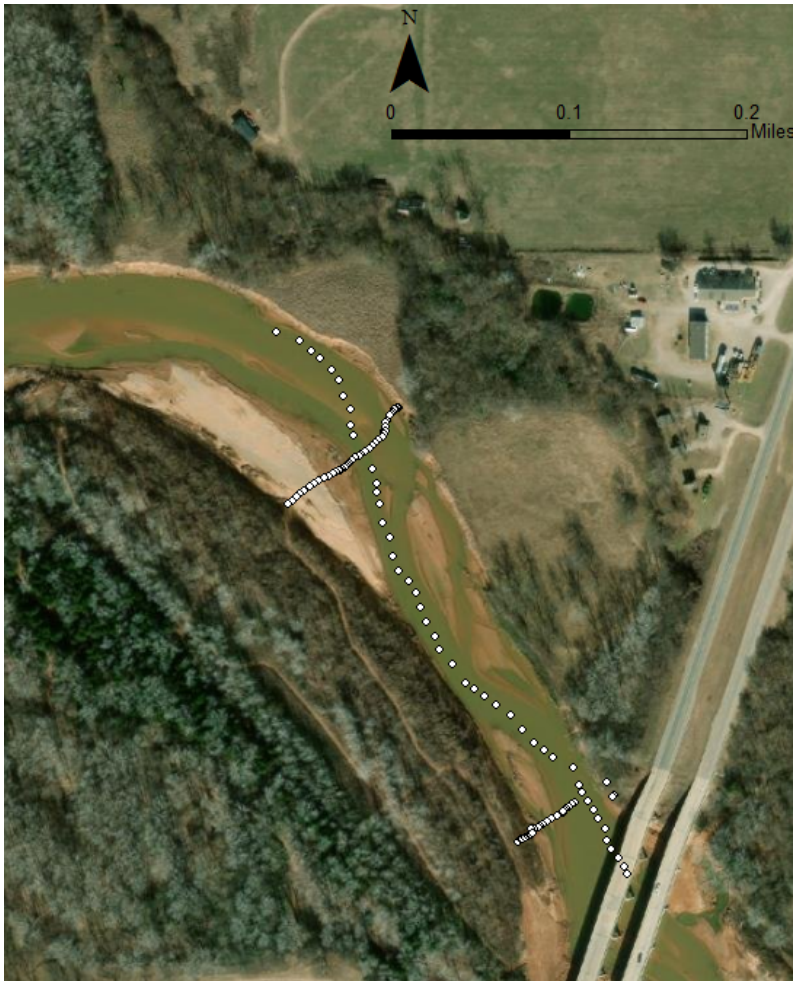

Figure 17: Site 18, Washita River and U.S 77 South of Davis in Murray county, thalweg data points.

The thalweg at site 18 moves laterally across the stream along the reach that was studied. Lateral movement of the thalweg is common in the Washita River, creating strong meanders and many high eroding banks. The average stream slope on the Washita River was 0.023%, with a minimum of 0.01% and a maximum of 0.04%. Overall, the Washita had very gentle stream slopes with little variability site-to-site.

The next major river is the North Canadian River, which flows east to west through central Oklahoma. Figure 18 is a map of the North Canadian River in Oklahoma (MapSof 2021).

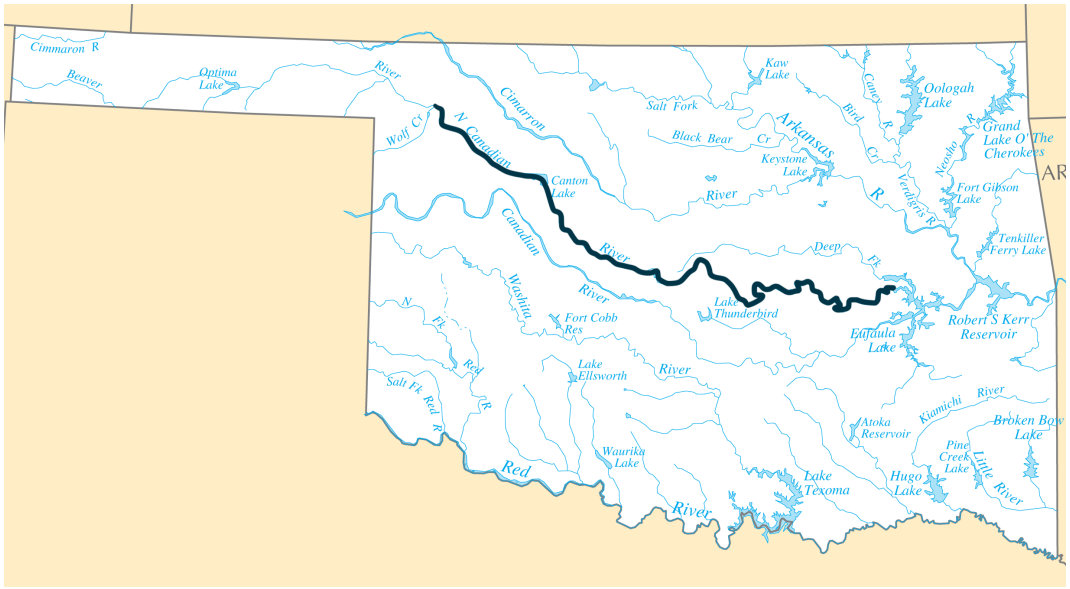

Figure 18: Map of North Canadian River in Oklahoma (MapSof 2021).

Figure 19 is an example of a longitudinal profile on the North Canadian River at site 27 south of Prague.

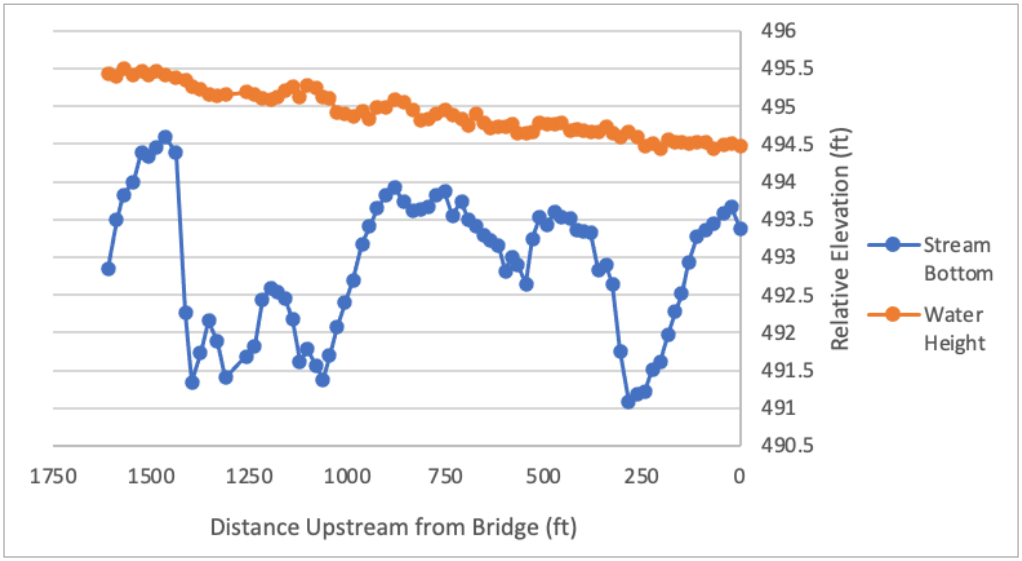

Figure 19: Site 27, North Canadian River and S.H. 99 south of Prague in Seminole county longitudinal profile.

Riffles are located around 1500 feet and 750 feet upstream from the bridge with pools around 1250 and 250 feet upstream from the bridge. There is little variability in the stream slope but

high variability in depth along this reach of the river. The location of the thalweg at site 27 is shown in Figure 20.

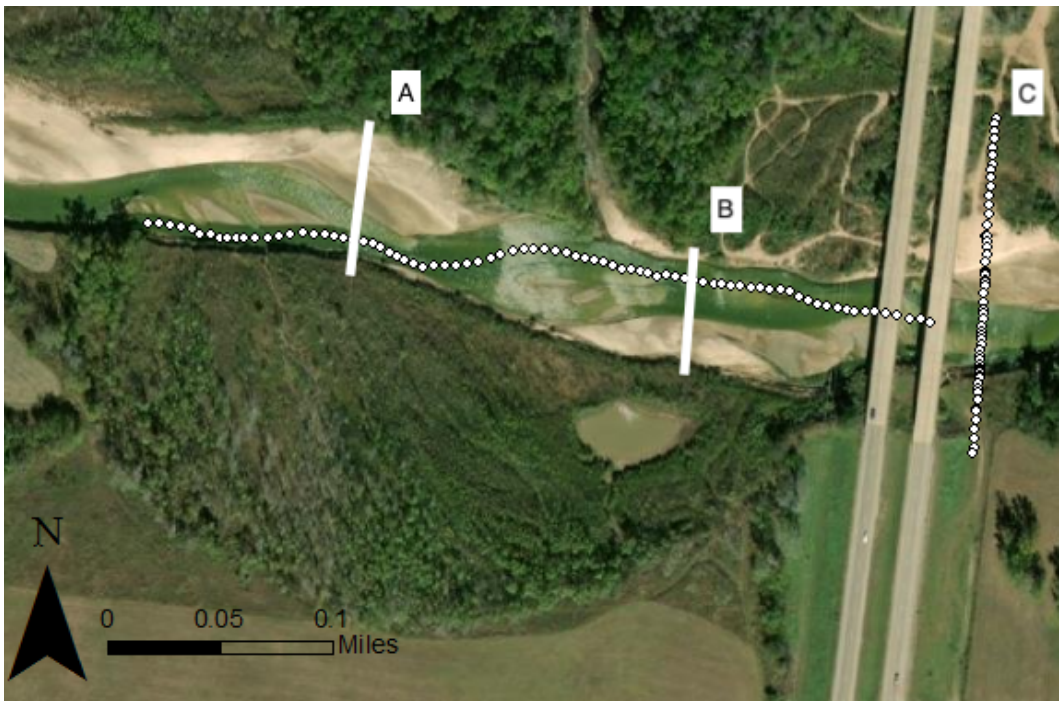

Figure 20: Site 27, North Canadian River and S.H. 99 south of Prague in Seminole county thalweg data points.

The thalweg moves laterally in the North Canadian River, but it moves more gently and creates fewer meanders than the Washita River. The average stream slope at sites on the North Canadian River is 0.040%, with a minimum of 0.026% and a maximum of 0.063%. These slopes are steeper than those in the Washita River, which may contribute to the lack of lateral movement in the thalweg.

The Canadian River, also sometimes referred to as the South Canadian River, has a similar characteristics to the North Canadian River. It also flows east to west through central Oklahoma. Figure 21 is a map of the Canadian River in Oklahoma (MapSof 2021).

Figure 21: Map of Canadian River in Oklahoma (MapSof 2021).

An example of a longitudinal profile in the Canadian River is shown in Figure 22.

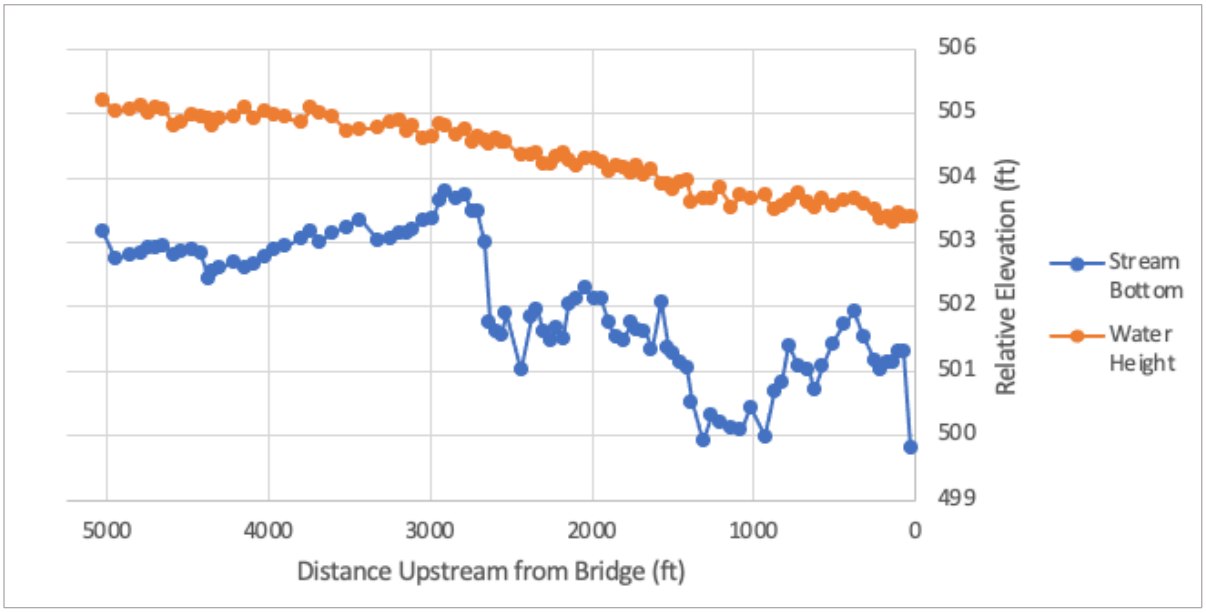

Figure 22: Site 13, Canadian River and S.H. 48 north of Atwood in Cotton county longitudinal profile.

A riffle was located around 3000 feet upstream of the bridge, with pools around 5000 and 1000 feet upstream of the bridge. The location of the thalweg at site 13 is shown in Figure 23. There is

very little lateral movement of the thalweg at this site, which is common in the Canadian and North Canadian rivers.

Figure 23: Site 13, Canadian River and S.H. 48 north of Atwood in Cotton county thalweg data points.

The average stream slope at sites on the Canadian River is 0.042%, with a minimum of 0.038% and a maximum of 0.048%. These slopes are very similar to the North Canadian River. The stream slopes are slightly steeper than the those on the Washita River, but they are still very gentle slopes, which is expected in Oklahoma.

The Cimarron River flows east to west through northern Oklahoma into Keystone Lake. Figure 24 is a map of the Cimarron River in Oklahoma (MapSof 2021).

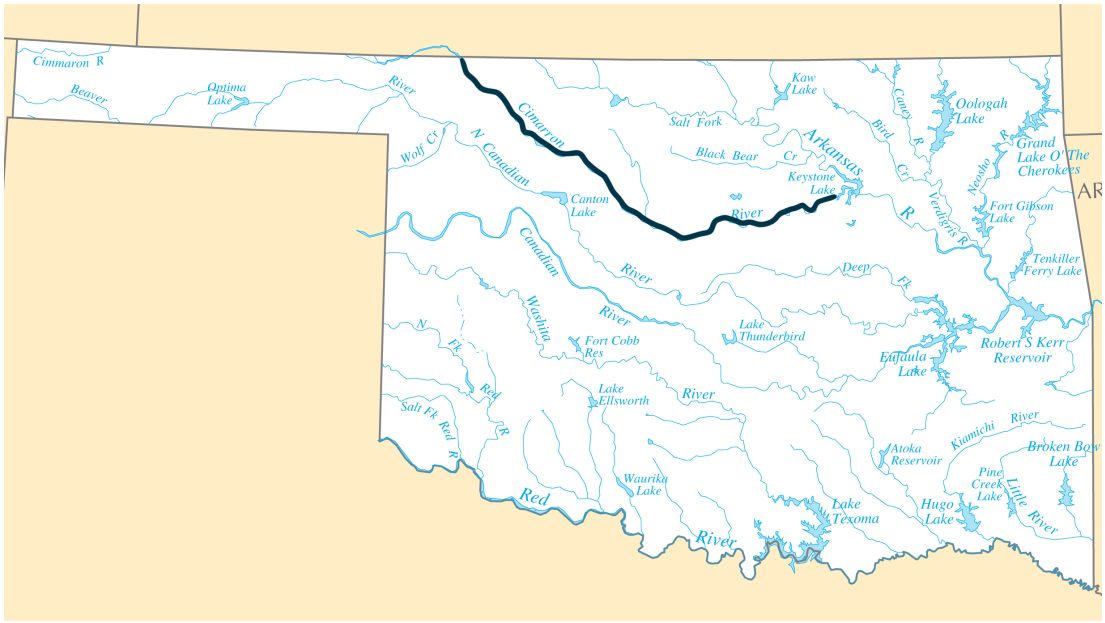

Figure 24: Map of Cimarron River in Oklahoma (MapSof 2021).

Figure 25 is an example of a longitudinal profile on the Cimarron River.

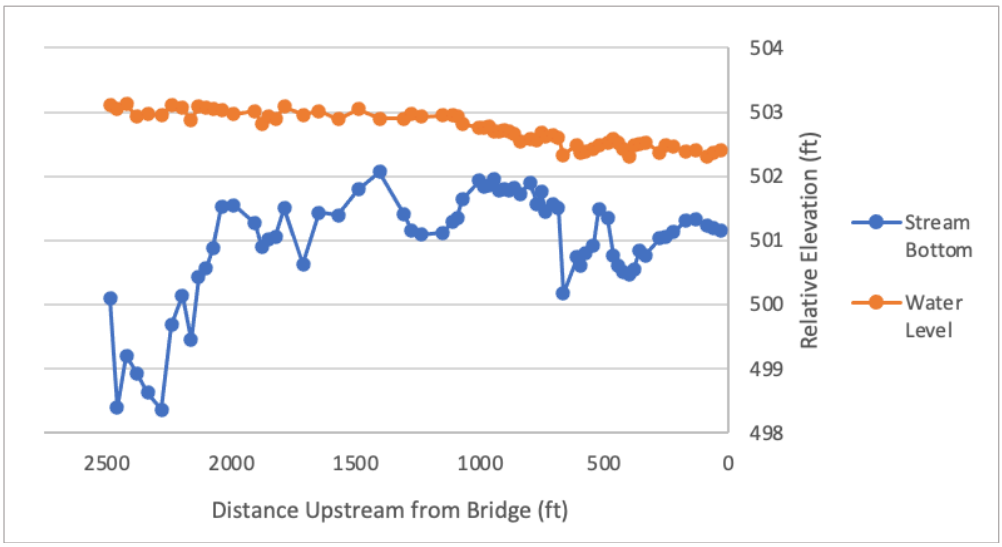

Figure 25: Site 17, Cimarron River and S.H. 74 south of Crescent in Logan county longitudinal profile.

Riffles are located at 1000 and 600 feet upstream of the bridge, and pools are located at 2500 and 1200 feet upstream. Figure 26 is a map of the data points taken along the thalweg at site 17. The thalweg moves gradually at this site, which is characteristic of the Cimarron River. It does not

move from bank-to-bank as much as the thalweg in the Washita River, but there is slight lateral movement of the thalweg along this river.

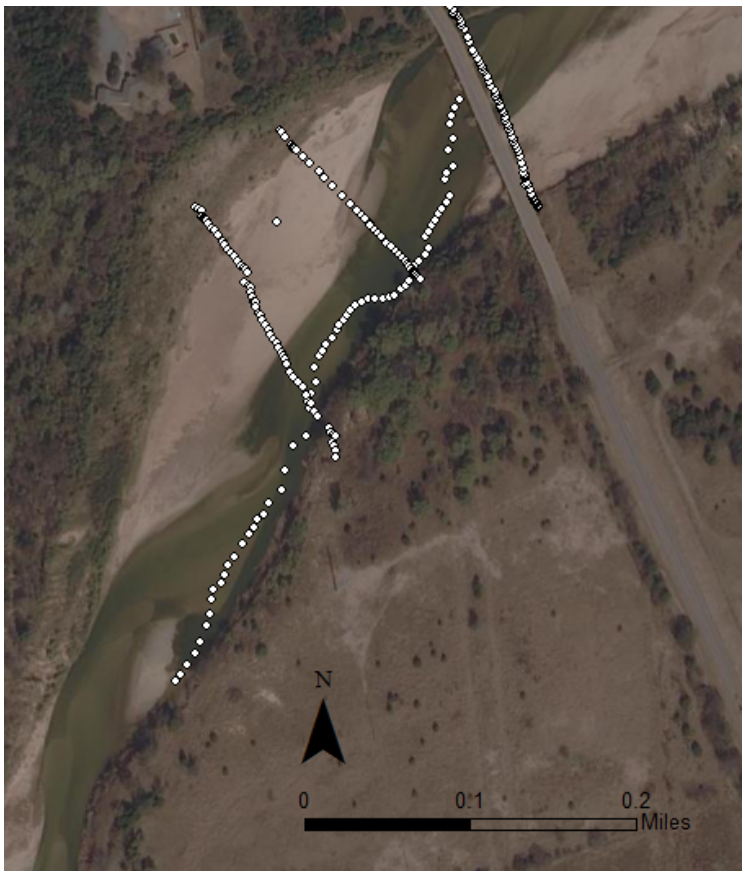

Figure 26: Site 17, Cimarron River and S.H. 74 south of Crescent in Logan county thalweg data points.

The average stream slope at sites on the Cimarron River is 0.037%, with a minimum of 0.032% and a maximum of 0.044%. These slopes are slightly more gentle than the North Canadian and Canadian rivers, but steeper than the Washita River.

The last major river basin that was investigated was the Red River, which flows east to west along the southern border of Oklahoma. Figure 27 is a map of the Red River in Oklahoma (MapSof 2021).

Figure 27: Map of Red River in Oklahoma (MapSof 2021).

Figure 28 is an example of a longitudinal profile in the Red River.

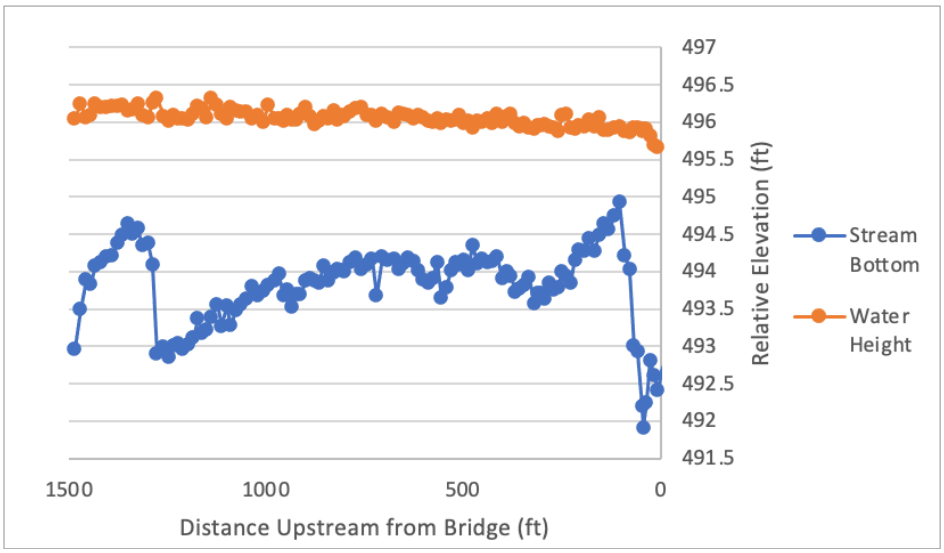

Figure 28: Site 21, Red River and S.H. 79 west of Waurika in Jefferson county longitudinal profile.

There is very little variability in the stream slope at this site, but there is a riffle 1400 feet upstream and a pool 1250 feet upstream from the bridge. Figure 29 shows the location of the

thalweg at a site on the Red River. The thalweg does not move laterally much, staying along the left bank for the reach of the river shown until the bridge crossing.

Figure 29: Site 21, Red River and S.H. 79 west of Waurika in Jefferson thalweg data points.

The average stream slope at sites in the Red River basin is 0.054%, with a minimum of 0.021% and a maximum of 0.088%. These slopes have a large range, but they are close to the average slopes of streams studied.

3.2 Bank Material Particle Size Distributions

The particle size distributions describe the texture of the soil and is used to characterize the soil based on percentages of clay, sand, and silt, according to the Unified Soil Classification System (USCS) (U.S. Department of Agriculture 2012). Appendix G contains all particle size distributions taken at the banks of concern at each site.

Geology varies greatly across Oklahoma, and this is true for the river throughout the state as well. Particle size distribution is an important factor in streambank erosion because sand is much more erodible than either silt or clay. Because of the variability in geology, an example bank particle size distribution will be shown for each major river with multiple sites.

Figure 30 is an example of a particle size distribution on the Washita River.

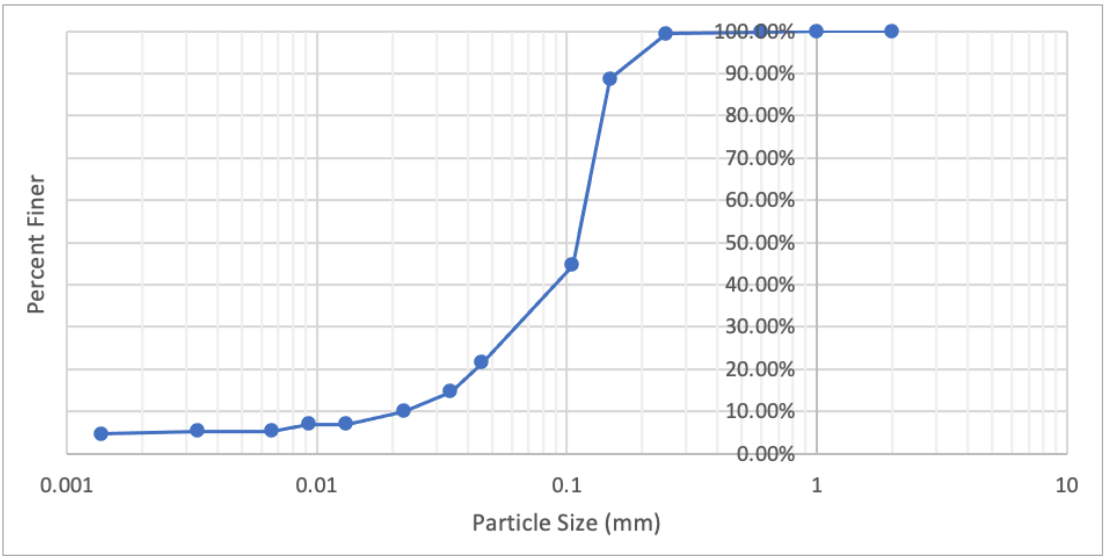

Figure 30: Site 11, Washita River and S.H. 74 north of Maysville in Garvin County, right bank particle size distribution.

Table 8 is a summary of the bank material particle size analyses on the eight Washita River sites. 50% of the samples on the Washita River were well graded, with high uniformity coefficients and coefficients of curvature between one and three. The other 50% had coefficients of curvature outside of the well-graded soil range.

Table 8: Washita River bank soil particle size analysis summary (n=8) (C_u = uniformity coefficient; C_c = coefficient of curvature).

	% clay	% sand	% silt	% gravel	d10	d40	C_u	C_c
Average	6.8	75	16	2.0	0.03	0.08	66	1.9
Minimum	1.6	53	2.0	0.0	0.0	0.01	2.0	0.31
Maximum	15	95	24	11	0.10	0.17	430	4.8

The soil types varied site-to-site on the Washita River, including sandy loam, loamy sand, and sand. They were all above 50% sand, with a maximum of 95% sand. Figure 31 is an example of a particle size distribution on the North Canadian River.

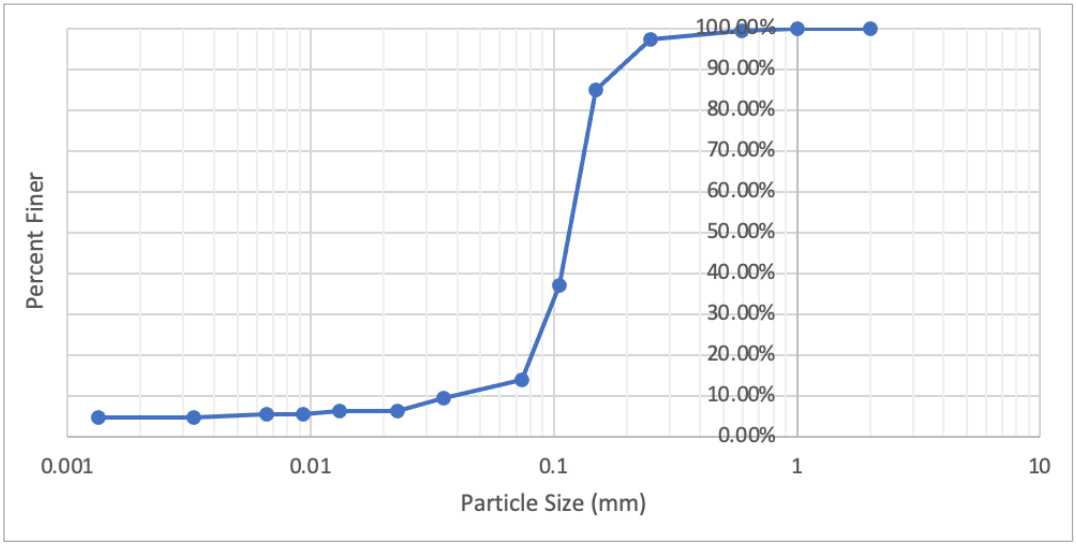

Figure 31: Site 25, North Canadian River and S.H. 48 north of Bearden in Okfuskee county left bank particle size distribution.

Table 9 is a summary of the bank material particle size analyses on the five North Canadian River sites. The samples on the North Canadian River had lower uniformity coefficients, meaning they were poorly graded, but the coefficients of curvature were mostly between one and three, meaning the samples were well graded. For sandy soils to be considered well graded, the uniformity coefficient must be above six, which was not the case for 80% of the samples. Thus, the soils in the North Canadian River were mostly poorly graded.

Table 9: North Canadian River bank soil particle size analysis summary (n=5) (C_u = uniformity coefficient; C_c = coefficient of curvature).

	% clay	% sand	% silt	% gravel	d10	d40	C_u	C_c
Average	1.5	93	5.3	0.14	0.08	0.25	5.4	2.5
Minimum	1.5	89	1.5	0.00	0.05	0.18	1.7	1.1
Maximum	1.5	97	9.0	0.28	0.12	0.32	9.1	4.0

All of the bank samples taken on the North Canadian River are classified as sand. The minimum sand percentage of a bank sample on this river was 89%, with a maximum of 97%. There was little variability between the samples. Figure 32 is an example of a particle size distribution on the Canadian River.

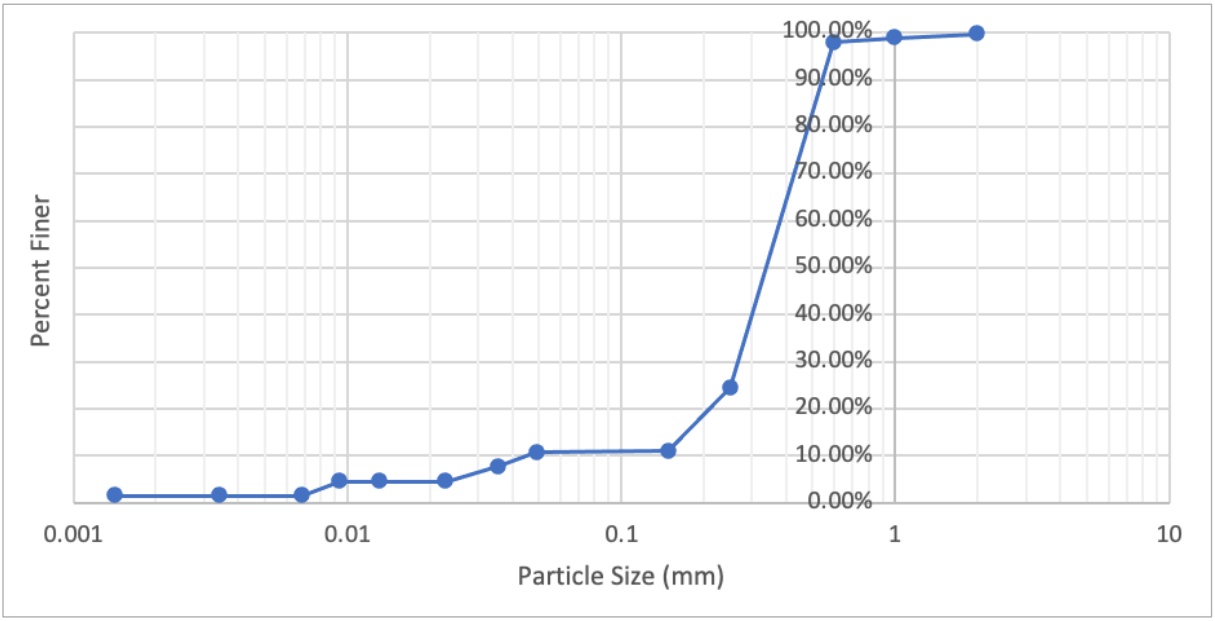

Figure 32: Site 7, Canadian River and U.S. 281 east of Bridgeport in Canadian county right bank particle size distribution.

Table 10 is a summary of the bank material particle size analyses on the two sites on the Canadian River. The samples taken at sites on the Canadian River both classified as sandy loam. There was little variability in the textures of the soils at these two sites, and neither was well graded, based on the uniformity coefficients and coefficients of curvature.

Table 10: Canadian River bank soil sample particle size analysis summary (n=2) (C_u = uniformity coefficient; C_c = coefficient of curvature).

	% clay	% sand	% silt	% gravel	d10	d40	C_u	C_c
Average	5.4	78	16	0.18	0.04	0.10	7.5	2.9
Minimum	4.4	72	14	0.01	0.005	0.08	1.9	1.1
Maximum	8.3	82	19	0.68	0.07	0.12	24	8.7

An example of a particle size distribution of bank soil at site 12 on the Cimarron River is shown in Figure 33. There were a total of four samples from the Cimarron River included in this analysis.

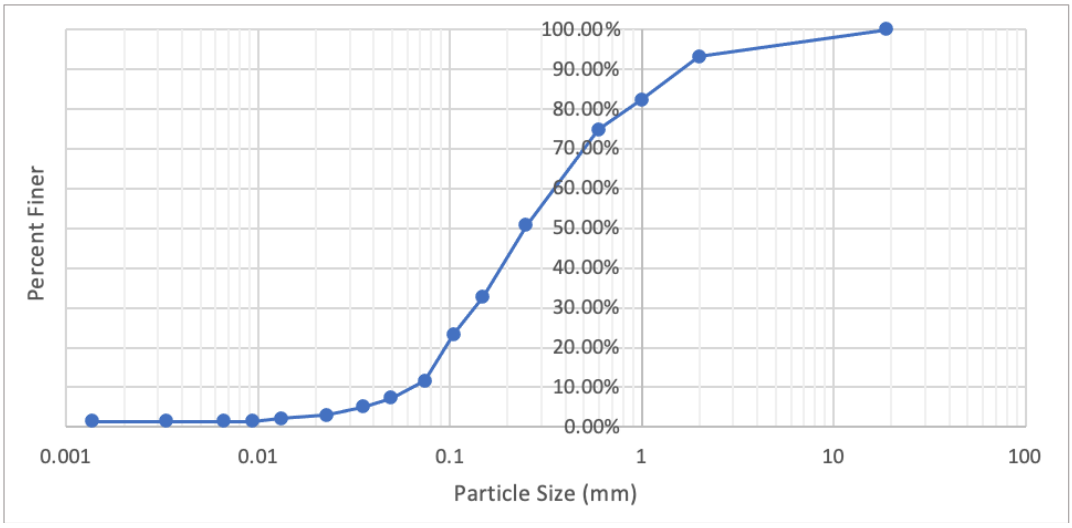

Figure 33: Site 12, Cimarron River and S.H. 33 north of Coyle in Logan county left bank particle size distribution.

The more gradual particle size distribution curve is characteristic of the bank samples collected at the Cimarron sites that were studied in this project. This corresponds to the higher uniformity coefficient (C_u) in Table 11, which means these sites had a higher variability in particle sizes with the sample than others. This is also represented by the coefficient of curvature (C_c), as none of the samples were in the range of well-graded soils.

Table 11: Cimarron River bank sample particle size analysis summary (n=4 (C_u = uniformity coefficient; C_c = coefficient of curvature).

	% clay	% sand	% silt	% gravel	d10	d40	C_u	C_c
Average	5.7	74	10	10	0.08	0.20	129	5.8
Minimum	0.0	47	0.0	1.3	0.001	0.0	2.0	0.74
Maximum	12	99	21	19	0.27	0.43	461	15

In addition to particle size variability within the samples, there was variability between the samples. The soils varied site-to-site along the Cimarron River. The textures included sandy loam, loamy sand, and sand, which were the same textures found along the Washita River. An example of a particle size distribution on the Red River is shown in Figure 34.

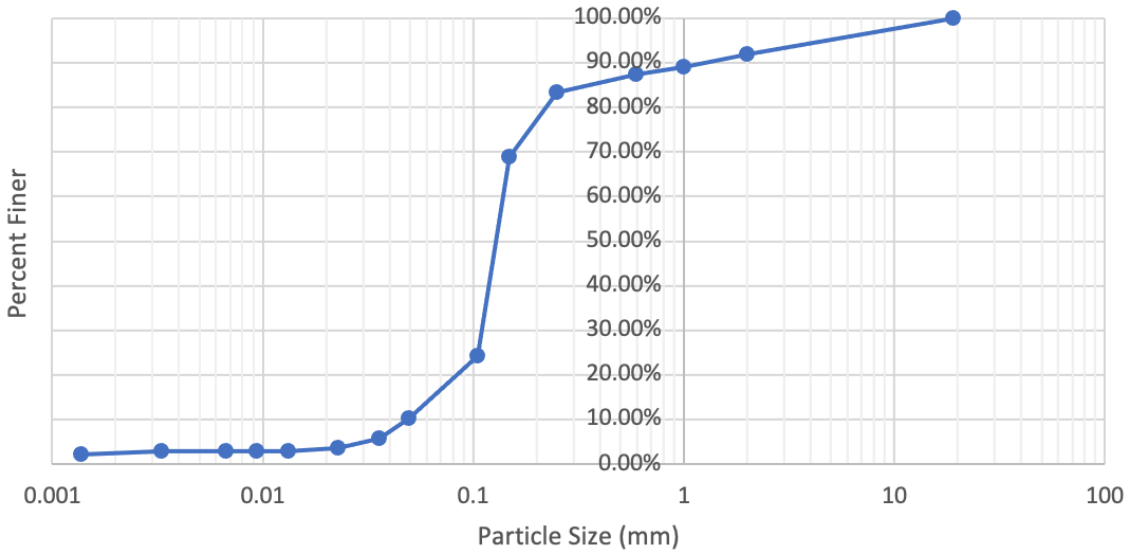

Figure 34: Site 24, Red River and U.S. 259 south of Harris in McCurtain county left bank particle size distribution.

A summary of the particle size analysis of bank samples taken in the Red River basin is shown in Table 12. This analysis included two sites on the Red River and one on the Salt Fork of the Red River. All bank soil samples collected at sites in the Red River basin classified as poorly graded sand or loamy sand. None of the samples had both the uniformity coefficient and the coefficient of curvature in the ranges of well-graded soils.

Table 12: Red River bank soil sample particle size analysis summary (n=3) (C_u = uniformity coefficient; C_c = coefficient of curvature).

	% clay	% sand	% silt	% gravel	d10	d40	C_u	C_c
Average	3.5	90	4.7	5.2	0.08	0.21	18	41
Minimum	0.24	79	0.44	0.33	0.01	0.12	2.3	0.91
Maximum	7.9	99	7.7	8.0	0.17	0.30	50	9.6

3.3 Cross Sections and Bank Erosion Hazard Index

Cross sections were taken at the structures, a local riffle, and at the bridge at each site. Cross sections show the height and angle of the bank, which are both factors that contribute to the BEHI analysis. They also provide information about the shape of the stream and banks upstream of the structures compared to at the structures and at the bridge. High and steep banks are at a higher risk of erosion, which represents the instability of the stream channel. The locations of the cross sections were carefully chosen to represent the variability in the bank along the stream reach. Site 6, on the North Canadian River, had Kellner jetties installed along the right (south) bank in 1927. The cross sections help show how the Kellner jetties have impacted the slope of the banks. The locations of the cross sections taken at site 6 are shown in white in Figure 35.

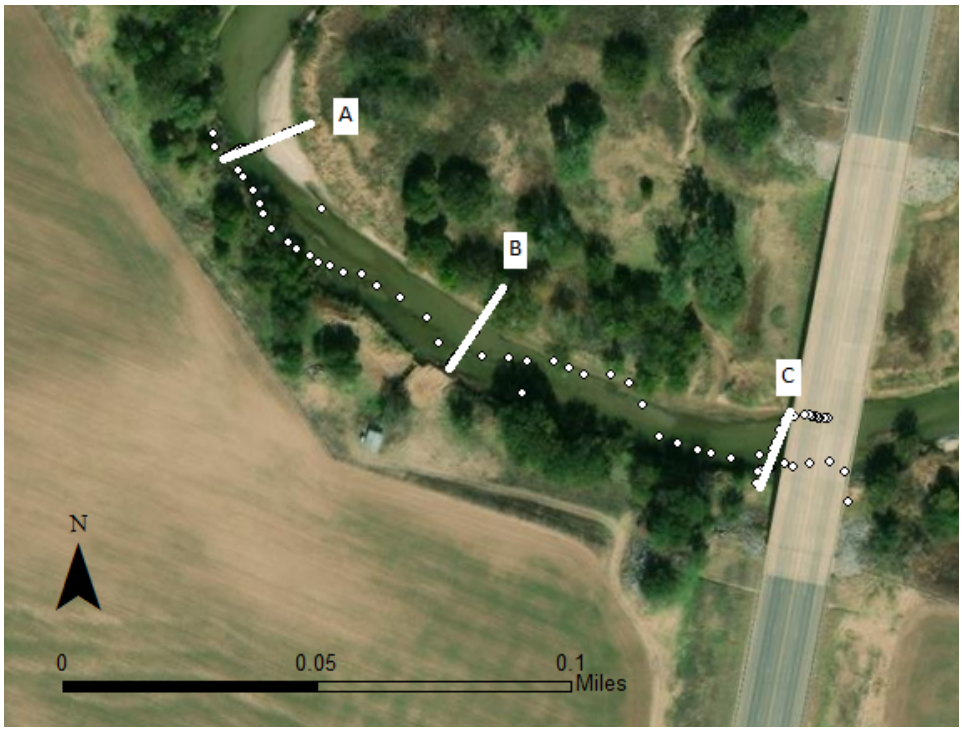

Figure 35: Site 6, North Canadian River and U.S. 281 near Watonga, cross section locations.

At site 6, cross sections were taken upstream of the Kellner jetties, at the Kellner jetties, and downstream of the bridge. The resulting cross sections are Figure 36, Figure 37, and Figure 38 for cross sections 6A, 6B, and 6C, respectively.

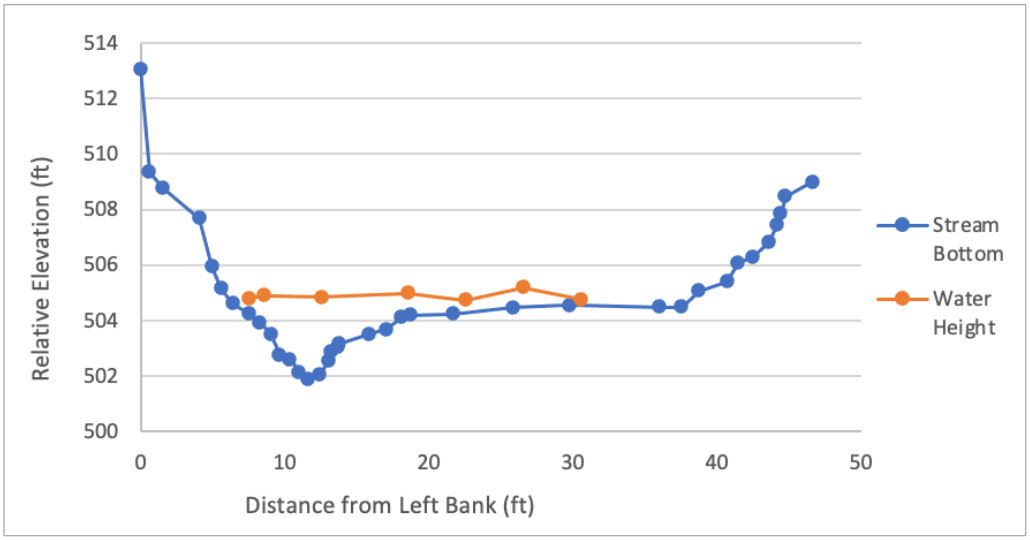

Figure 36: Site 6, North Canadian River and U.S. 281 near Watonga, cross section A upstream of structures facing downstream.

The slope of the right bank at cross section A was 0.47, and it was approximately 5 feet high.

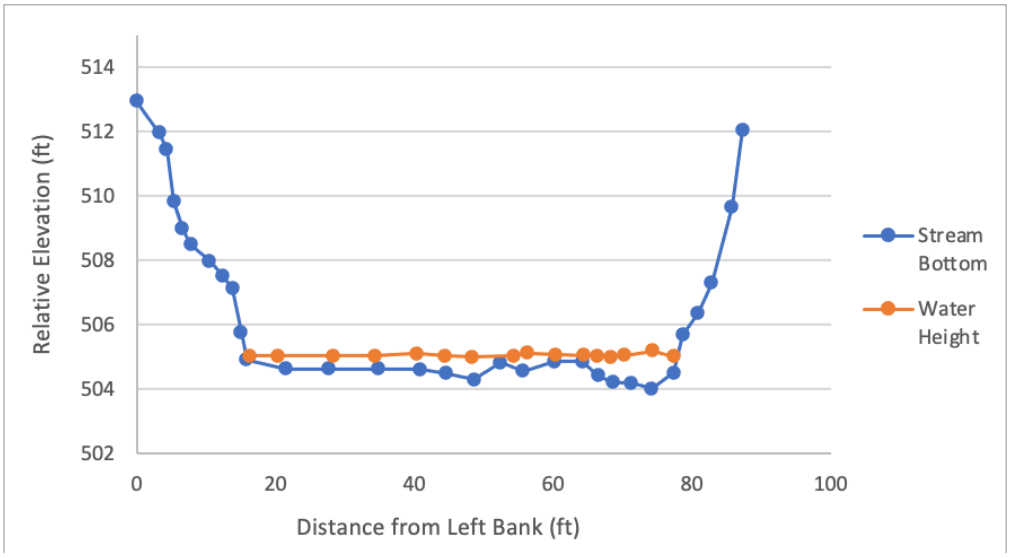

Figure 37: Site 6, North Canadian River and U.S. 281 near Watonga, cross section B at structures facing downstream.

The slope of the right bank at cross section B was 0.70, and it was 7 feet high, slightly steeper and higher than upstream of the structures.

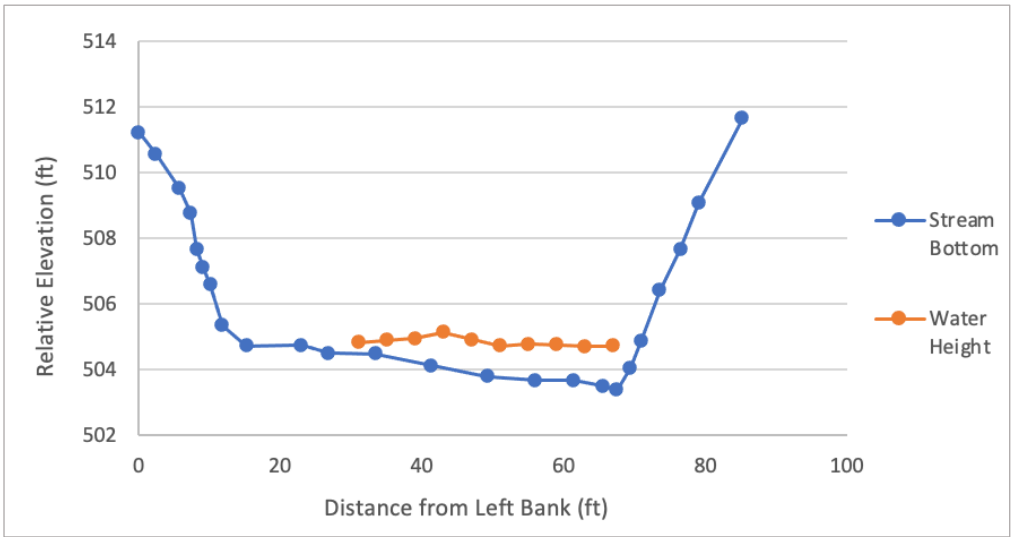

Figure 38: Site 6, North Canadian River and U.S. 281 near Watonga, cross section C downstream of bridge facing downstream.

The slope of the right bank at cross section C was 0.47, and it was 7 feet high.

In addition to bank angle and bank height, the BEHI analysis also includes root depth, root density, and surface protection. Figure 39 shows a section of the bank of concern near cross section B and its condition for site 6 on the North Canadian River near Watonga, Oklahoma. The bank is about 60% vegetated with mostly grasses. Overall, this bank had a BEHI rating of 18, which puts it in the category of “moderate”.

Figure 39: Site 6, North Canadian River and U.S. 281 near Watonga right bank with Kellner jetties.

The lowest BEHI rating was in the category of "very low" with a rating of 5.5 at site 11, Washita River and S.H. 74 north of Maysville in Garvin county, near an installation of bendway weirs.

The cross section at the bendway weirs is shown in Figure 40.

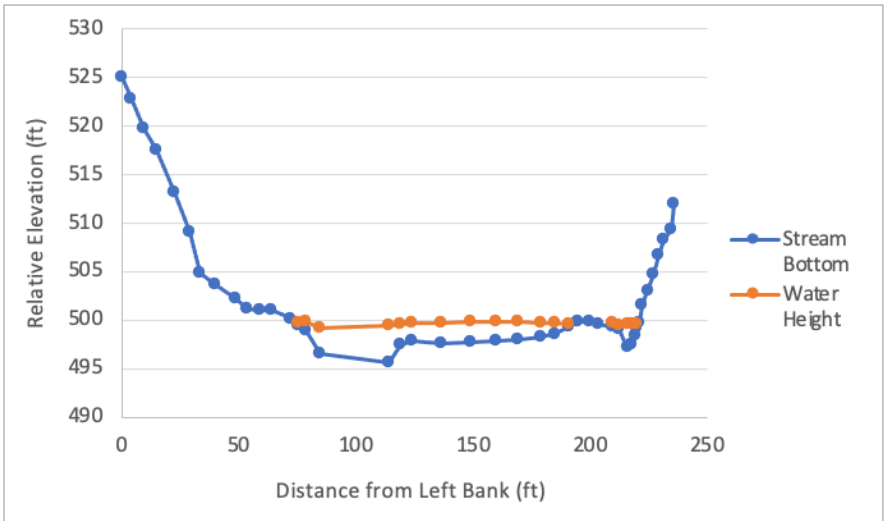

Figure 40: Site 11, Washita River and S.H. 74 north of Maysville in Garvin county, cross section at bendway weirs facing downstream.

The slope of the bank of concern (left bank) was 0.58, with a height of nearly 25 feet. These measurements correspond to a low BEHI rating, but the bendway weirs provided surface

protection, resulting in a rating of very low. The entire bank was covered in stones because of their installation, as shown in Figure 41. This surface protection classified the bank material as cobbles, which greatly decreases the risk of erosion on this bank.

Figure 41: Site 11, Washita River and S.H. 74 north of Maysville in Garvin county, upstream left bank.

The highest BEHI rating on the sites studied was a rating of 32, in the category of "very high" at Site 32, Washita River and S.H. 7 west of Davis in Murray county. Site 32 has Kellner jetties installed along the left bank on a meander. These jetties have worked to slow the velocity down along the left bank and start building up a new bank. However, since they are a relatively new installment of Kellner jetties (2004), they need more time to fully build a new bank and encourage vegetation growth. The cross section at the Kellner jetties at site 32 is shown in Figure 42. The angle of the left bank was 2.1, with a height of about 14 feet. These measurements put the bank in the BEHI category of "high".

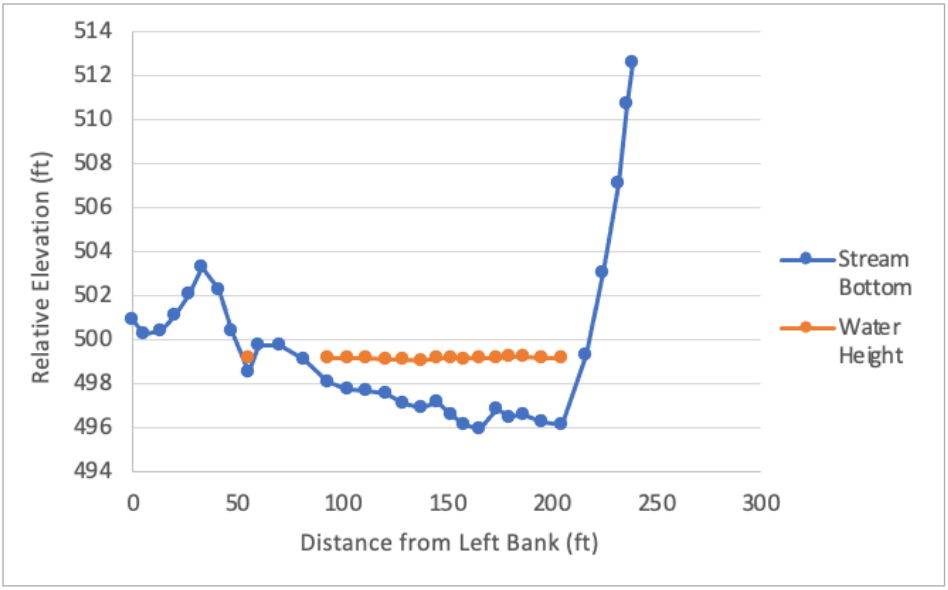

Figure 42: Site 32, Washita River and S.H. 7 west of Davis in Murray county, cross section at Kellner jetties facing downstream.

A photo showing the condition of the Kellner jetties and surrounding bank of concern is shown in Figure 43. The vegetation that has filled in around the Kellner jetties is mostly short grasses. These Kellner jetties were deemed a success despite the high BEHI rating because they are building up a bank on the outside of the meander.

Figure 43: Site 32, Washita River and S.H. 7 west of Davis in Murray county, left bank with Kellner jetties.

BEHI analyses were completed on each site based on measurements from the cross sections and observations on-site. The full BEHI scores for each bank of concern at each site are in Appendix H. Table 13 summarizes all of the BEHI results.

Table 13: Summary of bank erosion hazard index (BEHI) results at all banks of concern at all sites (n=41).

	Average	**Minimum**	**Maximum**
Rating	20.5	5.5	32
Category	Moderate-High	Very Low	Very High

The average rating was 20.5, which is directly between the "moderate" and "high" categories. The BEHI ratings should be expected to lean towards the higher end on average because the bank material of sand added 10 to most sites' ratings. Sand is highly erodible and makes these sites more at risk for streambank erosion, which is reflected in these BEHI ratings.

3.4 Velocity Profiles and Near-Bank Stress

Velocity profiles are a two-dimensional representation of water velocity at a cross section. Higher velocities correspond to higher energy in the stream. High velocity located near a vulnerable bank can cause erosion. Velocity profiles from site 29 on the Washita River at S.H. 19 South of Lindsay in Garvin county are included below. This site had Kellner jetties installed along the right bank in 1999 to keep it from moving closer to S.H. 19. The locations of the velocity profiles taken at site 29 are shown in Figure 44. The upstream velocity profile shows the stream at a riffle in that reach, upstream of the Kellner jetties at the site. The upstream velocity profile is shown, looking downstream, in Figure 45.

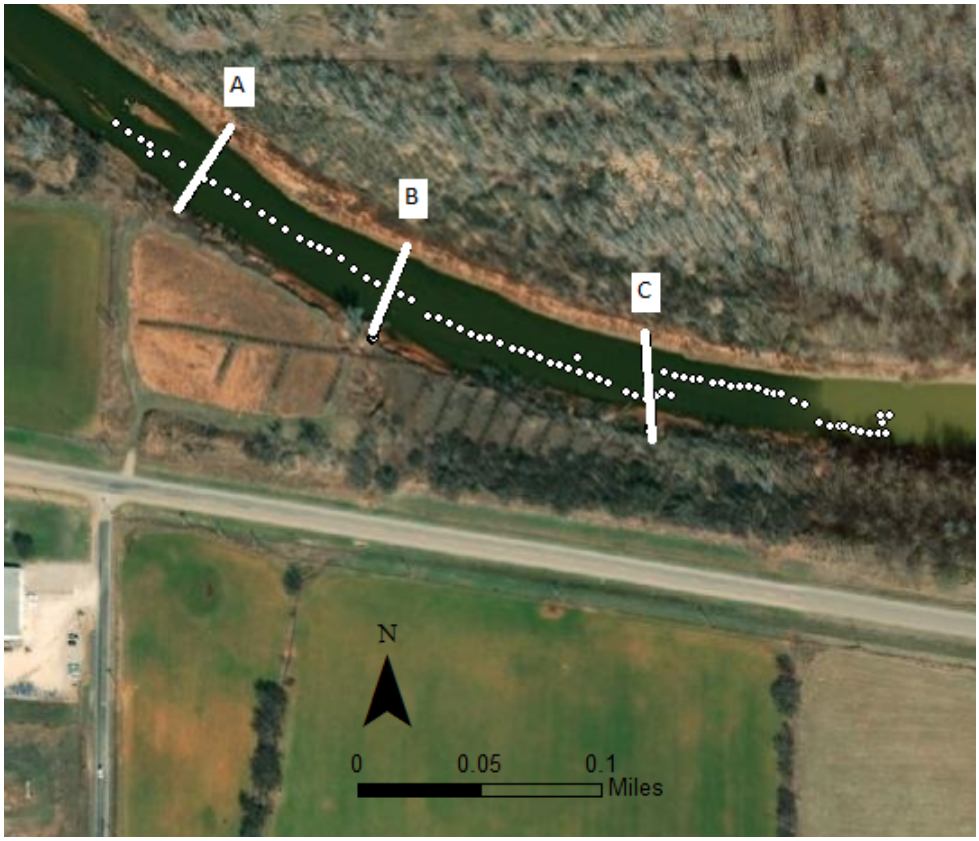

Figure 44: Locations of velocity profiles at site 29, Washita River at S.H. 19 South of Lindsay in Garvin county.

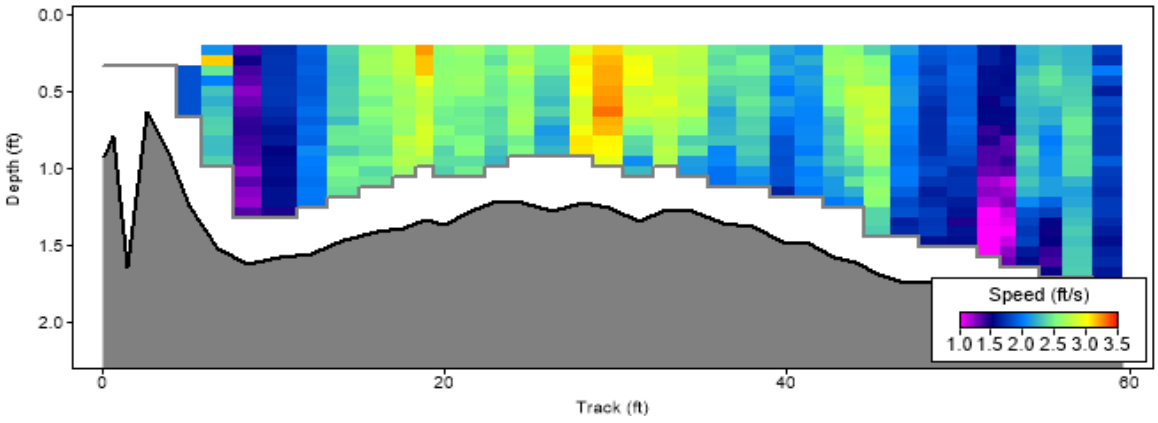

Figure 45: Site 29, Washita River at S.H. 19 South of Lindsay in Garvin county, velocity profile at cross section A, facing downstream. The near-bank stress rating at this cross section along the bank of concern (right bank) is low. The velocity profile ended 3 feet from either bank.

The energy in the stream is mostly in the center of the stream at this location. The near bank stress along the right bank at the upstream cross section is classified as "low," because it is between 1.01 and 1.60 ft/sec/ft. The middle cross section at site 29 shows the distribution of the

energy in the stream with the impact of the Kellner jetties along the right bank. This cross section is shown in Figure 46.

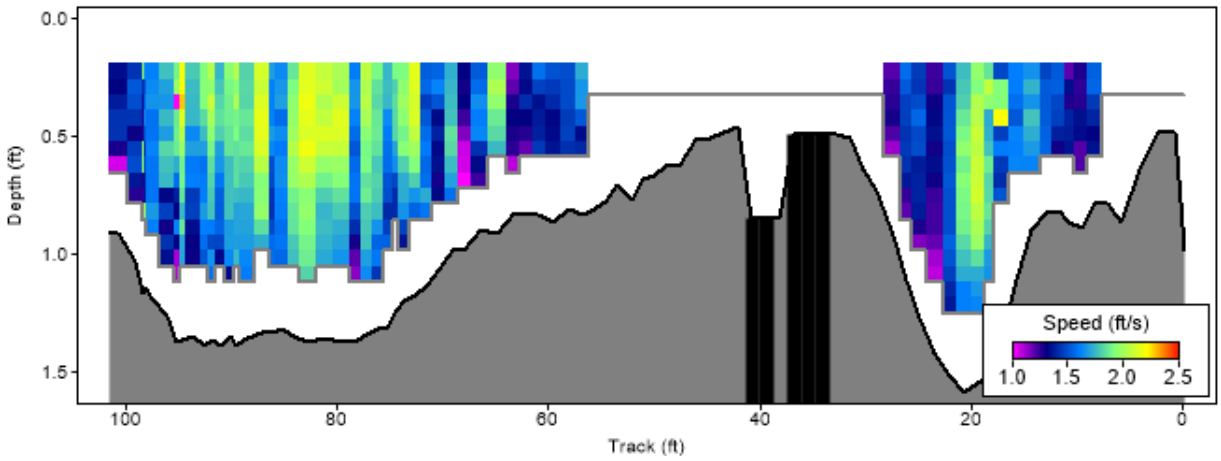

Figure 46: Site 29, Washita River at S.H. 19 South of Lindsay in Garvin county, velocity profile at cross section B, facing downstream. The near-bank stress rating at this cross section along the bank of concern (right bank) is very low. The velocity profile ended 2 feet from the left bank and 5 feet from the right bank.

The stream is split along the two sides of the stream at this location, but the energy is concentrated on the left bank, and the flow along the right bank is slow. The Kellner jetties seem to have slowed the flow of the stream along the right bank, which has allowed for sediment to settle out and extend the bank. The near bank stress along the right bank at the middle cross sections is categorized as "very low," as it is less than 0.5 ft/s/ft. Another velocity profile was taken downstream of the Kellner jetties, shown in Figure 47.

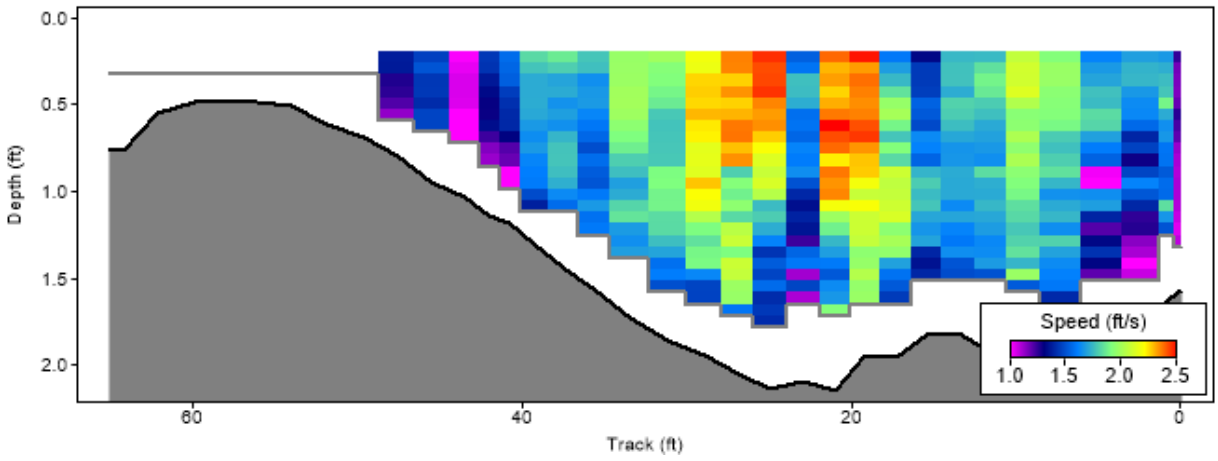

Figure 47: Site 29, Washita River at S.H. 19 South of Lindsay in Garvin county, velocity profile at cross section C, facing downstream. The near-bank stress rating at this cross section along the bank of concern (right bank) is very low. The velocity profile ended 10 feet from the left bank and 2 feet from the right bank.

The energy is focused in the center of the stream at this cross section, with slow flow along the right bank, meaning this bank is at low risk of erosion. This is confirmed by the Near Bank Stress, which is less than 0.5 ft/sec/ft, putting it in the category of "very low".

The velocity profiles can also show how the stream velocity has changed with the addition of bendway weirs. Site 12, Cimarron River and S.H. 33 north of Coyle in Logan county, is an example of a site where bendway weirs pushed the thalweg and energy of the stream away from the bank of concern and towards the center of the stream. Two bendway weirs were installed on the left bank at this site in 2003. They are a newer construction, so the site has not fully stabilized yet. This is an interesting point in time to see how the bendway weirs are impacting the stream while it is still changing in response to the installation. Velocity profiles were taken upstream of the bendway weirs as well as between the bendway weirs. If the bendway weirs are successful, the flow should stagnate between the weirs, and sediment should settle out to build up a bank. The locations of the velocity profiles taken at site 12 are shown in Figure 48.

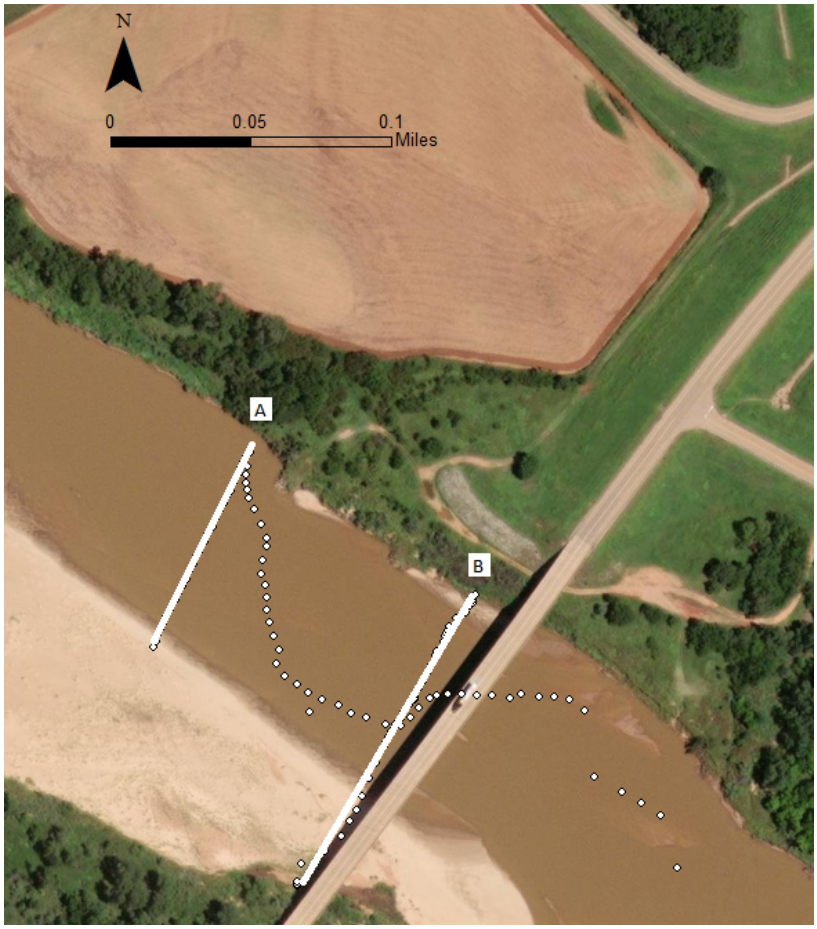

Figure 48: Site 12, Cimarron River and S.H. 33 north of Coyle in Logan county, velocity profile locations.

Velocity profile A, taken upstream of the bendway weirs at site 12 is Figure 49. The thalweg is on the left side of the stream, along the bank of concern. The near bank stress is categorized as "low" along the left bank at this location.

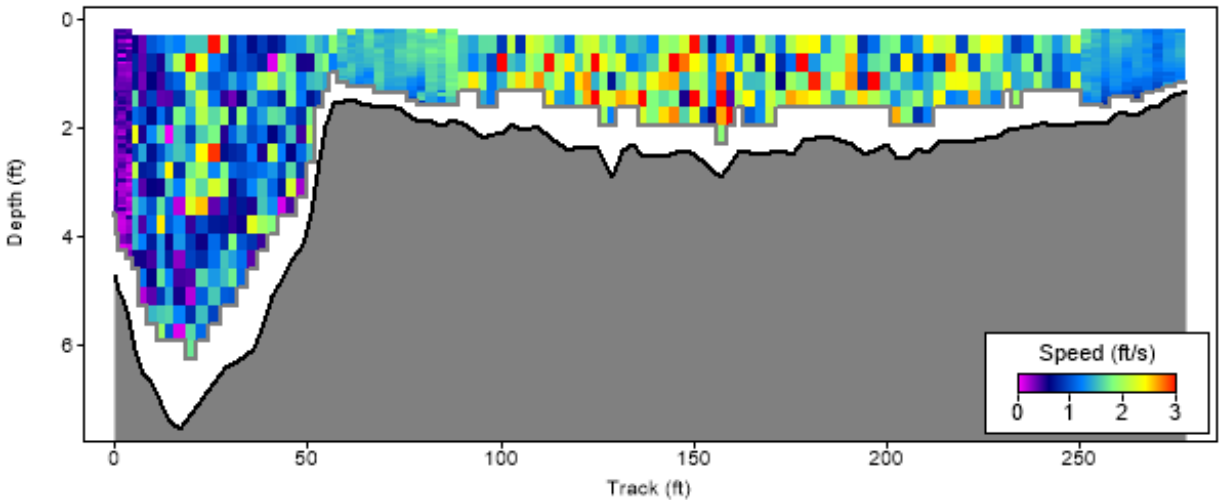

Figure 49: Site 12, Cimarron River and S.H. 33 north of Coyle in Logan county, velocity profile A upstream of bendway weirs, facing downstream. The near-bank stress rating at this cross section along the bank of concern (left bank) is low. The velocity profile ended 2 feet from either bank.

The bendway weirs have pushed the energy of the stream closer towards the center, as seen in velocity profile B taken between the weirs in Figure 50.

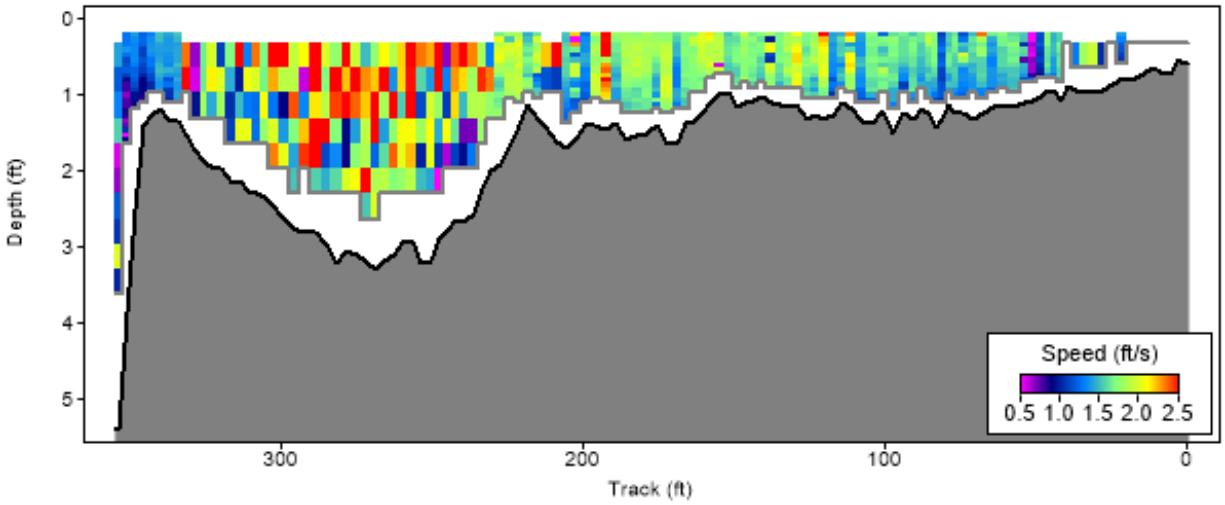

Figure 50: Site 12, Cimarron River and S.H. 33 north of Coyle in Logan county, velocity profile B between bendway weirs, facing downstream. The near-bank stress rating at this cross section along the bank of concern (left bank) is very low. The velocity profile ended 2 feet from either bank.

The energy of the stream is around 100 feet from the left bank. While the depth drops off in a scour pool near the weirs on the left bank, the flow is nearly stagnant, so erosion is not a concern.

This is confirmed by the near bank stress rating of "very low" along the left bank at this location. The creation of a scour pool near the bendway weirs is to be expected (Khosronejad et al. 2017). The bendway weirs were highly successful in this case, pushing the high velocity part of the stream towards the center by about 100 feet.

Table 14: Summary of near-bank stress (NBS) results at all banks of concern at all sites with velocity profiles (n=34).

	Average	**Minimum**	**Maximum**
Rating	0.37	0.05	1.9
Category	Very Low	Very Low	High

The average near-bank stress was in the lowest category: "very low", but the maximum was in the category "high". There were no sites with near-bank stress in the "very high" or "extreme" categories, which could have a few explanations. Firstly, most of the measurements were taken at low flow because that was when the river was accessible by wading or floating. The low flow measurements would have lower velocities, which would lower the near-bank stress. The ideal time for taking velocity profiles for a near-bank stress assessment is at bankfull, which is not when these velocity profiles were collected (Rosgen 2014). Additionally, the measurements were almost all taken near in-stream structures, and the purpose of many of these structures is to slow water down along the bank, which inherently reduces near-bank stress. This does not invalidate the data, but it may explain why the data is skewed towards the low categories.

Velocity profiles are crucial to understanding the risk of bank erosion at a particular site. In this study, they directly show the impact of the in-stream structure on the stream hydraulics and the bank of concern.

3.5 Historic Photos and Thalweg Movement

Historic photos were used, qualitatively and quantitatively, to evaluate how the river has moved over time and measure the thalweg movement distance. Bridge plans and stream surveys

were also used to the location of the thalweg at the bridge crossing since it cannot be determined from aerial images (Lewis 2020). Positive thalweg movement represents movement away from bank of concern while a negative thalweg movement represents movement towards the bank of concern. The absolute value of the thalweg movement was also taken to find the smallest movement of the thalweg. Appendix H contains all historic image overlays. The lateral thalweg movement is summarized by river in Table 15.

Table 15: Thalweg movement summary, separated by major river.

River	Washita (n=12)	Canadian (n=2)	North Canadian (n=10)	Cimarron (n=7)	Red (n=3)
Average	10	330	102	-236	1060
Minimum	-1125	40	-30	-1210	-150
Maximum	1125	710	260	250	2950
Minimum Absolute Value	10	40	10	10	150

The river with the most movement was the Red River. This could be due to the size of the river, as the larger the river, the larger its movements will be. It should also be noted that there were only two sites on the Red River, so it is a small sample size. The Cimarron and Washita rivers also had sites with thalweg movements above 1000 feet.

The thalweg movement data was normalized by the width of the river at each site. This data is summarized in Table 16. After normalization, the Washita River had the most movement, at site 1, near Wynnewood, OK, but the Red River maintained the highest average thalweg movement.

Table 16: Thalweg movement data normalized by river width at each site, separated by major river.

River	Washita (n=12)	Canadian (n=2)	North Canadian (n=10)	Cimarron (n=7)	Red (n=3)

Average	0.28	1.5	0.6	-0.6	2.5
Minimum	-5.6	0.2	-0.7	-2.8	-3.0
Maximum	5.6	2.8	1.7	0.4	3.0
Minimum Absolute Value	0.05	0.2	0.05	0.03	0.4

The amount of movement varied between rivers, as well as within a river. Site 1 had the most thalweg movement of any site on the Washita River. The bridge at this site used to be located on a meander, but over time it straightened. Kellner jetties were installed on the right (west) bank in 1949, and pile diversions and spur dikes were installed on both banks in 1959. The difference in the stream between 1956 and 2019 is shown in Figure 51.

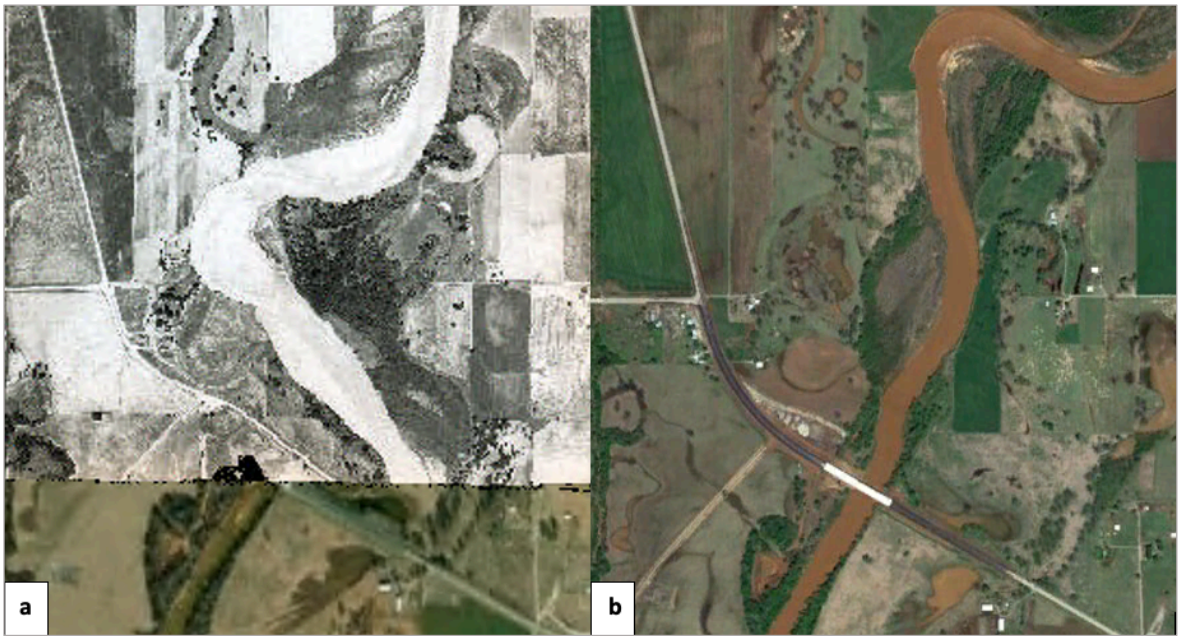

Figure 51: Site 1, Washita River and U.S. 77 north of Wynnewood in Garvin county, in 1956 and 2019.

Site 27, on the North Canadian River, also had a large thalweg movement over time. The bridge crossing was on a meander that was continuously eroding, so Kellner jetties were installed on the right (south) bank. The river continued eroding through these Kellner jetties, though, so bendway weirs were installed in the meander in 2001. These rapidly straightened out the river,

making it nearly perpendicular to the bridge crossing. The change in this river between 1995 and 2019 is shown in Figure 52.

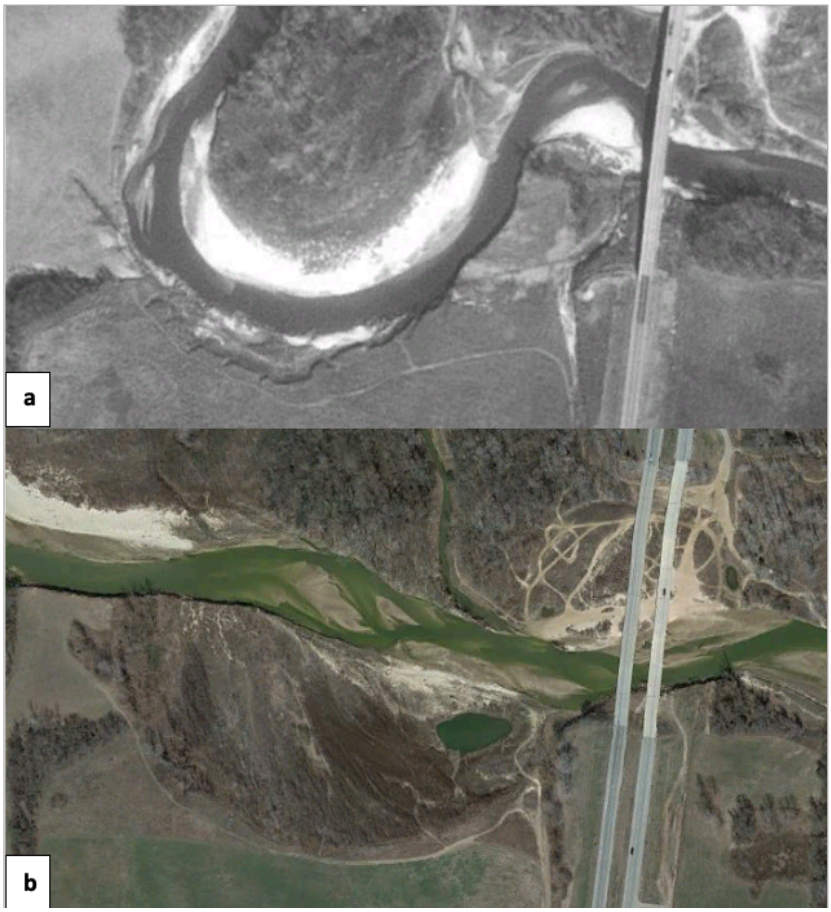

Figure 52: Site 27, North Canadian River and S.H. 99 south of Prague in Seminole county in a) 1995 and b) 2019.

A site with very little thalweg movement is site 25, on the North Canadian River. The stream meander moved east, towards S.H. 48, after 1961, so Kellner jetties were installed along this left (east) bank in 1989. Since installation, the stream seems to have remained stable, with very little movement seen between 1995 and 2019. Photos showing the location of this meander in 1961, 1995, and 2019 is shown in Figure 53.

Figure 53: Site 25, North Canadian River and S.H. 48 north of Bearden in Okfuskee county in a) 1961, b) 1995, and c) 2019.

3.6 Precipitation Data

Streambank erosion is caused by high flows and runoff from large precipitation events in a stream's watershed. A large precipitation event is defined at an event totaling greater than 0.5in of precipitation within 24 hours, as defined by the U.S. Department of Agriculture (Wischmeier and Smith 1978; Renard 1997). Precipitation data was taken into consideration when looking at the effectiveness of the structures on each site. Historical precipitation data covered five years after the installation of the structures, both near the site and across the watershed. The results of the precipitation data near the sites are summarized in Table 17, including large precipitation events (LPE) and maximum return periods of storm events at the site.

Table 17: Summary of historical precipitation data at the sites. Data includes the number of large precipitation events (LPE), defined as precipitation events with greater than 0.5in of rain in 24 hr. (Wischmeier and Smith 1978; Renard 1997), and maximum return periods (T) within 1, 3, and 5 years of installation of the structures.

	# LPE in 1 year	# LPE in 3 years	# LPE in 5 years	Maximum T in 1 year	Maximum T in 3 years	Maximum T in 5 years
Average	20	62	102	39	41	49
Minimum	7	25	43	0.04	0.12	0.61
Maximum	34	91	147	935	935	935

The largest precipitation event that occurred was a 935-year storm in May of 1950, at site 1 in the Washita River near Wynnewood, OK. This event was documented in both old reports on this site (Keeley 1971; Harp and Thomas 1989). Some sites saw very few precipitation events in the five years after installation, with the lowest return periods at site 2 in the Cimarron River near Perkins, OK.

LPEs in the watershed can contribute to erosion in addition to LPEs near the site, so precipitation data was taken from three weather stations throughout the watershed of each site. The maximum return period within 1, 3, and 5 years of installation of the structure was found at each of the three weather stations in each watershed. Then, the geometric mean, average, and maximum of the three maximum return periods for each site were collected. This data is what was used in the analysis for this study. The results of precipitation data throughout the sites' watersheds are summarized in Table 18.

The number of LPEs were averaged across the three weather stations throughout the watershed of each site, and they were similar to the values in Table 17. The total maximum return periods had magnitudes of difference between sites. The 935-year storm at site 1 in May, 1950, was again the largest storm in any of the watersheds represented. The minimum return

periods were again, at site 2, near Perkins, OK. This site had the lowest return periods in every category represented in Table 18.

Table 18: Summary of precipitation data in sites' watersheds. Data includes the number of large precipitation events (LPE), defined as precipitation events with greater than 0.5in of rain in 24 hr. (Wischmeier and Smith 1978; Renard 1997), and maximum return periods (T) within 1, 3, and 5 years of installation of the structures. The arithmetic mean of the number of LPEs at each weather station in each site's watershed is included. The geometric mean, arithmetic mean, and maximum of the maximum return periods at each weather station in each site's watershed are included.

	# LPE in 1 year	**# LPE in 3 years**	**# LPE in 5 years**	**Arithmetic Mean Maximum T in 1 year**	**Arithmetic Mean Maximum T in 3 years**	**Arithmetic Mean Maximum T in 5 years**
Average	56	167	272	15	19	22
Minimum	26	84	157	0.09	1.0	1.3
Maximum	92	256	447	313	313	313
	Geo. Mean Maximum T in 1 year	**Geo. Mean Maximum T in 3 years**	**Geo. Mean Maximum T in 5 years**	**Total Maximum T in 1 year**	**Total Maximum T in 3 years**	**Total Maximum T in 5 years**
Average	1.8	4.1	6.9	43	51	56
Minimum	0.05	0.4	1.2	0.15	1.9	2.0
Maximum	10	18	26	935	935	935

The precipitation data provides information on what the structures endured shortly after they were installed. Large precipitation events have historically caused damage to some structures in this study (Keeley 1971; Harp and Thomas 1989), but it is also possible that precipitation events can assist the structures by washing sediment into the stream that can fill in permeable structures, such as Kellner jetties.

3.7 Linear Regressions

Linear regressions were run prior to logistic regressions. The first regressions were run on all of the structure types together. To narrow the variables down a correlation matrix was completed first. Variables and their R-square values in relation to the binary success or failure variable are listed in Table 19.

Table 19: All structures and variables R-square values from correlation with binary success or failure variable (C_u = uniformity coefficient; C_c = coefficient of curvature, LPE = large precipitation event, T = return period; BEHI = bank erosion hazard index, NBS = near-bank stress).

Variable	**R^2**	**Variable**	**R^2**
Other Structure on bank when installed	-0.17	# LPE in 1yr in Watershed	0.03
Percent Clay	0.11	# LPE in 3yr in Watershed	-0.14
Percent Sand	-0.17	# LPE in 5yr in Watershed	-0.12
Percent Silt	0.32	Arithmetic Mean T in 1yr in Watershed	-0.07
d10	-0.15	Arithmetic Mean T in 3yr in Watershed	-0.08
d40	-0.14	Arithmetic Mean T in 5yr in Watershed	-0.08
Cu	0.10	Geo. Mean Maximum T in 1yr in Watershed	0.15
Cc	-0.12	Geo. Mean Maximum T in 3yr in Watershed	0.02
Percent Gravel	-0.07	Geo. Mean Maximum T in 5yr in Watershed	0.00
Arithmetic Mean Depth to Bedrock	0.00	Total Maximum T in 1yr in Watershed	-0.07
Coefficient of Variation of Depth to Bedrock	0.14	Total Maximum T in 3yr in Watershed	-0.09
Minimum Depth to Bedrock	-0.08	Total Maximum T in 5yr in Watershed	-0.09
Angle of installation	0.10	Sinuosity	-0.15
Angle in 1971	0.53	Percent Watershed Developed	0.24
Angle in 1989	-0.28	Average Streamflow	-0.15
Current KJ angle	0.66	BEHI	-0.07
Oldest KJ Angle	0.10	NBS	-0.12
Most Recent KJ Angle	-0.03	Root Density	-0.05
# LPE in 1yr at Site	0.07	Drainage Area	-0.21
# LPE in 3yr at Site	-0.15	Stream Slope	0.12
# LPE in 5yr at Site	-0.13	Thalweg Movement	-0.28
Maximum T in 1yr at Site	-0.07	Location of Structures (1=meander, 0=straight)	-0.11
Maximum T in 3yr at Site	-0.07		
Maximum T in 5yr at Site	-0.06		

The variables with the highest R-square values for each concept, based on the correlation matrix were used. The p values for the multiple variable linear regression with these variables are listed in Table 20. Since there were no p values below 0.1, the linear regressions were not continued on this specific dataset.

Table 20: All structures multiple variable linear regression results.

Variable	**p value**
Intercept	0.63
% silt	0.33
d10	0.54
d40	0.50
Cc ((D30)^2/(d60*d10)	0.13
Depth to BR (min) (ft)	0.48
Geo mean max return period in 1 yr	0.58
Sinuosity	0.11
% Watershed developed	0.30
Average Streamflow	0.63
BEHI rating	0.57
Root Density (%)	0.27
Drainage area	0.55
Stream Slope	0.58
Distance thalweg has moved in relation to bank of concern at installation	0.31

Linear regressions were also run on Kellner jetties and pile diversions individually. The variables were chosen based on correlation matrices for these datasets. The p values for the multiple regression run on Kellner jetties are listed in Table 21. There were no p values below 0.1, so these regressions were not continued.

Table 21: Kellner jetties multiple variable linear regression p values.

Variable	p value
Intercept	0.31
Percent Silt	0.72
Minimum Depth to Bedrock	0.16
Oldest KJ Angle	0.17
Geometric Mean Maximum T in 5yr in Watershed	0.28
Thalweg Movement	0.18

The p values for the multiple regression run on pile diversions are listed in Table 22. There were no p values below 0.1, so these regressions were not continued.

Table 22: Pile diversions multiple variable linear regression p values.

Variable	p value
Intercept	0.29
Percent Sand	0.51
Minimum Depth to Bedrock	0.25
Arithmetic Mean Maximum T in 3yr at Site	0.26
Percent Watershed Developed	0.23

Logistic regressions were deemed more appropriate for analysis of this data because the dependent variable is binary (success of failure). Statistical analysis in research typically uses logistic regressions for categorical data (Dowdy et al. 2004).

3.8 Bendway Weirs Analysis

The purpose of bendway weirs is to push the energy of the stream away from the bank of concern and towards the middle of the stream (Thornton et al. 2007). They were installed at four sites included in this study, and they were deemed successful at all sites. They were installed at sites 11, 12, 16, and 27 on the Washita, Cimmaron, and North Canadian rivers. They were installed between 2000 and 2004, so they range from 17 to 21 years old. At site 16 and site 27, some of the bendway weirs were not visible from the river because the river had drastically

shifted course away from the original bank of concern. The shift at site 27 was shown in Figure 52. At all of the sites, velocity profiles showed the energy of the stream was pushed towards the center, and all of the visible bendway weirs had developed sand bars between the weirs, which is a sign of success (Thornton et al. 2007).

The velocity profiles and location of the thalweg most directly showed the impact of the bendway weirs on the stream. A typical velocity profile taken near the bendway weirs had a scour pool around the bendway weir, which is to be expected, but the highest velocity was in the center of the stream. This is what is expected of a successful implementation of a bendway weir (Thornton et al 2007). Additionally, at each of the sites, the thalweg could be seen moving away from the bank of concern as it moved from upstream of the bendway weirs downstream. This is another way to visualize the bendway weir pushing the energy of the stream away from the bank of concern.

The average stream flows at sites with bendway weirs ranged from 339 to 1380 cubic feet per second, so these structures were successful over a range of base stream flows. Additionally, the sinuosity at sites with bendway weirs varied between 1.1 and 2.1. The range of sinuosities at all of the sites was 1.0-2.1, so bendway weirs succeeded in nearly the entire range of sinuosities present in this project. The thalweg movement ranged from 80 to 260 feet. These data support the positive change, away from the bank of concern, supporting the conclusion of reach improvement.

The bendway weirs were installed in the Washita, North Canadian, and Canadian Rivers, with a range of sediment types, including sandy loam, loamy sand, and sand. The sediment data for sites with bendway weirs is summarized in Table 23.

Table 23: Summary of sediment data at sites with bendway weirs (n=4) (C_u = uniformity coefficient; C_c = coefficient of curvature).

	% clay	% sand	% silt	% gravel	d10	d40	Cu	Cc
Average	4.0	82	13	1.4	0.02	0.12	4.6	1.6
Minimum	1.4	79	5.8	0.01	0.04	0.09	3.9	0.7
Maximum	4.9	86	16	6.8	0.07	0.19	5.9	2.1

The success of bendway weirs in a variety of sediment types is to be expected because they change the hydraulics of the stream when they are installed (Thornton et al. 2007). Additionally, the sediments of sites where bendway weirs were installed are all classified as poorly graded, meaning they are unstable and susceptible to erosion (Vargas-Luna et al. 2018). The erodibility of the poorly graded sandy sediments may work to the bendway weirs' advantage because they will quickly shift course. With the shift in the thalweg away from the bank of concern, the sandy streams will quickly erode in the center or far bank, shifting in that direction over time.

The bendway weirs withstood erosion from a range of storm events without allowing the rivers to cut behind them, erode the bank of concern, or wash away the protective rip-rap. The precipitation data at sites with bendway weirs is summarized in Table 24.

Table 24: Summary of precipitation data at sites with bendway weirs including number of large precipitation events (LPE), defined as precipitation greater than 0.5in in 24 hours and maximum return period (T) (n=4).

	# LPE in 1 year	# LPE in 3 years	# LPE in 5 years	Maximum T in 1 year	Maximum T in 3 years	Maximum T in 5 years
Average	18	58	98	0.4	6.3	9.4
Minimum	16	54	94	0.1	0.4	5.6
Maximum	20	68	112	0.8	24	24

The largest storm the bendway weirs faced was a 24-year storm. This occurred at site 27, on the North Canadian River near Prague, in 2003. This site also had the largest thalweg shift of the sites with bendway weirs, but the shift occurred between 2014 and 2017, so it was not related

to the 2003 precipitation event. The sites also faced a minimum of 94 erosion-causing storms, as defined by the U.S. Department of Agriculture (Wischmeier and Smith 1978; Renard 1997) without allowing excessive bank erosion along the bank of concern.

Table 25: Summary of precipitation data in watersheds of sites with bendway weirs including number of large precipitation events (LPE), defined as precipitation greater than 0.5in in 24 hours (Wischmeier and Smith 1978; Renard 1997), and the arithmetic mean, geometric mean, and total maximum of the maximum return period (T) in the sites' watersheds (n=4).

	# LPE in 1 year	**# LPE in 3 years**	**# LPE in 5 years**	**Arithmetic Mean Maximum T in 1 year**	**Arithmetic Mean Maximum T in 3 years**	**Arithmetic Mean Maximum T in 5 years**
Average	44	142	247	1.4	6.8	8.0
Minimum	37	128	240	0.7	4.9	6.6
Maximum	59	171	262	2.9	11	11
	Geo. Mean Maximum T in 1 year	**Geo. Mean Maximum T in 3 years**	**Geo. Mean Maximum T in 5 years**	**Total Maximum T in 1 year**	**Total Maximum T in 3 years**	**Total Maximum T in 5 years**
Average	0.7	1.9	3.0	3.6	17	17
Minimum	0.5	1.1	2.6	1.5	14	14
Maximum	1.1	3.5	3.7	7.6	24	24

Among the reaches studied herein, the largest storm documented within five-years post installation of bendway weirs was the 24-year storm at site 27, on the North Canadian River near Prague. In addition to this high-intensity storm, all of the bendway weir sites were subjected to at least 240 erosion-causing storms within their watersheds. From this study, all bendway weirs were able to maintain a stable bank and prevent excessive bank erosion.

The range of circumstances within which bendway weirs were successful is broad. This shows how versatile and effective bendway weirs are. Literature supports that these structures are effective in many different stream types (Abad et al. 2008; Thornton et al. 2007; Scurlock 2014). They are recommended as a streambank protection method to be used in any Oklahoma river in the future.

3.9 Pile Diversions Analysis

The purpose of pile diversions is similar to that of bendway weirs, but they are less structurally sound. They are intended to divert energy away from the bank of concern and eventually allow sediment to settle to extend the bank (Harp and Thomas 1989). Pile diversions were installed at 10 different sites in the Washita, Cimmaron, Canadian, North Canadian, and Arkansas rivers. They were installed between 1950 and 1969, making them 51 to 70 years old. Some sites had multiple sets of pile diversions, which were split up as different structures. This resulted in a total of 14 different data points. Because of their age, the majority of pile diversions could not be found at the sites or were badly deteriorated. Success was determined based on historic images and old reports (Keeley 1971, Harp and Thomas 1989). If the bank had developed where the pile diversions were installed, and the stream had not cut behind the initial installation of pile diversions, they were deemed a success. There were six failures and eight successes, for a success rate of 57%.

The average stream flows at sites with pile diversions ranged from 167 to 1820 cubic feet per second, so these structures were installed in small to medium size streams. Additionally, the sinuosity at sites with pile diversions varied between 1.3 and 1.9. The range of sinuosities at all of the sites was 1.0-2.1, so pile diversions were located in the middle of the range of sinuosities present in this project. The thalweg movement ranged from -1125 to 1125 feet. Both of the extremes in the thalweg movement measurements were at the same site, but there were pile diversions on both banks, so one was positive and one was negative. There were no distinct differences between these variables in pile diversions that succeeded, compared to those that failed.

The pile diversions were installed in a range of sediment types, including sandy loam, loamy sand, and sand. Table 23 is a summary of the sediment data for sites with pile diversions.

Table 26: Summary of sediment data at sites with pile diversions (n=10 (C_u = uniformity coefficient; C_c = coefficient of curvature).

	% clay	% sand	% silt	% gravel	d10	d40	Cu	Cc
Average	5.5	77	12	5.9	0.001	0.05	82	4.9
Minimum	0.0	47	0.0	0.0	0.04	0.09	1.7	0.8
Maximum	12	99	24	27	0.07	0.19	461	15

The sediments of 93% of the sites where pile diversions were installed were classified as poorly graded, based on their C_u and C_c values, meaning they are unstable and susceptible to erosion (Vargas-Luna et al. 2018). The one site with well-graded soil was a site with successful pile diversions. This is not enough data to make any conclusions about the impact of soil grading on pile diversions. Logistic regressions were used show the impact of sediment type on pile diversions.

The pile diversions faced a range of storm events within five years of their installation. The precipitation data at sites with pile diversions is summarized in Table 24.

Table 27: Summary of precipitation data at sites with pile diversions including number of large precipitation events (LPE), defined as precipitation greater than 0.5in in 24 hours and maximum return period (T) (n=14).

	# LPE in 1 year	# LPE in 3 years	# LPE in 5 years	Maximum T in 1 year	Maximum T in 3 years	Maximum T in 5 years
Average	22	63	99	2.0	2.9	13
Minimum	9	30	43	0.04	0.5	0.7
Maximum	34	91	128	20	20	132

The largest storm the pile diversions faced was a 132-year storm. This occurred at site 4, on the Cimarron River near Waynoka, OK, in 1963. This site remained successful, despite this large precipitation event. The sites also faced a minimum of 43 erosion-causing storms, as

defined by the U.S. Department of Agriculture (Wischmeier and Smith 1978; Renard 1997), within five years of installation. There were no distinct differences between the precipitation events at sites with pile diversions that succeeded, compared to those that failed.

Table 28 summarizes the precipitation data in the watersheds of sites with pile diversions within five years of installation.

Table 28: Summary of precipitation data in watersheds of sites with pile diversions including number of large precipitation events (LPE), defined as precipitation greater than 0.5in in 24 hours, and the arithmetic mean, geometric mean, and total maximum of the maximum return period (T) in the sites' watersheds (n=13).

	# LPE in 1 year	**# LPE in 3 years**	**# LPE in 5 years**	**Arithmetic Mean Maximum T in 1 year**	**Arithmetic Mean Maximum T in 3 years**	**Arithmetic Mean Maximum T in 5 years**
Average	59	170	269	1.8	3.3	3.9
Minimum	35	118	196	0.1	1.1	2.0
Maximum	82	218	312	7.1	8.6	10
	Geo. Mean Maximum T in 1 year	**Geo. Mean Maximum T in 3 years**	**Geo. Mean Maximum T in 5 years**	**Total Maximum T in 1 year**	**Total Maximum T in 3 years**	**Total Maximum T in 5 years**
Average	0.9	2.2	3.0	70	73	74
Minimum	0.1	0.7	1.0	0.2	1.9	3.1
Maximum	2.4	5.2	7.6	935	935	935

Among the reaches studied, the largest storm documented within five-years post installation of pile diversions was the 935-year storm at site 1, on the Washita River near Wynnewood. In addition to this high-intensity storm, all of the pile diversion sites were subjected to at least 196 erosion-causing storms within their watersheds. Logistic regressions were used to show the impact of these precipitation events on the pile diversions.

Logistic regressions were run on the pile diversion data to determine any variables that had a significant impact on the structures' failure or success. Because of the limited number of data points, a confidence limit of 90% has been used. When all of the variables were considered in

logistic regressions, three were significant: percent sand, arithmetic mean maximum return period in the watershed within three years of installation, and percent of the watershed developed. Regressions with combinations of these variables were insignificant, but these singular variable regressions were significant. These results are summarized below.

Figure 54 shows the logistic regression model with percent sand and the data points for comparison. Data points with a y-value of 1 were successful pile diversions, while failures are represented by a y-value of 0.

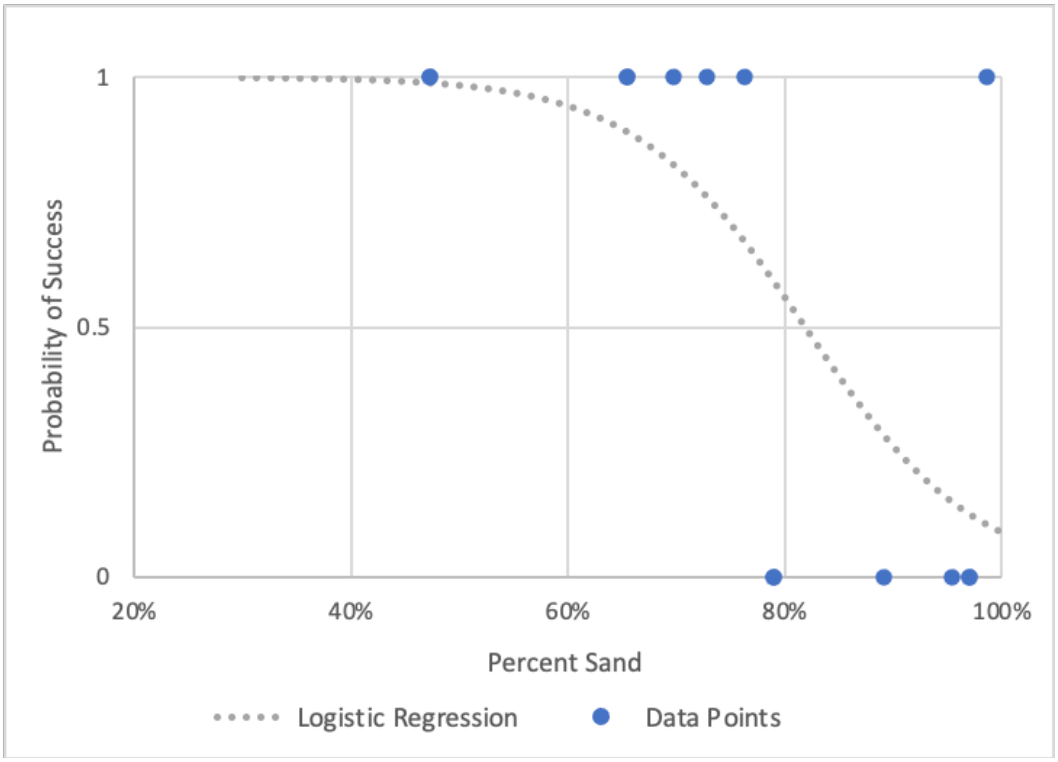

Figure 54: Pile diversion logistic regression with percent sand ($p < 0.1$).

Coefficients and p values from the logistic regression with percent sand are listed in Table 29.

Table 29: Pile diversion logistic regression with percent sand results.

	Coefficient	**p Value**
Intercept	10.5	0.049
Percent Sand (as a fraction)	-12.8	0.049

The percent sand coefficient shows that pile diversions installed on banks with higher sand content are more likely to fail. This makes sense, since sandy streambeds are highly mobile, and pile diversions are an instable structure, compared to other structures studied (Harp and Thomas 1989). There is an exception to this pattern at site 4 on the Cimarron River near Waynoka, but the regression remains significant. More data is needed to confirm this regression.

The next variable that resulted in a significant logistic regression was the arithmetic mean maximum return period in the watershed within three years of installation. These results are shown in Figure 55 with data points for comparison. Data points with a y-value of 1 were successful pile diversions, while failures are represented by a y-value of 0.

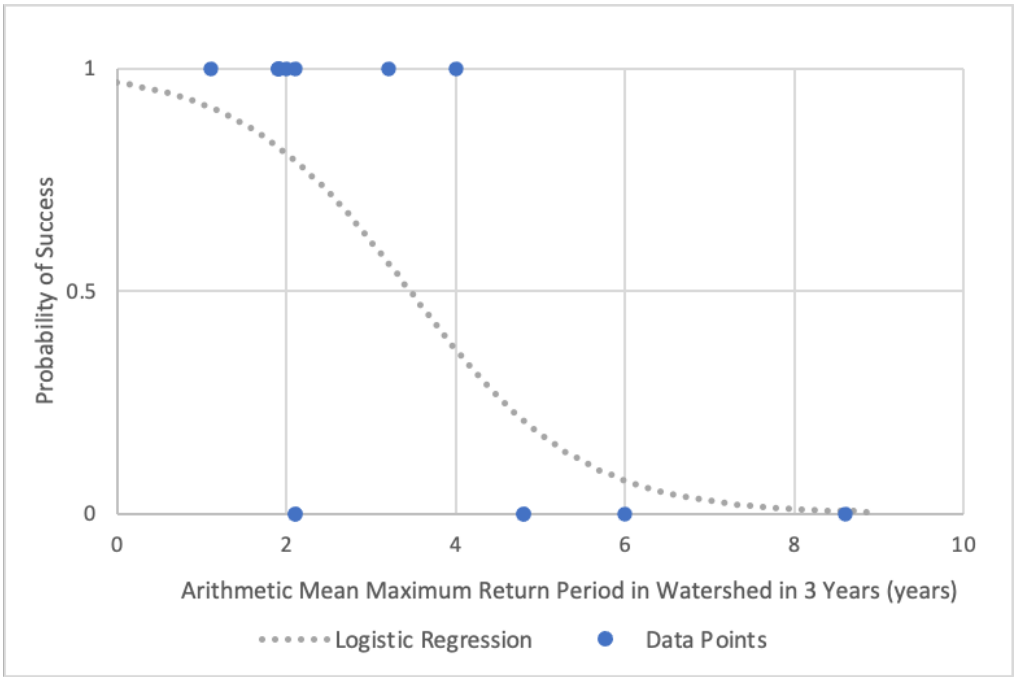

Figure 55: Pile diversion logistic regression with arithmetic mean maximum return period in the watershed within three years of installation ($p < 0.1$).

The coefficients and p values from the logistic regression with the return period variable are shown in Table 30.

Table 30: Pile diversion logistic regression with return period results.

	Coefficient	p Value
Intercept	3.42	0.047
Arithmetic Mean Maximum Return Period in the Watershed within Three Years of Installation (years)	-0.99	0.065

The return period coefficient shows that larger precipitation events within three years of installation makes the pile diversions more likely to fail. Harp and Thomas hypothesized that pile diversions failed because of the weakness of wood (1989). Additionally, unlike rock and steel, wood is weakened by the addition of moisture because of its porous nature, so it would be weakened more quickly in streams than other materials (Rammer and Winistorfer 2007). Large precipitation events could lead to the destruction of the pile diversions, and if this occurred before sediment has settled out and built up bank, the structure would be ineffective.

The third variable that was significant in a logistic regression is the percent of the watershed that is developed. The resulting regression and data points for comparison are shown in Figure 56.

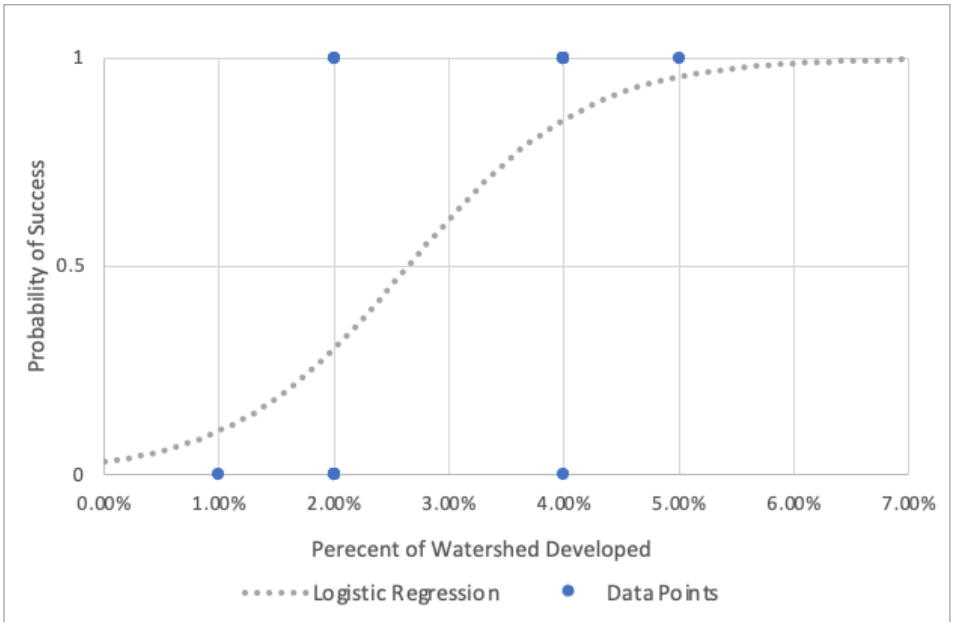

Figure 56: Pile diversion logistic regression with percent watershed developed ($p < 0.1$).

The coefficients and p values from the logistic regression with percent watershed developed are shown in Table 31.

Table 31: Pile diversion logistic regression with percent watershed developed results.

	Coefficient	**p Value**
Intercept	-3.43	0.069
Percent Watershed Developed (as a fraction)	130	0.045

The percent watershed developed coefficient shows that pile diversions in a stream with a more developed watershed is more likely to succeed. A more developed watershed would have more runoff and higher flows during storm events, so a negative coefficient, such as the one seen with the return period variable, would be expected. It should be noted that the percent of the watersheds that were developed, based on the National Land Cover Database (2016) ranged from 1% to only 5%, so there was little variation. To fully understand the impact of development on the success of these structures, a different variable could be used, such as a binary urban or rural variable or a variable that takes into account agricultural land use, which also leads to increased runoff. Additionally, more data from urban watersheds is to confirm this regression because the sites were nearly all located in rural Oklahoma.

The resulting p values of the combinations of these regressions are shown in Table 32. None of these regressions had all p values below 0.1.

Table 32: Pile diversion multiple variable logistic regression p values, including percent sand, percent watershed developed, and arithmetic mean maximum return period (T) in the watershed within three years of installation.

Regression Inputs	Variable	p Value
% Sand + Arithmetic Mean Maximum T in 3 years	Intercept	0.075
	% Sand	0.13
	Avg Max T - 3yr	0.18
% Watershed Developed + Arithmetic Mean Maximum T in 3 years	Intercept	0.46
	% Watershed Developed	0.14
	Avg Max T - 3yr	0.078
Percent Watershed Developed + Percent Sand	Intercept	0.32
	% Watershed Developed	0.28
	% Sand	0.14
Percent Watershed Developed + Percent Sand + Arithmetic Mean Maximum T in 3 years	Intercept	0.78
	% Watershed Developed	0.30
	% Sand	0.55
	Avg Max T - 3yr	0.16

This shows there is interference with these variables that the logistic regression simply cannot account for. The lack of significance in these regressions only shows that these variables must be looked at individually, rather than together, when making decisions on pile diversion installation (Dowdy et al. 2004). Overall, pile diversions are unsuccessful in comparison to other structures providing a similar function, so they are not recommended for future use in Oklahoma.

3.10 Rip Rap Analysis

Rip rap works differently than the other structures, since it is simply a revetment intended to protect the bank material from erosion, rather than diverting energy away from the bank of concern. Rip rap was installed at 12 different sites in the Washita, Cimmaron, Canadian, North Canadian, Red, and Arkansas rivers. One site had rip rap on both banks, which were split up as different structures. This resulted in a total of 13 different data points, with seven failures and six successes. Rip-rap was deemed a failure if it had washed away from the site. It only protects the

bank if it is still present, so if the majority of the rip-rap that was initially installed was not found on the site, it was deemed a failure.

The average stream flows at sites with rip rap ranged from 346 to 7390 cubic feet per second, so these structures were installed in medium to large size streams. Additionally, the sinuosity at sites with rip rap varied between 1.2 and 2.0. The range of sinuosities at all of the sites was 1.0-2.1, so rip rap was located in sites covering nearly the entirety of the range of sinuosities present in this project. The thalweg movement ranged from -1125 to 2950 feet, covering the entirety of the range in thalweg movement seen in this study. There were no distinct differences between these variables in rip rap that succeeded, compared to those that failed.

The sites with rip rap were in many different rivers with different geomorphology. Figure 57 shows the ranges of sediment factors at sites with rip rap, separated by failures and successes.

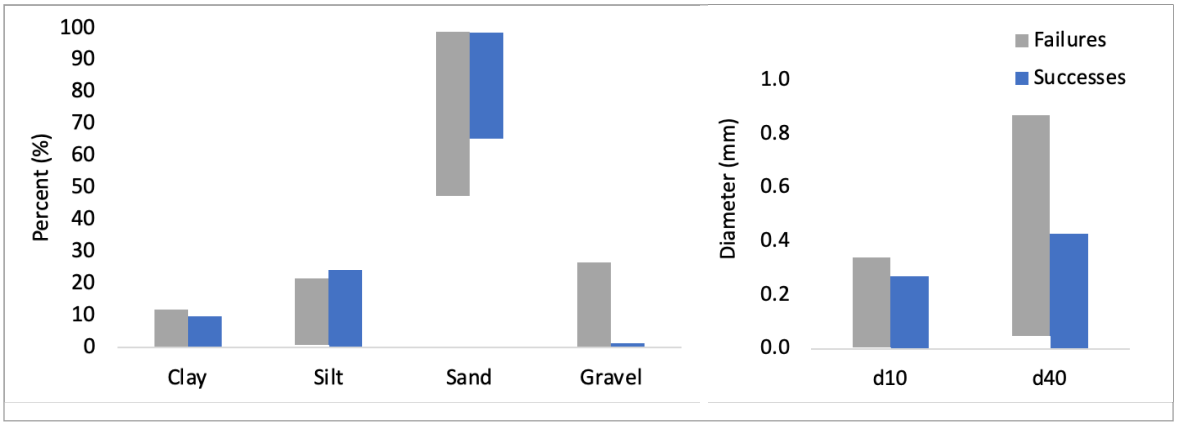

Figure 57: Ranges of sediment factors at sites with rip rap, separated by failures and successes.

Based on this data, the major difference between the bank material at sites where rip rap failed and where rip rap succeeded is the amount of gravel; however, the percent gravel is not a significant variable in a logistic regression. This lack of significance is likely due to the small number of data points (n=13).

The sites with rip rap also faced a range of precipitation events in the five years after their installation. The ranges of precipitation variables at sites with rip rap, split up by failures and successes, are shown in Figure 58.

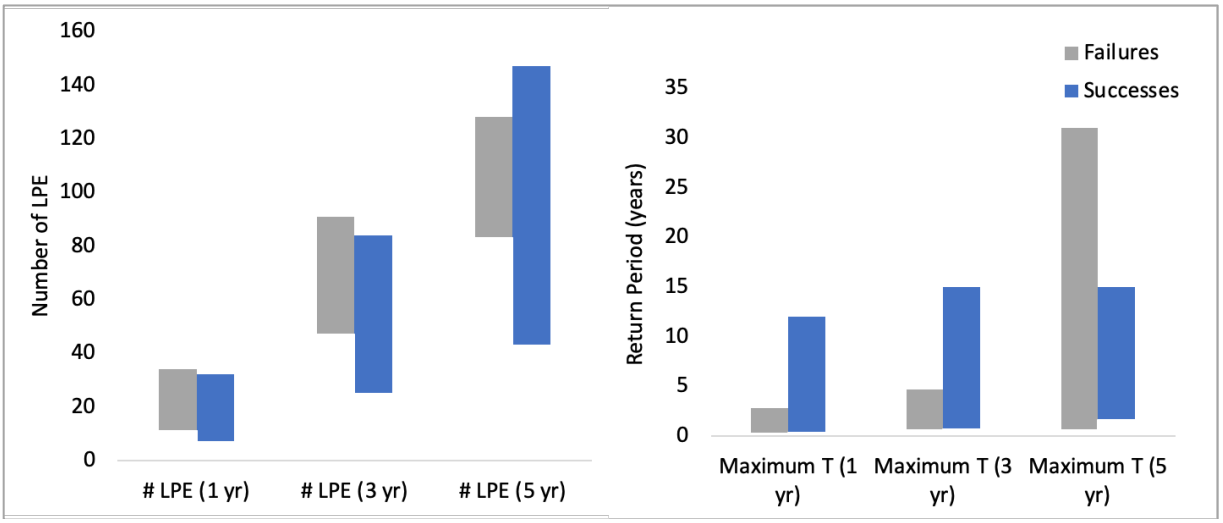

Figure 58: Ranges of precipitation data at sites with rip rap, separated by failures and successes (LPE = large precipitation events, T = return period).

The number of large precipitation events at the sites did not vary much between the failures and successes. The maximum return periods in one and three years were both higher at the successful sites, but the maximum return periods in five years were higher at the sites with failed rip rap. The ranges of maximum return period variables within the watersheds of sites with rip rap, split up by failures and successes, are shown in Figure 59. The numbers of storms within the watershed were not included because they did not vary much between the successes and failures, and it was a distribution very similar to the storms at the site (Figure 58).

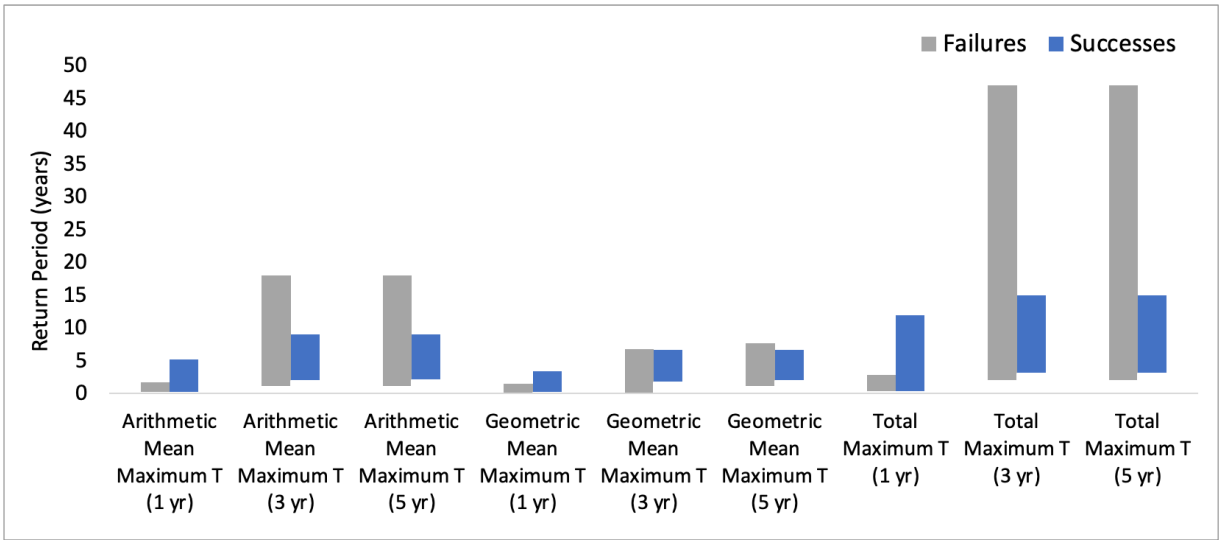

Figure 59: Ranges of arithmetic mean, geometric mean, and total maximum return periods (T) within the watersheds of sites with rip rap, separated by failures and successes

The arithmetic mean maximum return periods and the total maximum return periods in the watersheds in one year were higher at the successful sites, but the arithmetic mean maximum return periods in three and five years were higher at the sites with failed rip rap. The geometric means, however, did not vary much between the successes and failures. There is not enough data to draw a conclusion from the precipitation data. More sites with rip rap would need to be studied to understand how precipitation events impact the structure's success.

Overall, rip rap had a 46% success rate at the sites studied. It is a simple and commonly used streambank stabilization structure, but it is not reliably successful. The variability in success is also present in literature (Keown et al. 1977; Froehlich 2013; Radecki-Pawlik 2019). Some engineers think the most common cause of rip rap failure is poor installation or the size of the rip rap, which was beyond the scope of this study (Keown et al. 1977; Froehlich 2013). Data should be collected on installation practices, such as excavation or the use of a geotextile, and stone size to determine if these were potential causes of failure at sites in this study.

Logistic regressions were run on this data, but no significant variables were found. The regressions and the corresponding p values are summarized in Table 33.

Table 33: Rip rap logistic regression p values, including percent silt, percent of the watershed developed, and return periods (T) (p > 0.1)

Regression	Variable	p Value
1	Intercept	0.30
	Percent Silt	0.19
2	Intercept	0.27
	Percent of Watershed Developed	0.29
3	Intercept	0.17
	Maximum T at Site in 3 years	0.20
4	Intercept	0.28
	Maximum T at Site in 3 years	0.19
	Percent Silt	0.17
	Percent of Watershed Developed	0.48
5	Intercept	0.15
	Maximum T at Site in 3 years	0.17
	Percent Silt	0.16
6	Intercept	0.16
	Geometric Mean Maximum T in 1 year	0.16
7	Intercept	0.78
	Geometric Mean Maximum T in 1 year	0.17
	Percent Silt	0.17
	Percent of Watershed Developed	0.33
8	Intercept	0.13
	Geometric Mean Maximum T in 1 year	0.24
	Percent Silt	0.21

The variables run in these regressions were determined from their individual p values and how they collectively contribute to streambank erosion. Precipitation in a more developed watershed will create higher flows, and high flows lead to erosion or the bank material. The erodibility of this bank material depends on its soil type. The specific precipitation and sediment variable(s) chosen had the lowest p values in their respective categories. More data is needed to find what variables impact the success or failure of rip rap before recommendations on the implementation of this structure are made.

3.11 Spur Dikes Analysis

Spur dikes differ from other structures in this study because they are located only immediately upstream of the bridge abutment. Their purpose is to protect the bridge abutment from attacks from the stream. Spur dikes were installed at seven different sites in the Washita, Cimmaron, and Arkansas rivers. One site had spur dikes on both banks, which were split up as different structures. This resulted in a total of eight different data points, with one failure and seven successes. Spur dikes were deemed a failure if the stream had eroded and cut around the spur dike. Otherwise, they were considered successful.

The one failed site was site 17, on the Cimmaron River at S.H. 74 near Crescent, OK. At this site, the Cimarron River is cutting behind the spur dike. There were no variables that had an outlying data point at site 17. All of the data collected at site 17 fell in the range of the sites with successful spur dikes. Thus, a cause of failure cannot be determined from the data collected. However, the spur dike at this site is part of an embankment from an old bridge that was rip rapped once the bridge was taken down in 1943. The failure of the spur dike at this site could be because it was not originally designed as a spur dike. Additionally, the old bridge was too narrow, which is why it was removed. The location of the spur dike is based on the old bridge, so it is not located in the ideal place for the current bridge. The failure of this spur dike is not representative of the typical design. If site 17 is removed from consideration, spur dikes were 100% successful. Because of the lack of spur dike failures, regressions were not run on this data.

The average stream flows at sites with spur dikes ranged from 19 to 2440 cubic feet per second, so these structures were installed in small to medium size streams. Additionally, the sinuosity at sites with spur dikes varied between 1.1 and 1.5. The range of sinuosities at all of the sites was 1.0-2.1, so spur dikes were located in sites on the lower range of sinuosities present in

this project. The thalweg movement ranged from -1125 to 1125 feet, and both of those extremes occurred at site 1, on the Washita River at U.S. 77 near Wynnewood, OK. Site 1 has spur dikes on either bank, so movement of the thalweg in relation to one bank is the opposite of the thalweg movement for the other bank. The movement of the thalweg at site 1 was shown in Figure 51.

Spur dikes were installed on streams with varying geomorphology. A summary of sediment data at sites where spur dikes succeeded is shown in Table 34.

Table 34: Summary of sediment data at sites with spur dikes.

	% clay	% sand	% silt	% gravel	d10	d40	Cu	Cc
Average	6.6	70	16	8.1	0.06	0.19	85	4.0
Minimum	0.0	47	0.6	0.4	0.001	0.04	4.5	0.7
Maximum	12	86	24	27	0.34	0.87	461	15

A summary of precipitation data at sites where spur dikes were successful is shown in Table 35. There were no distinct differences in sediment characteristics between spur dikes that succeeded and those that failed.

Table 35: Summary of precipitation data at sites with spur dikes including the number of large precipitation events (LPE), defined as precipitation events with greater than 0.5in of rain in 24 hr., and maximum return periods (T) within 1, 3, and 5 years of installation of the structures.

	# LPE in 1 year	# LPE in 3 years	# LPE in 5 years	Maximum T in 1 year	Maximum T in 3 years	Maximum T in 5 years
Average	22	64	98	2.1	6.0	11
Minimum	10	41	60	0.2	0.5	0.7
Maximum	34	91	128	11	31	31

The spur dikes studied faced a maximum of a 31-year storm within five years of their installation, which occurred at site 1 on the Washita River, near Wynnewood, OK. They also faced a minimum of 60 erosion-causing storms within five years of their installation.

A summary of precipitation data in the watersheds of sites where spur dikes were successful is shown in Table 36.

Table 36: Summary of precipitation data in watersheds of sites with spur dikes. Data includes the number of large precipitation events (LPE), defined as precipitation events with greater than 0.5in of rain in 24 hr., and maximum return periods (T) within 1, 3, and 5 years of installation of the structures. The geometric mean, average, and maximum of the maximum return periods at each weather station in each site's watershed are included.

	# LPE in 1 year	**# LPE in 3 years**	**# LPE in 5 years**	**Arithmetic Mean Maximum T in 1 year**	**Arithmetic Mean Maximum T in 3 years**	**Arithmetic Mean Maximum T in 5 years**
Average	60	170	261	7.0	8.7	1.6
Minimum	39	114	157	1.1	2.1	0.2
Maximum	92	226	334	34	34	8.1
	Geo. Mean Maximum T in 1 year	**Geo. Mean Maximum T in 3 years**	**Geo. Mean Maximum T in 5 years**	**Total Maximum T in 1 year**	**Total Maximum T in 3 years**	**Total Maximum T in 5 years**
Average	1.6	4.4	5.6	3.2	13	17
Minimum	0.2	0.7	1.5	0.4	1.9	3.1
Maximum	8.1	18	18	16	68	68

The spur dikes studied faced a maximum of a 68-year storm within five years of their installation, which occurred at site 1 on the Washita River near Wynnewood, OK. Additionally, they faced a minimum of 157 erosion-causing storms throughout their watersheds within five years of installation.

The spur dikes protected the bridge abutments at all sites where they were properly installed. They are a simple structure that is easy to install and highly effective. The disadvantage of spur dikes is that they only protect the bridge abutments. If the river is in need of a change in course, spur dikes are not a solution. However, if the stream is eroding the bridge abutment, a spur dike could successfully protect this bridge abutment and decrease the chance of bridge failure.

3.12 Kellner Jetties Analysis

Kellner jetties are a permeable structure that jets out from the streambank into the stream. They work by slowing the water down and allowing sediment to settle out, slowly building a new bank. Kellner jetties were installed at 22 different sites in the Washita, Cimmaron, Canadian, North Canadian, Red, and Arkansas rivers. Some sites had multiple sets of jetties, which were split up as different structures. This resulted in a total of 28 different data points to be used in regressions, with six failures and 22 successes, for a total success rate of 79%. The Kellner jetties were deemed a failure if they had been washed away or eroded around. If the Kellner jetties were not visible, they may have washed away, but they may have also been covered by sediment. To determine between these two occurrences, the old reports were referenced (Keeley 1971; Harp and Thomas 1989).

The average stream flows at sites with Kellner jetties ranged from 19 to 10,300 cubic feet per second, so these structures were installed in all size streams. Additionally, the sinuosity at sites with Kellner jetties varied between 1.1 and 2.1 The range of sinuosities at all of the sites was 1.0-2.1, so Kellner jetties were located in sites covering the range of sinuosities present in this project. The thalweg movement ranged from -1210 to 2950, covering the entire range of thalweg movement in this project.

Logistic regressions were run on the Kellner jetty data to determine variables that impacted the success or failure of these structures. Because of the limited number of data points, a confidence limit of 90% has been used. When all of the variables were considered in logistic regressions, the only individual significant variable was the angle of the Kellner jetty in relation to the thalweg. The oldest available Kellner jetty angle is assumed to be close to the Kellner jetty angle at the time of installation. Some of these angles were from original plans, and many were

from Keeley (1971). Angles from newer sites were from Harp and Thomas (1989) or aerial Images (GoogleEarth 2020). This variable was combined with the thalweg movement variable to create a stronger regression, but it was found that site 21 skewed this regression. Other variables were tested in combination with these variables, but none were significant. These results are summarized below.

Figure 60 shows the logistic regression model with the oldest available Kellner jetty angle and the data points for comparison. Data points with a y-value of 1 were successful pile diversions, while failures are represented by a y-value of 0.

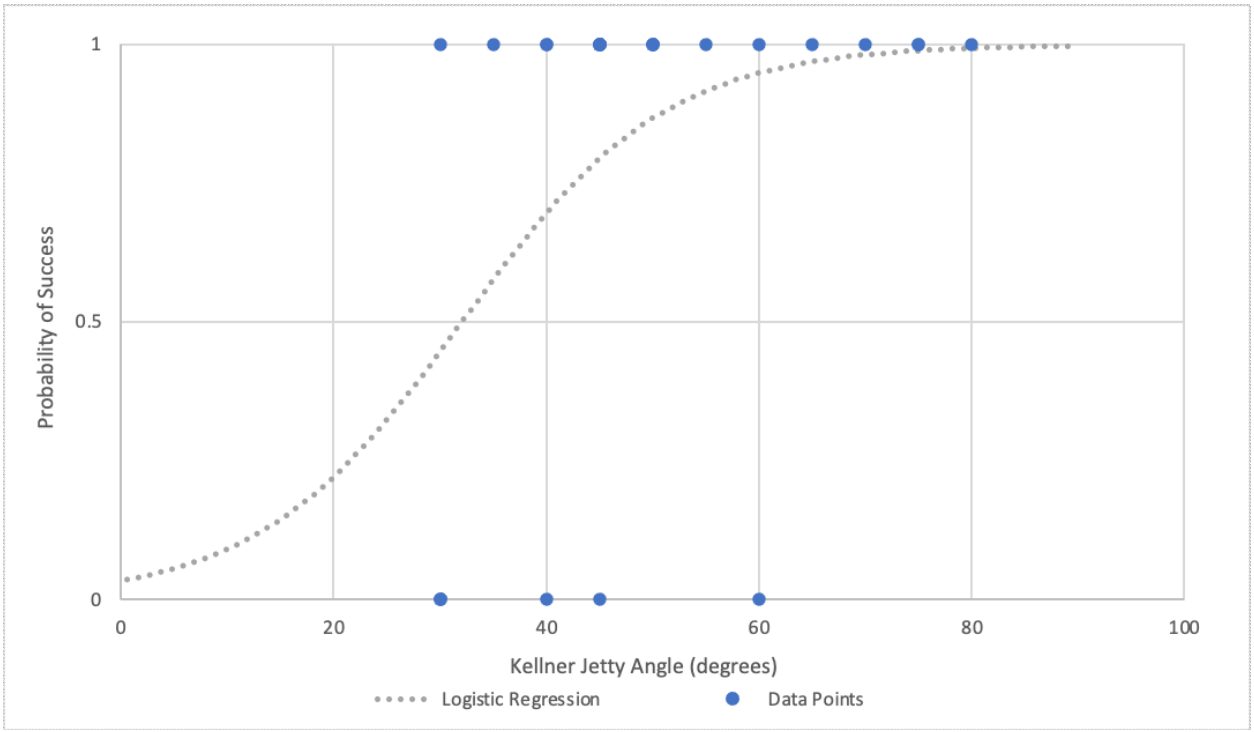

Figure 60: Kellner jetty logistic regression with oldest Kellner jetty angle ($p < 0.1$)

The Kellner jetty angles ranged from 30 to 80 degrees, and above 60 degrees, they were consistently successful. Only one failure occurred at 60 degrees (site 21) while the rest were all at 45 degrees or below. The results of this regression are summarized in Table 37.

Table 37: Kellner jetty logistic regression with oldest Kellner jetty angle results

	Coefficient	p Value
Intercept	-3.35	0.17
Oldest Kellner Jetty Angle (degrees)	0.104	0.068

The high p value on the intercept does not take away from the significance of the oldest Kellner jetty angle variable. The positive coefficient for the Kellner jetty angle shows that the larger the angle the jetties make with the thalweg, the more likely they are to succeed. This means the water hitting the jetties at an angle closer to perpendicular causes the water to slow down more and allow sediment to settle out.

The p values in this regression decreased with the addition of the thalweg movement variable when site 21 was included. To show the impact of each of the variables on the regression, the variables were isolated and shown in two separate models, where one was held constant while the other was changed. First, the thalweg movement was held constant at the average value of 55 feet, and the Kellner jetty angle was changed. The regression and data points in respect to Kellner jetty angles are shown in Figure 61. This regression is similar to the one without thalweg movement, as the steepest part of the curve is around 20 to 50 degrees.

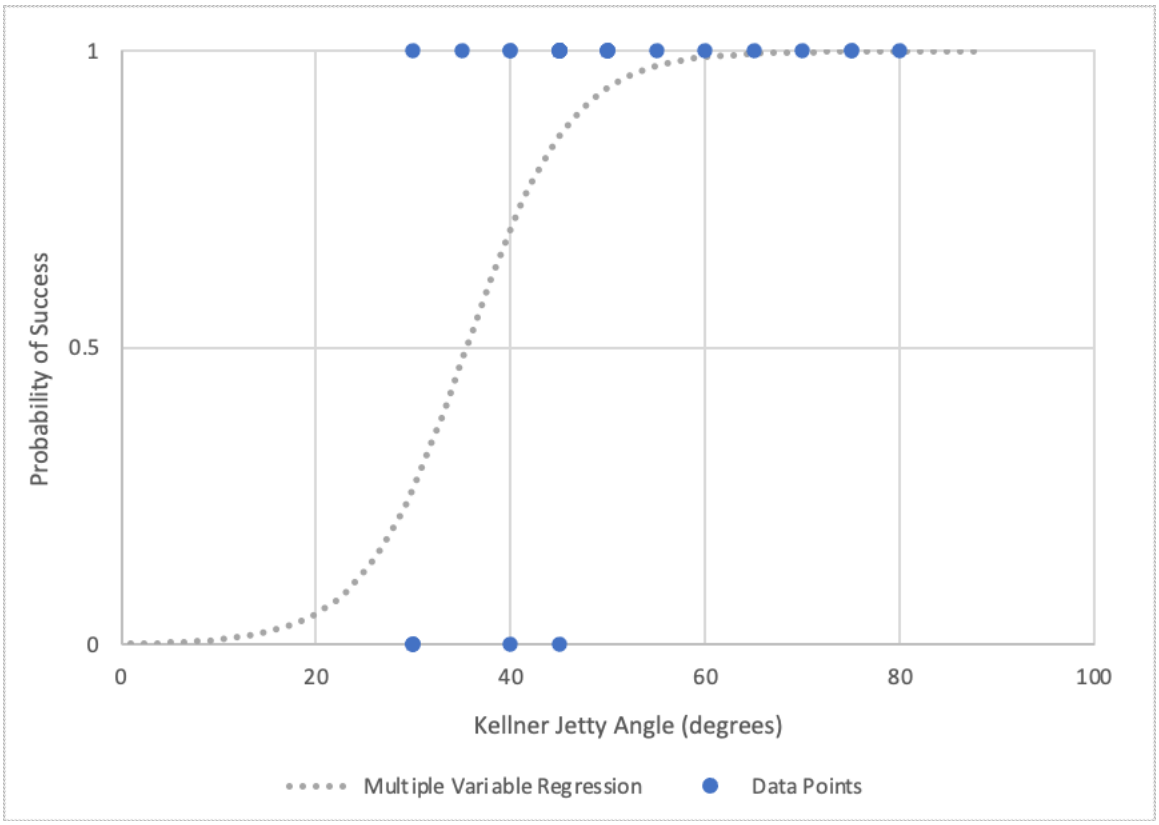

Figure 61: Kellner jetty multiple variable logistic regression in respect to Kellner jetty angle ($p < 0.1$)

To evaluate the impact of the thalweg movement on the regression, the Kellner jetty angle was held constant at the average value of 49 degrees, and the thalweg movement was changed. The regression and data points in respect to thalweg movement are shown in Figure 62. This regression shows that the further away from the bank of concern the thalweg moves, the more likely the structure is to fail. This is counterintuitive but may be due to the erroneous data point with a thalweg movement of 2950. This is site 21, which is the only failed structure with a positive thalweg movement. The impact of this data point on the regression is further analyzed after the presentation of these regressions.

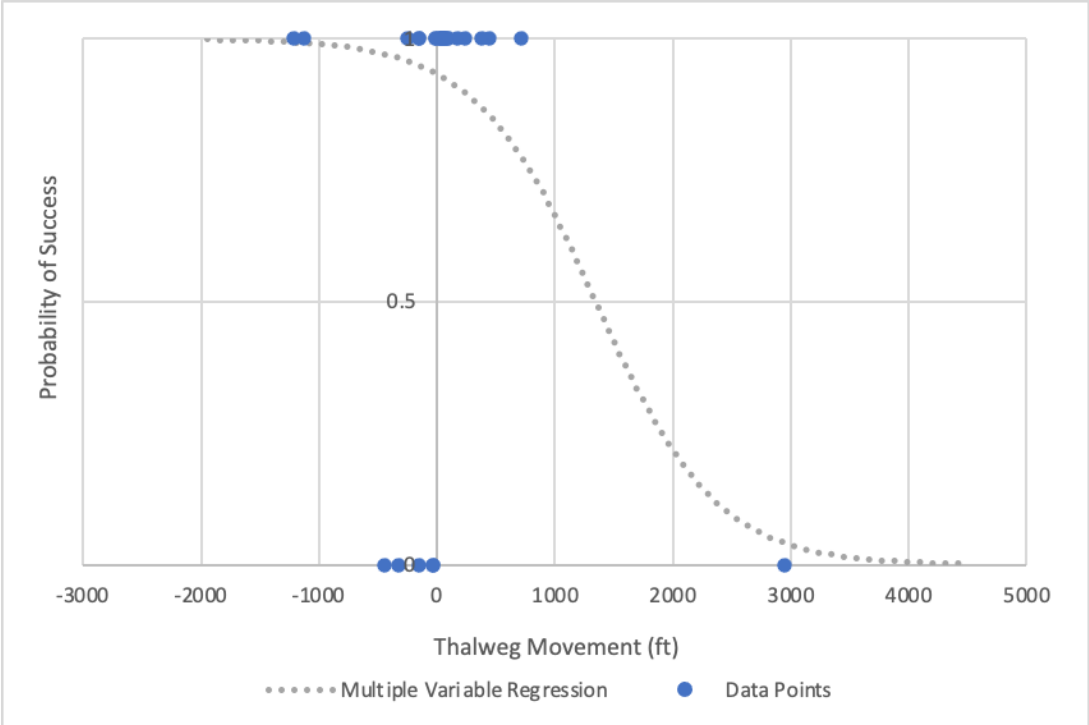

Figure 62: Kellner jetty multiple variable logistic regression in respect to thalweg movement ($p < 0.1$)

To evaluate how the variables worked in the regression together, they were combined into one model. Figure 63 shows the logistic regression with the oldest available Kellner jetty angle and thalweg movement and the data points in respect to both variables for comparison. The regression is similar to the others in respect to the Kellner jetty angles, where Kellner jetties installed at angles greater than 60 degrees in respect to the thalweg are predicted to be consistently successful, but thalweg movement is also considered here. Based on this regression, sites with thalweg movement greater than about 400 feet away from the bank of concern and Kellner jetties angles of above 60 degrees will almost always succeed.

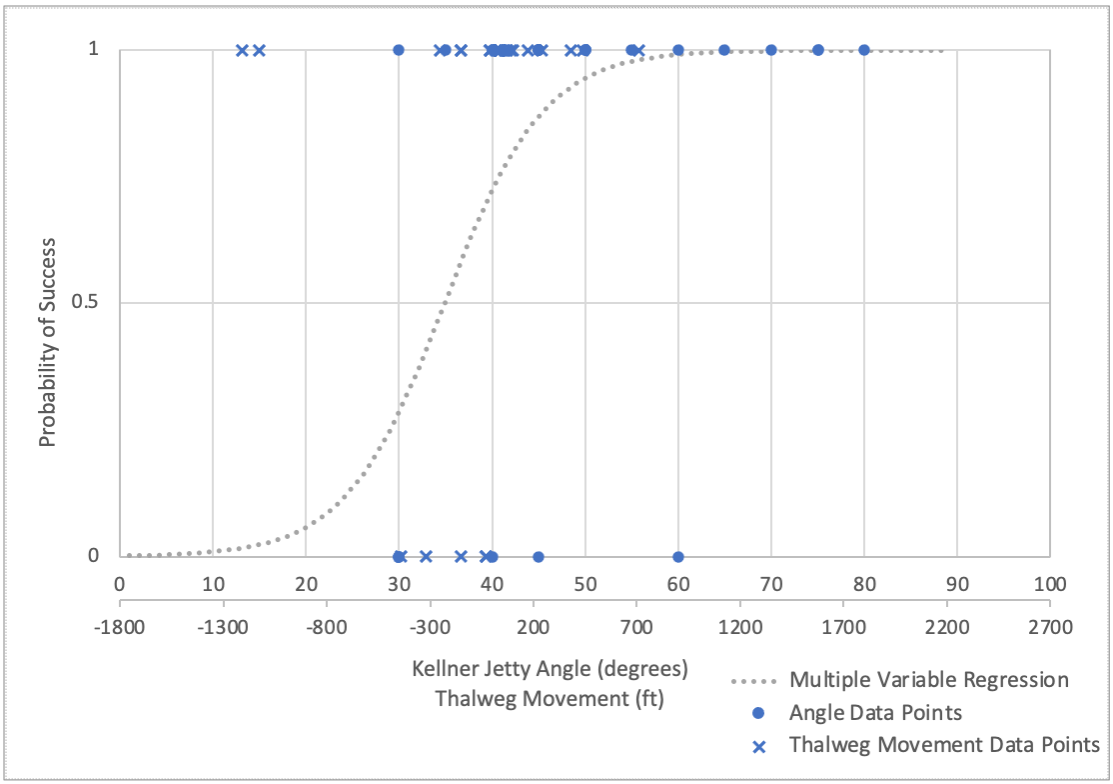

Figure 63: Kellner jetties multiple variable logistic regression in respect to oldest Kellner jetty angle and thalweg movement ($p < 0.1$)

The results of the multivariable regression are summarized in Table 38.

Table 38: Kellner jetty logistic regression with oldest Kellner jetty angle and thalweg movement results

	Coefficient	**p Value**
Intercept	-3.33	0.062
Oldest Kellner Jetty Angle (degrees)	0.101	0.057
Thalweg Movement	-0.0013	0.035

The thalweg movement was negative when the thalweg moved towards the bank with structures and positive when it moved away. A negative coefficient means that thalweg movement towards the structures lead to successful structures. This is shown in Figure 62 when the Kellner jetty angle was held constant. When an individual logistic regression was run with thalweg movement, the p value was 0.30, so it was not significant. It was only made significant by the

addition of the Kellner jetty angle variable. The Kellner jetty angle and thalweg movement data for the failed Kellner jetty sites are shown in Table 39.

Table 39: Kellner jetty angles and thalweg movement data for failed Kellner jetty sites

Site	Oldest KJ Angle (degrees)	Thalweg Movement (ft)
5	30	-440
6	30	-30
8	30	-150
11	40	-30
17	45	-320
21	60	2950

Site 21 has a much higher thalweg movement value than any other site and was the only failed site with a positive value for this variable. This one data point makes the thalweg movement coefficient negative. Site 21 also had the highest angle of all of the failed sites. The negative coefficient for thalweg movement would balance these two variables at this site to make this regression significant. This site was deemed a failure because the river cut through and around the Kellner jetties, and none of the Kellner jetties could be found in 1971, 1989, or 2021 (Keeley 1971; Harp and Thomas 1989). Work was continuously done on this site, 40 years after the Kellner jetties were installed until the river changed course. This change in course, which is reflected in the high positive thalweg movement value, was not caused by the Kellner jetties, so it does not fit in these regressions. Because of the circumstances surrounding the failure at site 21, the data point was removed, and the regressions were rerun. Without this data point, the results from the regression with the Kellner jetty angle and thalweg movement variables are shown in Table 40.

Table 40: Kellner jetty logistic regression with oldest Kellner jetty angle and thalweg movement results without site 21

	Coefficient	p Value
Intercept	-7.18	0.045
Oldest Kellner Jetty Angle (degrees)	0.213	0.020
Thalweg Movement	0.00145	0.41

Without site 21, the thalweg movement is no longer significant. The results without site 21 for a logistic regression with just the Kellner jetty angles are shown in Table 41.

Table 41: Kellner jetty logistic regression with oldest Kellner jetty angle results without site 21

	Coefficient	p Value
Intercept	-3.54	0.044
Oldest Kellner Jetty Angle (degrees)	0.091	0.022

The regression without site 21 is shown in Figure 64 with data points for comparison. This regression looks very similar to the one with site 21 included, showing it is a relatively reliable regression despite the inclusion of the erroneous data point. The curve is still steepest between 20 and 50 degrees, as it was in Figure 60.

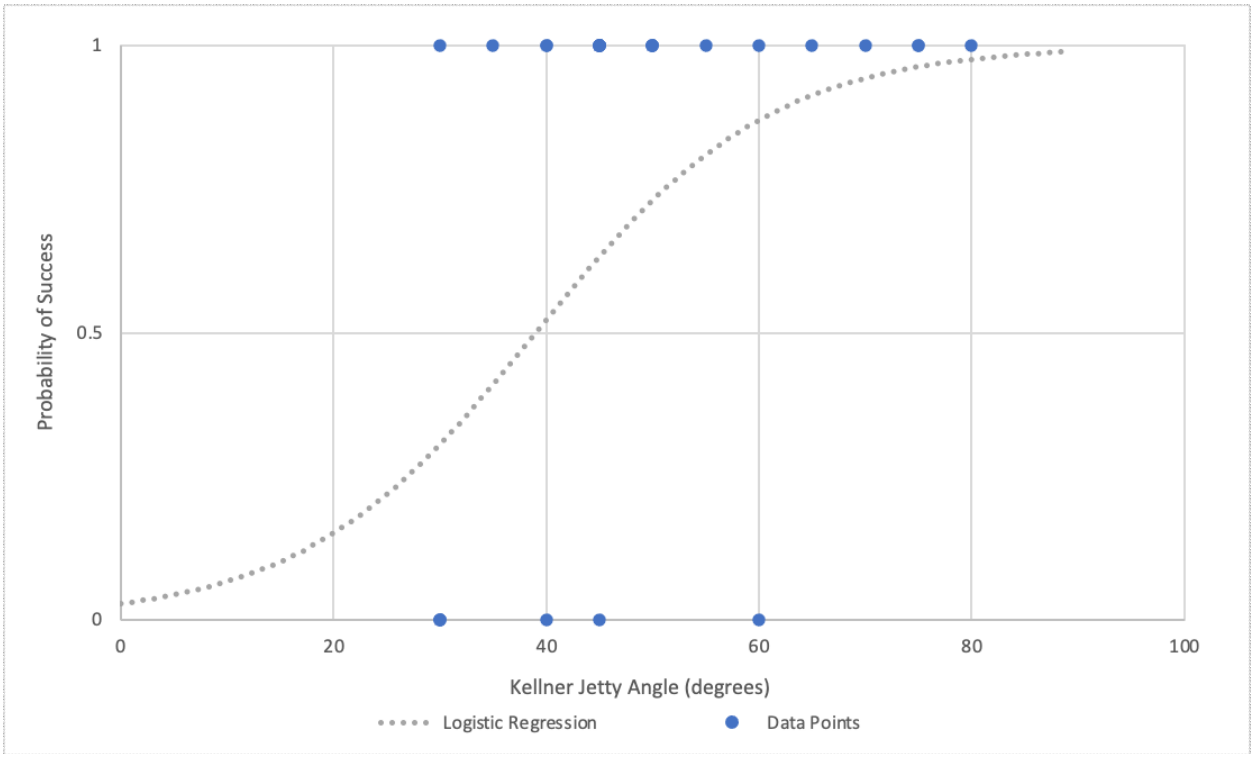

Figure 64: Kellner jetties logistic regression with oldest Kellner jetty angle without site 21 ($p < 0.1$)

To evaluate what other variables were not significant when used in logistic regressions, p values were determined (Table 42). First, a multivariable regression was run with six variables, chosen based on their R^2 values in a correlation with the binary success or failure variable: coefficient of curvature (C_c), percent gravel, geometric mean of maximum return period (T) in three years after installation, stream slope, and thalweg movement. These variables were then narrowed down by p value and analyzed in different combinations based on their conceptual relationships. For example, precipitation and sediment variables were run together and geomorphology variables were run together. All of these regressions were run without site 21.

Table 42: Kellner jetty regressions for all variables. Variables with p values > 0.10 are considered moderately significant and are shown in bold. (LPE = large precipitation events)

Variable	p value	Variable	p value
Other Structure on Bank	1.0	# LPE in 1yr in Watershed	0.52
Percent Clay	0.49	# LPE in 3yr in Watershed	0.69
Percent Sand	0.37	# LPE in 5yr in Watershed	0.72
Percent Silt	0.70	Maximum T in 1yr in Watershed	0.57
d10	0.73	Maximum T in 3yr in Watershed	0.59
d40	0.46	Maximum T in 5yr in Watershed	0.63
Cu	0.69	Geo. Mean Max T in 1yr in Watershed	0.57
Cc	0.16	Geo. Mean Max T in 3yr in Watershed	0.30
Percent Gravel	0.17	Geo. Mean Max T in 5yr in Watershed	0.33
Average Depth to Bedrock	0.69	Total Max T in 1yr in Watershed	0.56
Coefficient of Variation Depth to Bedrock	0.18	Total Max T in 3yr in Watershed	0.56
Minimum Depth to Bedrock	0.26	Total Max T in 5yr in Watershed	0.59
KJ Angle of Installation	1.00	Sinuosity	0.59
KJ Angle in 1971	**0.04**	Percent Watershed Developed	0.86
KJ Angle in 1989	0.38	Average Streamflow	0.82
Current KJ Angle	1.00	BEHI	0.63
Oldest KJ Angle	**0.02**	NBS	0.63
Most Recent KJ Angle	0.06	Root Density	0.81
# LPE in 1yr at Site	0.52	Drainage Area	0.66
# LPE in 3yr at Site	0.75	Stream Slope	0.20
# LPE in 5yr at Site	0.70	Thalweg Movement	0.37
Maximum T in 1yr at Site	0.59		
Maximum T in 3yr at Site	0.60		
Maximum T in 5yr at Site	0.63		

To summarize, the angle of the Kellner jetties was the only significant variable in a logistic regression with this data. The angles in 1971 were significant, in addition to the oldest angle. The oldest angle included more sites in the analysis and was more significant. The larger the angle between the Kellner jetties and the thalweg, the more likely they are to succeed. Site 21 was deemed an error and will not be included in other analyses. More data is needed to confirm this regression and rule out the impact of thalweg movement.

3.13 Gabion Baskets

Gabion baskets were successful at site 31, on the Deer Creek tributary. However, they were unsuccessful on Sugar Creek, where they sunk into the bank and did not provide any protection. The gabion baskets at site 31 are shown in Figure 65.

Figure 65: Gabion baskets at site 31

Vegetation has filled in around the gabion baskets, and they have little to no damage. These gabion baskets have been successful at site 31. Figure 66 shows the gabion baskets at site 26 on Sugar Creek that have sunken completed into the bank. The wire and rocks from the gabion baskets could be seen in some areas on the streambank but were completely covered in others.

Figure 66: Sunken gabion baskets at site 26

This difference in success is likely due to the bank materials at these sites. Bank material at site 31 had 60% sand, classifying as a sandy loam while site 26 has 94% sand, classifying as sand. Literature confirms that gabion baskets are often unsuccessful in sandy soils because they have the potential to sink into the bank (Freeman and Fischenich 2000). Soil type should be taken into consideration before gabion baskets are installed in the future.

3.14 Rock Vanes

Rock vanes were installed at site 28 on the Illinois River in 2016 and are working very effectively. This project also included plantings to help vegetation develop on the site. The rock vanes have been on the site for less than five years, so it cannot yet be concluded that they were successful. The rock vanes were submerged when the site was visited, but one is located towards the center of the stream in Figure 67.

Figure 67: Rock vane at site 28 on the Illinois River

The other part of this site is the vegetation along the bank. Although it was winter when this site was visited, the vegetation is shown in Figure 68.

Figure 68: Right bank of Illinois River at site 28

Dense tall grasses have filled in the right bank, along S.H. 10, and with more time, shrubs and trees should start growing as well. This will assist the rock vanes in preventing the Illinois River from moving closer to the roadway.

3.15 Rock Drop Structures

Rock drop structures were installed at sites 26 and 34 on Sugar Creek to prevent the incision of the stream. Residents of the land near these sites had dug the stream out to try to prevent

flooding, but it only made the stream erode more. The rock drop structure creates patterns of riffles and pools to control the slope of the stream and decrease erosion. A photo of a riffle in the rock drop structure at site 26 is shown in Figure 69.

Figure 69: Rock drop structure at site 26

These structures were very successful at both site 26 and 34. Vegetation along the banks is dense, tall grass, as seen in Figure 69. These sites on this incised stream were successfully rehabilitated with the installation of rock drop structures.

3.16 All In-Stream Structures

Regressions were run on all of the sites together, combining all of the structures. This shows what makes a river difficult to control with any kind of streambank stabilization structure. There were 30 sites in total, and many had multiple structures, for a total of 79 structures studied. Of these structures, 25 failed, and 54 succeeded. With the higher number of data points in this regression analysis, a higher confidence limit of 95% was used. Many variables were run, but few were significant. The only individual variable that was significant in a logistic regression was percent silt in the bank material. The logistic regression model with data points for comparison is shown in Figure 70.

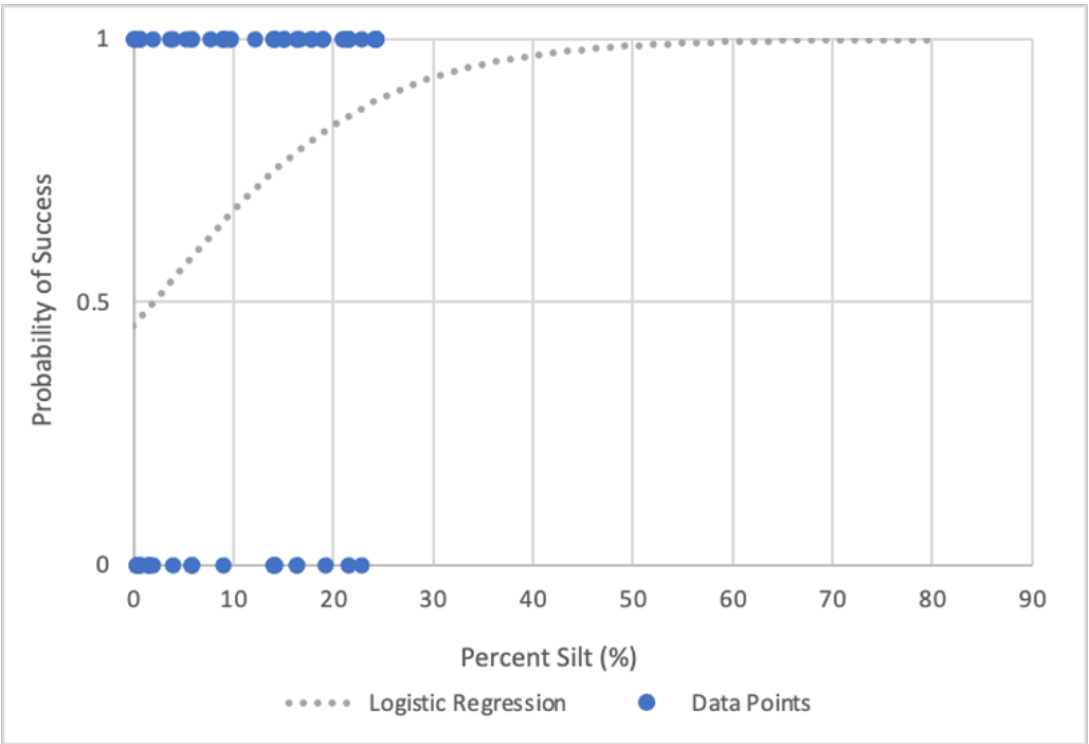

Figure 70: All structures logistic regression with percent silt ($p < 0.05$)

This regression shows that streams with bank material with silt fractions above about 40% will almost always respond positively to streambank stabilization structures, but the data points do not quite line up with this regression.

The results of this regression are summarized in Table 43.

Table 43: All structures logistic regression with percent silt results

Variable	Coefficient	p Value
Intercept	-0.183	0.66
Percent Silt (as a fraction)	9.05	0.007

The insignificant intercept may be the explanation for the difference in the regression and data points in Figure 70, but it does not take away from the significance of the impact of silt on success rates. A threshold of the silt fraction that will make structures most likely to succeed cannot be determined; however, the positive coefficient for percent silt shows that more silt in the bank material leads to more successful streambank stabilization by a variety of structures.

Many of the structures rely on sediment settling out to build up a bank, and silty streams work well with these structures (Army Corps of Engineers 1963; Harp and Thomas 1989; Abad et al. 2008; Scurlock 2014). Sandy or rocky streams often do not carry enough sediment to work well with these structures, or the structures will sink into the streambed and banks before they have time to be effective. Clay is typically too fine to settle out in these structures, so it has little impact on their effectiveness. This regression supports literature and previous reports showing the contribution of silt to the success of structures like Kellner jetties, pile diversions, and bendway weirs (Army Corps of Engineers 1963; Harp and Thomas 1989; Abad et al. 2008; Scurlock 2014). This means that a variety of structures on sites with high silt content can be successful. Other factors can go into the decision of which structure is installed, such as cost and ease of installation, without fear of failure of the structure.

3.17 Long Term Evaluation

To evaluate the long term effectiveness of the structures, the status of each structure was determined from the 1971 and 1989 reports and compared to the status determined in this study. The statuses of each structure in 1971, 1989, and 2020 are listed in

Table 44. The exact year of failure of the structures cannot be determined because they were not consistently evaluated, thus only estimations on the time of failure can be made based on their status in 1971, 1989, and 2020.

*Table 44: Comparison of structure statuses over time, based on reports from 1971 and 1989 and evaluations from 2020 (Keeley 1971; Harp and Thomas 1989). (US = Upstream, RB = Right bank, LB = left bank; 0=failed; 1=Success). Only structures constructed prior to 1989 are included.*Not included in current study*

Site No.	Structure Type (Bank)	Year of Installation	Status in 1971	Status in 1989	Status in 2020
1	Kellner jetties (RB)	1949	1	1	1
1	pile diversions(RB)	1959	1	1	1
1	rip-rap (RB)	1959	1	1	1
1	rip-rapped dike (RB)	1959	1	1	1
1	pile diversions (LB)	1959	1	1	1
1	rip-rapped dike (LB)	1959	1	1	1
2	Kellner jetties (RB)	1940	1	1	1
2	pile diversions (RB)	1950	1	1	1
2	pile diversions (RB)	1963	1	1	1
2	rip-rapped dikes (LB)	1963	1	1	1
2	rip-rap (LB)	1965	1	0	0
3*	Rock dike (RB)	1934	1	1	N/A
3*	Kellner jetties (RB)	1938	0	0	N/A
3*	Pile diversions (RB)	1957	0	0	N/A
3*	Spur dike (RB)	1957	1	1	N/A
4	Kellner jetties (LB)	1950	1	1	1
4	Pile diversions (LB)	1958	1	1	1
4	rip-rap (LB)	1958	1	1	1
5	Kellner jetties (LB)	1939	1	1	1
5	rock spur dike (LB)	1959	1	1	1
5	pile diversions(LB)	1959	1	1	1
5	Kellner jetties (RB)	1948	0	0	0
5	rip-rap (RB)	1959	0	0	0
6	Kellner jetties (RB)	1927	0	0	0
7	Kellner jetties (RB)	1937	0	0	0
7	Kellner jetties (RB)	1939	0	0	0
7	Kellner jetties (RB)	1949	0	0	0
7	Tetrahedron jetties (RB)	1951	1	0	0
7	rip-rap (RB)	1951	1	1	1
7	pile diversions (RB)	1958	0	0	0
7	Kellner jetties (RB)	1980	N/A	1	1
8	Kellner jetties (RB)	1939	0	0	0
8	pile diversions (RB)	1957	1	0	0
8	pile diversions (LB)	1957	1	0	0
9*	Kellner jetties	1950	0	N/A	N/A
10	pile diversions (LB)	1953	0	0	0
11	Kellner jetties (LB)	1949	1	1	1
11	Kellner jetties (RB)	1949	1	0	0
12	Spur dike (LB)	1957	1	1	1
13	Pile diversions (LB)	1958	0	0	0
13	Pile diversions (LB)	1958	0	0	0

Site No.	Structure Type (Bank)	Year of Installation	Status in 1971	Status in 1989	Status in 2020
13	Rip Rap (LB)	1958	0	0	0
14	Kellner jetties (RB)	1949	0	0	0
14	Rip Rap (RB)	1958	1	0	0
14	pile diversions (RB)	1958	1	0	0
15*	Rip-rap	1947	1	1	N/A
15*	Pile diversions	1948	1	1	N/A
15*	Bank retards	1948	1	1	N/A
16	Kellner jetties (RB)	1949	1	1	1
17	Rayfield jetties (RB)	1937	0	0	0
17	rip-rap (RB)	1957	1	0	0
17	dikes (RB)	1957	1	0	0
18	rip-rap (LB)	1966	1	1	0
18	Kellner jetties (RB)	1966	1	1	1
19	Kellner jetties (RB)	1949	1	1	1
19	Dikes (RB)	1949	1	1	1
20	Kellner Jetties (RB)	1979	N/A	1	1
20	Pile diversions (RB)	1969	N/A	1	0
21	rip-rap (RB)	1983	N/A	1	0
21	trilock block (RB)	1983	N/A	1	0
21	Kellner jetties (RB)	1983	N/A	0	0
21	Henson type fence (RB)	1983	N/A	0	0
22	Spur dike (LB)	1972	N/A	1	1
22	Kellner jetties (LB)	1981	N/A	0	0
23	Kellner jetties (LB)	1988	N/A	1	1
23	rip-rap (LB)	1988	N/A	1	1
24	Kellner jetties (LB)	1960	N/A	1	1
25	Kellner jetties (LB)	1985	N/A	1	1
25	rip-rap (LB)	1985	N/A	1	1
25	rip-rap (RB)	1985	N/A	1	1

Of the structures that failed over the course of the studies, 73% failed within 20 years. This means if a structure is going to fail, there is a 73% chance it will fail within 20 years. Only 53% of the structures studied were evaluated within 20 years of installation, though, so this does not account for all of the structures listed in Table 44. Within 20 years, the structures are likely covered in sediment, and vegetation, such as grasses, shrubs, and some trees have begun developing around them. These provide protection for the structures, making them more likely to succeed, as supported by the data.

Of the structures that failed over the course of the studies, 97% failed within 50 years of installation. If the structures did not fail within 50 years of installation, they have a 97% chance of still being successful today. Kellner jetties accounted for 39% of these failures, and their design lifetime is 50 years, meaning many of the Kellner jetties have remained successful beyond their expected lifetime (Army Corps of Engineers 1963; Cochran 1963). Other structures included in these failures were pile diversions and rip rap, but their exact design lifetimes are unknown because they depend on material or rock size (Keeley 1971; Harp and Thomas 1989).

Once a structure has been successful for 50 years, sediment has filled in, and vegetation has fully developed. This was seen at many of the sites visited in this study. Numerous structures could not be found during the 2020 site visits because they were covered in sediment or vegetation. Once the structure is buried or surrounded in vegetation, it is highly unlikely that it will suffer damage. Thus, if the structure has survived 50 years, it is unlikely to fail in the future, as supported by the data. These studies provide a unique opportunity to evaluate in-stream structures past their intended lifetime. Many of the structures were successful beyond their design lifetimes, and will likely continue to prove effective for more years to come.

Chapter 4: Findings, Conclusions, and Recommendations

4.1 Findings

The most noteworthy findings from this study are listed below:

- All bendway weirs studied were successful.
- All spur dikes, when initially installed as spur dikes, were 100% successful.
- Gabion baskets failed in sandier soils.

- Pile diversions had a 57% success rate. Based on logistic regressions, they were more likely to fail in sandy stream banks or if a large storm occurred within three years of installation.
- Rip rap had a 46% success rate, but there was no significant distinction between the variables at sites that failed and those that succeeded.
- Kellner jetties had a 79% success rate. Kellner jetties installed at higher angles were more likely to succeed.
- Overall, higher silt content was linked to a higher success rate of all structure types combined.

4.2 Conclusions

The conclusions developed from the findings of this study are listed below:

- Bendway weirs often caused the stream to drastically shift after they were installed. Sandbars built up between the bendway weirs, helping to stabilize the bank of concern.
- If pile diversions faced a storm within three years of installation, they became damaged and were more likely to fail.
- Sandy banks are unstable and difficult to control, which made pile diversions less successful. Other structures did not have the same failure rates on sandy banks.
- The cause of failure of rip rap could not be determined, but literature shows installation of the rip rap could play a large role in its success, which was not evaluated.
- Spur dikes are a simple structure that protects the bridge abutment from attacks by the stream with proper installation.
- Higher angles between Kellner jetty retard lines and the thalweg at the time of installation makes them more likely to succeed.

- Banks with higher silt content are more stable since silt is more cohesive than sand. The maximum silt content in the banks studied was less than 25%, so higher variability in data points could help confirm this regression.

In addition to these findings, a method of evaluating the condition of the structures and streams was developed. Standardization of this method will allow for more data to be collected to strengthen the patterns found in this project.

4.3 Recommendations

Scour is the leading cause of bridge failure, costing $50 million in damage each year (Lagasse et al. 1995). However, bridge failures can be prevented by the installation of in-stream streambank stabilization structures. The main objective of this study was to determine variables that contribute to the failure of different streambank stabilization structures, including bendway weirs, pile diversions, rip rap, spur dikes, and Kellner jetties. Understanding these variables and choosing and designing the structures accordingly could save money and lives in the future. Data was collected at 30 sites where a total of 79 streambank stabilization structures were installed to protect transportation infrastructure across the state of Oklahoma. Most of these sites were previously studied in 1971 and 1989, making this a five-decade study, which has never been completed before on these types of structures (Keeley 1971; Harp and Thomas 1989). The long-term evaluation of these structures can inform engineers on how they function beyond their design lifetime. Each structure was deemed either a failure or a success, based on its current condition and its impact on the stream. Data was collected about each site, describing the bank sediment, historical precipitation, and stream characteristics. Then, logistic regressions showed what variables contributed to the failure or success of each type of structure and all the structures combined. Recommendations for engineers and decision makers are listed below:

- Bendway weirs are recommended in streams of any type where a radical change in the stream channel is required.
- Kellner jetties should be installed at higher angles.
- Spur dikes should be installed in rivers with wide flood plains, where erosion around the bridge abutment is a risk.
- Gabion baskets should not be installed in sandy soils.

Without examples of failed bendway weirs and spur dikes, no conclusion could be made about what contributes to their failure. To determine what variables (if any) may cause bendway weirs or spur dikes to fail, more of these structures, especially those that failed, need to be studied. In future studies, the installation of each structure should also be considered. No variables surrounding the installation of bendway weirs, spur dikes, rip rap, or pile diversions were included, and the only one evaluated for Kellner jetties was the angle of installation. With more data on the installation, more patterns may arise. Potential variables to describe the installation of these structures are listed below:

- Size and shape of rip rap rocks
- Number of bendway weirs, pile diversions, and Kellner jetties
- Spacing between bendway weirs, pile diversions, and Kellner jetties
- How far into the stream bendway weirs, pile diversions, or Kellner jetties protrude
- The height of bendway weirs or spur dikes
- Use of geotextiles with the structure
- Excavation depth during installation
- If any gradation was completed during installation

Additionally, to increase the number of data points and the range of the variables studied, this project should be expanded nationally. Oklahoma rivers have many similar characteristics, so to understand how these different structures behave in many different stream types, this project must go beyond the state of Oklahoma. A wider range within each variable could help strengthen the regressions or show that they are not applicable outside of Oklahoma.

Another interesting addition to this project could be a cost benefit analysis. No information on the cost of each of these structures was included in this study, but it is an important factor for deciding which structures to install on a given site. A risk analysis on each structure type could be completed based on the stream characteristics at the site, and the risk could be weighed against the cost of the different structures. This would be a useful decision-making tool for engineers working on streambank stabilization projects in the future.

Overall, this project provided the start of an understanding of the factors that influence the success of different types of in-stream streambank stabilization structures. The continuation of this project could save millions of dollars in damage to bridges and potentially save lives by preventing bridge failures.

Literature Cited

Abad, J. D., Rhoads, B. L., Güneralp, I., & García, M. H. (2008). Flow Structure at Different Stages in a Meander-Bend with Bendway Weirs. *Journal of Hydraulic Engineering*, *134*(8), 1052–1063. https://doi.org/10.1061/(ASCE)0733-9429(2008)134:8(1052)

Army Corps of Engineers. (1963). Symposium on Channel Stabilization Problems / Committee on Channel Stabilization. Washington, D.C.

ASTM D6913. (2017). Standard Test methods for particle-size distribution (gradation) of soils using sieve analysis. ASTM International, West Conshohocken, PA. doi:10.1520/d6913-04r09

ASTM D7928-17. (2017). Standard Test Method for particle-size distribution (gradation) of fine-grained soils using the sedimentation (hydrometer) analysis. ASTM International, West Conshohocken, PA. DOI: 10.1520/D6913-17

Bernhardt, E. S., (2005). "Synthesizing U.S. river restoration efforts." Science, 308, 636–637.10.1126/science.1109769

Budhu, M. (2011). *Soil mechanics and foundations*. John Wiley & Sons, Inc.

Cochran, A. L. (1963). Proceedings of the Federal inter-agency sedimentation conference: held at Jackson (Miss.), Jan 28th-Febr. 1st, 1963. Washington, D.C.

Dowdy, S., Weardon, S., Chilko, D. (2004). *Statistics for Research, Third Edition.* John Wiley & Sons, Inc. doi: 10.1002/0471477435

Freeman, G. E., & Fischenich, J. C. (2000). *Gabions for Streambank Erosion Control*.

Froehlich, D.C. (2013). Sizing Loose Rock Riprap to Protect Stream Banks. *River Research and Applications*., 29, 219-235. https://doi-org.ezproxy.lib.ou.edu/10.1002/rra.1587

Google Earth Pro 7.3.3.7786. (2020). NOAA DigitalGlobe 2021.

Harp, J. F., & Thomas, M. (1989). Effectiveness of riverbank protection and river control in Oklahoma. University of Oklahoma.

Keefer, T. N., McQuivey, R. S., & Simons, D. B. (1990). *Stream Channel Degradation and Aggradation: Uses and Consequences to Highways*. Washington, D.C.: Federal Highway Administration.

Keeley, J.W.. (1971). *Bank protection and river control in Oklahoma.* Federal Highway Administration.

Keown, M. P., Oswalt, N. R., Perry, E. B., & Dardeau, E. A. (1977). Literature Survey and Preliminary Evaluation of Streambank Protection Methods (WES-TR-H-77-9). Army Engineer Waterways Experiment Station, Vickburg, MS.

Khosronejad, A., Diplas, P. & Sotiropoulos, F. (2017). Simulation-based optimization of in–stream structures design: bendway weirs. *Environ Fluid Mech* 17, 79–109. https://doi-org.ezproxy.lib.ou.edu/10.1007/s10652-016-9452-5

Lagasse, P. F., Clopper, P. E., Thornton, C. I., Shields Jr, F. D., McCullah, J., & Spitz, W. J. (2016). Evaluation and Assessment of Environmentally Sensitive Stream Bank Protection Measures. *NCHRP Report*, *822*.

Lagasse, P. F., Schall, J. D., Johnson, F., Richardson, E. V., & Chang, F. (1995). *Stream Stability at Highway Structures* (2nd ed.). Washington, D.C.: Federal Highway Administration.

Lewis, L. (2020). Oklahoma Department of Transportation Archives, Oklahoma City, OK.

Li, M.-H. (2006). Learning from streambank failures at bridge crossings: A biotechnical streambank stabilization project in warm regions. *Landscape and Urban Planning*, *77*(4), 343–358. https://doi.org/10.1016/j.landurbplan.2005.04.006

Lindsey, C. G., Long, L. W., & Begej, C. W. (1982). Long-term survivability of riprap for armoring uranium-mill tailings and covers: A literature review (NUREG/CR--2642). Pacific Northwest Lab.

MapSof. (2021). *Oklahoma Rivers And Lakes*. Oklahoma Rivers And Lakes - MapSof.net. https://www.mapsof.net/oklahoma/oklahoma-rivers-and-lakes.

National Centers for Environmental Information (NCEI). (2021). *Climate Data Online*. Climate Data Online (CDO) | National Climatic Data Center (NCDC). https://www.ncdc.noaa.gov/cdo-web/.

NLCD Data. (2016). Retrieved July 06, 2020, from https://www.mrlc.gov/data?f%5B0%5D=category%3Aland+cover

NOAA, U.S. Department of Commerce. (2005). Precipitation Frequency Data Server. Retrieved March 29, 2021, from https://www.nws.noaa.gov/ohd/hdsc/index.html

Odgaard J.A., & Kennedy J. F. (1983). River-Bend Bank Protection by Submerged Vanes. Journal of Hydraulic Engineering, 109(8), 1161–1173. https://doi.org/10.1061/(ASCE)0733-9429(1983)109:8(1161)

Odgaard, J. A. & Lee, H.E. (1984). *Submerged Vanes for Flow Control and Bank Protection In Streams.* Iowa Institute of Hydraulic Research, Iowa City, Iowa.

Oklahoma Aerial Photo Inventory. (2019). Retrieved March 28, 2020, from https://www.arcgis.com/apps/webappviewer/index.html?id=e8eb5f5f19e943b3b43ff45a844c78b1

O'Neil, J., and Fitch, L. (1992). "Performance audit of in-stream habitat structures constructed during the period, 1982–1990, in southwestern Alberta." Abstracts for American Fisheries Society Meeting, 4.

Radecki-Pawlik, Artur, Radecki-Pawlik, Bartosz, Podkanowicz, Patryk, & Plesiński, Karol. (2019). RIP-RAP REVETMENT EXPLOITATION AND DESIGNING PROBLEMS: THE CZARNY DUNAJEC RIVER CASE STUDY. *Acta Scientiarum Polonorum Formatio Circumiectus,* 1(1), 175-192.

Rammer, D., & Winistorfer, S.G. (2007). Effect of Moisture Content on Dowel-Bearing Strength. *Wood and Fiber Science, 33*, 126-139.

Renard, K. G., Foster, G. R., Weesies, G. A., McCool, D. K., & Yoder, D. C. (1997). *Predicting soil erosion by water: A guide to conservation planning with the revised universal soil loss equation (RUSLE)*. Washington, D.C.: USDA Handbook No. 703.

Rosgen, D. L. (2014). *River stability: field guide*. Fort Collins, CO: Wildland Hydrology.

Scurlock, S.M. (2014). *Quantification of Hydraulic Effects from Transverse Instream Structures in Channel Beds* (Publication No. 3624360) [Doctoral dissertation, Colorado State University]. ProQuest LLC.

Smith, L. M., & Patrick, D. M. (1979). Engineering Geology and Geomorphology of Streambank Erosion. Report 1. EEl River Basin, California.

Thornton, C., Abt, S., Baird, D., & Padilla, R. (2007). *Hydraulics of bendway weirs*. Southampton: W I T Press. doi:http://dx.doi.org/10.2495/RM070371

U.S. Department of Agriculture. (2012). Engineering Classification of Earth Materials. *National Engineering Handbook Part 631.* 210-VI-NED, Ammend. 55.

U.S. Geological Survey (2020). The StreamStats program, online: http://streamstats.usgs.gov.

Vargas-Luna, A., Duró, G., Crosato, A., Uijttewaal, W. (2018) Morphological Adaptation of River Channels to Vegetation Establishment: A Laboratory Study. *Journal of Geophysical Research: Earth Surface* 124:7, pages 1981-1995.

Walters, W. H. (1982). Rock riprap design methods and their applicability to long-term protection of uranium mill tailings impoundments (NUREG/CR-2684; PNL-4252). Pacific Northwest Lab., Richland, WA (USA). https://doi.org/10.2172/6765539

Wardhana, K., Hadipriono, F.C. (2003). Analysis of recent bridge failures in the United States. Journal of Performance of Constructed Facilities, 17 (3), 144-150.

Wischmeier, W. H., & Smith, D. D. (1978). *Predicting rainfall erosion losses A guide to conservation planning.* Washington, D.C.: USDA Handbook No. 537.

Appendix A – Maps of Thalweg and Cross Section Locations

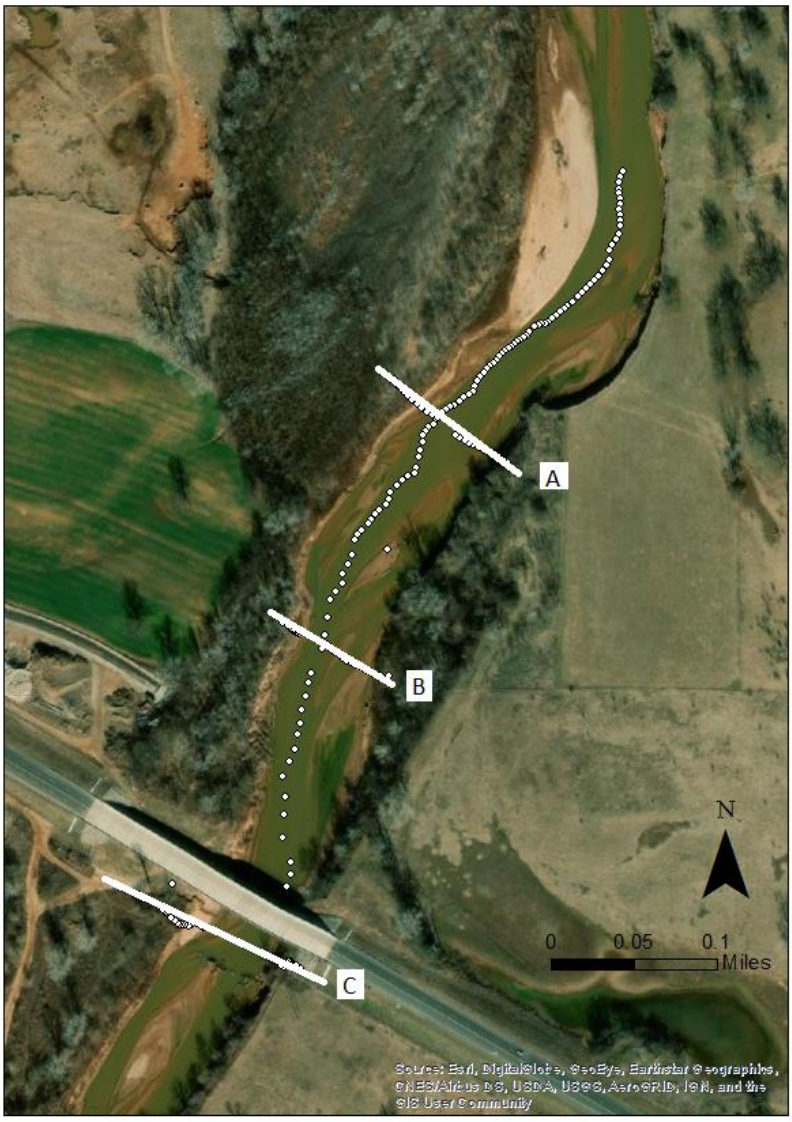

Figure A1: Site 1, Washita River and U.S. 77 north of Wynnewood in Garvin county, thalweg data points and cross section locations.

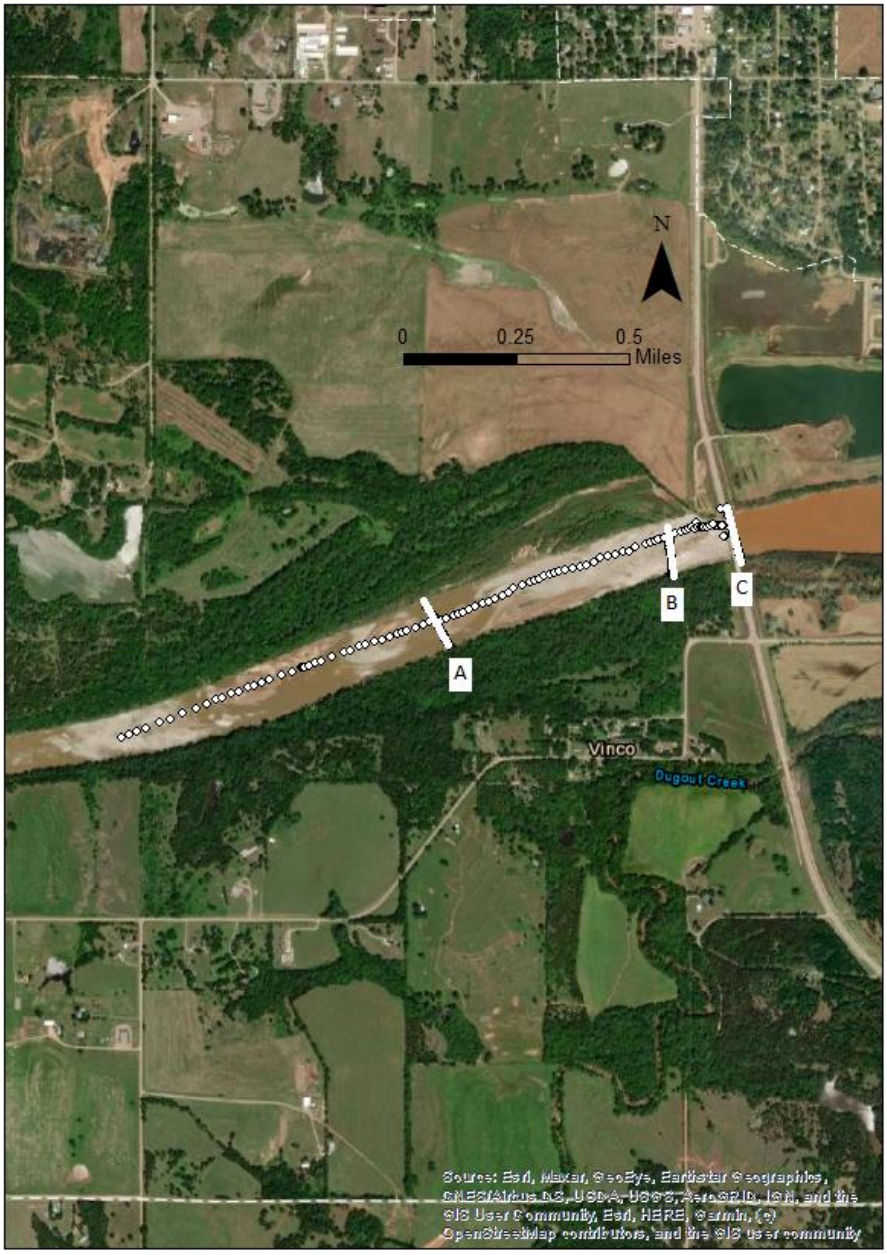

Figure A2: Site 2, Cimarron River and U.S. 177 south of Perkins in Payne county, thalweg data points and cross section locations.

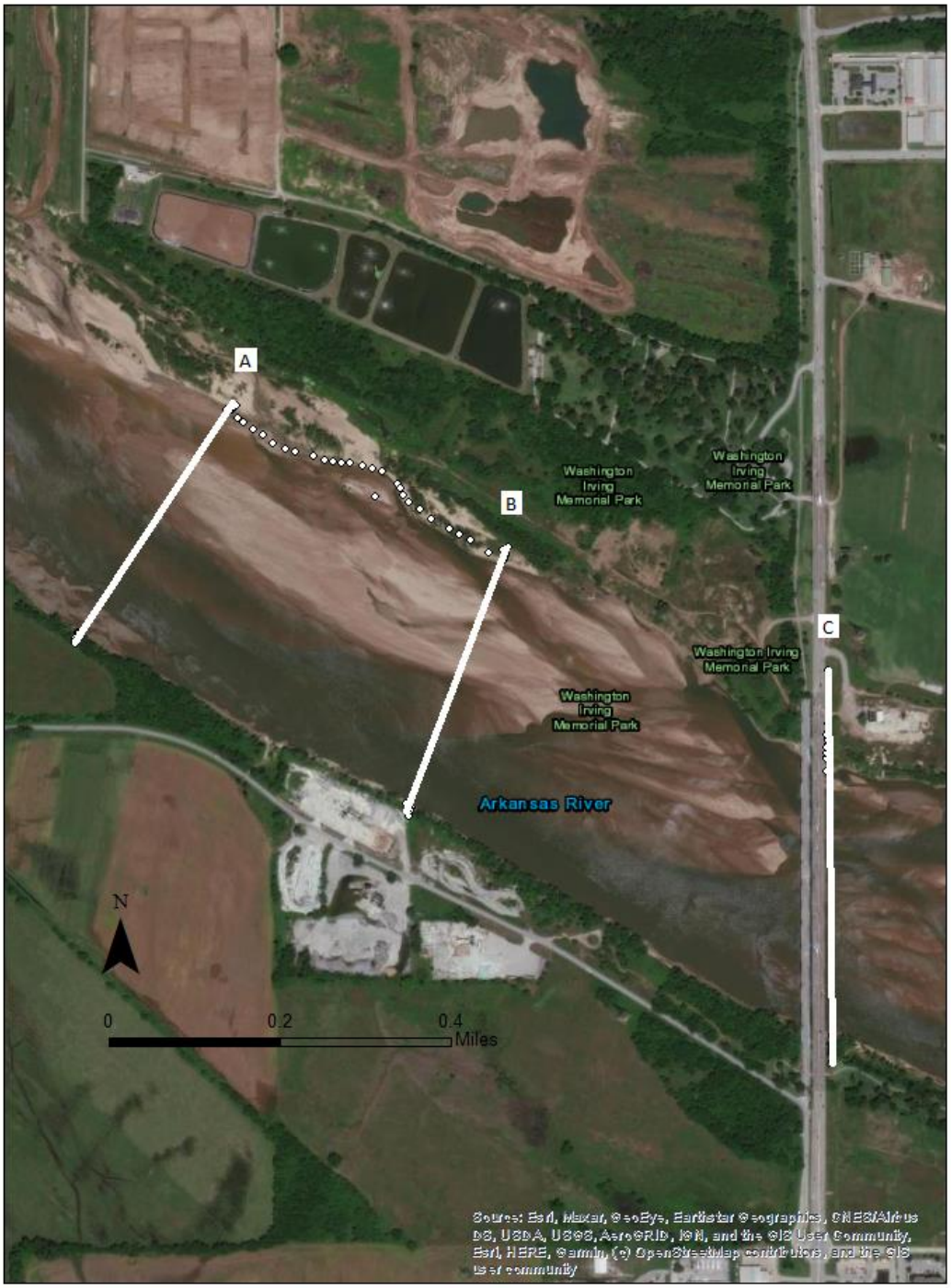

Figure A3: Site 5, Arkansas River and U.S. 64 north of Bixby in Tulsa county, thalweg data points and cross section locations.

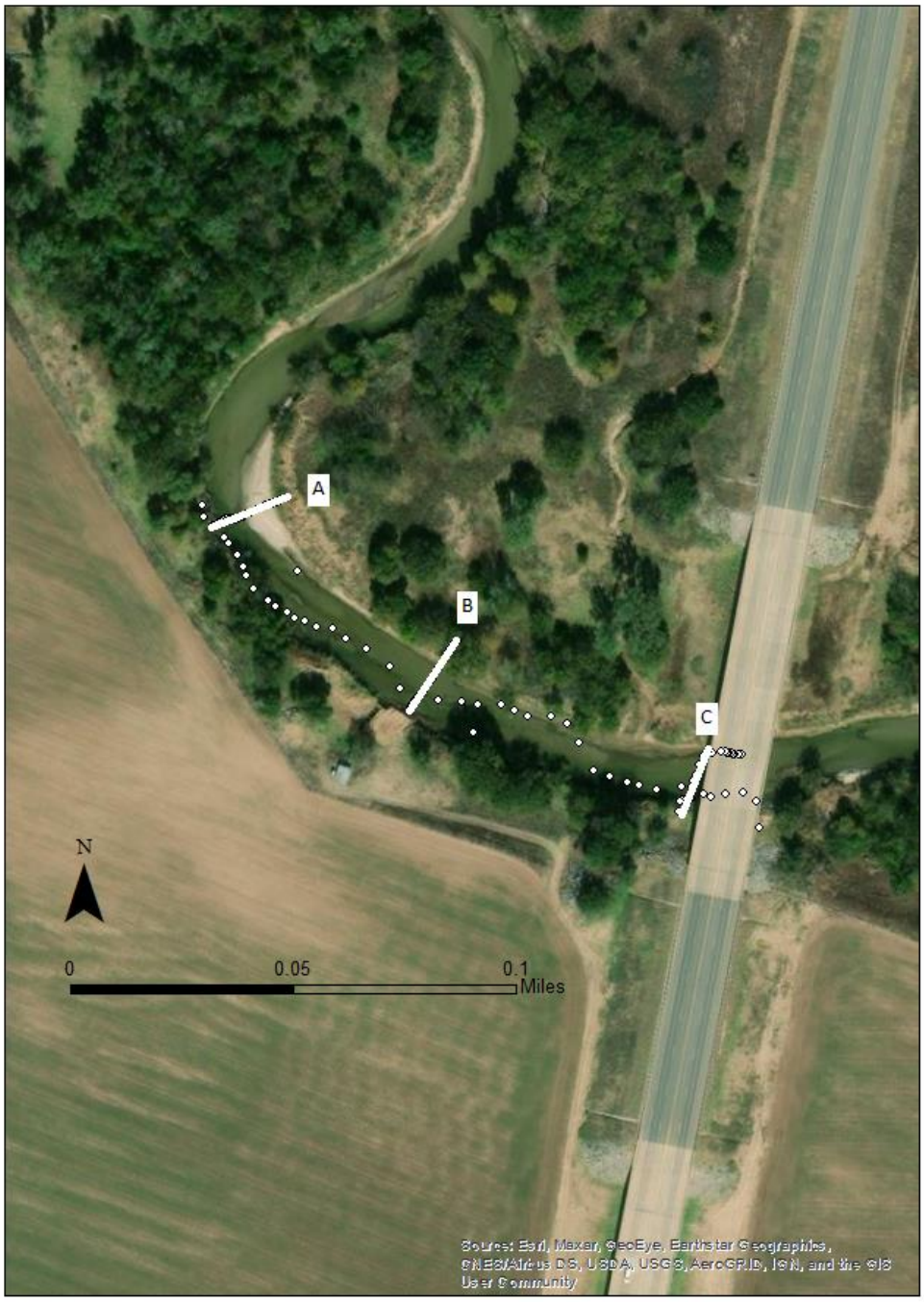

Figure A4: Site 6, North Canadian River and U.S. 281 south Watonga in Blaine county, thalweg data points and cross section locations.

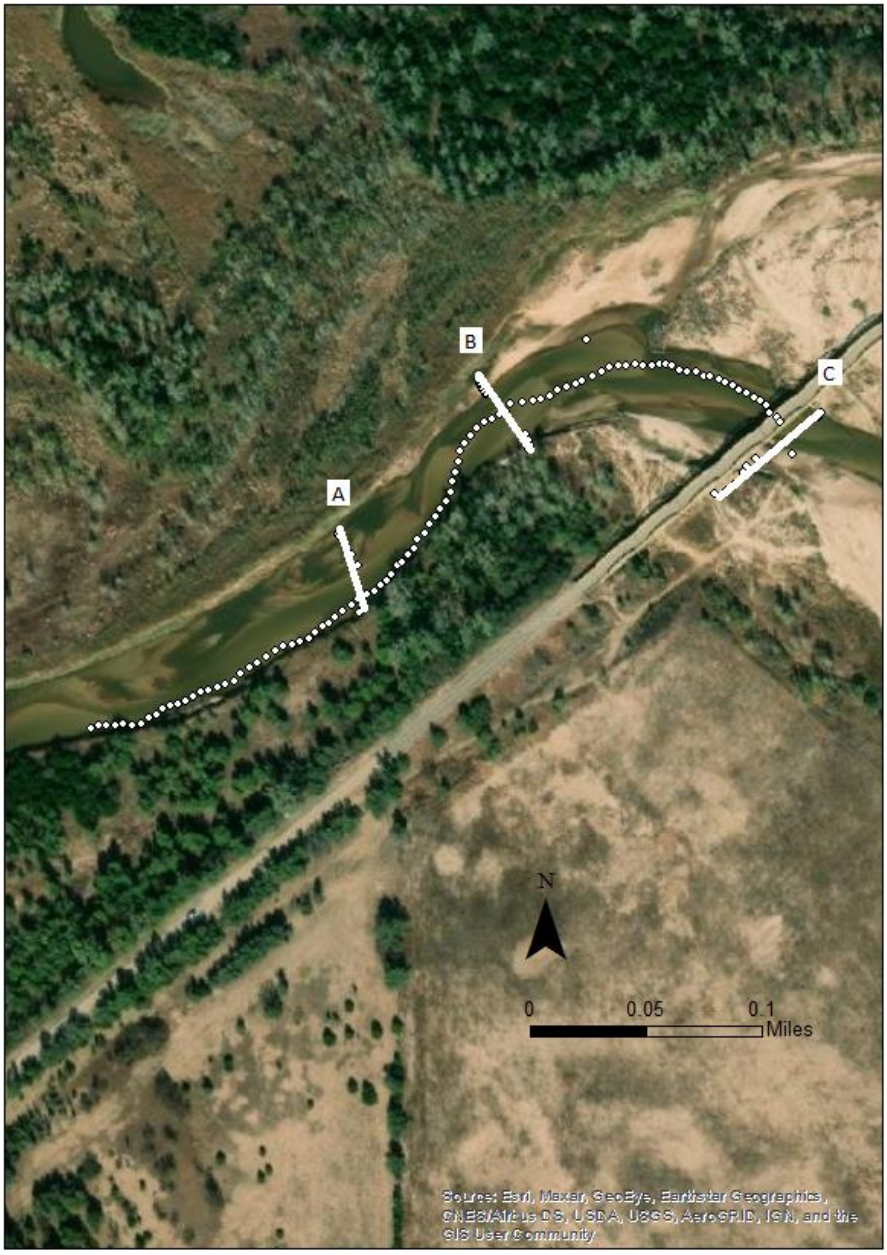

Figure A5: Site 7, Canadian River and U.S. 281 east of Bridgeport in Canadian county, thalweg data points and cross section locations.

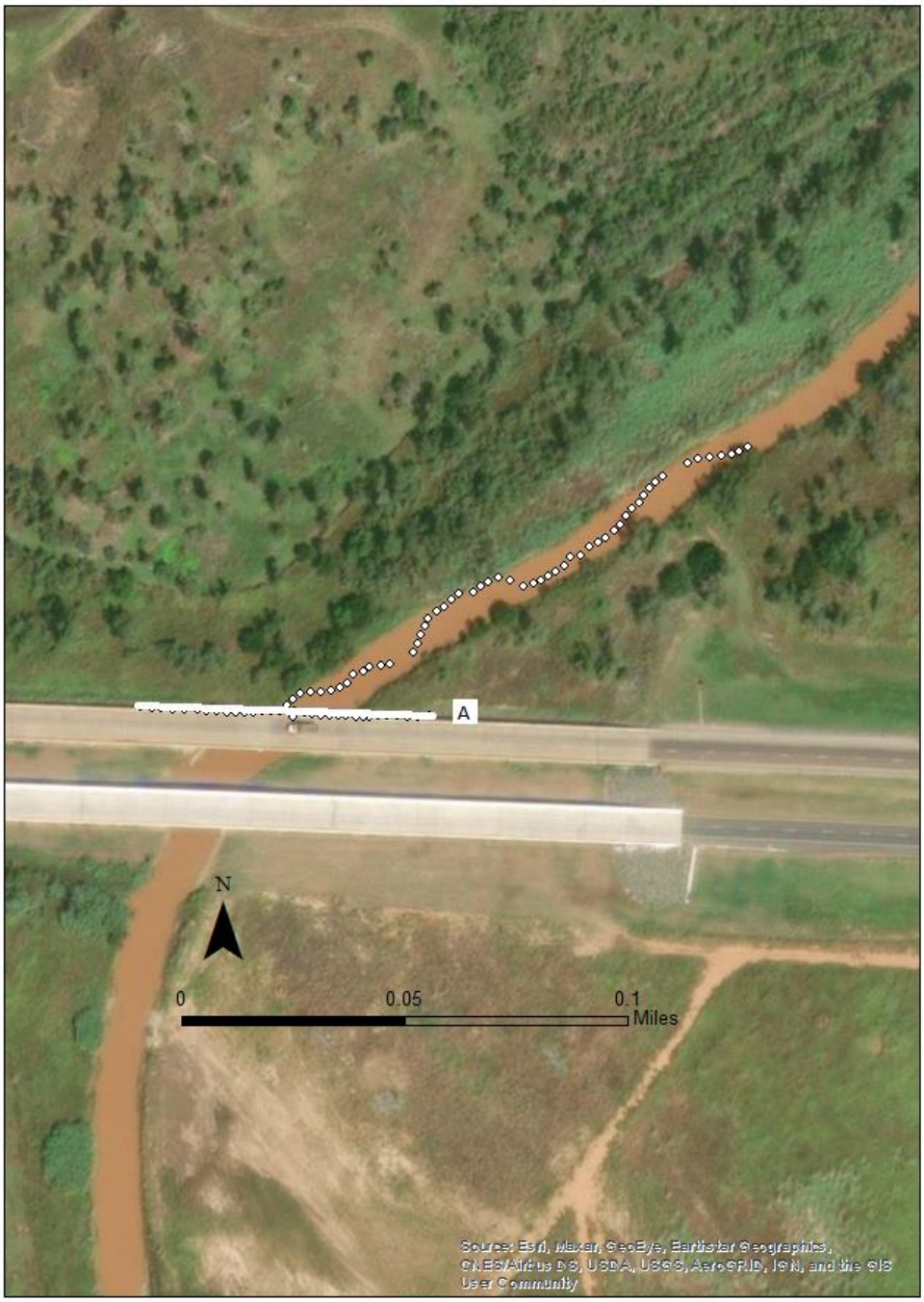

Figure A6: Site 8, Salt Fork of the Red River and U.S. 62 west of Altus in Jackson county, thalweg data points and cross section locations.

Figure A7: Site 10, Washita River and S.H. 76 south of Lindsay in Garvin county, thalweg data points and cross section locations.

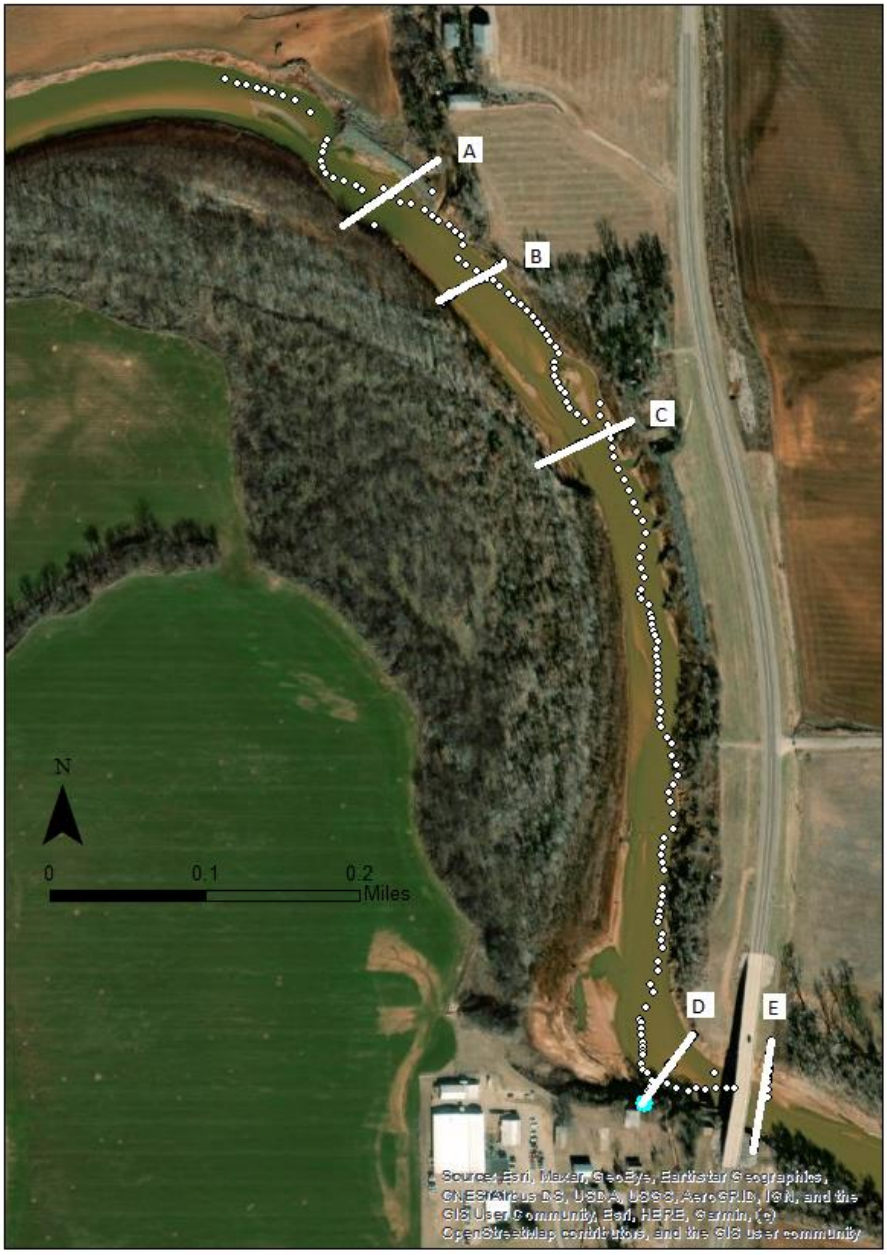

Figure A8: Site 11, Washita River and S.H. 74 north of Maysville in Garvin county, thalweg data points and cross section locations.

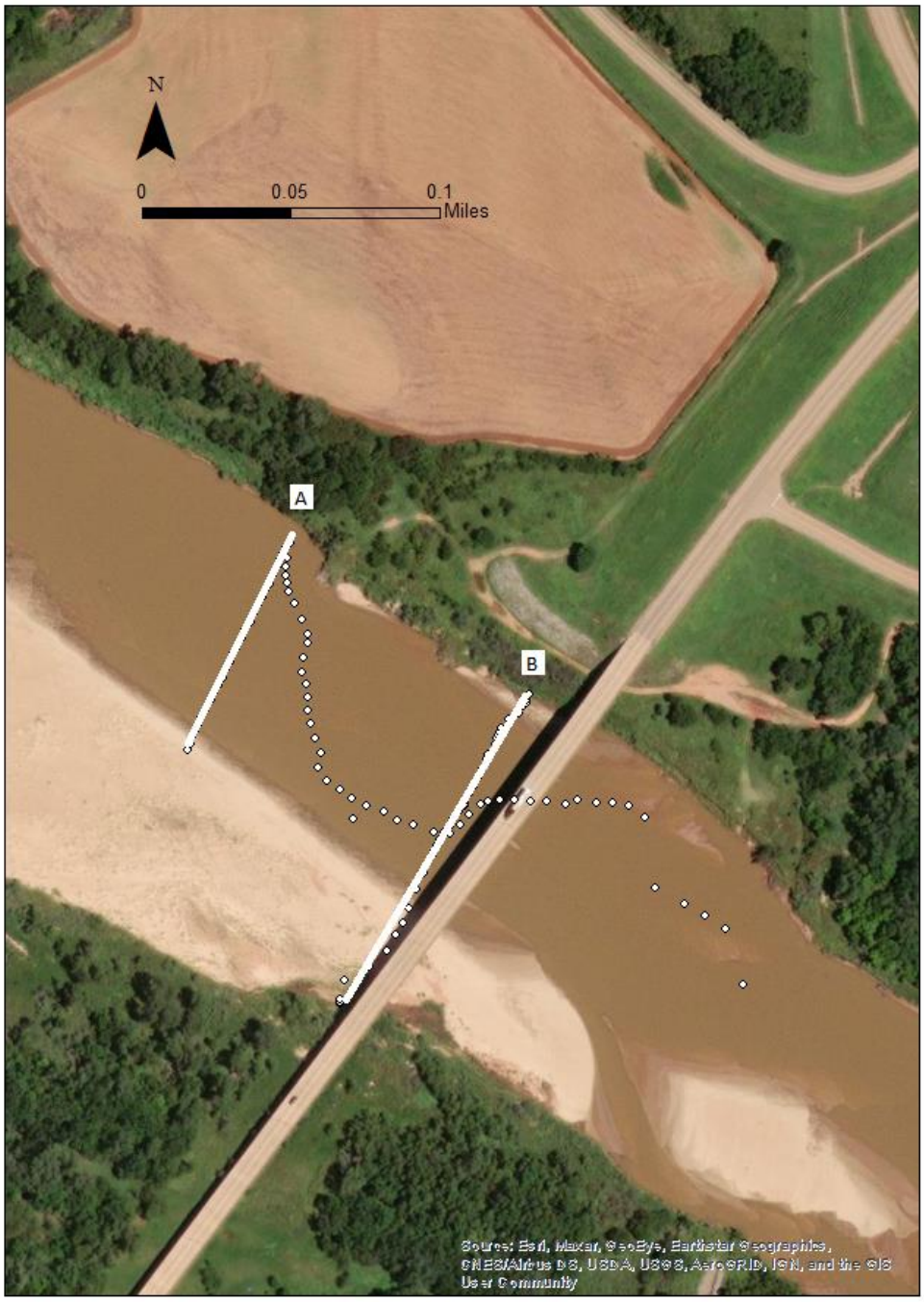

Figure A9: Site 12, Cimarron River and S.H. 33 north of Coyle in Logan county, thalweg data points and cross section locations.

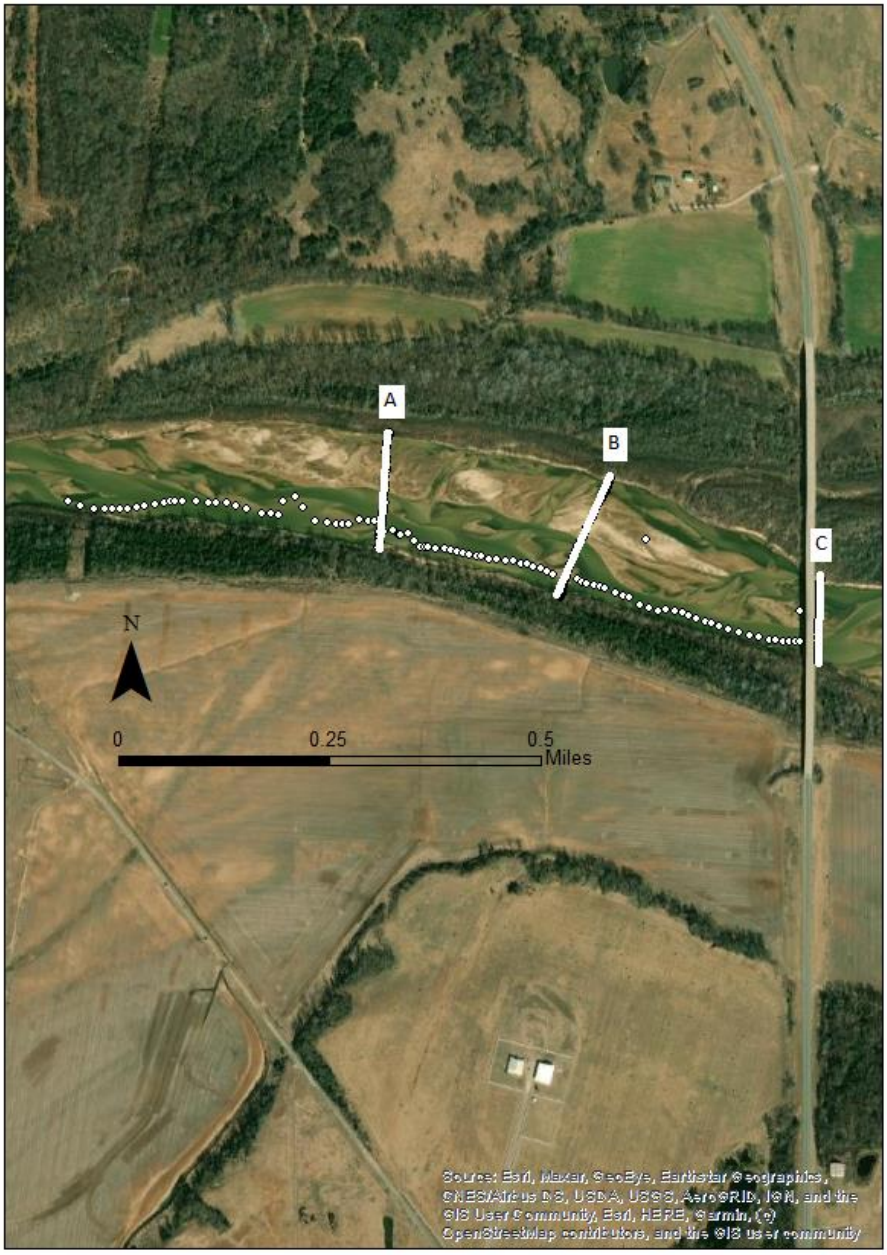

Figure A10: Site 13, Canadian River and S.H. 48 north of Atwood in Cotton county, thalweg data points and cross section locations.

Figure A11: Site 14, North Canadian River and S.H. 84 north of Dustin in Okfuskee county, thalweg data points and cross section locations.

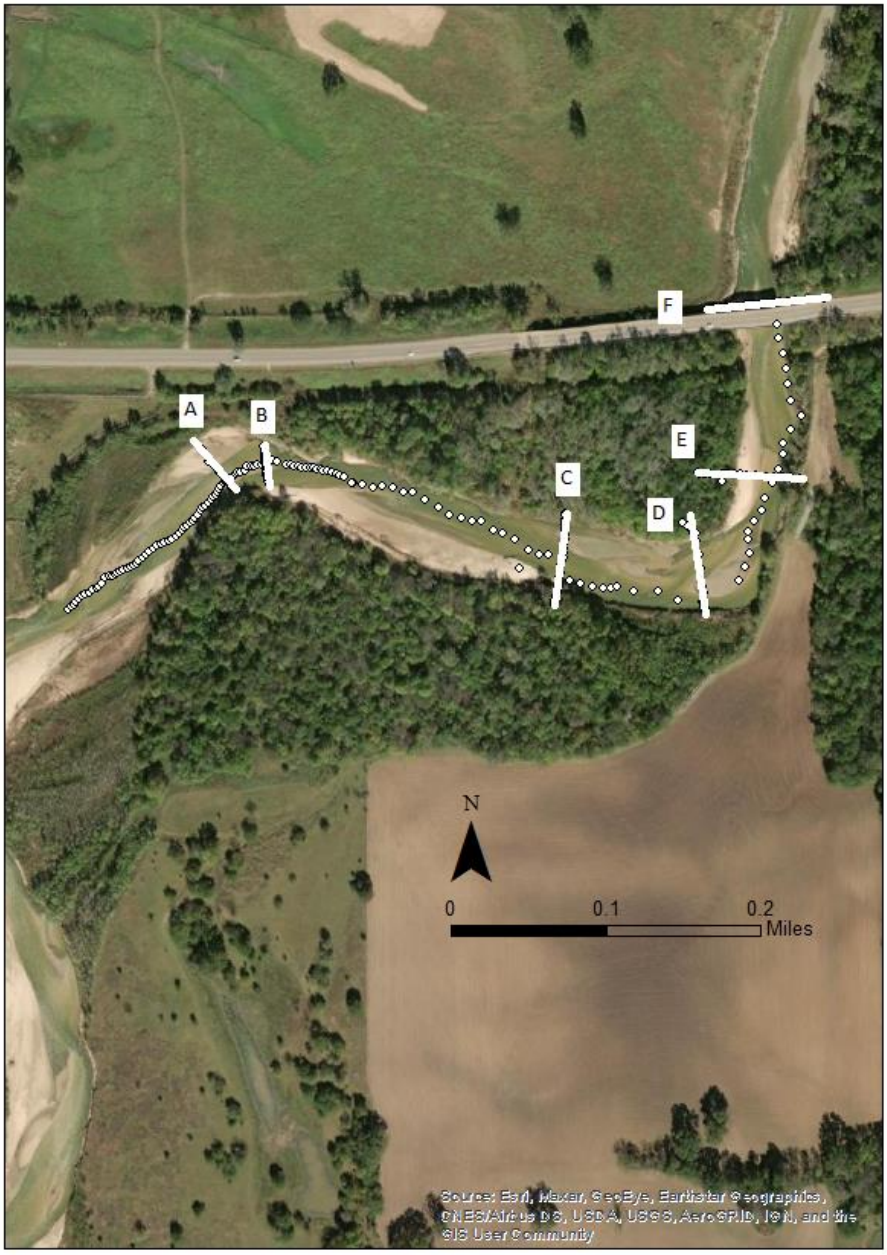

Figure A12: Site 16, North Canadian River and S.H. 3 east of Shawnee in Pottawatomie county, thalweg data points and cross section locations.

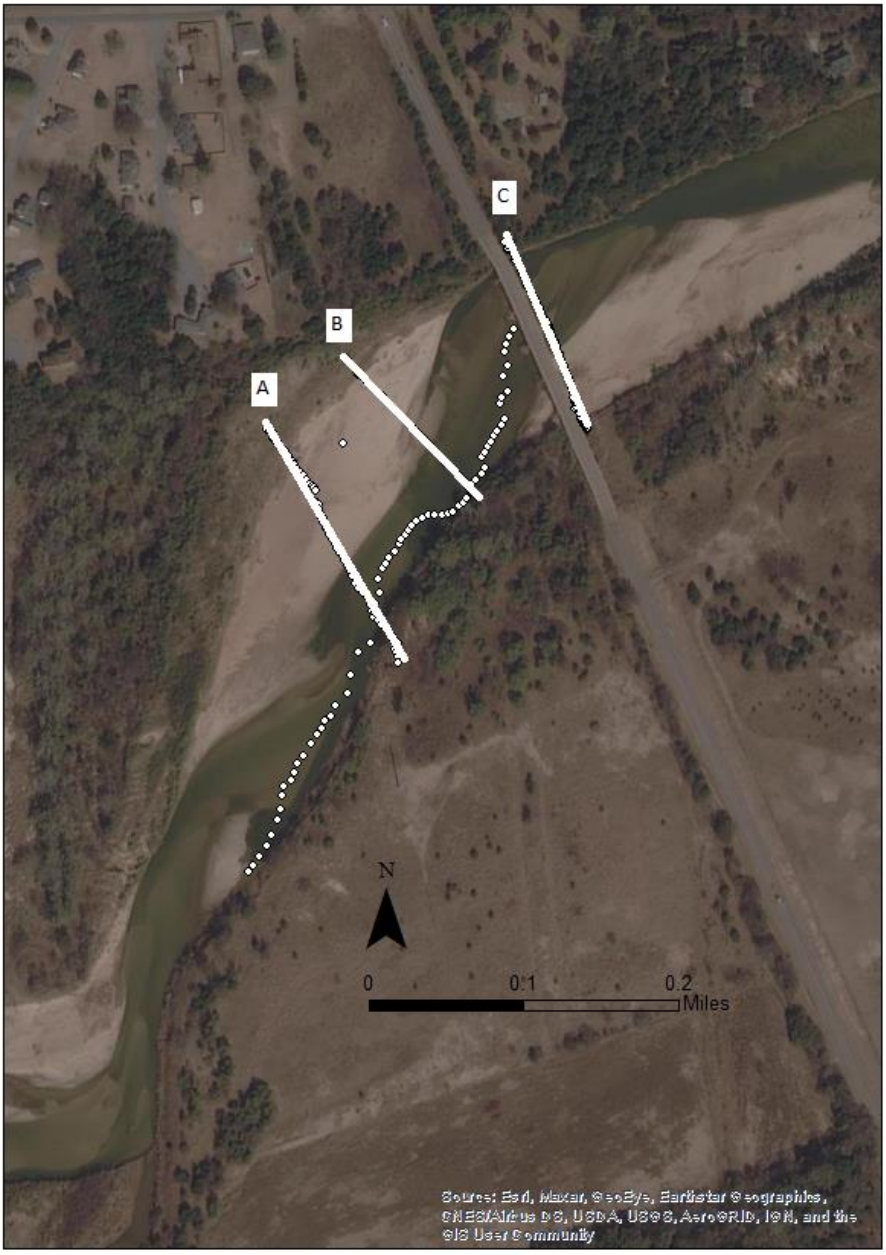

Figure A13: Site 17, Cimarron River and S.H. 74 south of Crescent in Logan county, thalweg data points and cross section locations.

Figure A14: Site 18, Washita River and U.S. 77 south of Davis in Murray county, thalweg data points and cross section locations.

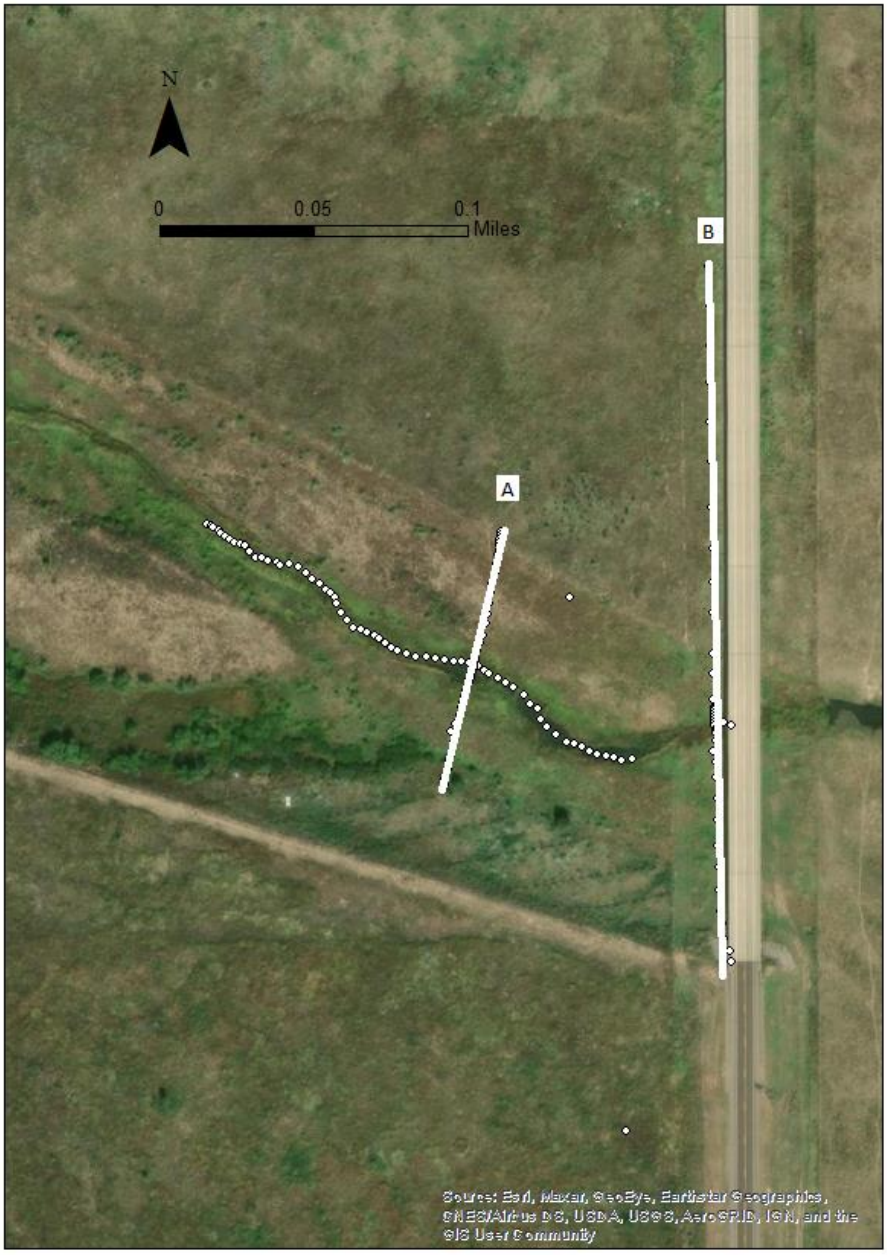

Figure A15: Site 19, Beaver River and U.S. 283 north of Laverne in Harper county, thalweg data points and cross section locations.

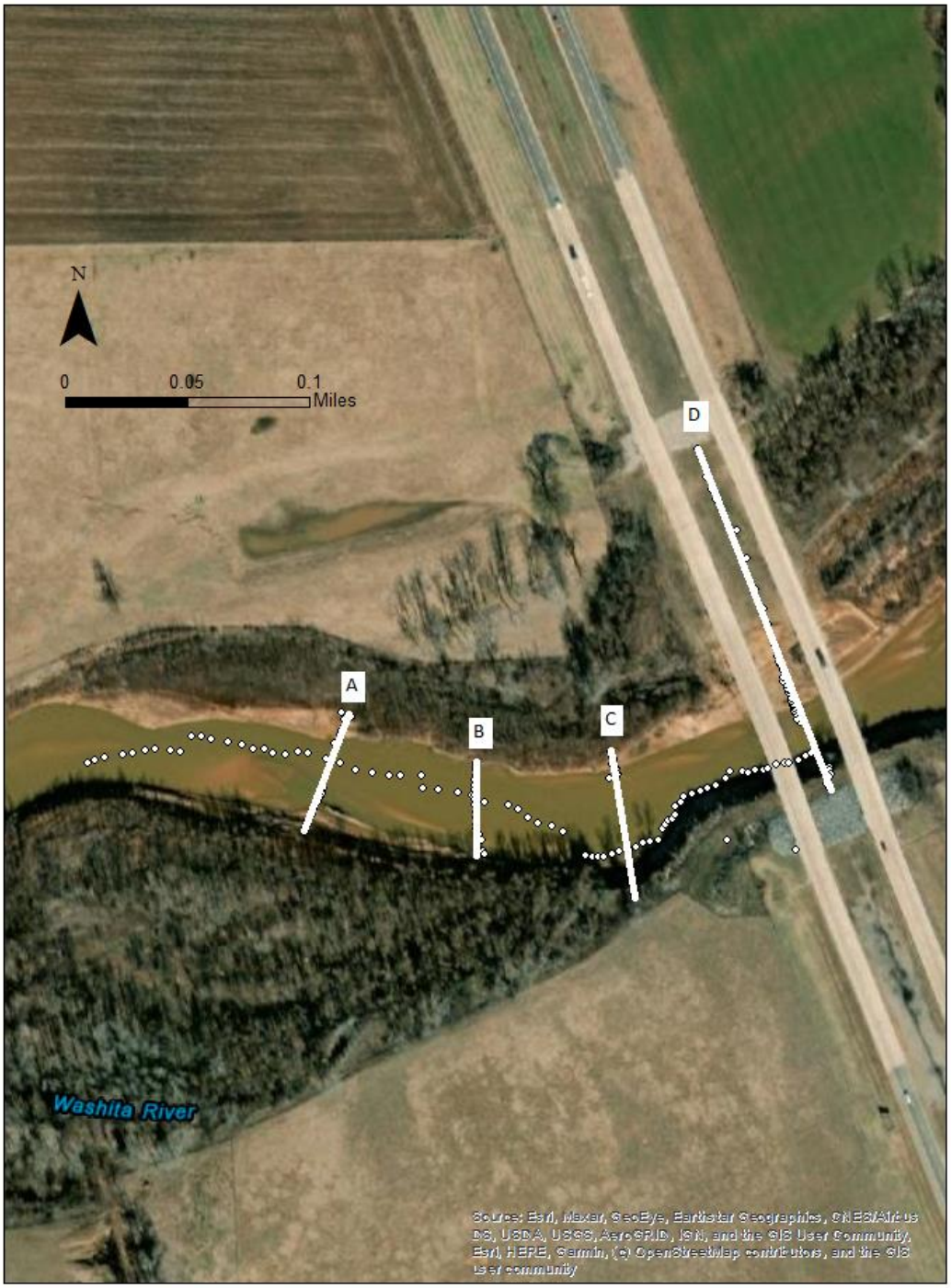

Figure A16: Site 20, Washita River and I-35 southwest of Paoli in Garvin county, thalweg data points and cross section locations.

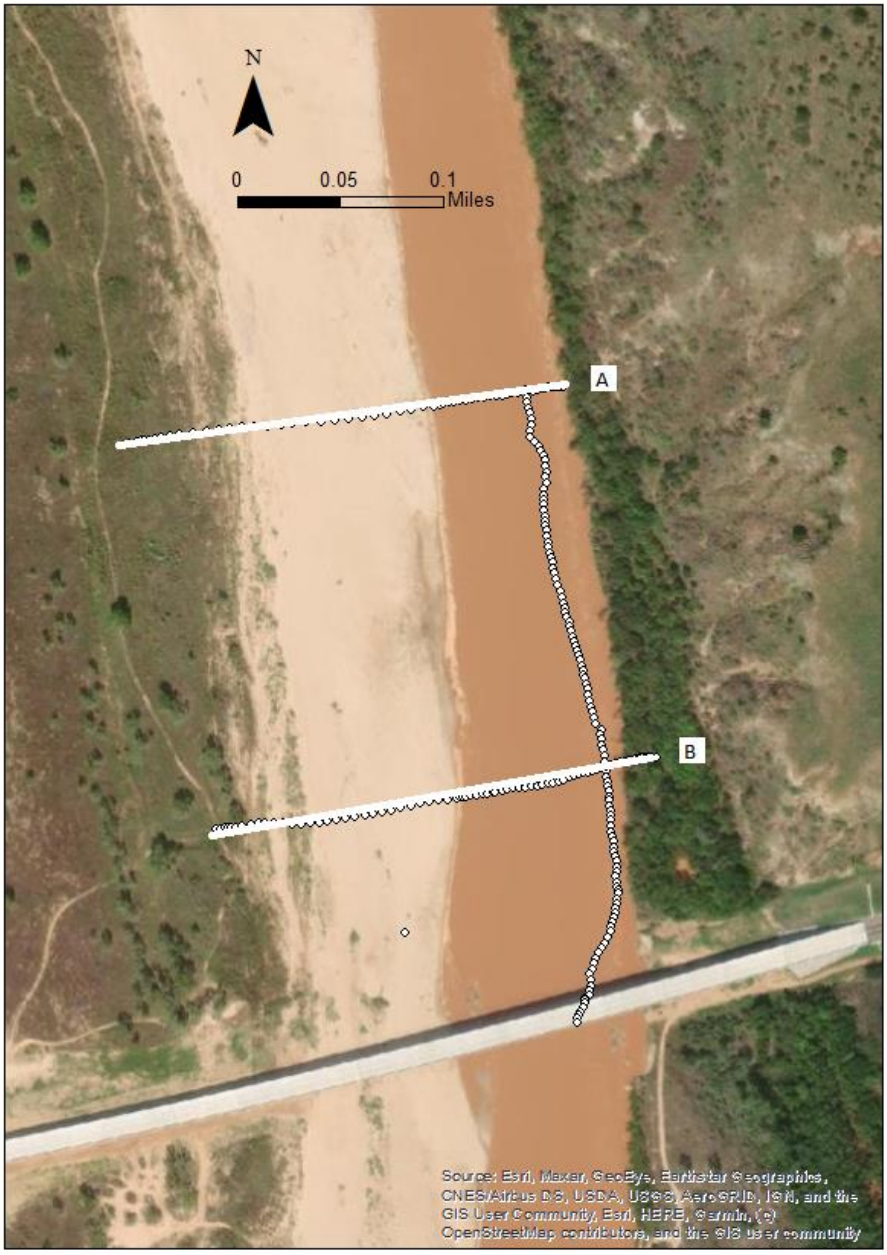

Figure A17: Site 21, Red River and S.H. 79 west of Waurika in Jefferson county, thalweg data points and cross section locations.

Figure A18: Site 22, Washita River and S.H. 53 east of Gene Autry in Carter county, thalweg data points and cross section locations.

Figure A19: Site 24, Red River and U.S. 259 south of Harris in McCurtain county, cross section locations.

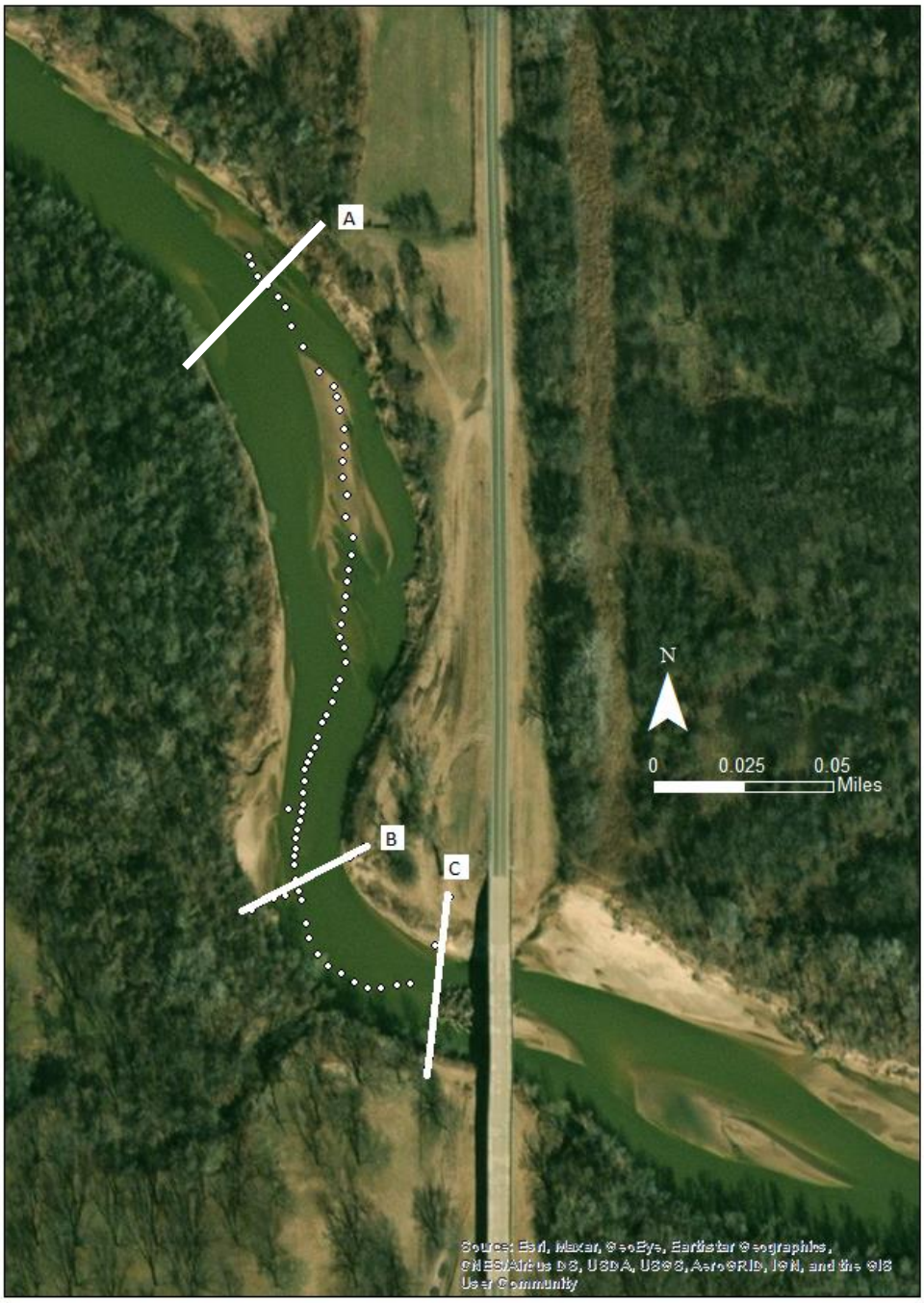

Figure A20: Site 25, North Canadian River and S.H. 48 north of Bearden in Okfuskee county, thalweg data points and cross section locations.

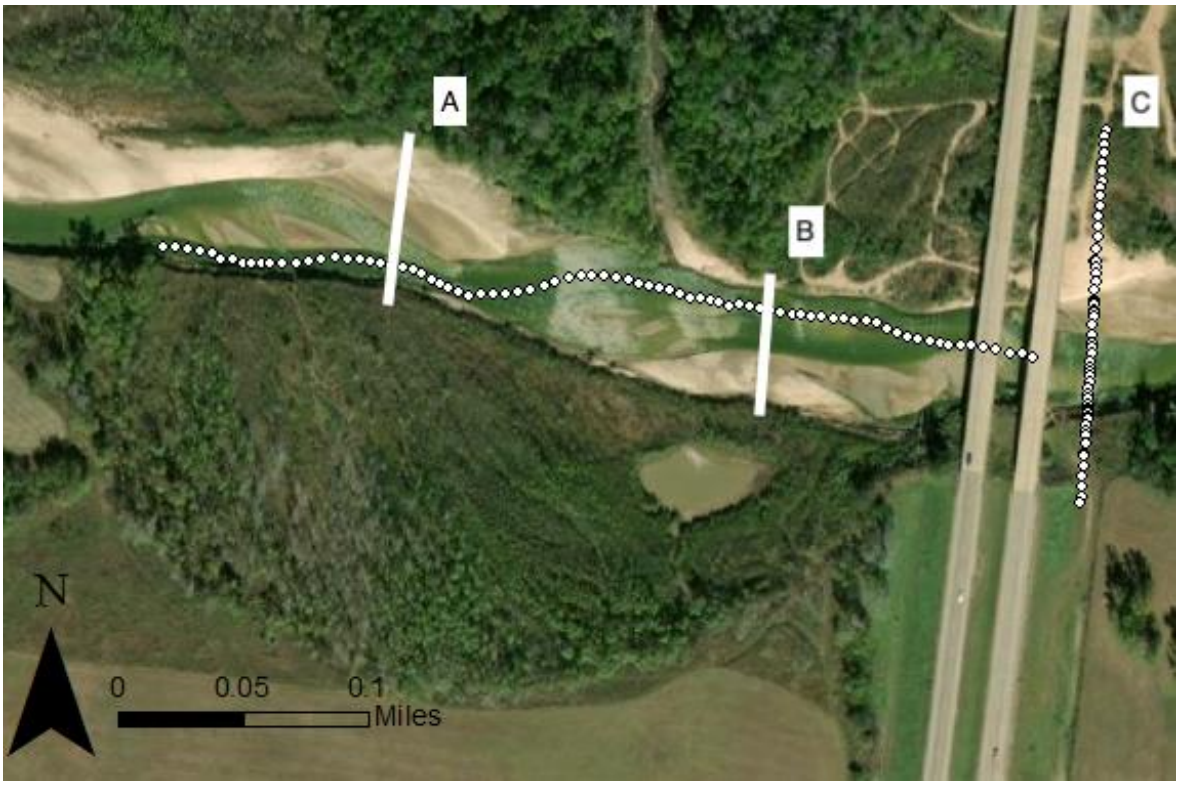

Figure A21: Site 27, North Canadian River and S.H. 99 south of Prague in Seminole county, thalweg data points and cross section locations.

Figure A22: Site 28, Illinois River and S.H. 10 east of Tahlequah in Cherokee county, thalweg data points and cross section locations.

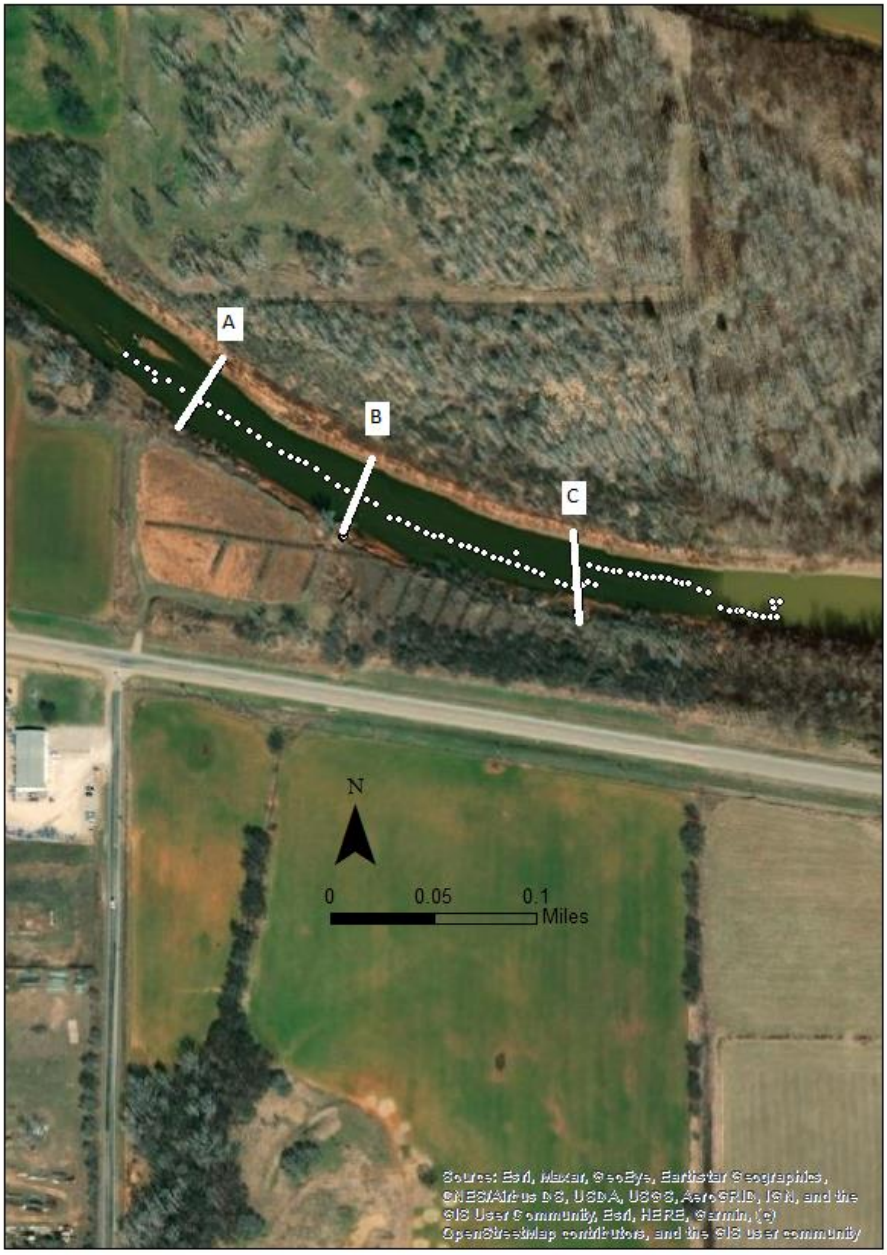

Figure A23: Site 29, Washita River and S.H. 19 east of Lindsay in Garvin county, thalweg data points and cross section locations.

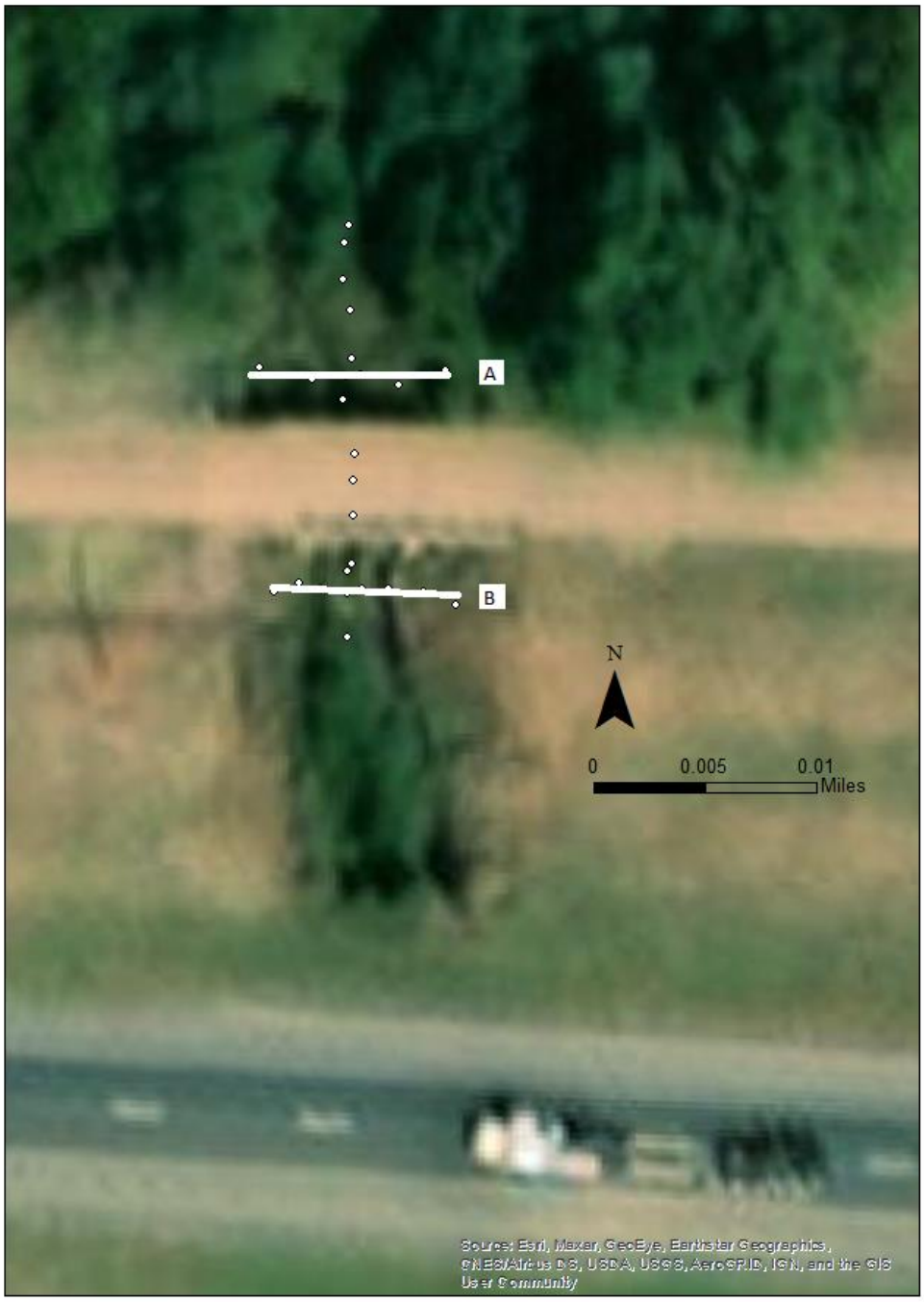

Figure A24: Site 31, Deer Creek Trib and U.S. 66 south of Hydro in Caddo county, thalweg data points and cross section locations.

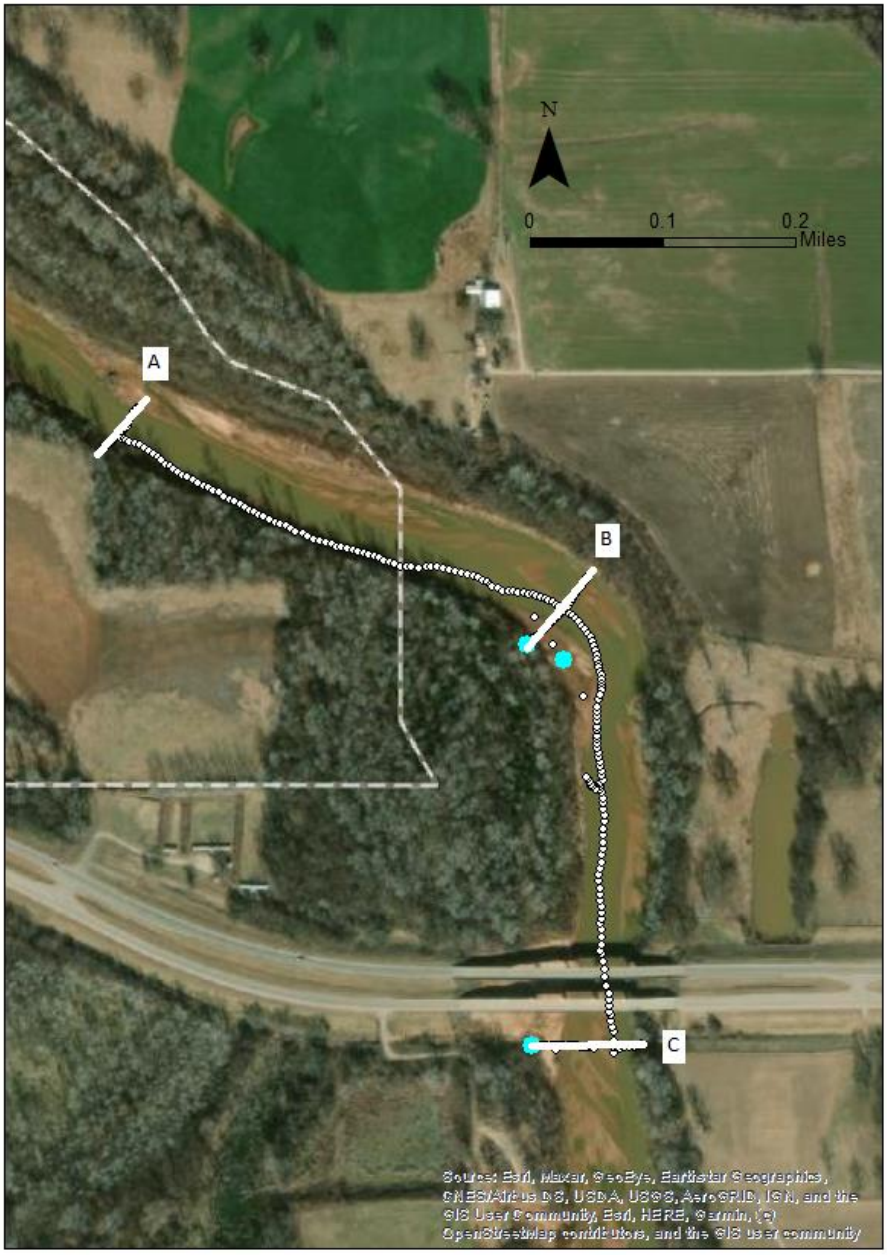

Figure A25: Site 32, Washita River and S.H. 7 west of Davis in Murray county, thalweg data points and cross section locations.

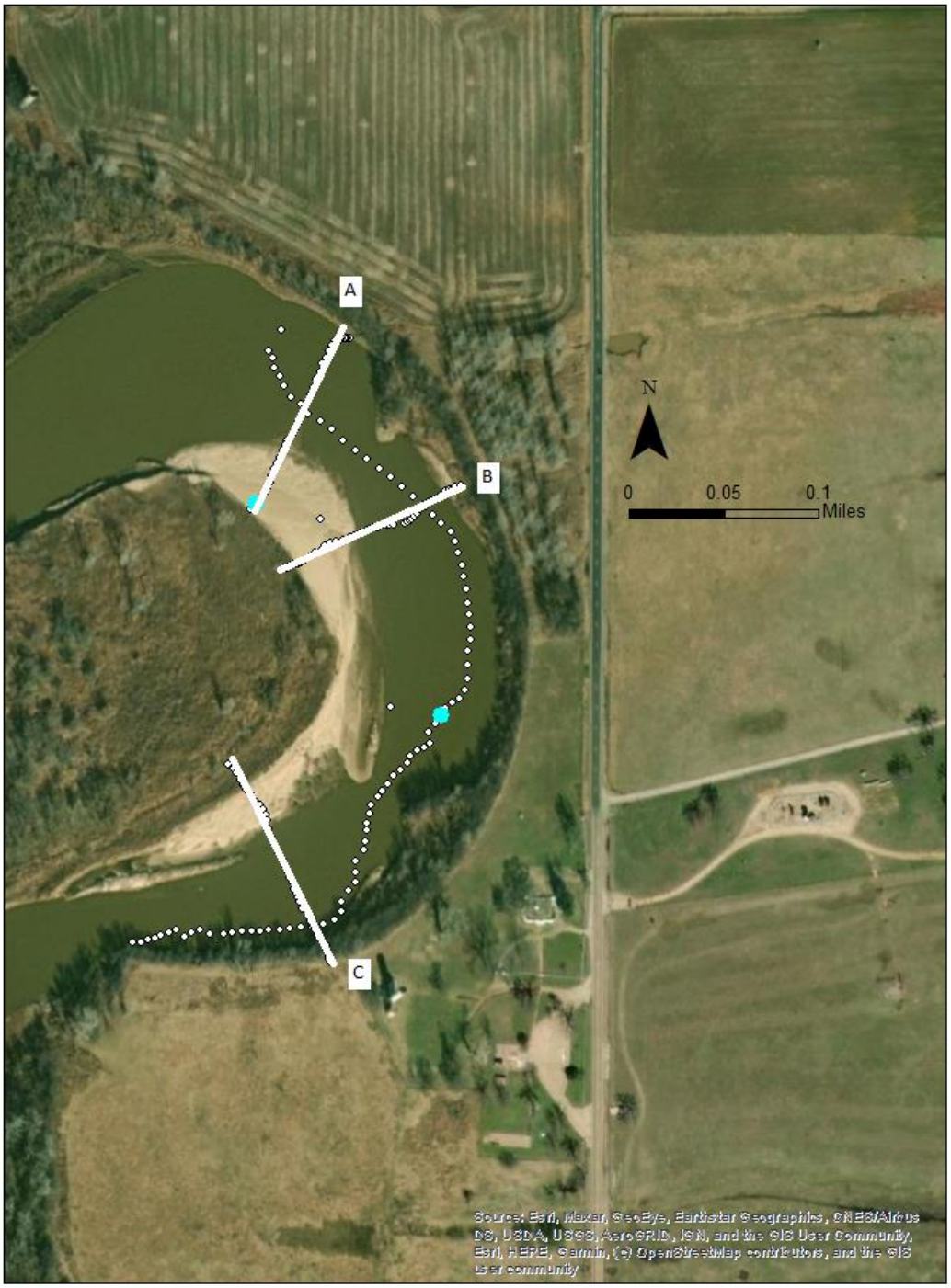

Figure A26: Site 33, Salt Fork of the Arkansas River and S.H. 156 north of Marland in Kay county, thalweg data points and cross section locations.

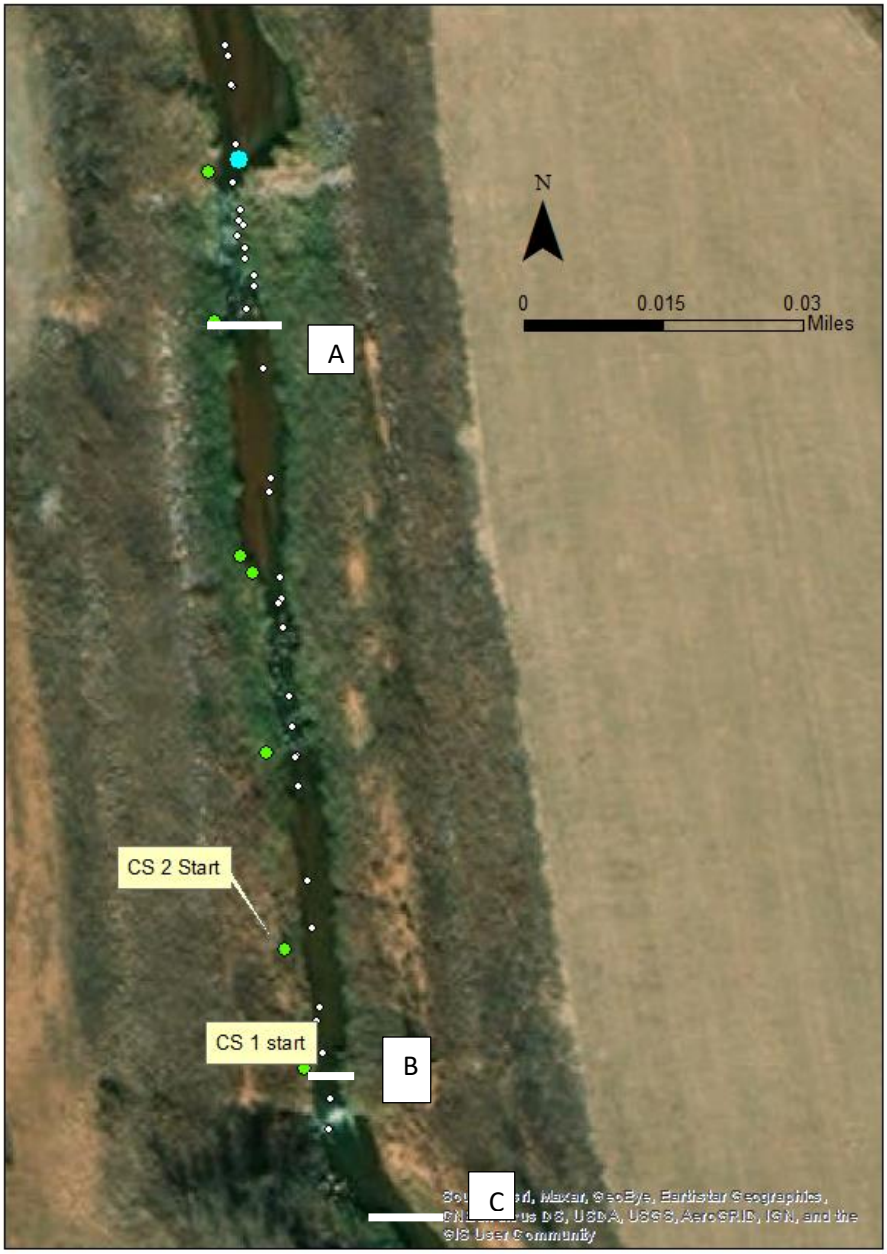

Figure A27: Site 34, Sugar Creek and U.S. 281 east of Binger in Caddo county, thalweg data points and cross section locations.

Appendix B – Longitudinal Profiles

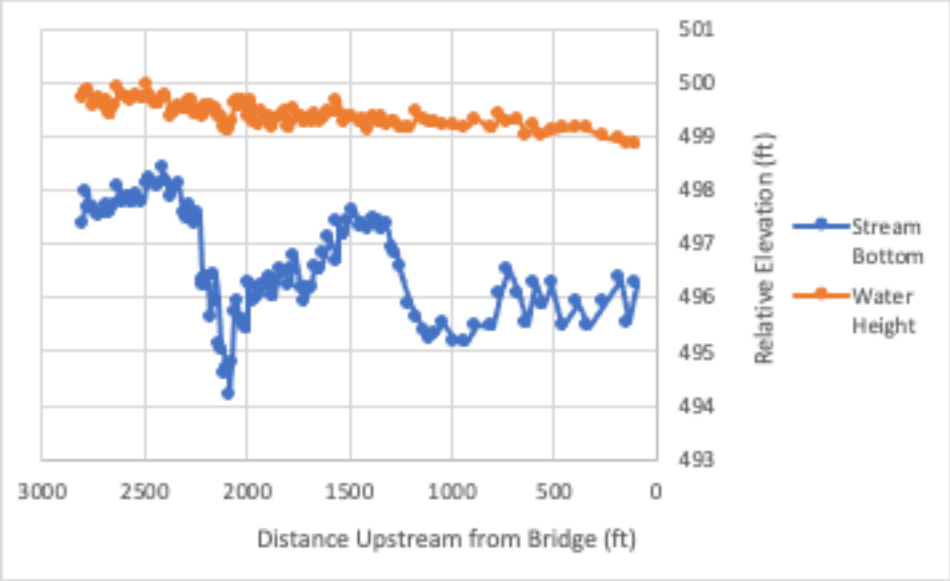

Figure B1: Site 1, Washita River and U.S. 77 north of Wynnewood in Garvin county, longitudinal profile

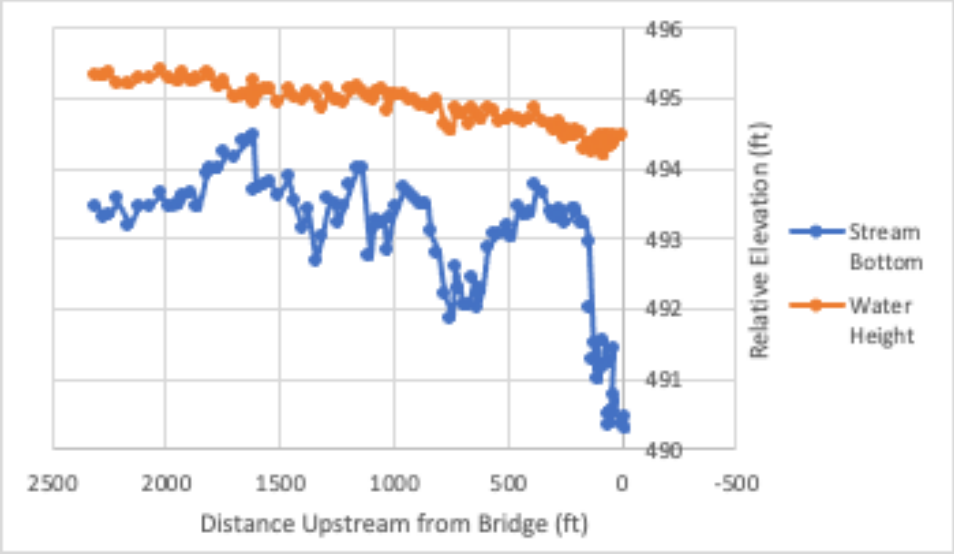

Figure B2: Site 2, Cimarron River and U.S. 177 south of Perkins in Payne county, longitudinal profile

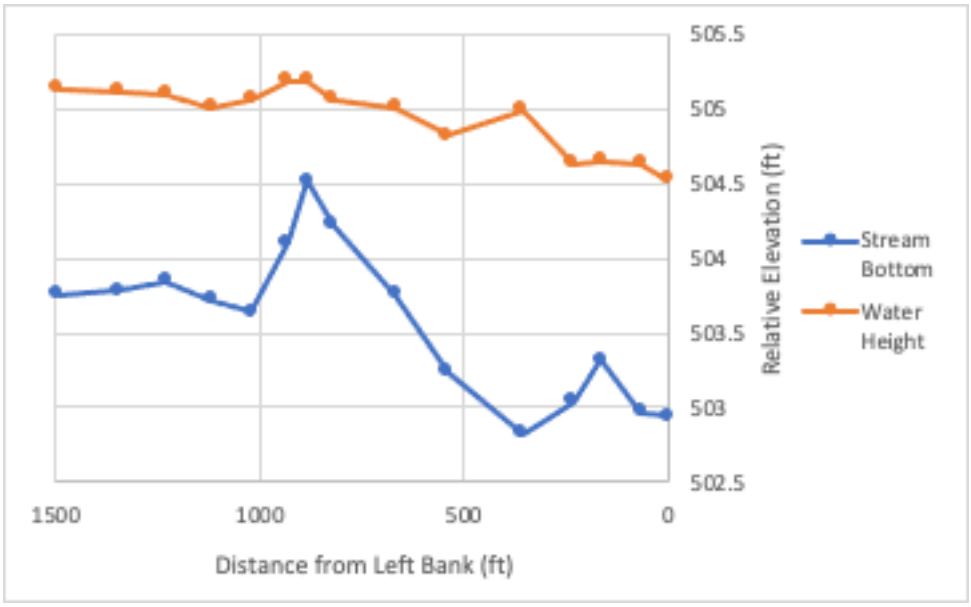

Figure B3: Site 4, Cimarron River and U.S. 281 south of Watonga in Blaine county, longitudinal profile

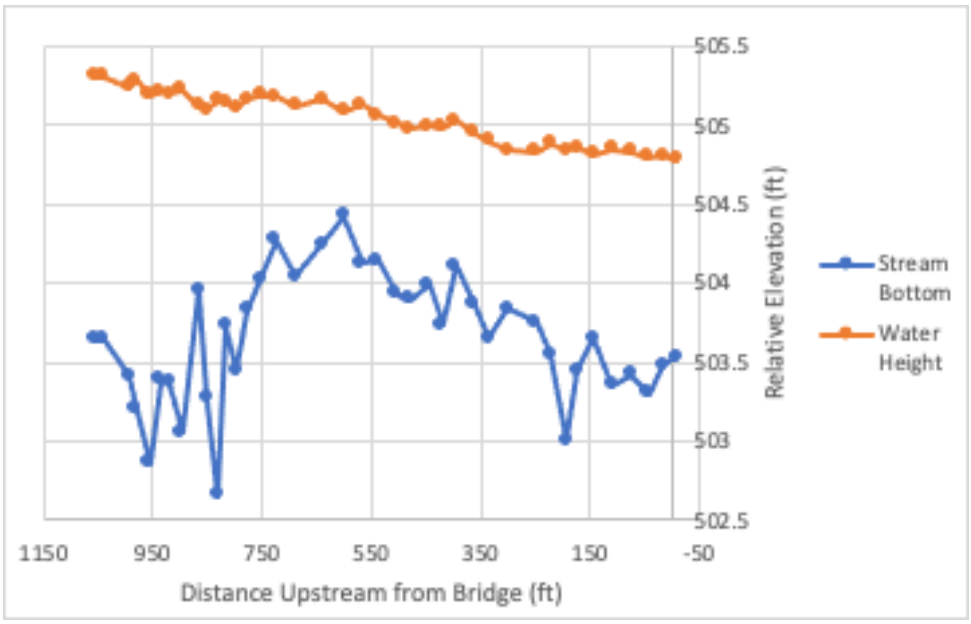

Figure B4: Site 6, North Canadian River and U.S. 281 south Watonga in Blaine county, longitudinal profile

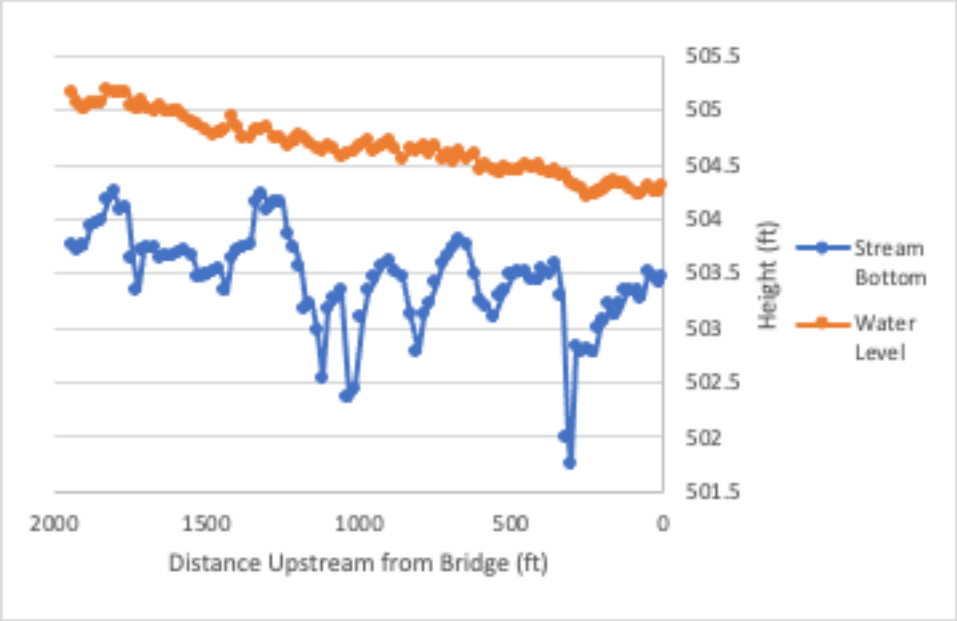

Figure B5: Site 7, Canadian River and U.S. 281 east of Bridgeport in Canadian county, longitudinal profile

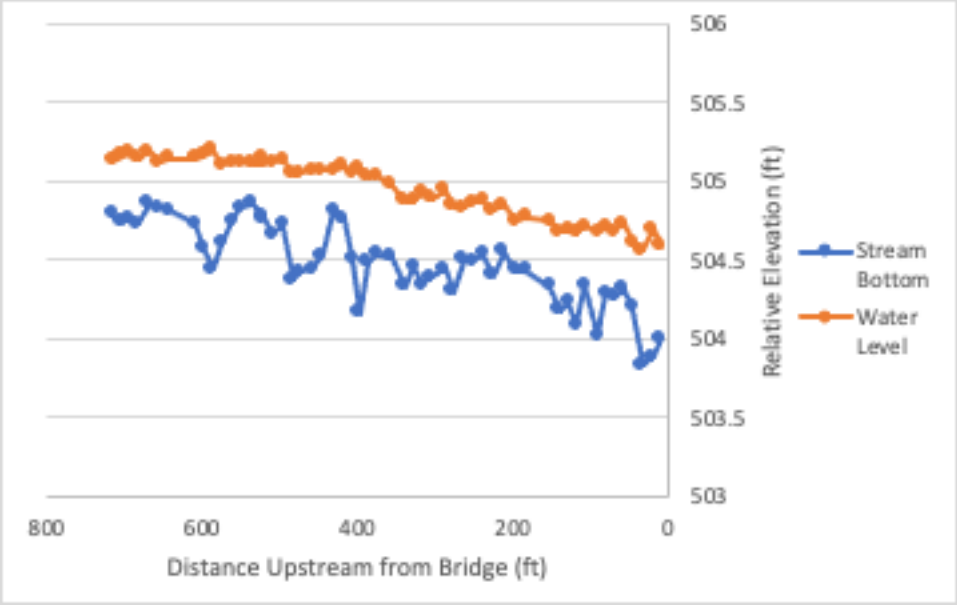

Figure B6: Site 8, Salt Fork of the Red River and U.S. 62 west of Altus in Jackson county, longitudinal profile

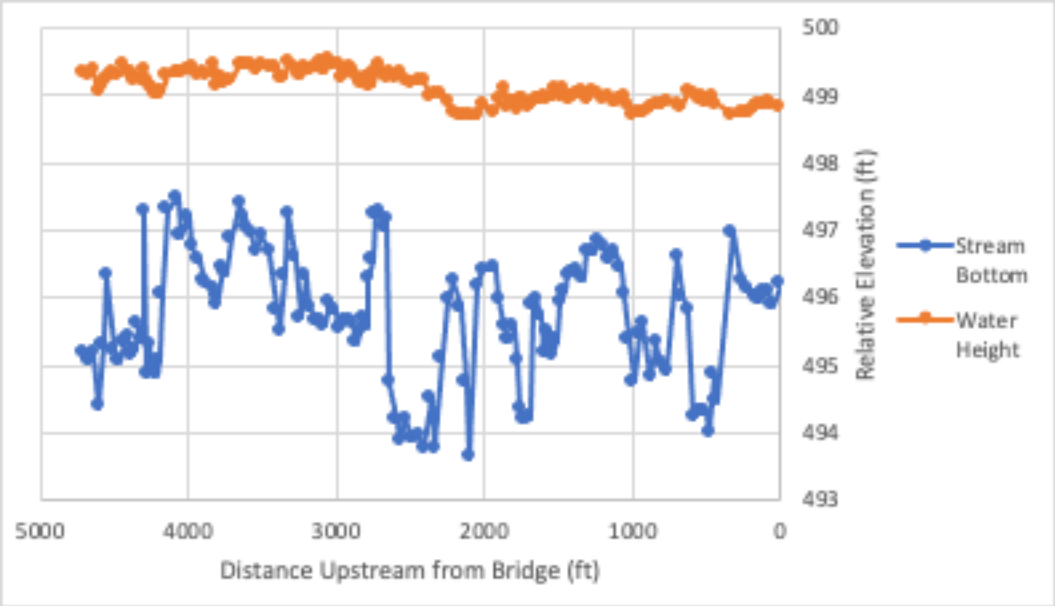

Figure B7: Site 11, Washita River and S.H. north of Maysville in Garvin county, longitudinal profile

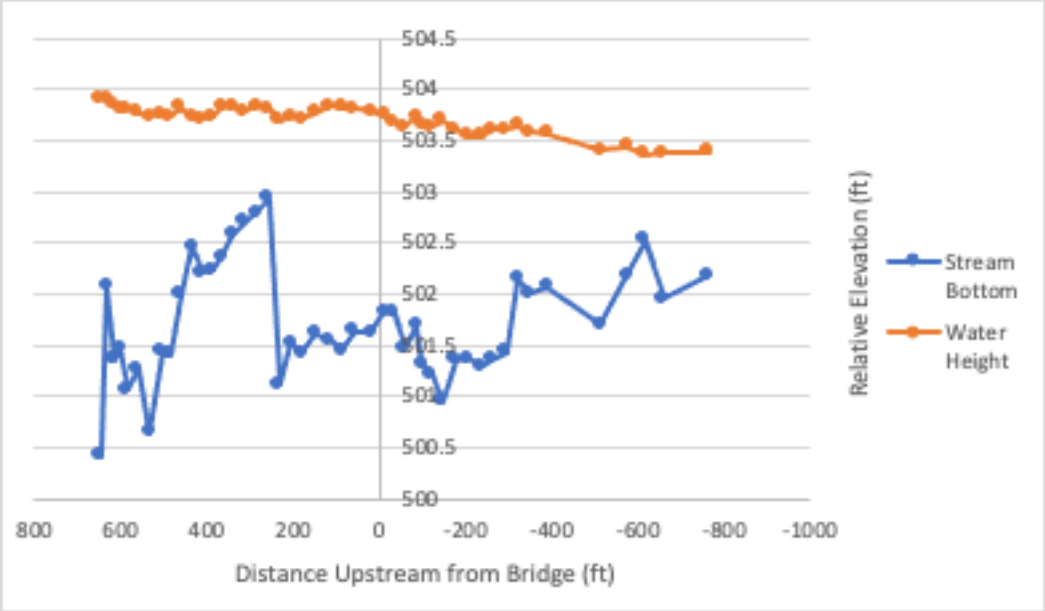

Figure B8: Site 12, Cimarron River and S.H. 33 north of Coyle in Logan county, longitudinal profile

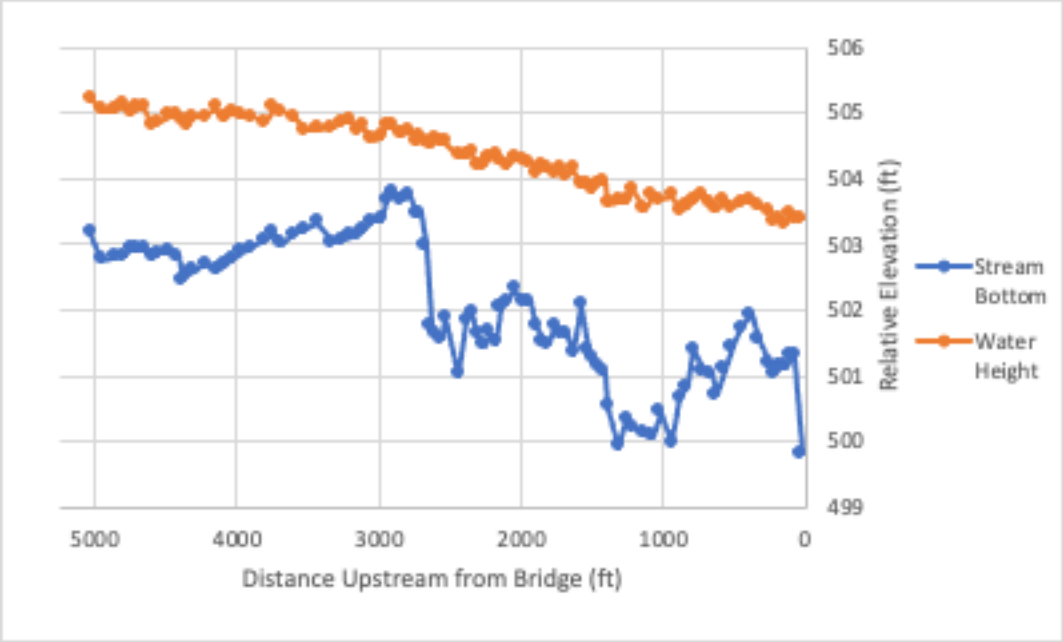

Figure B9: Site 13, Canadian River and S.H. 48 north of Atwood in Cotton county, longitudinal profile

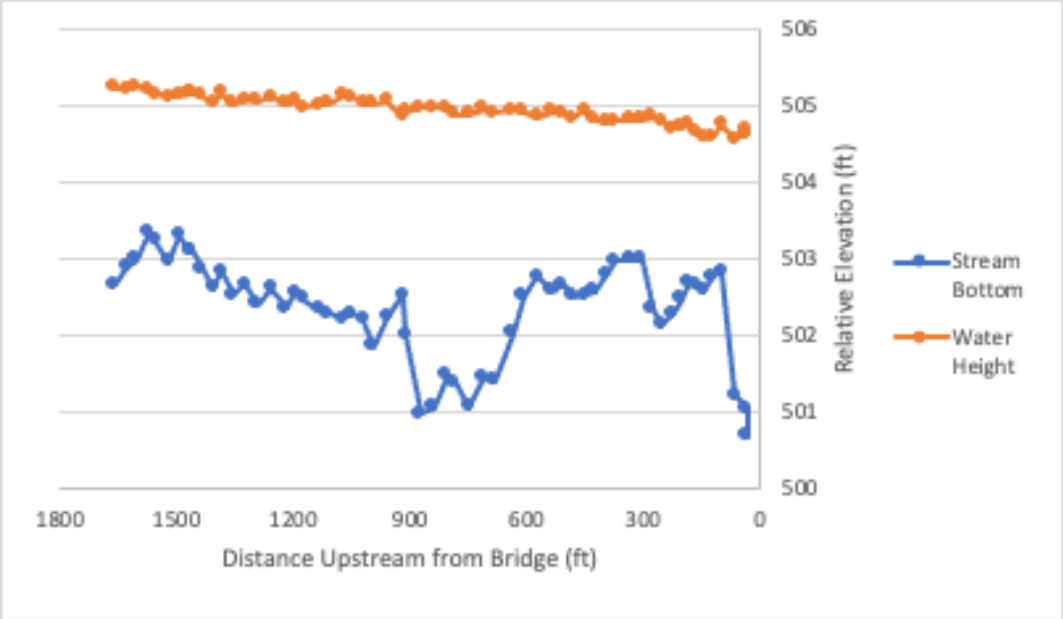

Figure B10: Site 14, North Canadian River and S.H. 84 north of Dustin in Okfuskee county, longitudinal profile

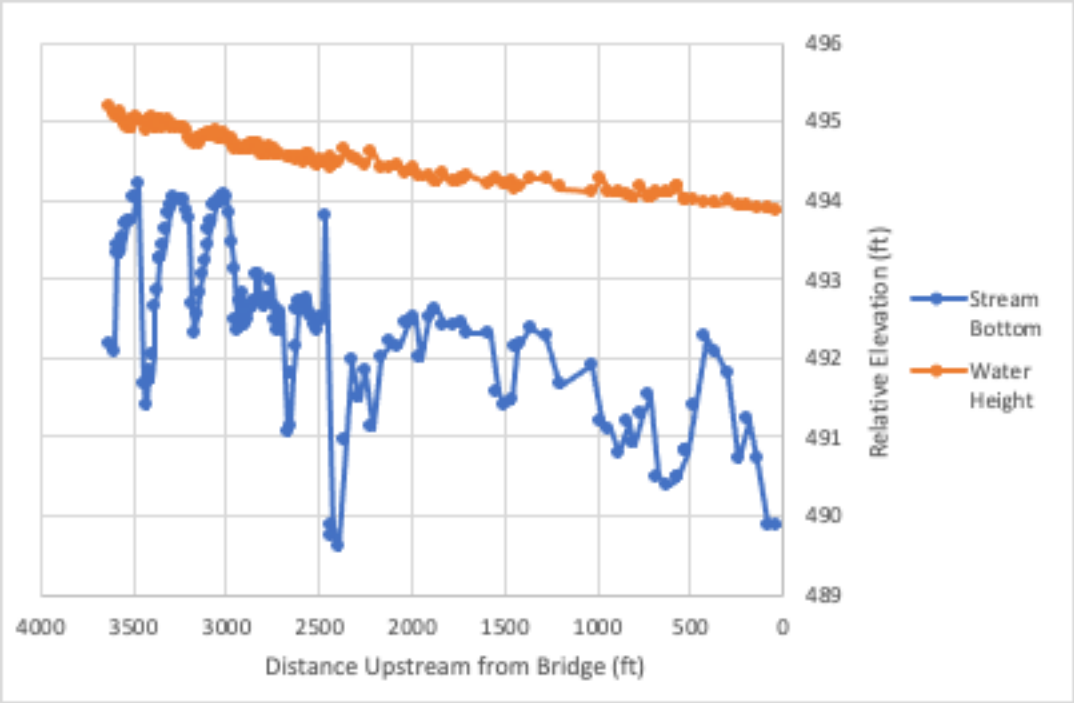

Figure B11: Site 16, North Canadian River and S.H. 3 east of Shawnee in Pottawatomie county, longitudinal profile

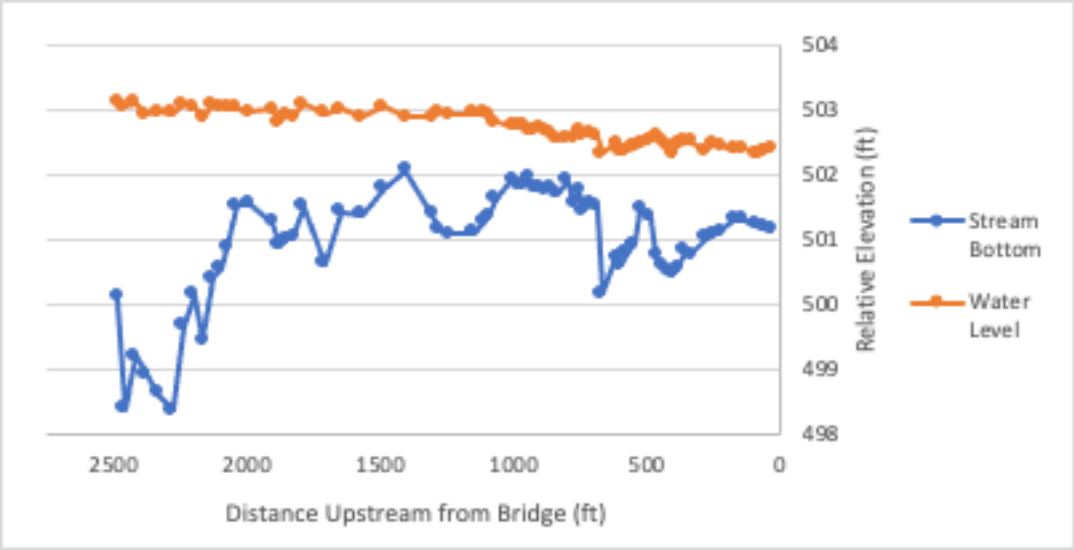

Figure B12: Site 17, Cimarron River and S.H. 74 south of Crescent in Logan county, longitudinal profile

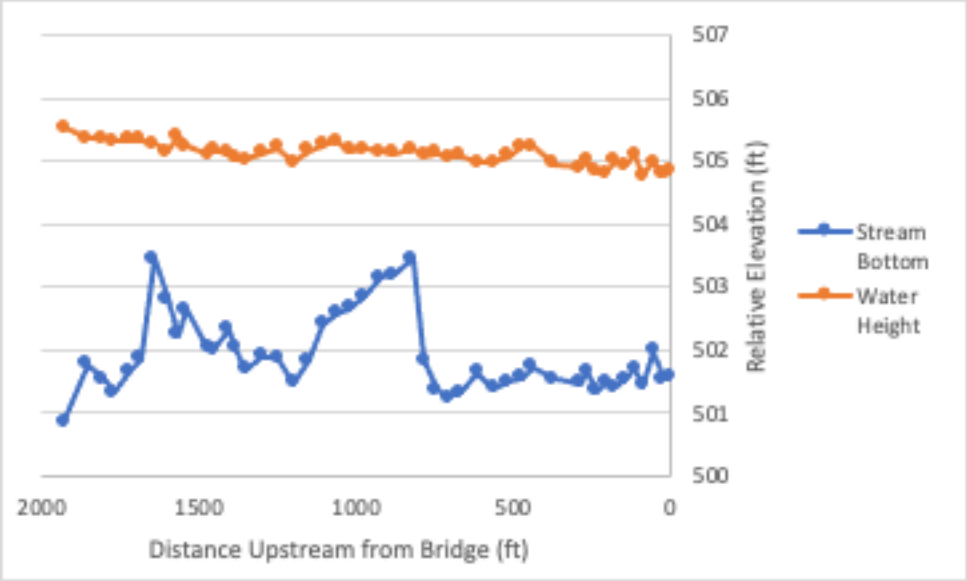

Figure B13: Site 18, Washita River and U.S. 77 south of Davis in Murray county, longitudinal profile

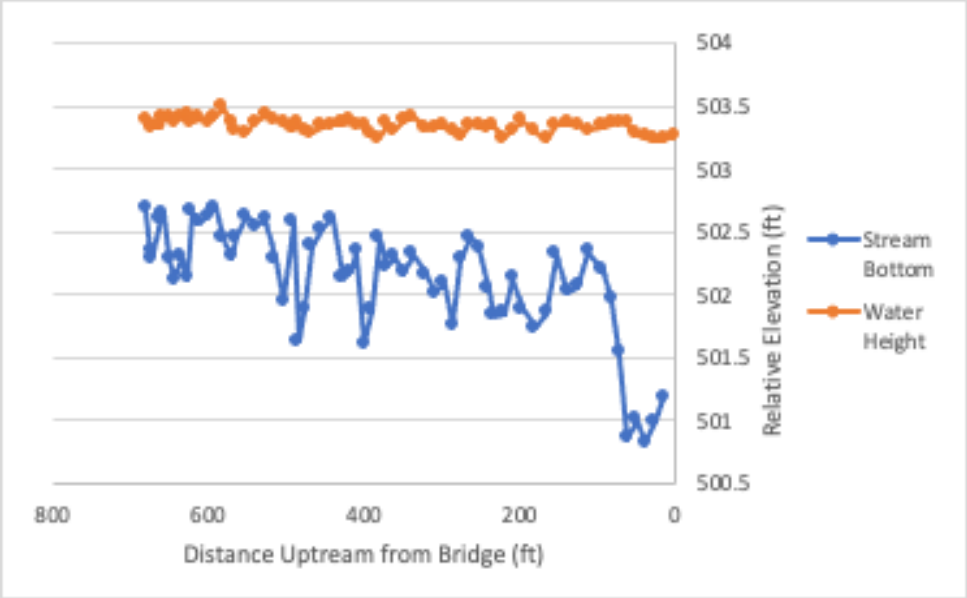

Figure B14: Site 19, Beaver River and U.S. 283 north of Laverne in Harper county, longitudinal profile

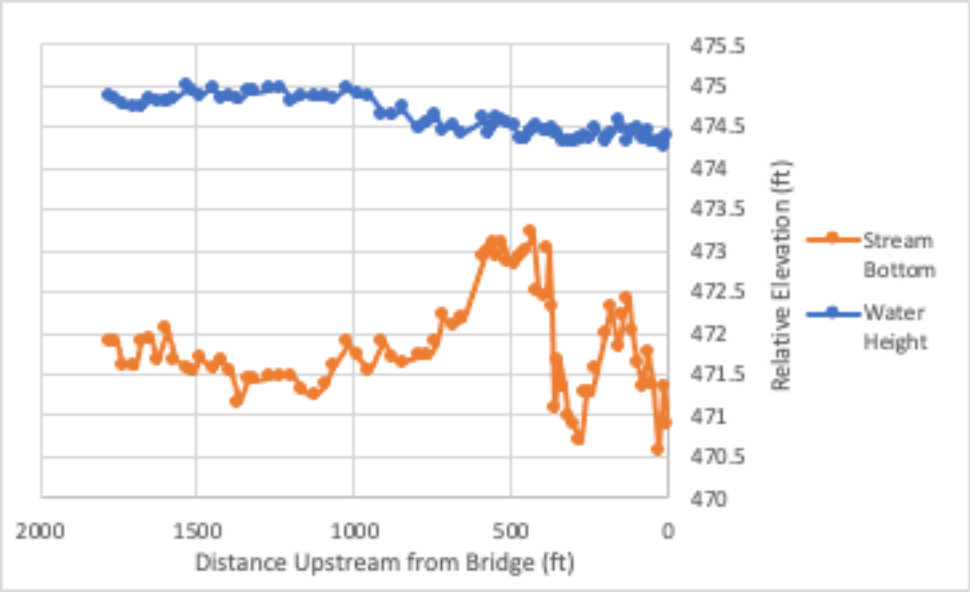

Figure B15: Site 20, Washita River and I-35 southwest of Paoli in Garvin county, longitudinal profile

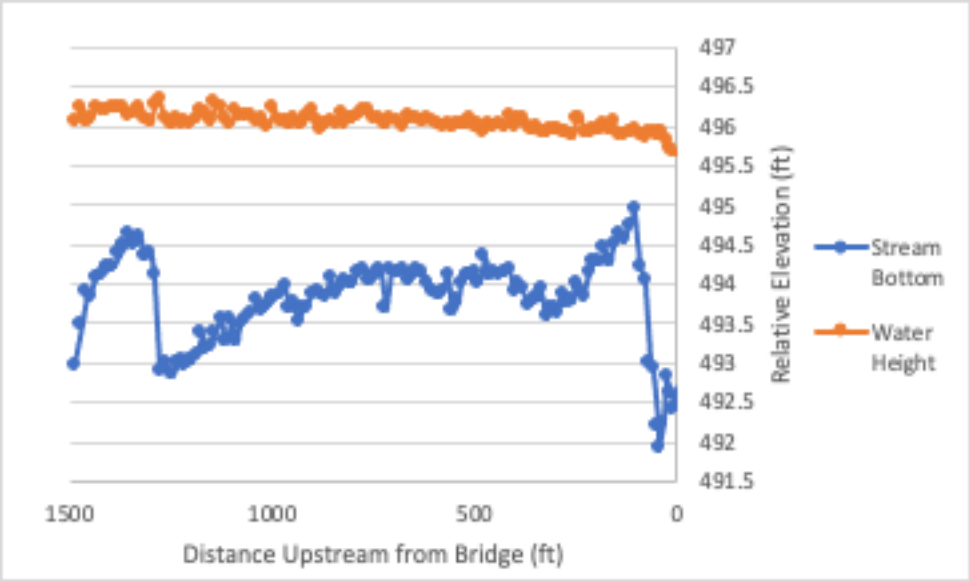

Figure B16: Site 21, Red River and S.H. 79 west of Waurika in Jefferson county, longitudinal profile

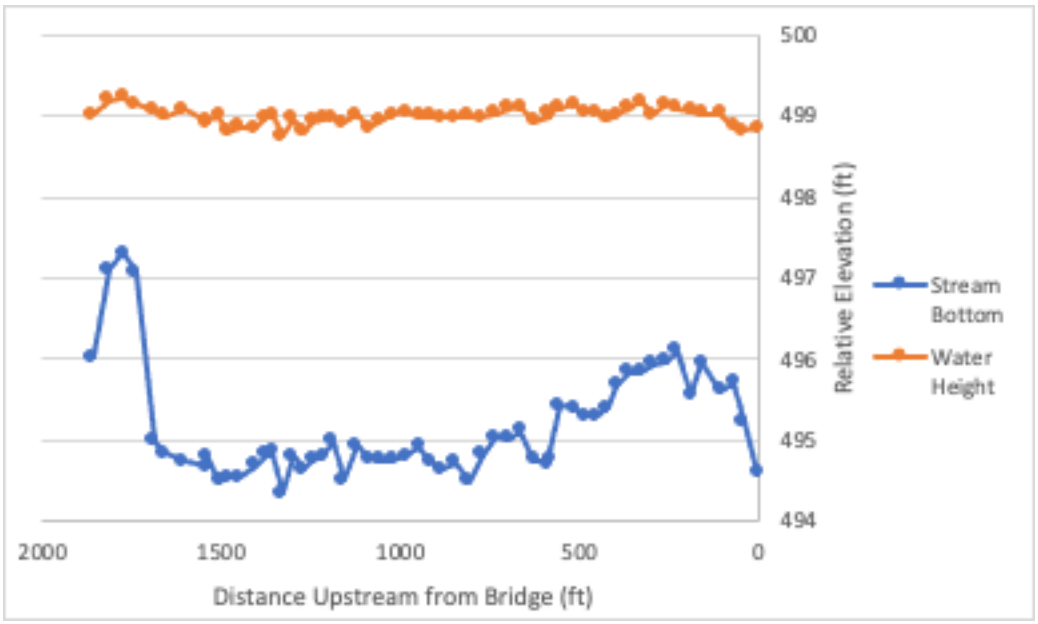

Figure B17: Site 22, Washita River and S.H. 53 east of Gene Autry in Carter county, longitudinal profile

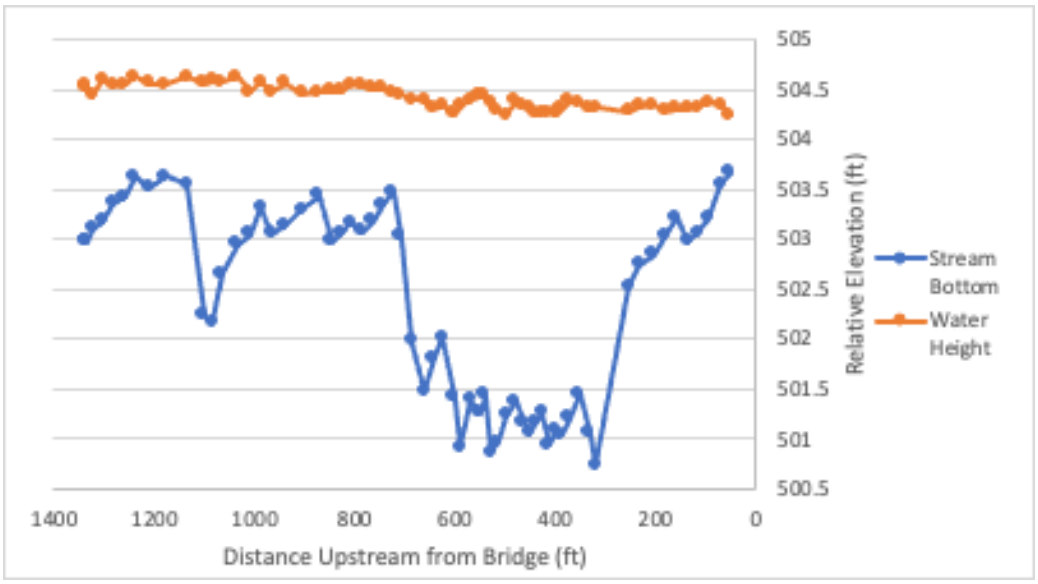

Figure B18: Site 25, North Canadian River and S.H. 48 north of Bearden in Okfuskee county, longitudinal profile

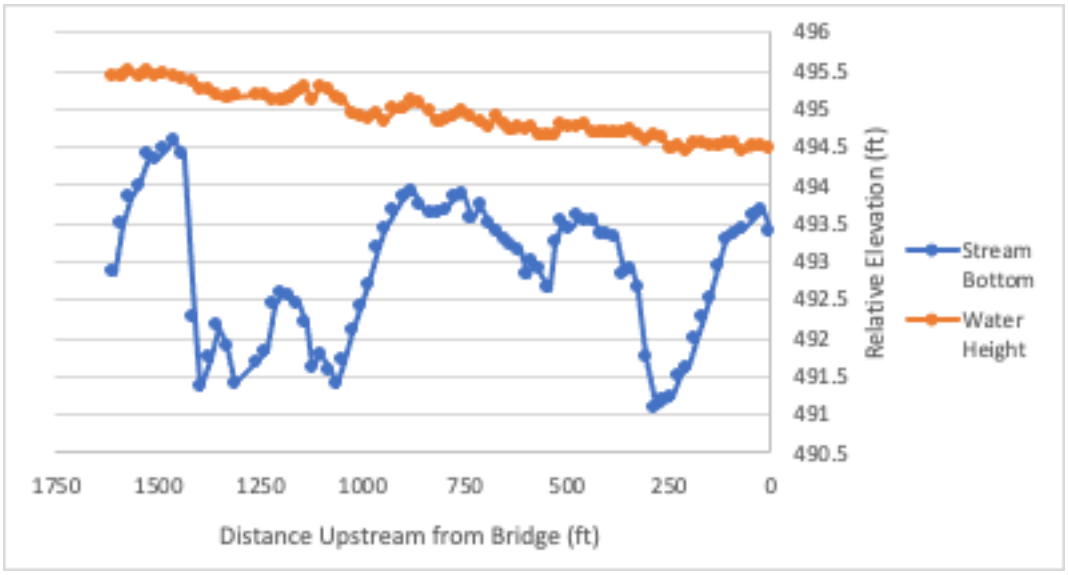

Figure B19: Site 27, North Canadian River and S.H. 99 south of Prague in Seminole county, longitudinal profile

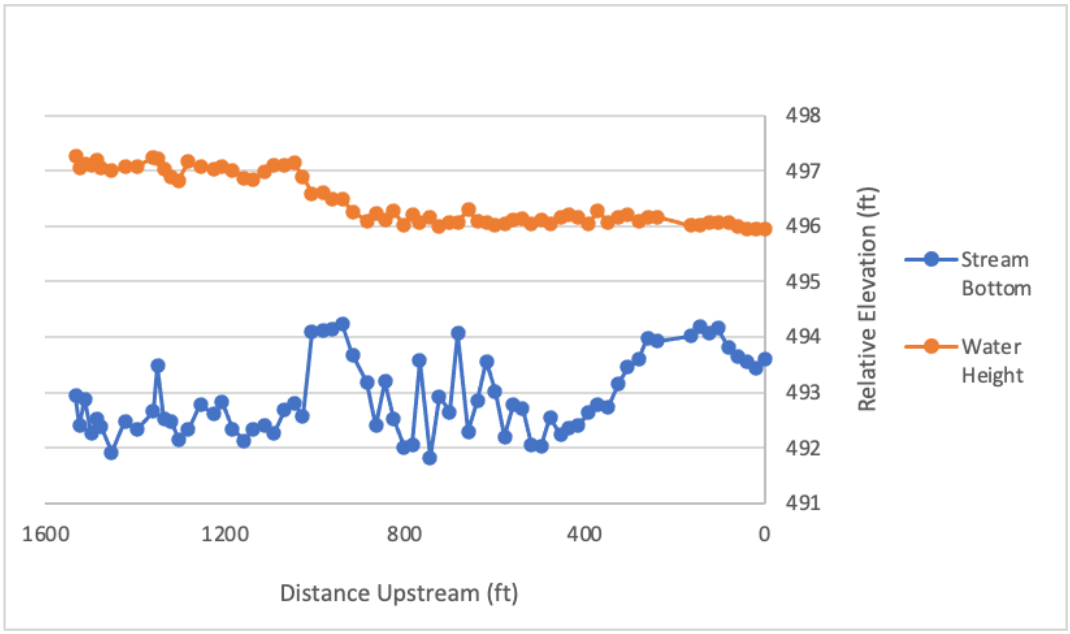

Figure B20: Site 28, Illinois River and S.H. 10 east of Tahlequah in Cherokee county, longitudinal profile

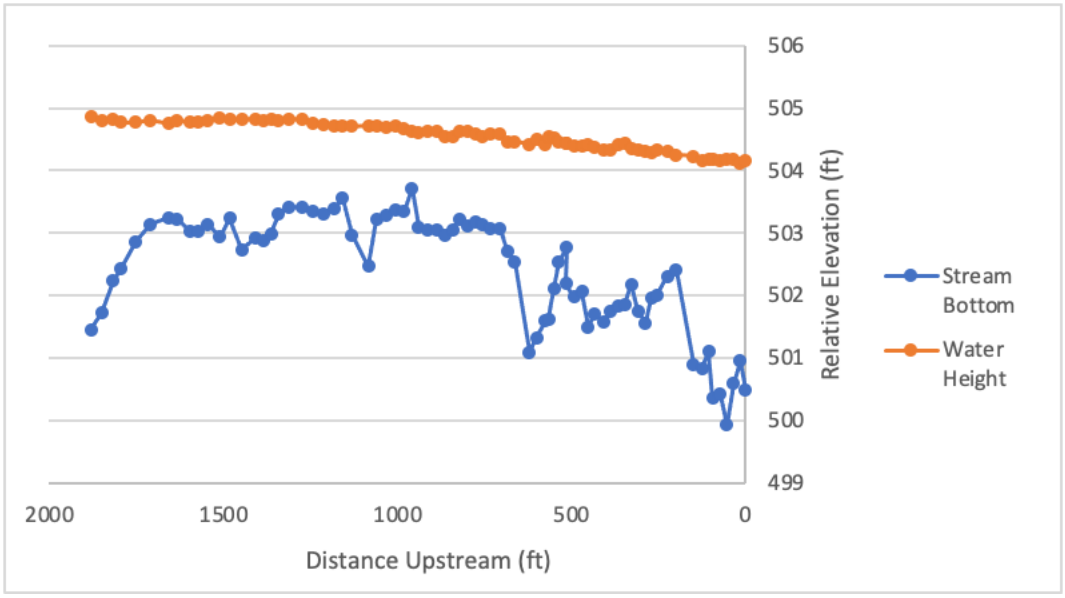

Figure B21: Site 29, Washita River and S.H. 19 east of Lindsay in Garvin county, longitudinal profile

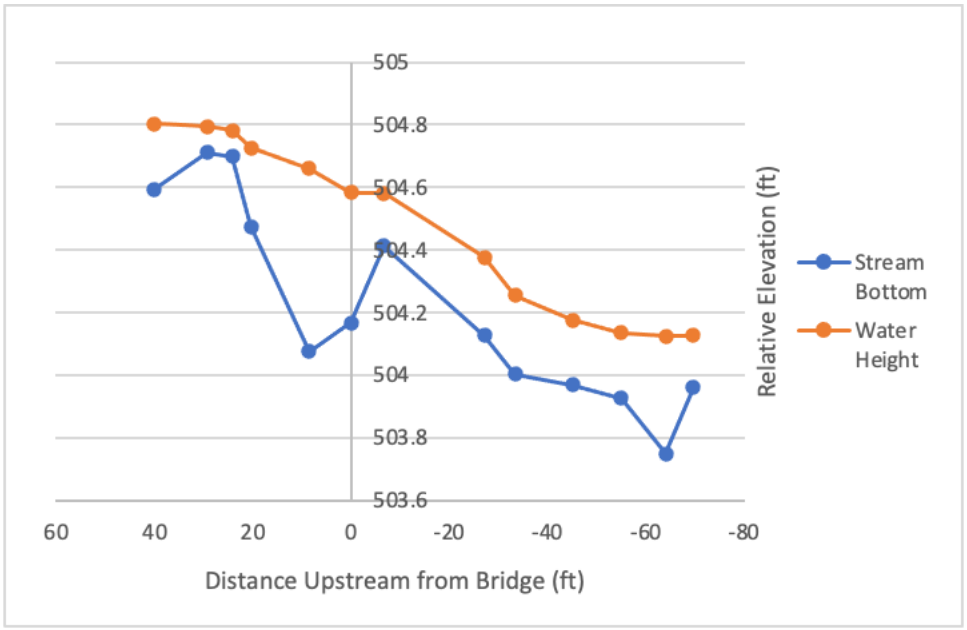

Figure B22: Site 31, Deer Creek Trib and U.S. 66 south of Hydro in Caddo county, longitudinal profile

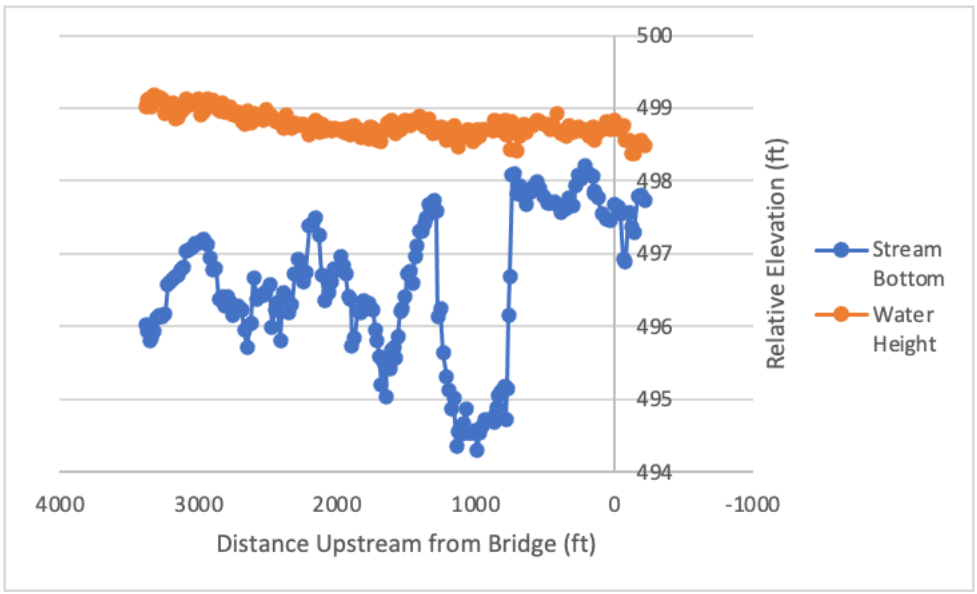

Figure B23: Site 32, Washita River and S.H. 7 west of Davis in Murray county, longitudinal profile

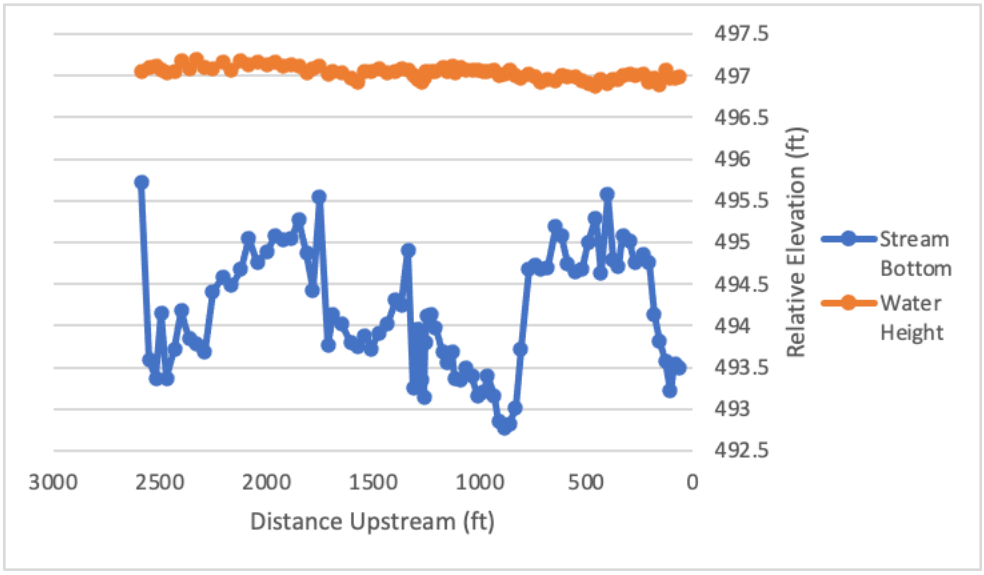

Figure B24: Site 33, Salt Fork of the Arkansas River and S.H. 156 north of Marland in Kay county, longitudinal profile

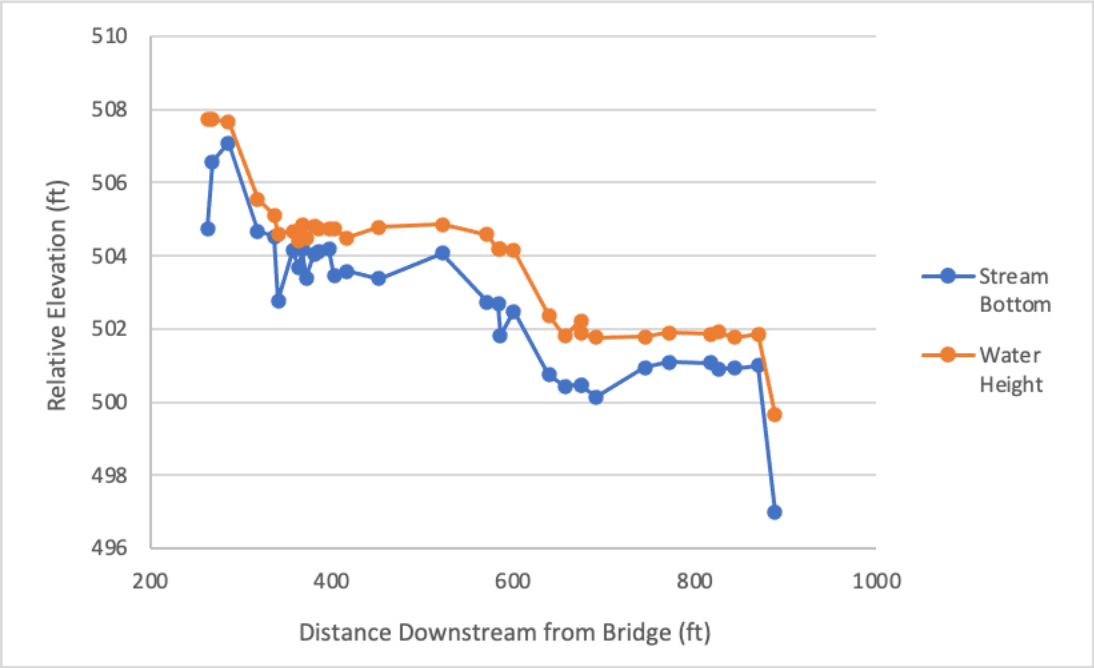

Figure B25: Site 34, Sugar Creek and U.S. 281 east of Binger in Caddo county, longitudinal profile

Appendix C – Cross Sections

Site 1 - Washita River and U.S. 77 north of Wynnewood in Garvin county

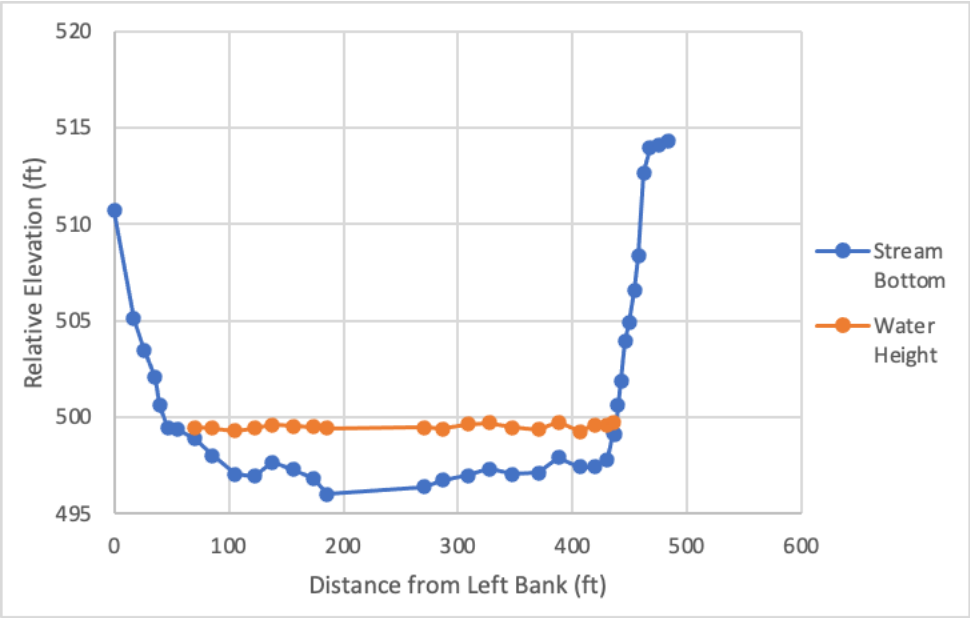

Figure C1: Site 1, Washita River and U.S. 77 north of Wynnewood in Garvin county, cross section A.

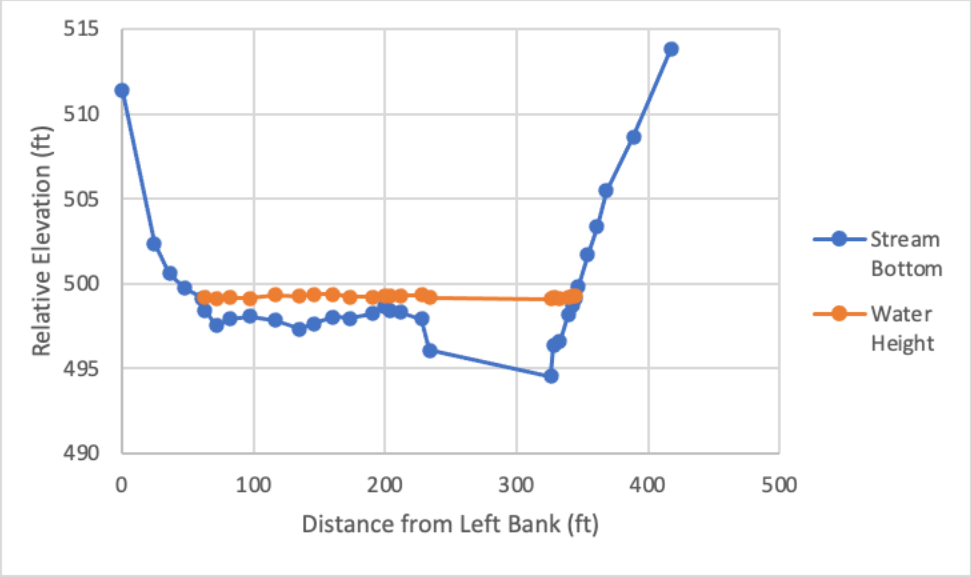

Figure C2: Site 1, Washita River and U.S. 77 north of Wynnewood in Garvin county, cross section B.

Site 2 - Cimarron River and U.S. 177 south of Perkins in Payne county

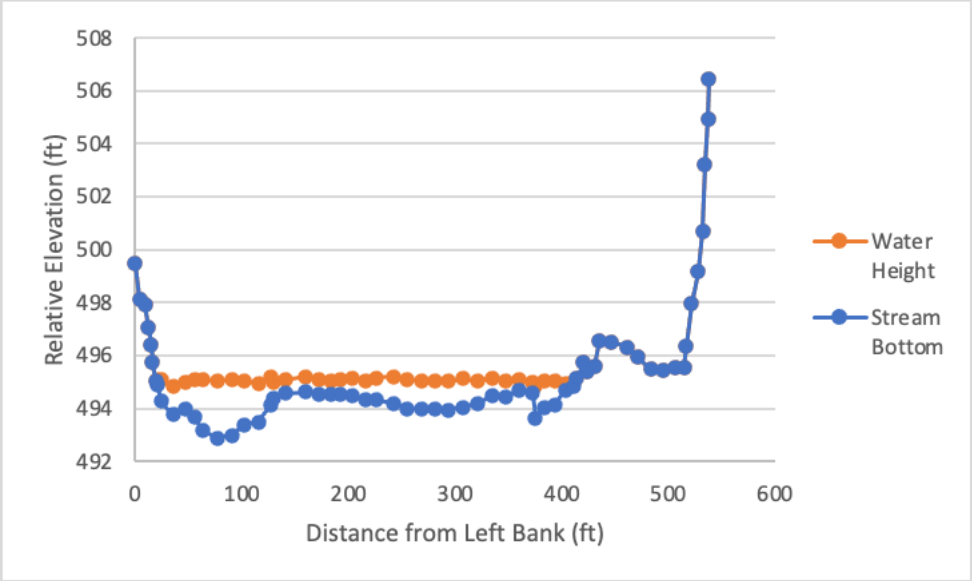

Figure C3: Site 2, Cimarron River and U.S. 177 south of Perkins in Payne county, cross section A.

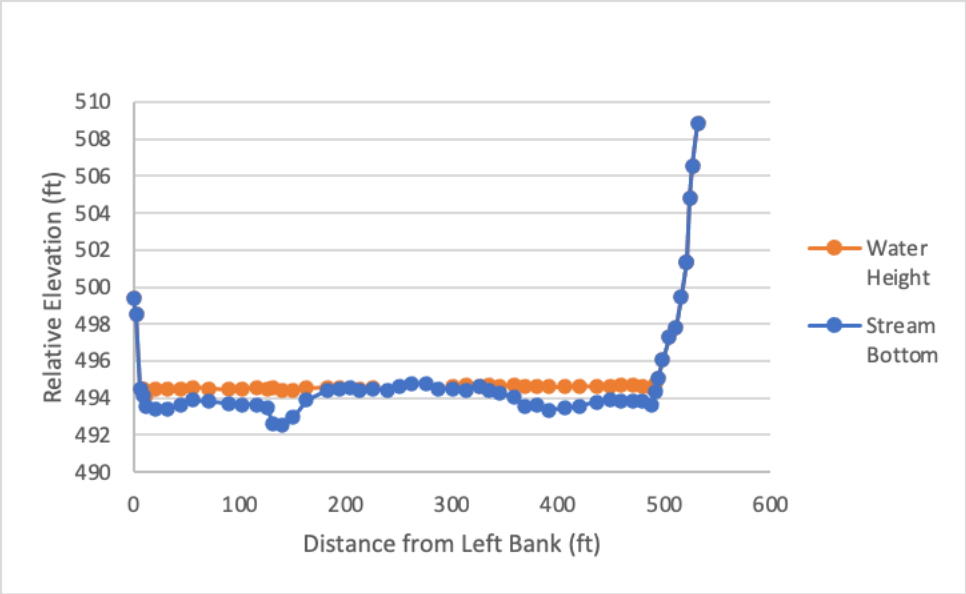

Figure C4: Site 2, Cimarron River and U.S. 177 south of Perkins in Payne county, cross section B.

Site 4 - Cimarron River and U.S. 281 south of Watonga in Blaine county

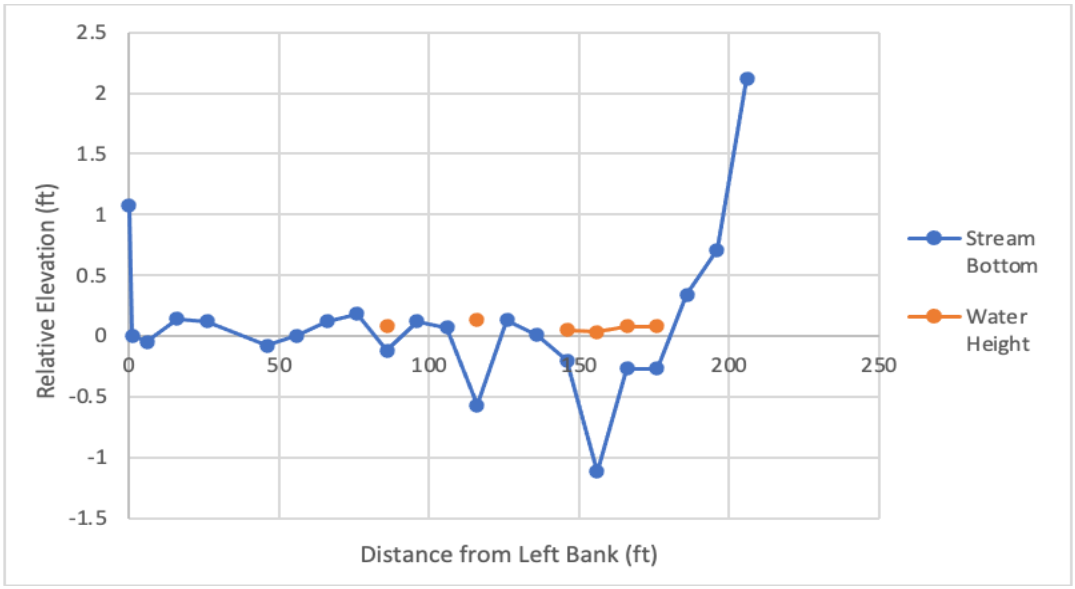

Figure C5: Site 4, Cimarron River and U.S. 281 south of Watonga in Blaine county, cross section A.

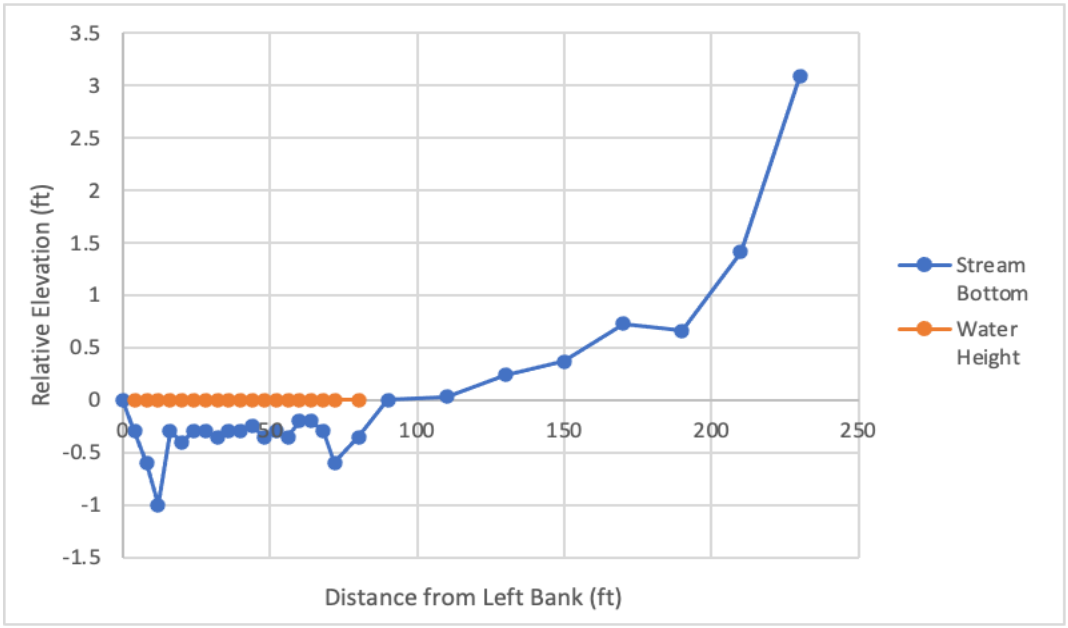

Figure C6: Site 4, Cimarron River and U.S. 281 south of Watonga in Blaine county, cross section B.

Site 6 - North Canadian River and U.S. 281 south Watonga in Blaine county

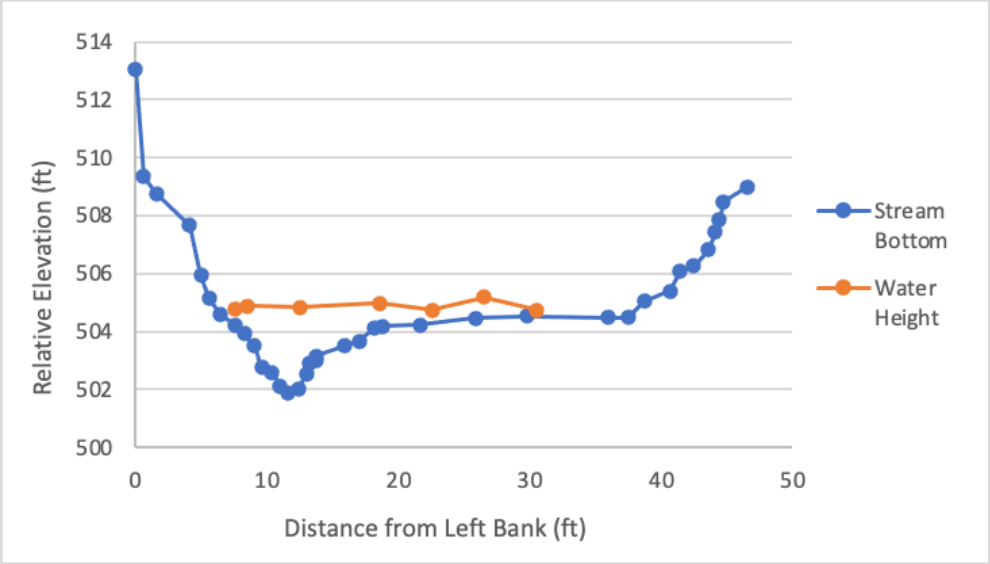

Figure C7: Site 6, North Canadian River and U.S. 281 south Watonga in Blaine county, cross section A.

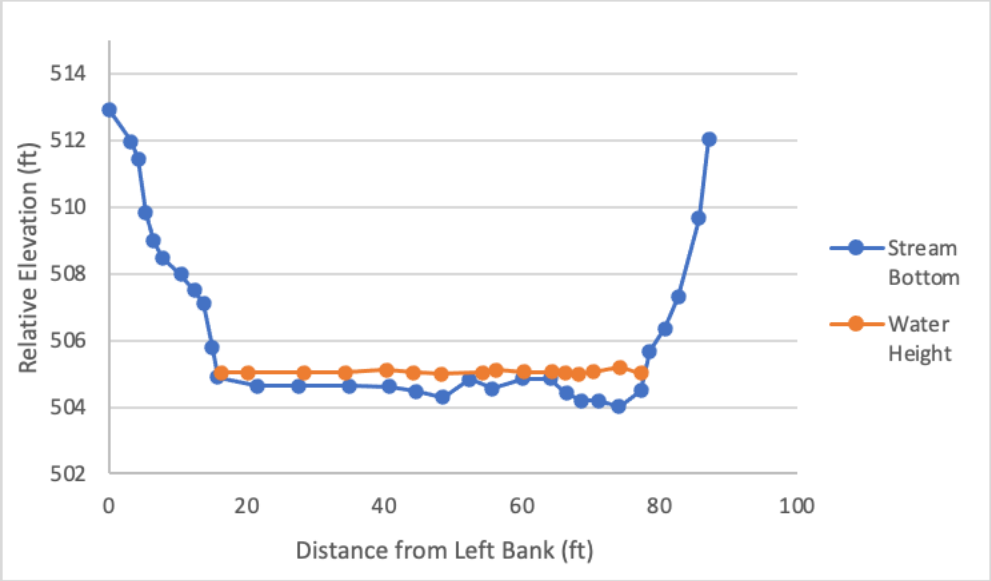

Figure C8: Site 6, North Canadian River and U.S. 281 south Watonga in Blaine county, cross section B.

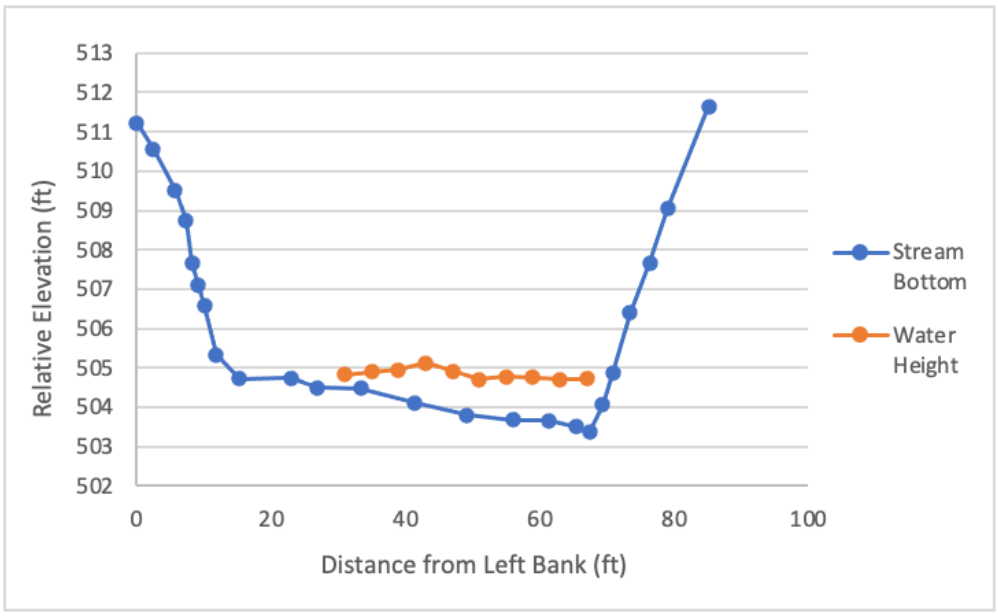

Figure C9: Site 6, North Canadian River and U.S. 281 south Watonga in Blaine county, cross section C.

Site 7 - Canadian River and U.S. 281 east of Bridgeport in Canadian county

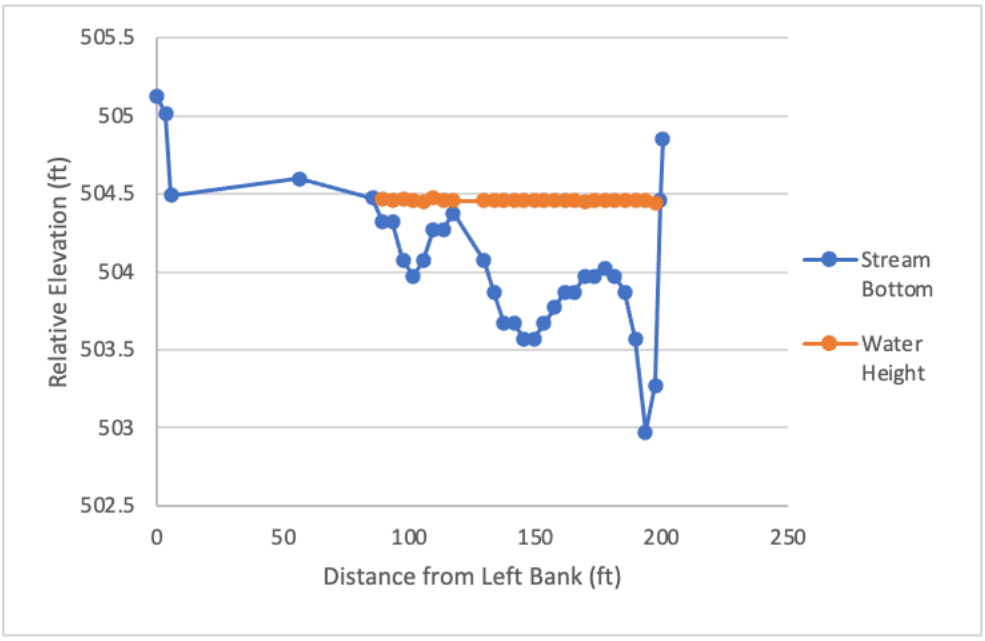

Figure C10: Site 7, Canadian River and U.S. 281 east of Bridgeport in Canadian county, cross section A.

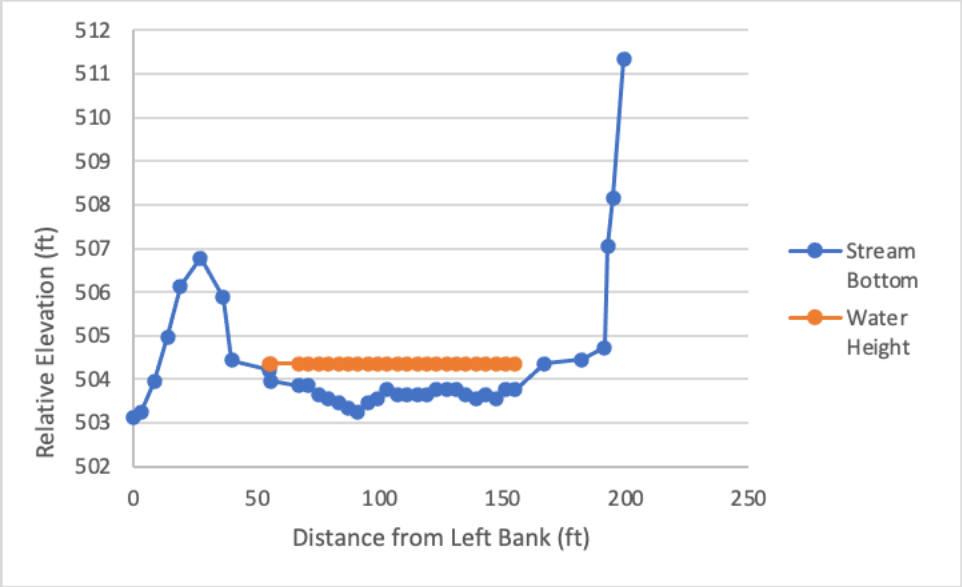

Figure C11: Site 7, Canadian River and U.S. 281 east of Bridgeport in Canadian county, cross section B.

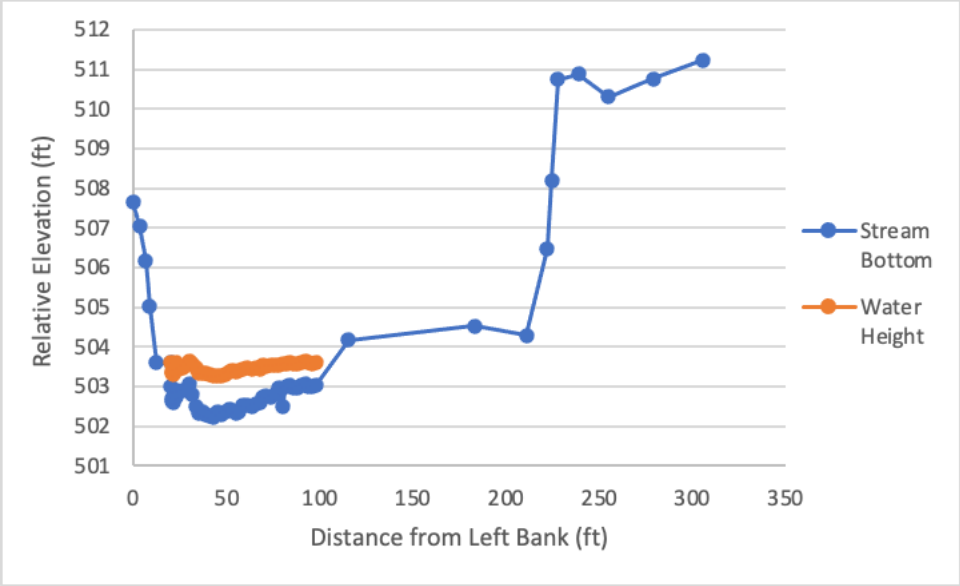

Figure C12: Site 7, Canadian River and U.S. 281 east of Bridgeport in Canadian county, cross section C.

Site 8 - Salt Fork of the Red River and U.S. 62 west of Altus in Jackson county

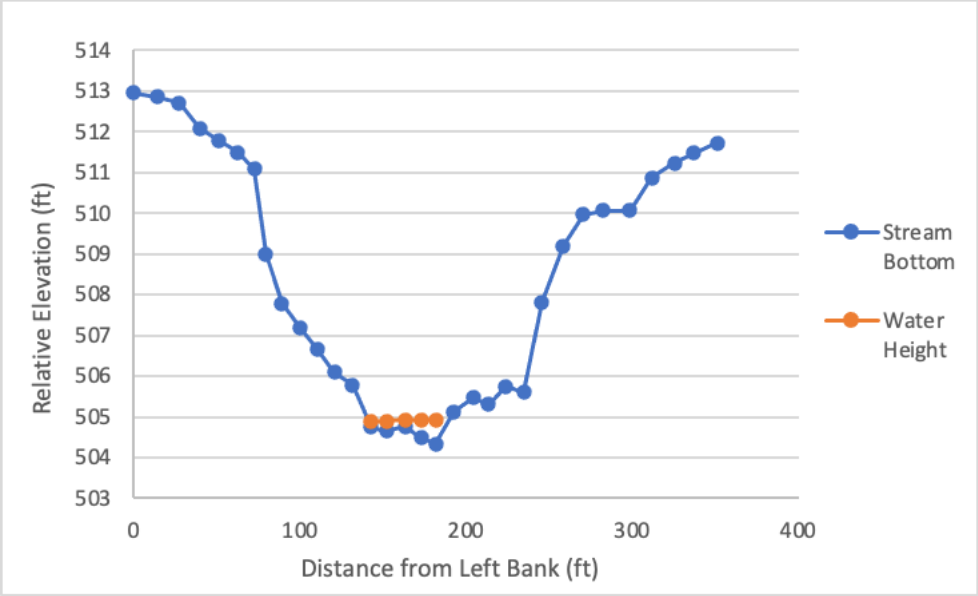

Figure C13: Site 8, Salt Fork of the Red River and U.S. 62 west of Altus in Jackson county, cross section A.

Site 10 - Washita River and S.H. 76 south of Lindsay in Garvin county

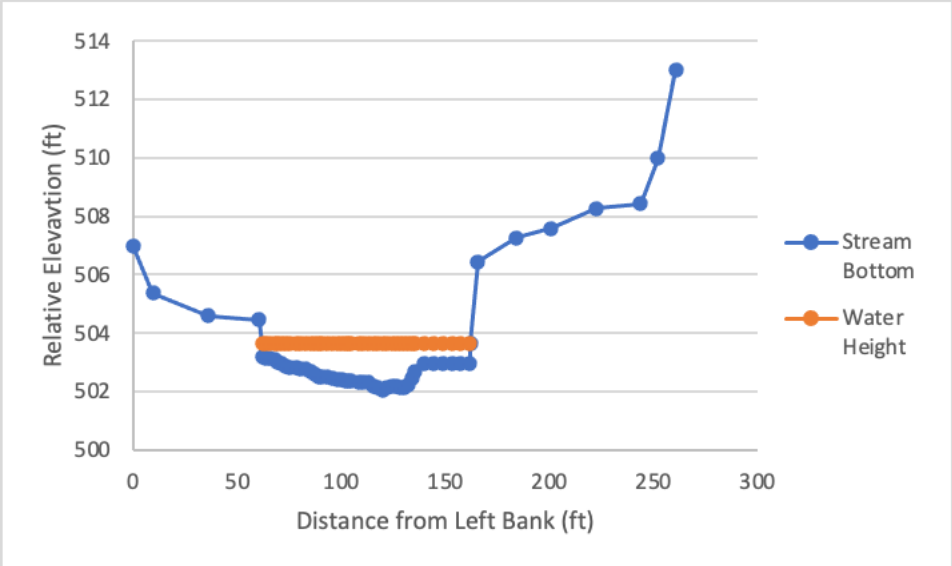

Figure C14: Site 10, Washita River and S.H. 76 south of Lindsay in Garvin county, cross section A.

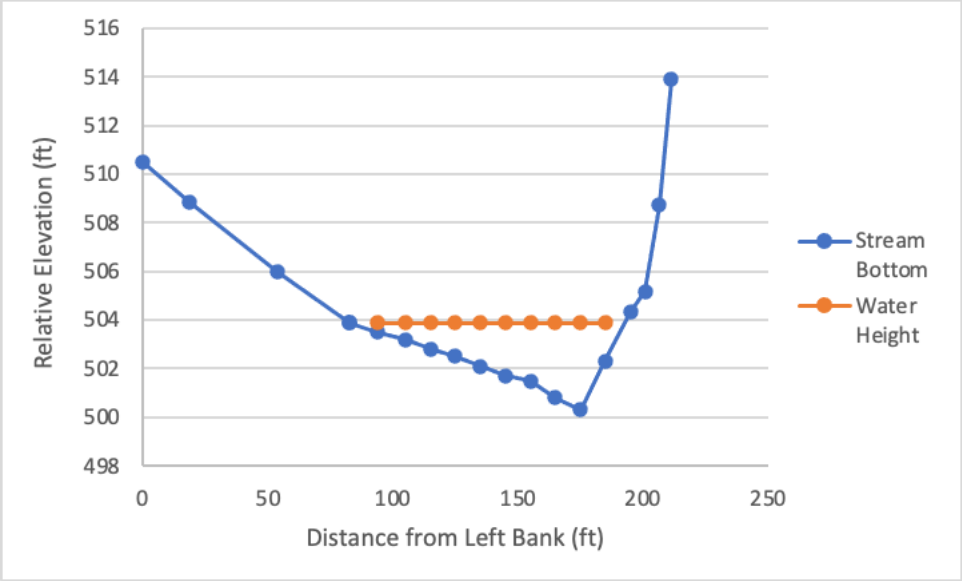

Figure C15: Site 10, Washita River and S.H. 76 south of Lindsay in Garvin county, cross section B.

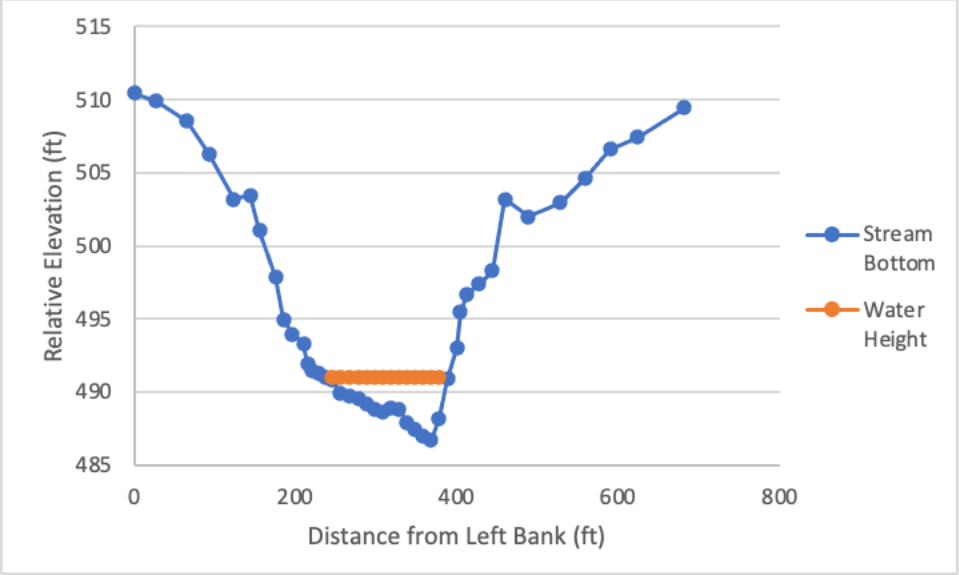

Figure C16: Site 10, Washita River and S.H. 76 south of Lindsay in Garvin county, cross section C.

Site 11 - Washita River and S.H. 74 north of Maysville in Garvin county

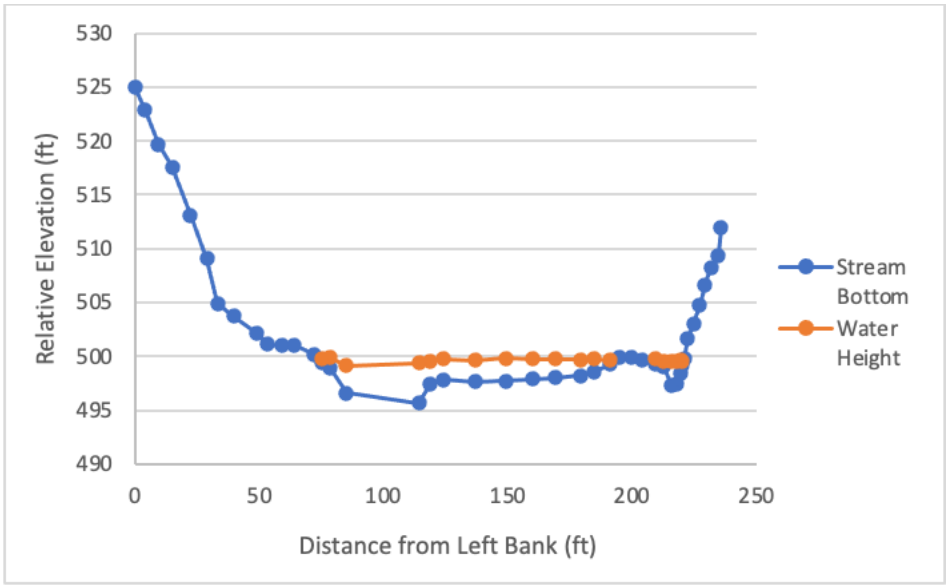

Figure C17: Site 11, Washita River and S.H. 74 north of Maysville in Garvin county, cross section A.

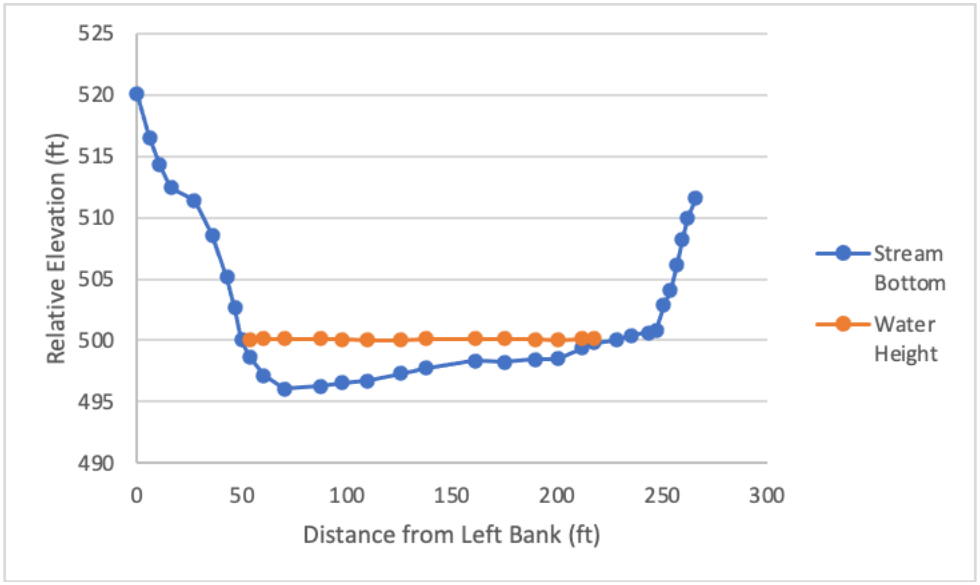

Figure C18: Site 11, Washita River and S.H. 74 north of Maysville in Garvin county, cross section B.

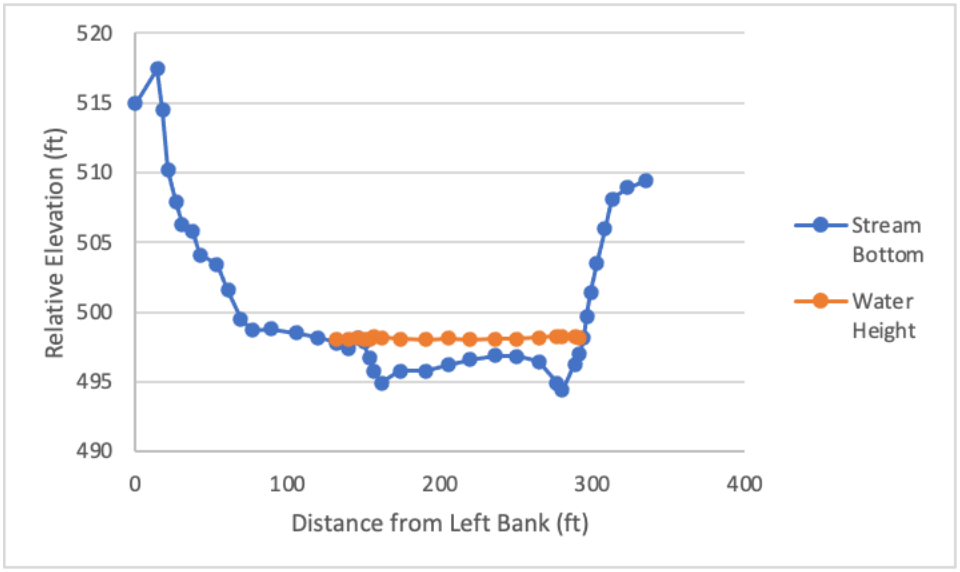

Figure C19: Site 11, Washita River and S.H. 74 north of Maysville in Garvin county, cross section C.

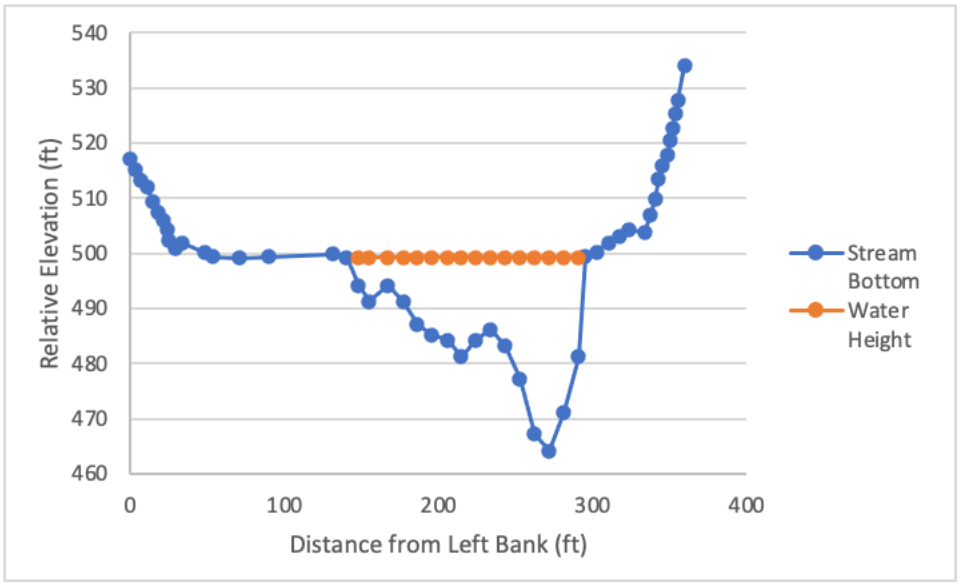

Figure C20: Site 11, Washita River and S.H. 74 north of Maysville in Garvin county, cross section D.

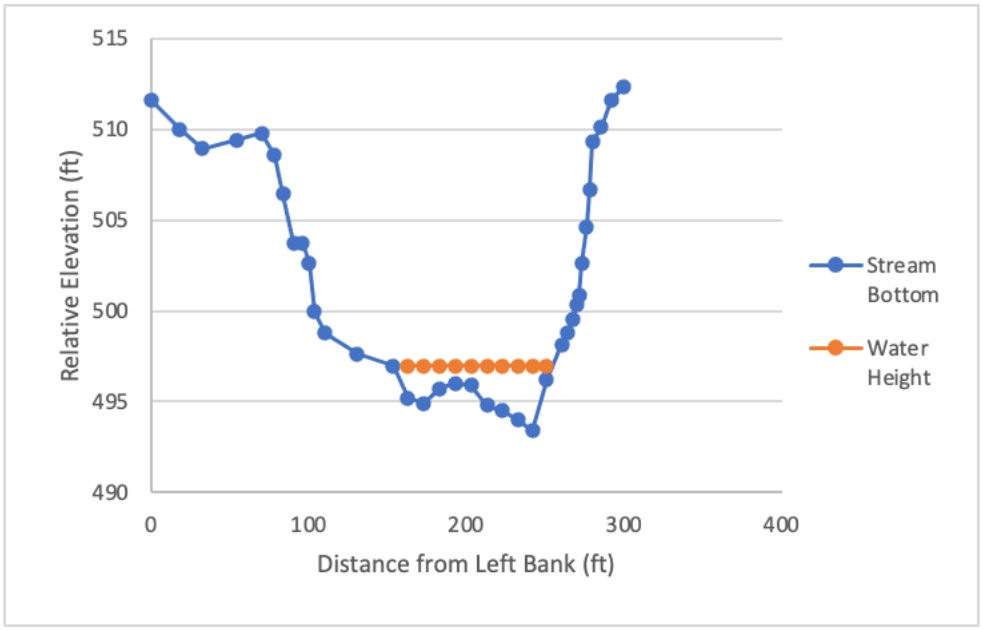

Figure C21: Site 11, Washita River and S.H. 74 north of Maysville in Garvin county, cross section E.

Site 12 - Cimarron River and S.H. 33 north of Coyle in Logan county

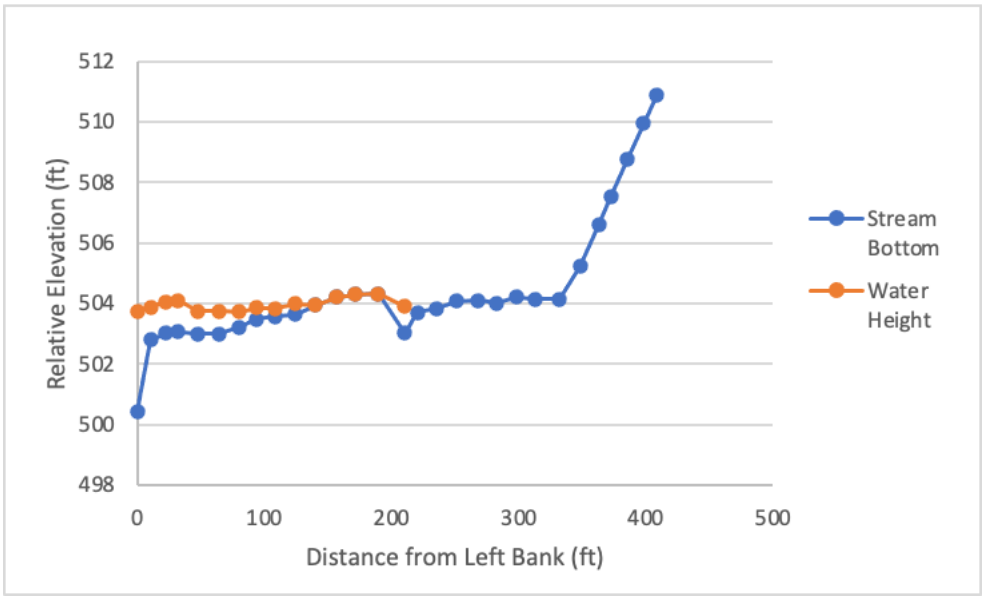

Figure C22: Site 12, Cimarron River and S.H. 33 north of Coyle in Logan county, cross section A

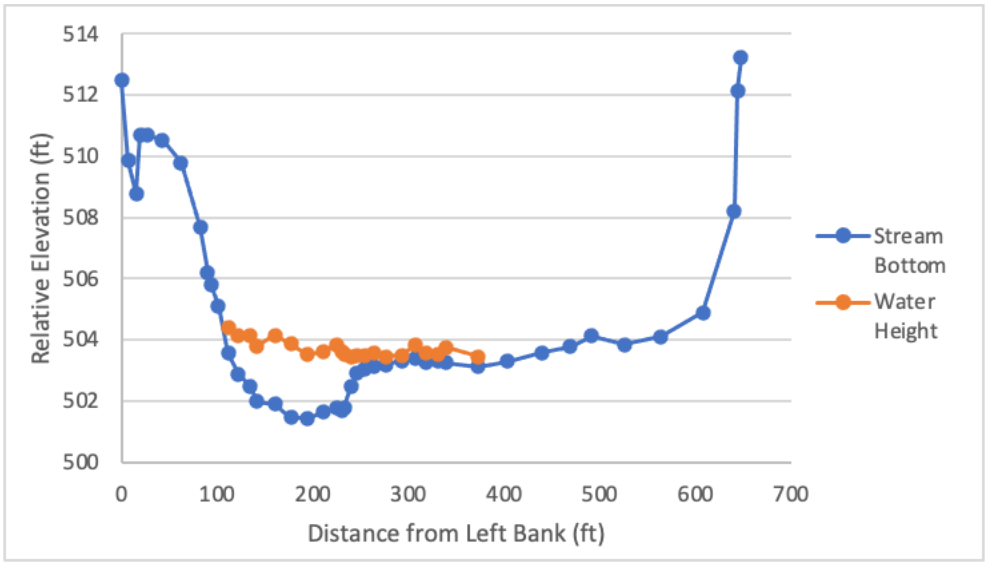

Figure C23: Site 12, Cimarron River and S.H. 33 north of Coyle in Logan county, cross section B

Site 13 - Canadian River and S.H. 48 north of Atwood in Cotton county

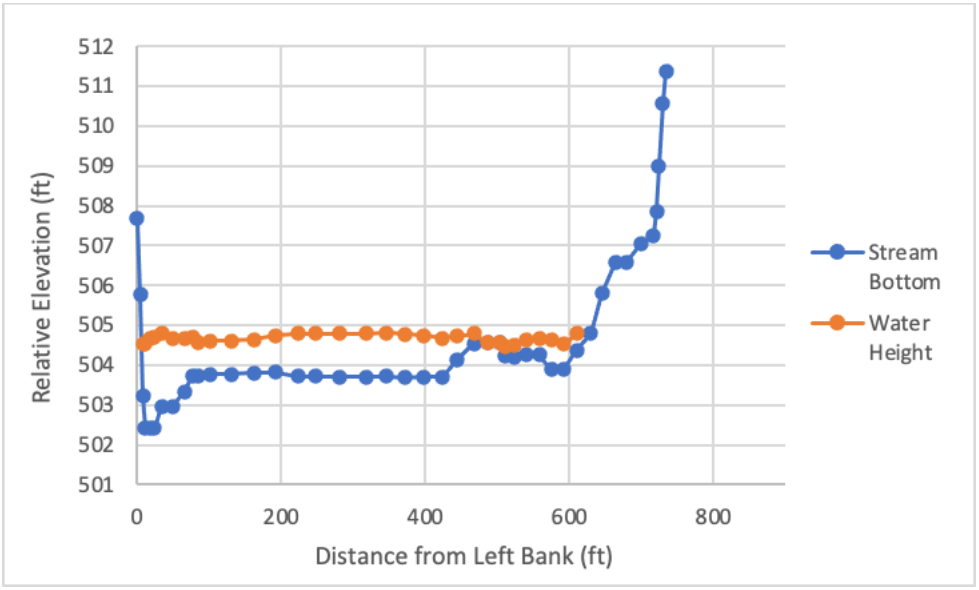

Figure C24: Site 13, Canadian River and S.H. 48 north of Atwood in Cotton county, cross section A

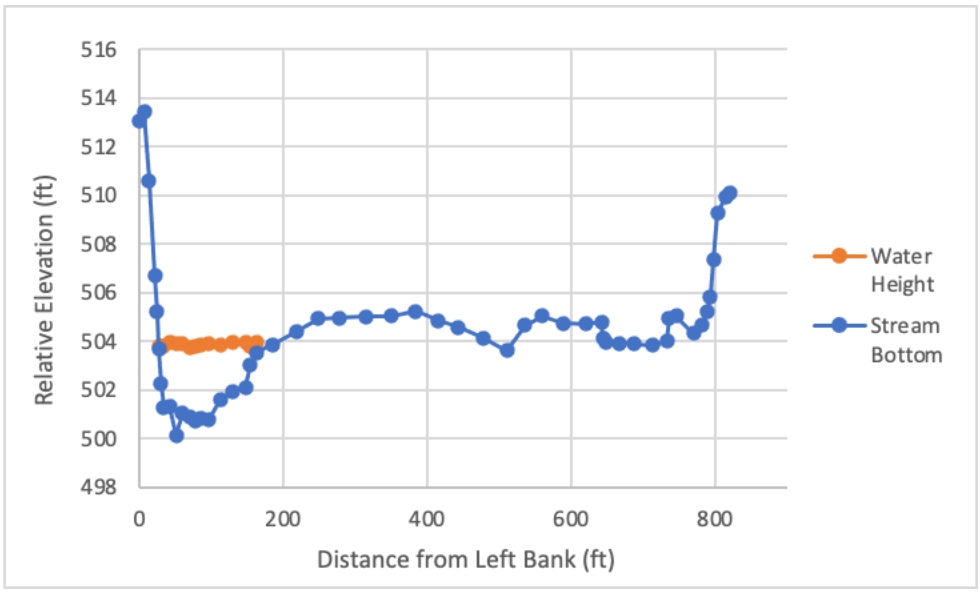

Figure C25: Site 13, Canadian River and S.H. 48 north of Atwood in Cotton county, cross section B

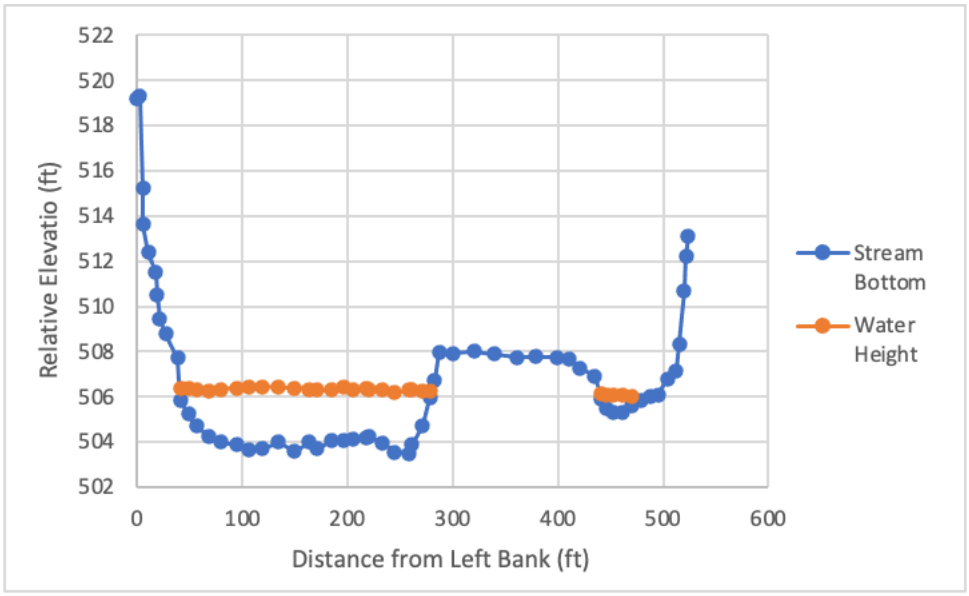

Figure C26: Site 13, Canadian River and S.H. 48 north of Atwood in Cotton county, cross section C

Site 14 - North Canadian River and S.H. 84 north of Dustin in Okfuskee county

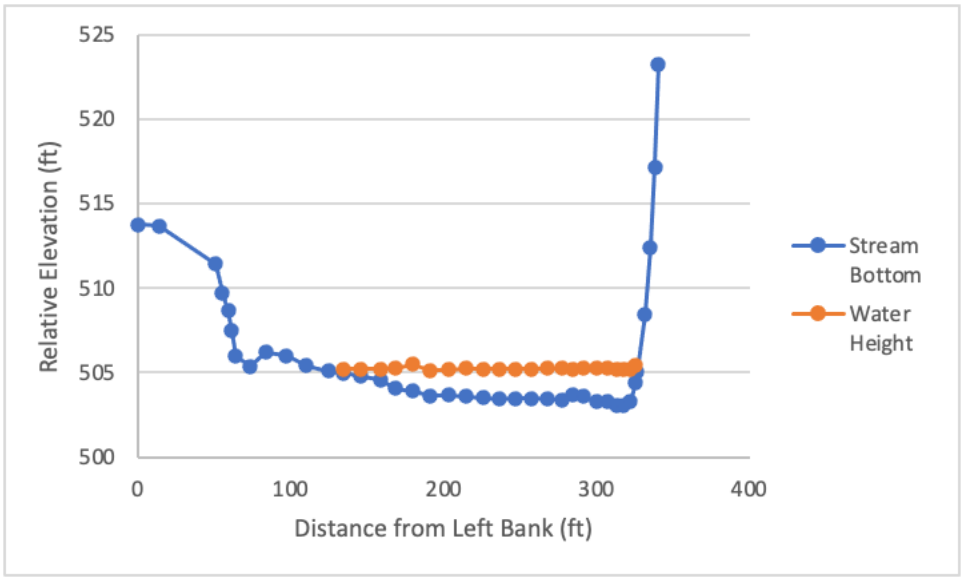

Figure C27: Site 14, North Canadian River and S.H. 84 north of Dustin in Okfuskee county, cross section A

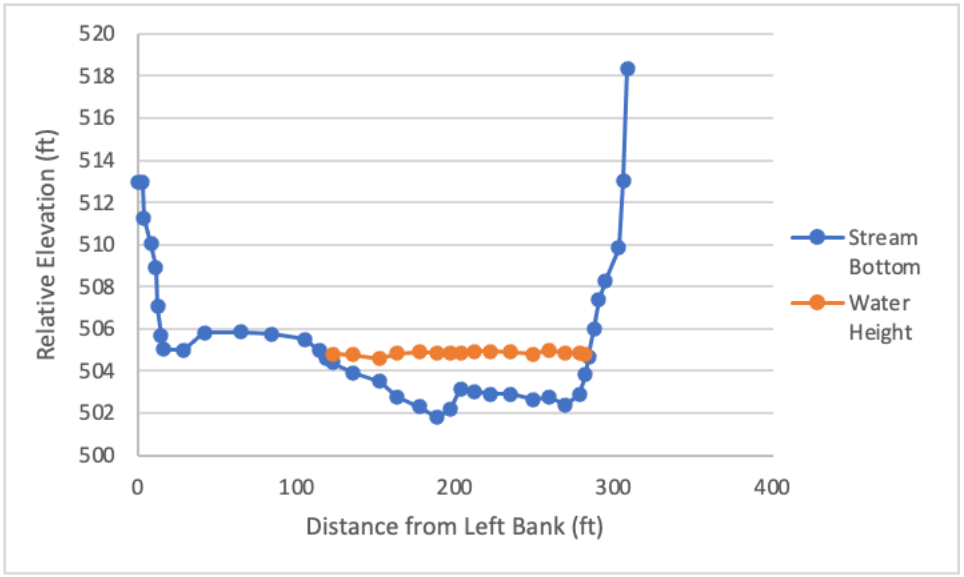

Figure C28: Site 14, North Canadian River and S.H. 84 north of Dustin in Okfuskee county, cross section B

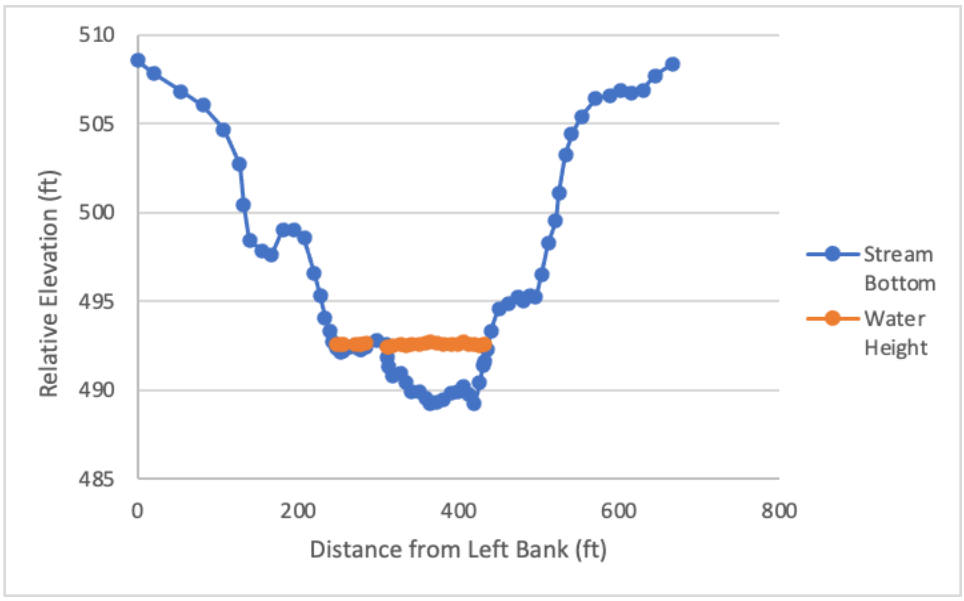

Figure C29: Site 14, North Canadian River and S.H. 84 north of Dustin in Okfuskee county, cross section C.

Site 16 - North Canadian River and S.H. 3 east of Shawnee in Pottawatomie county

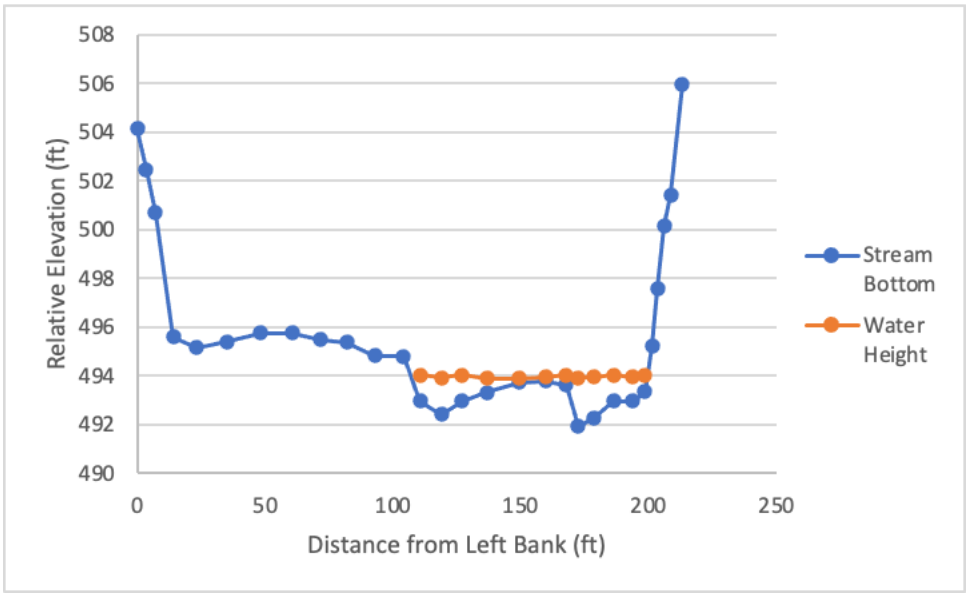

Figure C30: Site 16, North Canadian River and S.H. 3 east of Shawnee in Pottawatomie county, cross section A.

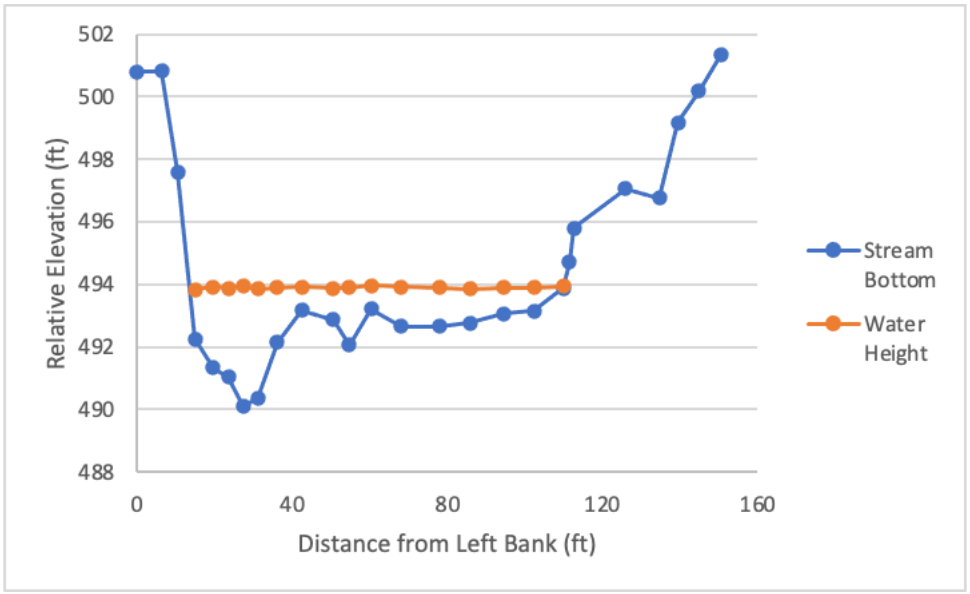

Figure C31: Site 16, North Canadian River and S.H. 3 east of Shawnee in Pottawatomie county, cross section B.

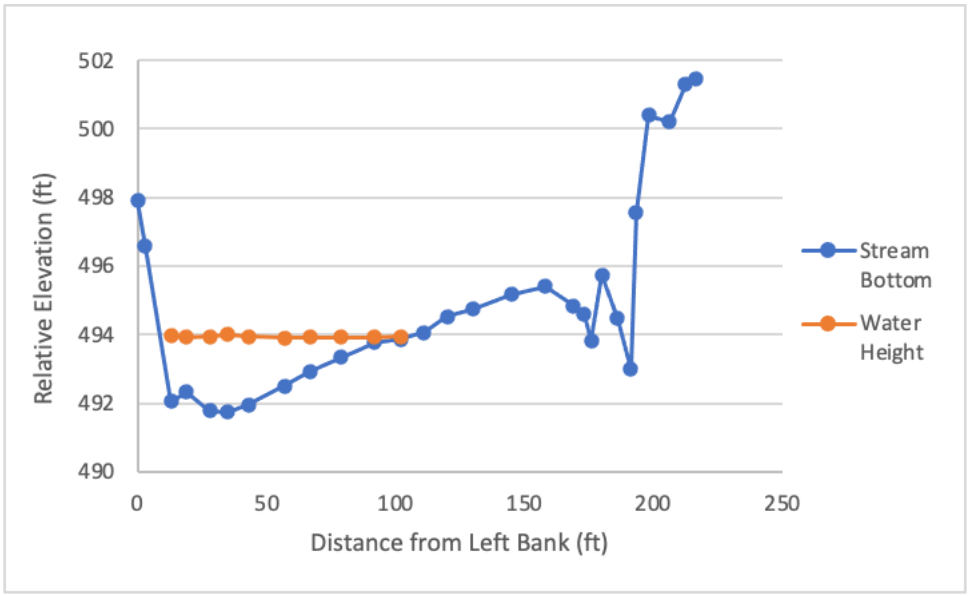

Figure C32: Site 16, North Canadian River and S.H. 3 east of Shawnee in Pottawatomie county, cross section C.

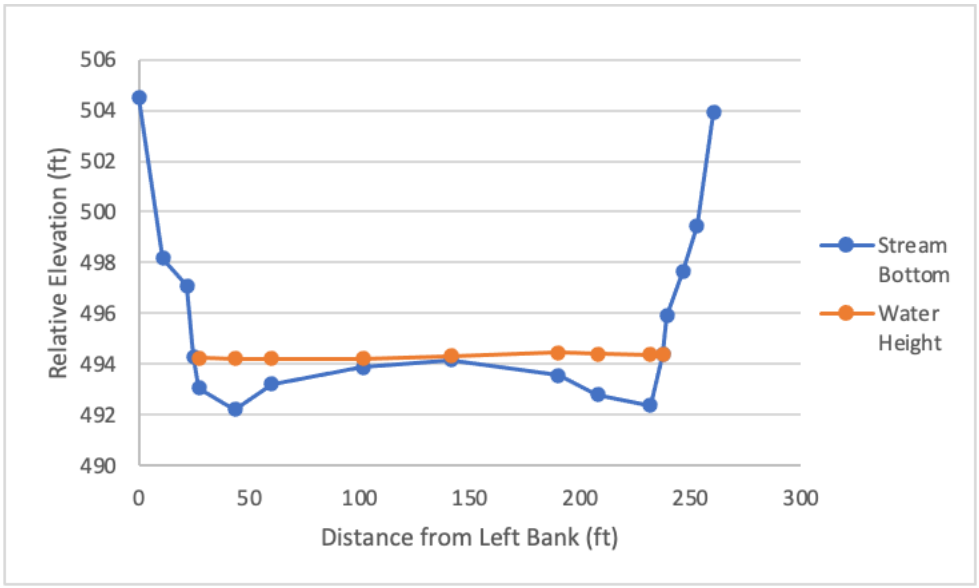

Figure C33: Site 16, North Canadian River and S.H. 3 east of Shawnee in Pottawatomie county, cross section D.

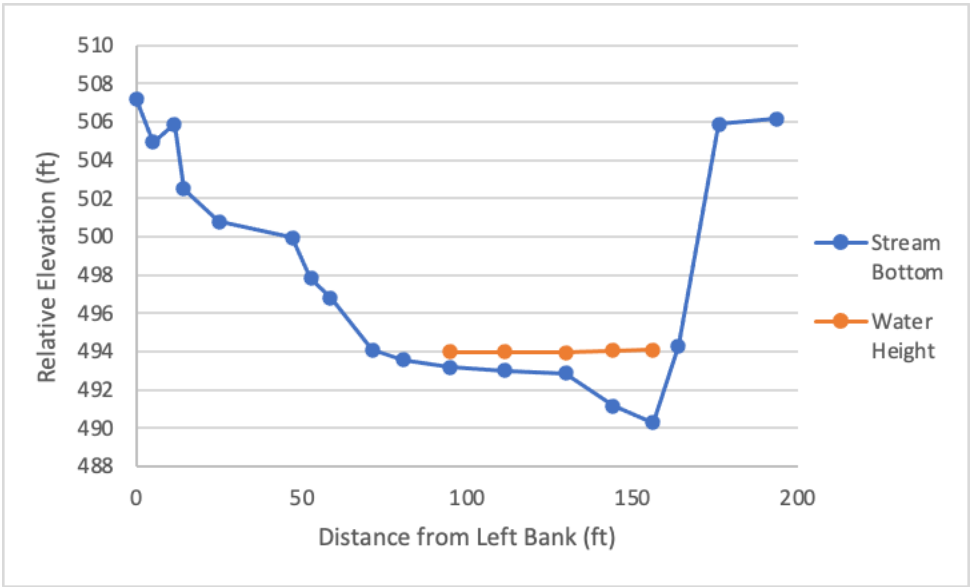

Figure C34: Site 16, North Canadian River and S.H. 3 east of Shawnee in Pottawatomie county, cross section E.

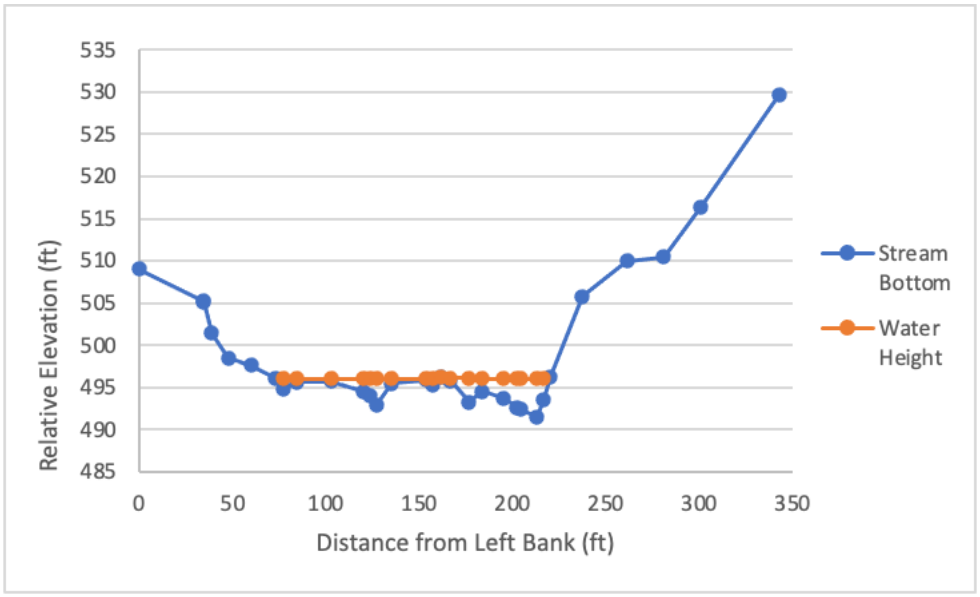

Figure C35: Site 16, North Canadian River and S.H. 3 east of Shawnee in Pottawatomie county, cross section F.

Site 17 - Cimarron River and S.H. 74 south of Crescent in Logan county

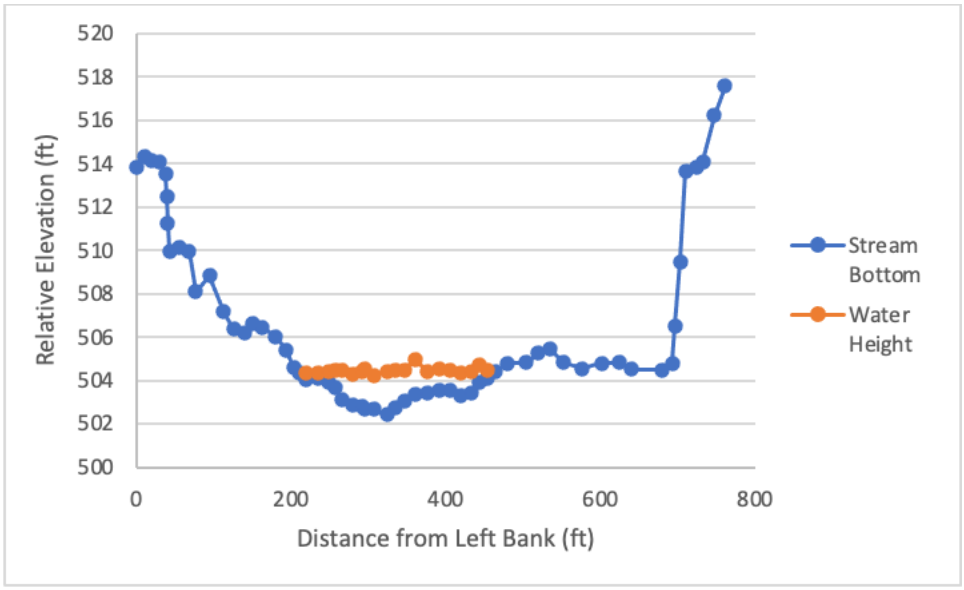

Figure C36: Site 17, Cimarron River and S.H. 74 south of Crescent in Logan county, cross section A.

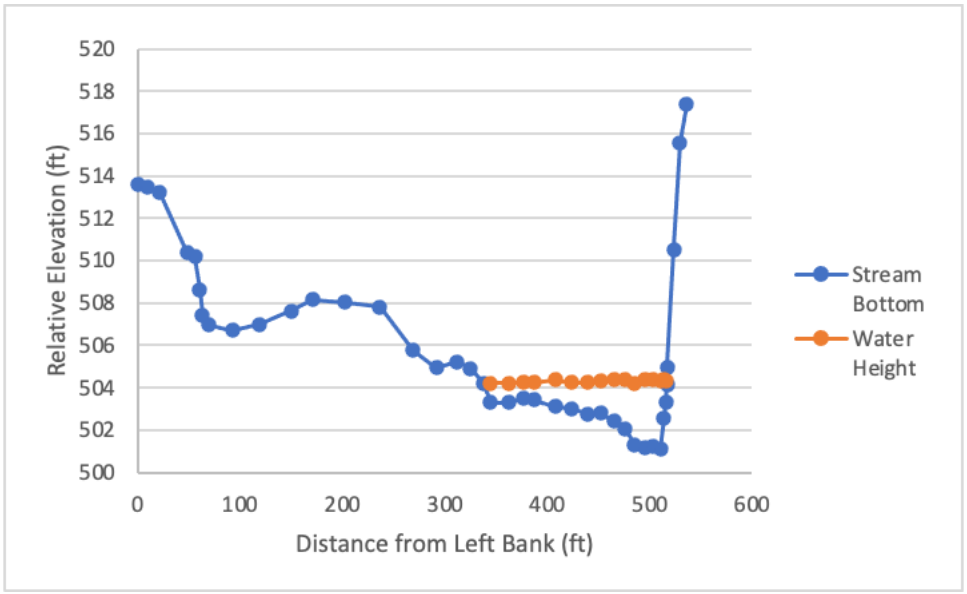

Figure C37: Site 17, Cimarron River and S.H. 74 south of Crescent in Logan county, cross section B.

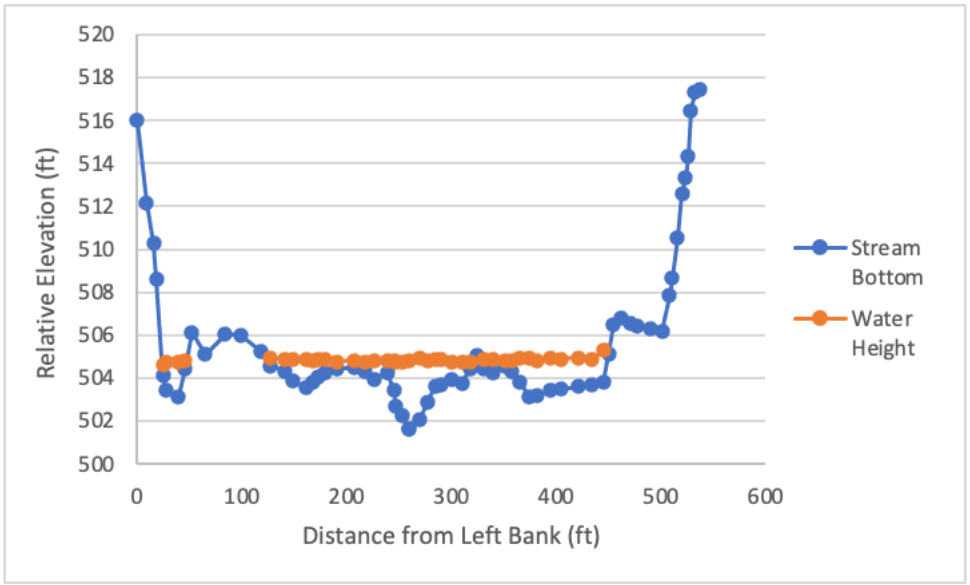

Figure C38: Site 17, Cimarron River and S.H. 74 south of Crescent in Logan county, cross section C.

Site 18 - Washita River and U.S. 77 south of Davis in Murray county

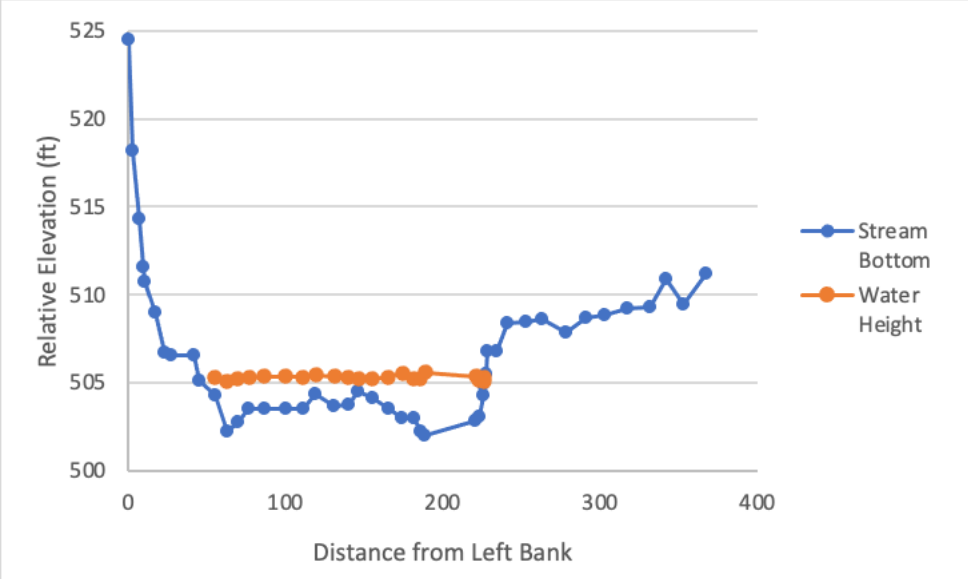

Figure C39: Site 18, Washita River and U.S. 77 south of Davis in Murray county, cross section A.

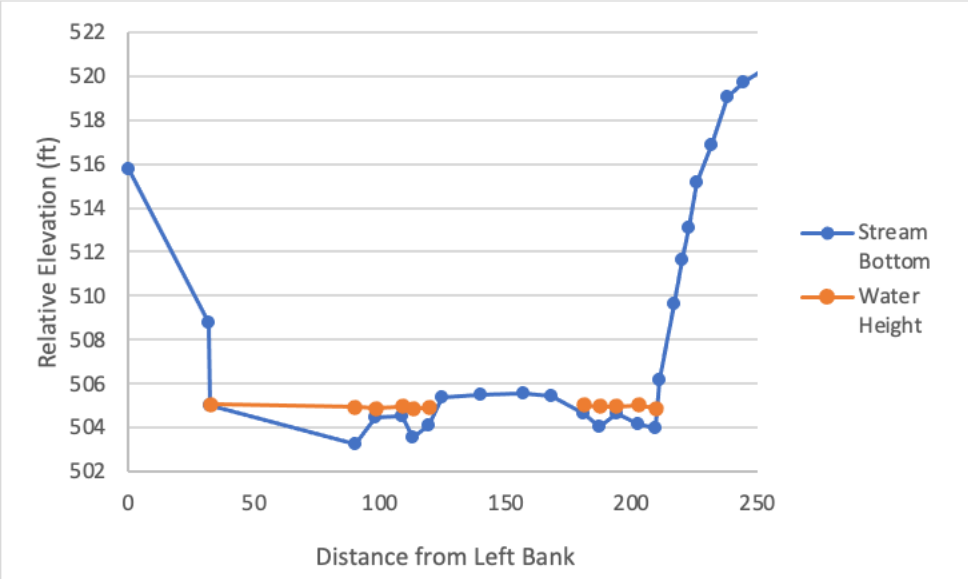

Figure C40: Site 18, Washita River and U.S. 77 south of Davis in Murray county, cross section B.

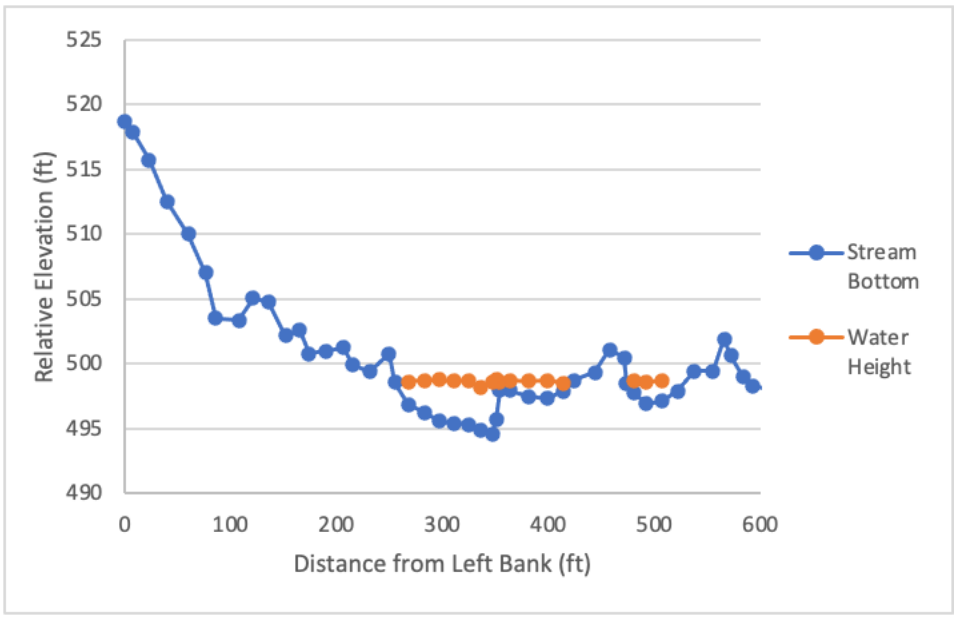

Figure C41: Site 18, Washita River and U.S. 77 south of Davis in Murray county, cross section C.

Site 19 - Beaver River and U.S. 283 north of Laverne in Harper county

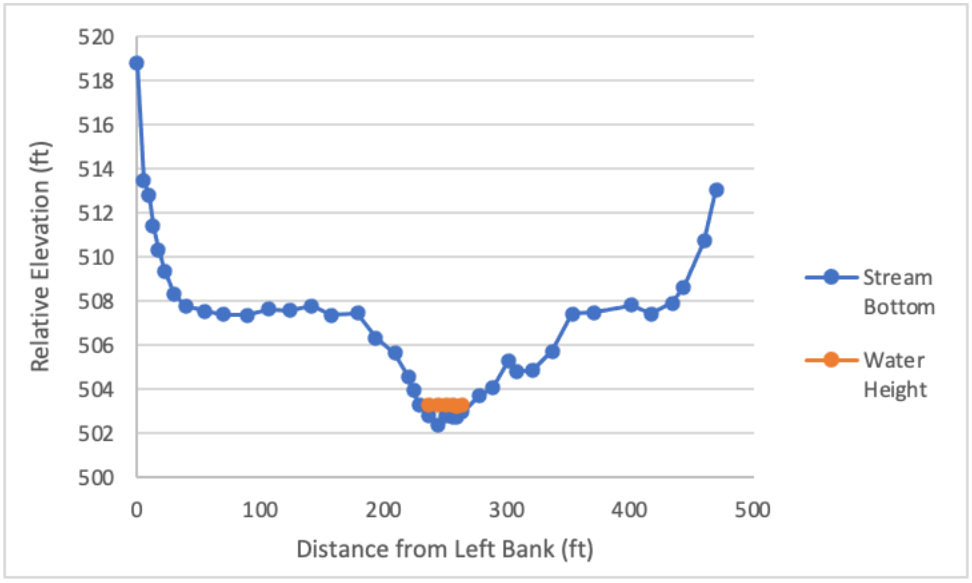

Figure C42: Site 19, Beaver River and U.S. 283 north of Laverne in Harper county, cross section A.

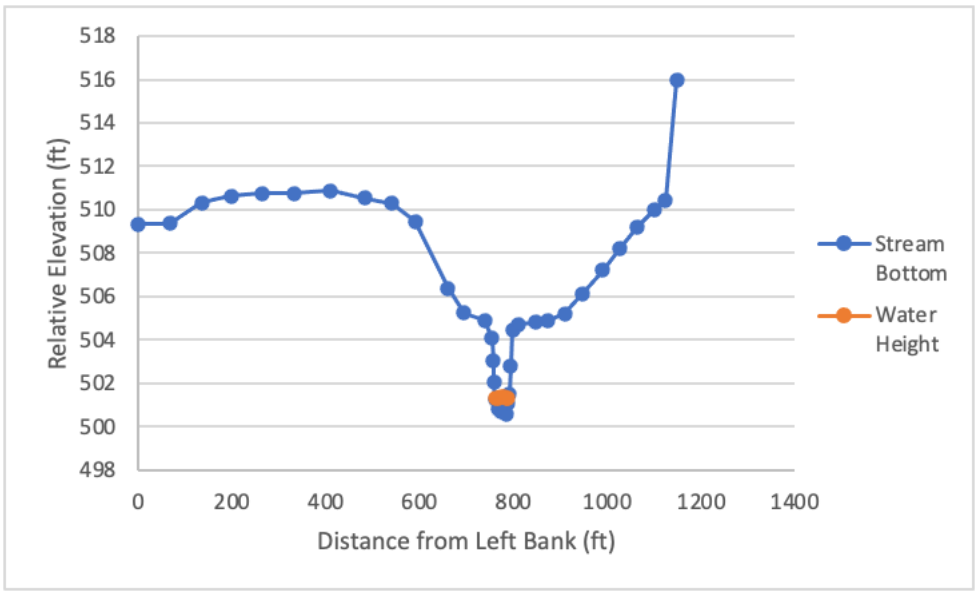

Figure C43: Site 19, Beaver River and U.S. 283 north of Laverne in Harper county, cross section B.

Site 20 - Washita River and I-35 southwest of Paoli in Garvin county

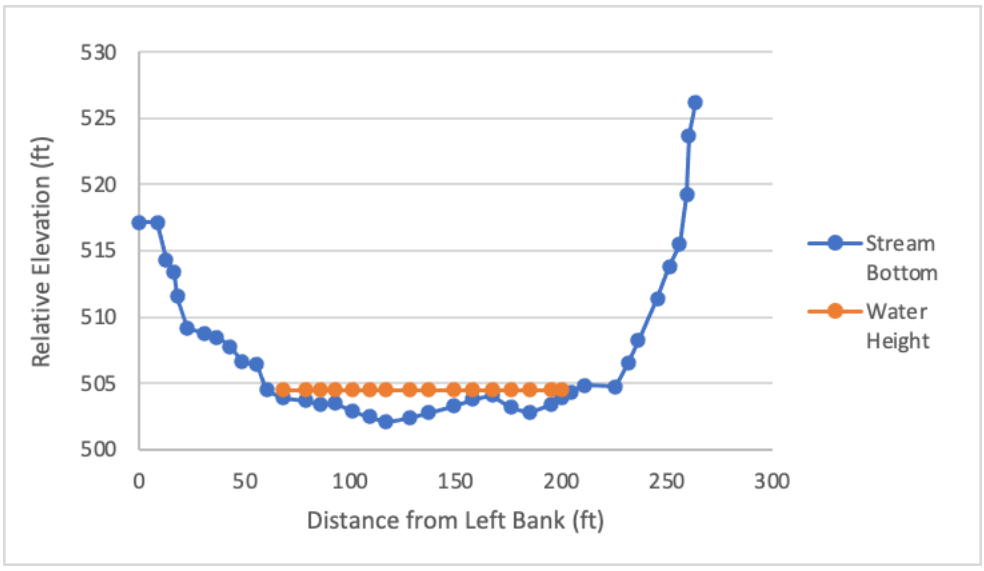

Figure C44: Site 20, Washita River and I-35 southwest of Paoli in Garvin county, cross section A.

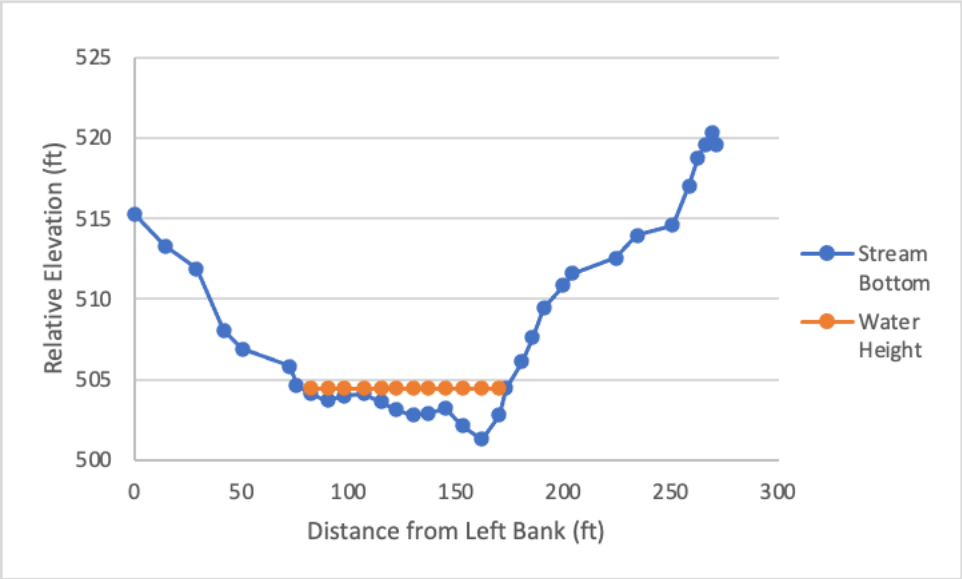

Figure C45: Site 20, Washita River and I-35 southwest of Paoli in Garvin county, cross section B.

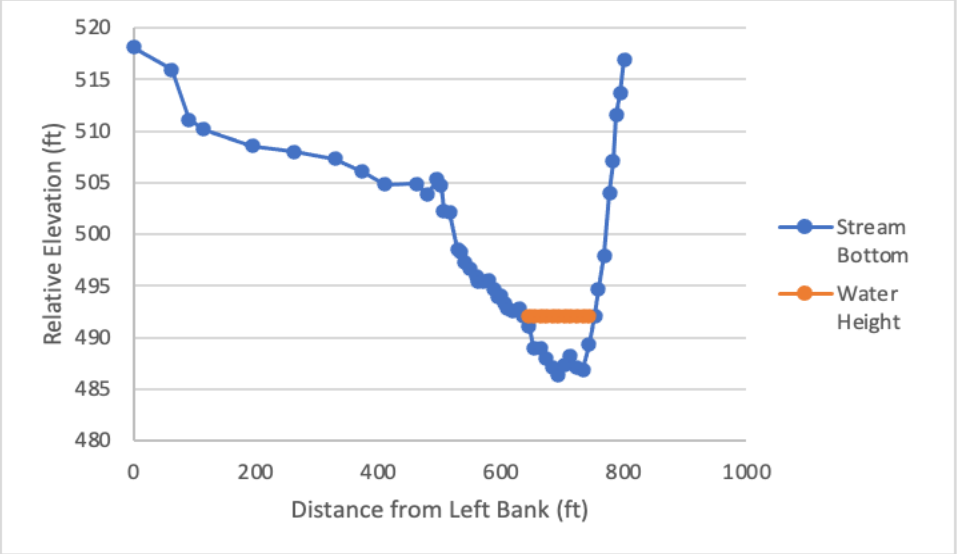

Figure C46: Site 20, Washita River and I-35 southwest of Paoli in Garvin county, cross section C.

Site 21 - Red River and S.H. 79 west of Waurika in Jefferson county

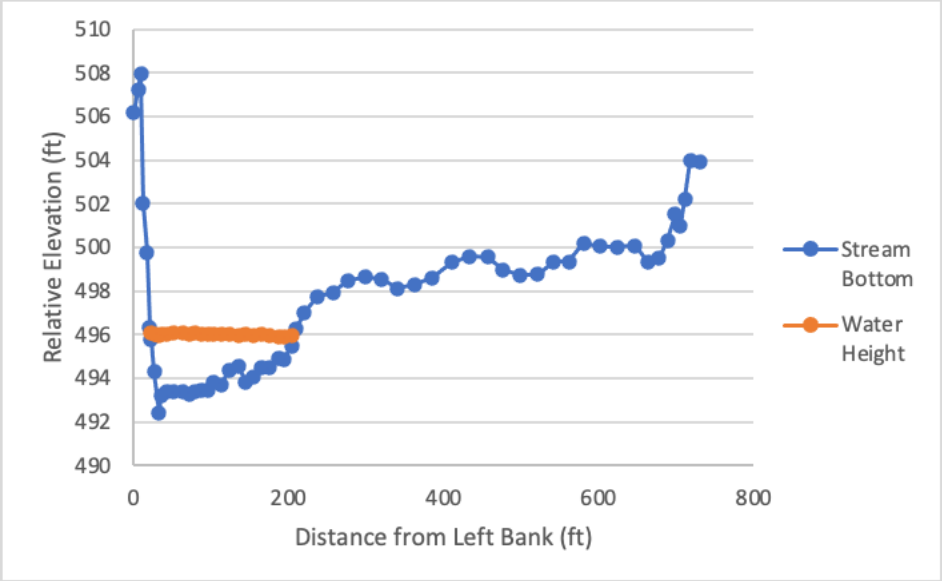

Figure C47: Site 21, Red River and S.H. 79 west of Waurika in Jefferson county, cross section A.

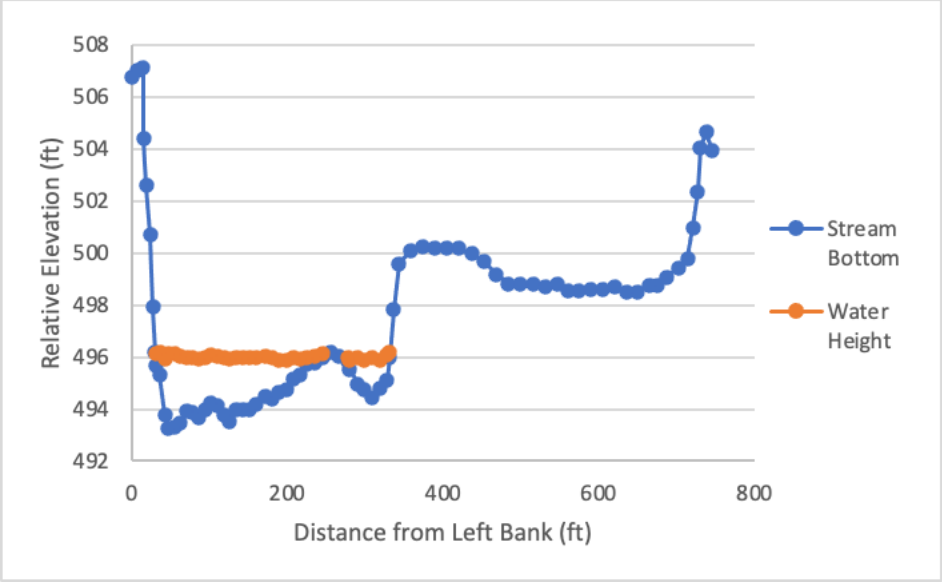

Figure C48: Site 21, Red River and S.H. 79 west of Waurika in Jefferson county, cross section B.

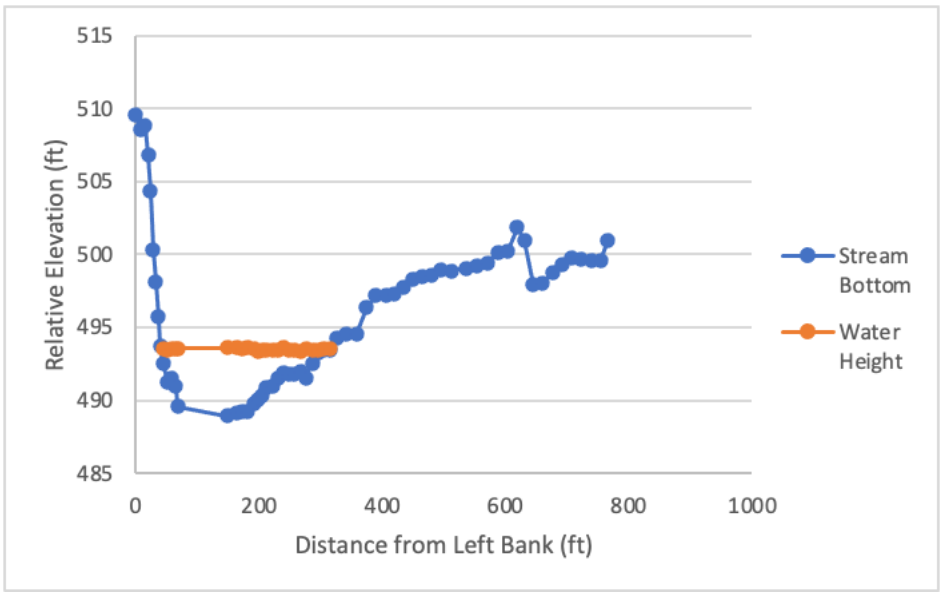

Figure C49: Site 21, Red River and S.H. 79 west of Waurika in Jefferson county, cross section C.

Site 22 - Washita River and S.H. 53 east of Gene Autry in Carter county

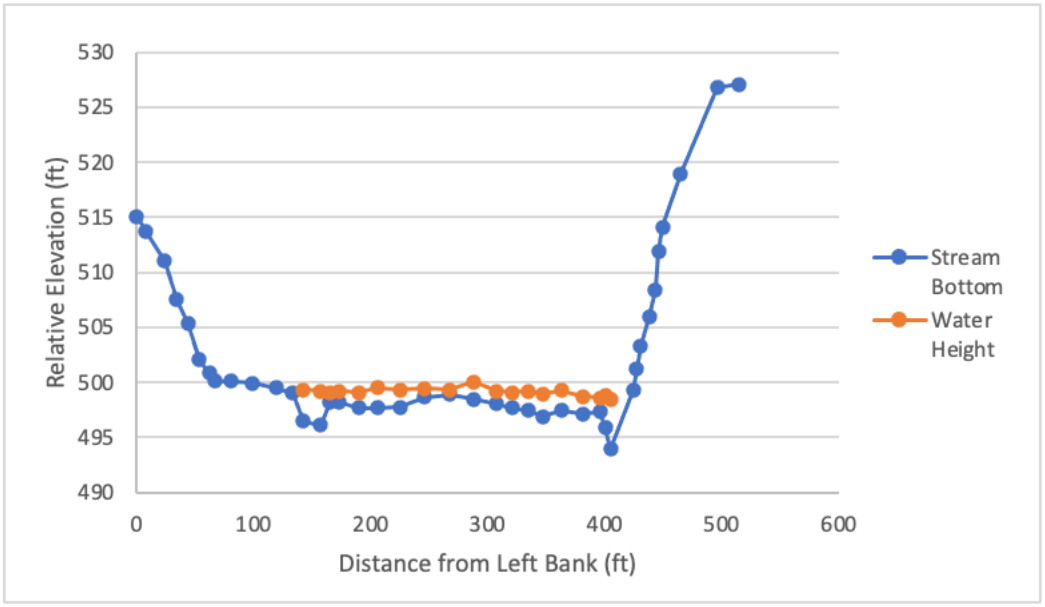

Figure C50: Site 22, Washita River and S.H. 53 east of Gene Autry in Carter county, cross section A.

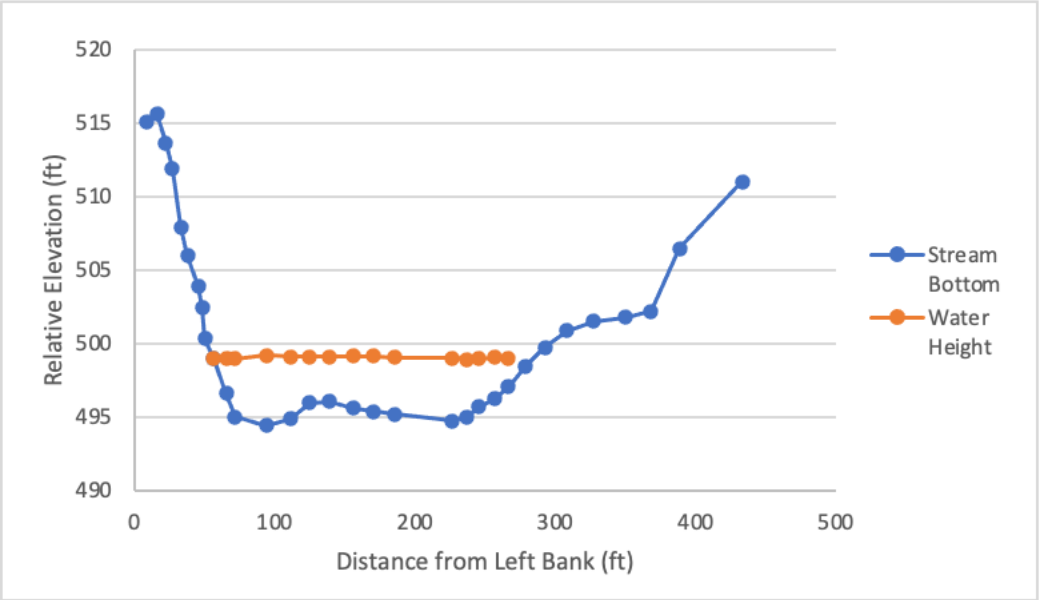

Figure C51: Site 22, Washita River and S.H. 53 east of Gene Autry in Carter county, cross section B.

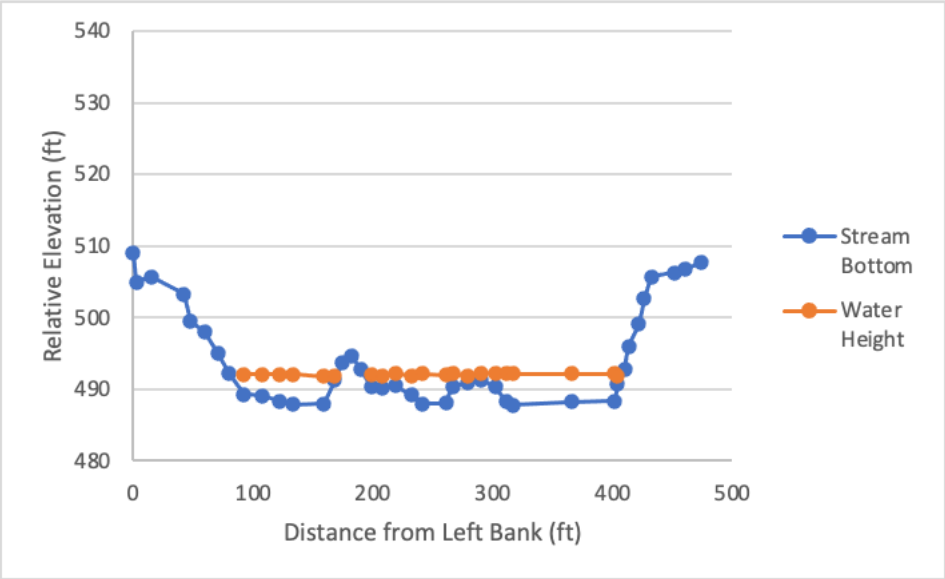

Figure C52: Site 22, Washita River and S.H. 53 east of Gene Autry in Carter county, cross section C.

Site 25 - North Canadian River and S.H. 48 north of Bearden in Okfuskee county

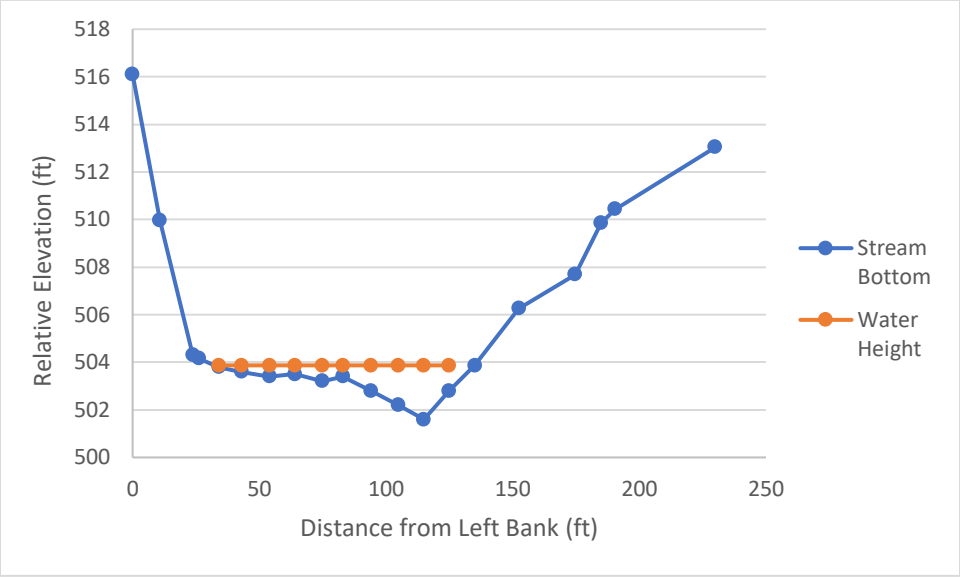

Figure C53: Site 25, North Canadian River and S.H. 48 north of Bearden in Okfuskee county, cross section A.

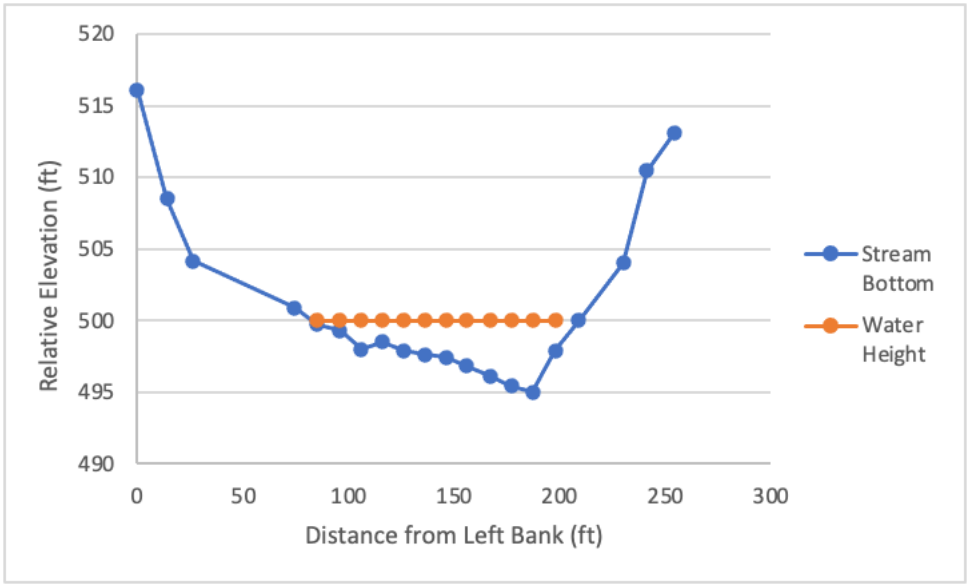

Figure C54: Site 25, North Canadian River and S.H. 48 north of Bearden in Okfuskee county, cross section B.

Site 27 - North Canadian River and S.H. 99 south of Prague in Seminole county

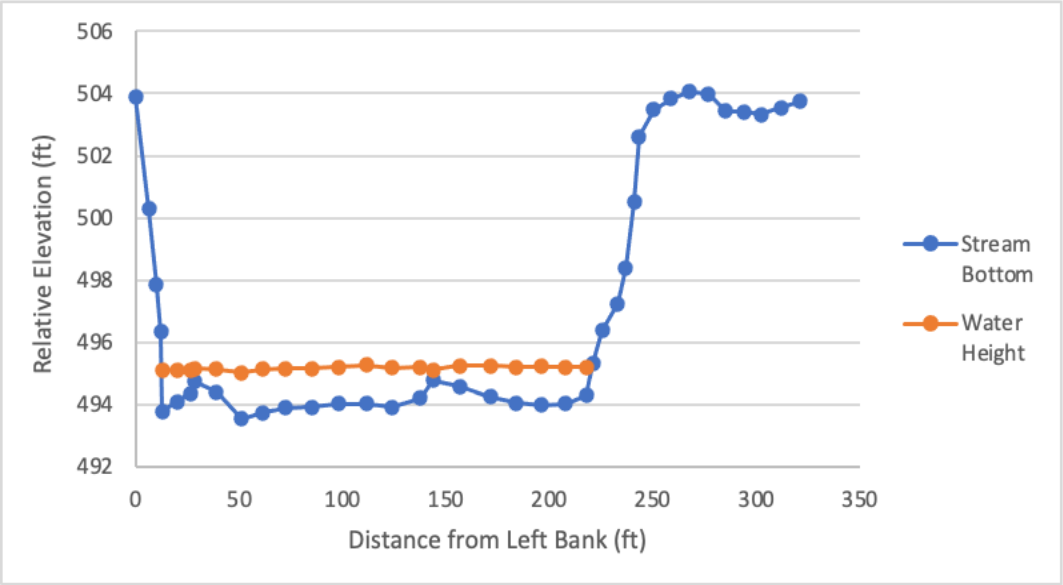

Figure C55: Site 27, North Canadian River and S.H. 99 south of Prague in Seminole county, cross section A.

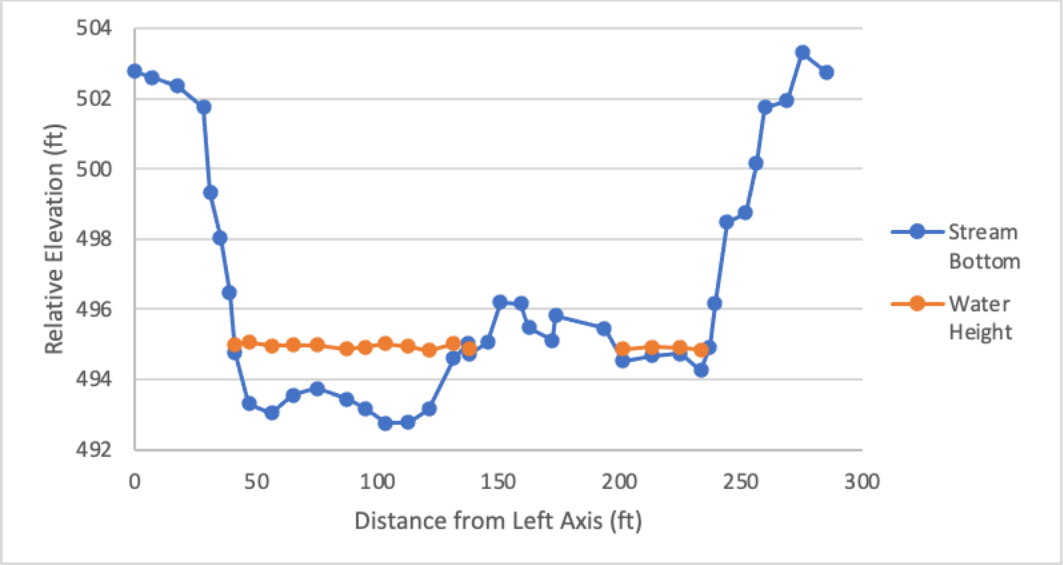

Figure C56: Site 27, North Canadian River and S.H. 99 south of Prague in Seminole county, cross section B.

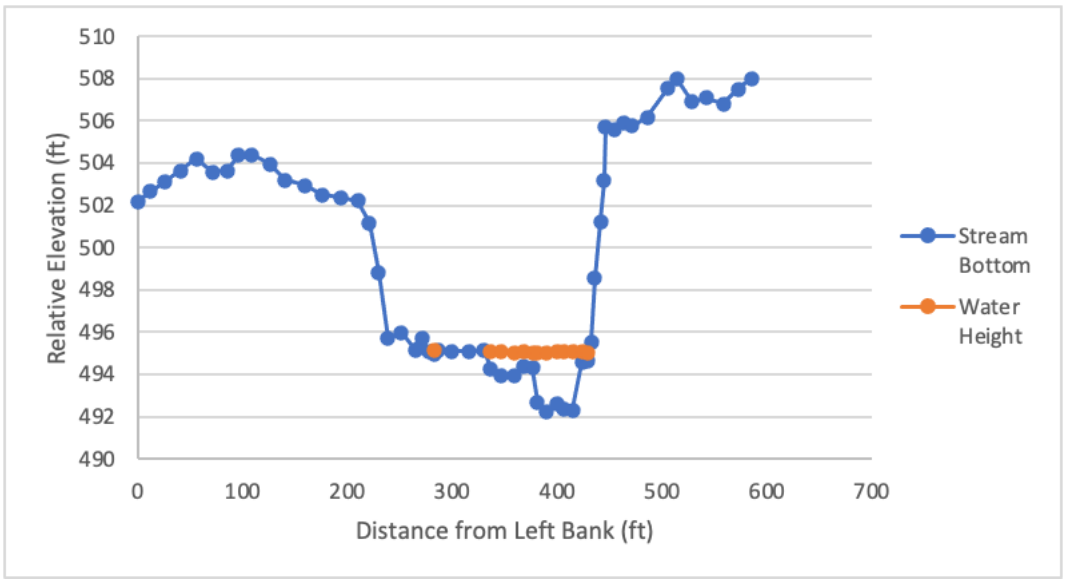

Figure C57: Site 27, North Canadian River and S.H. 99 south of Prague in Seminole county, cross section C.

Site 28 - Illinois River and S.H. 10 east of Tahlequah in Cherokee county

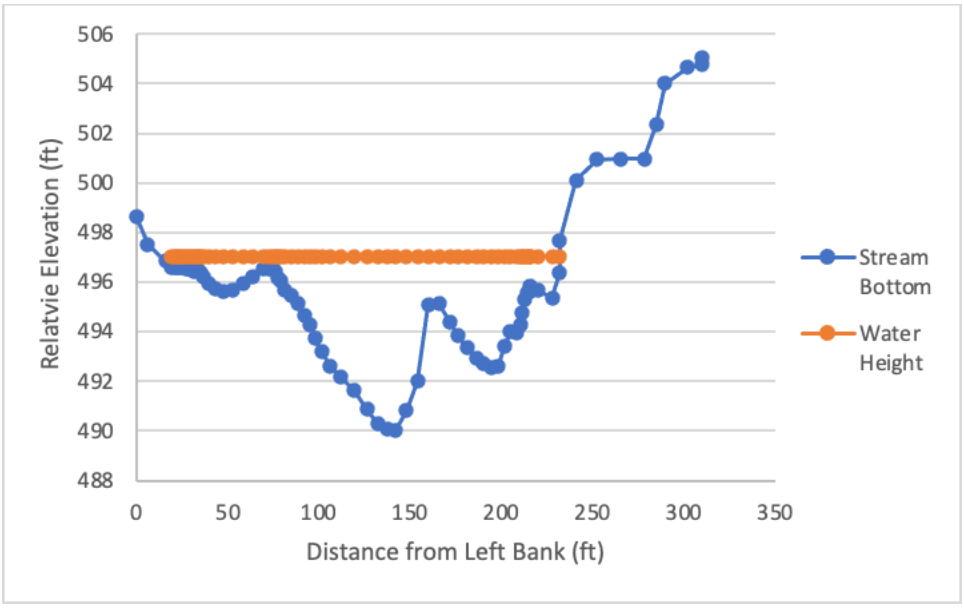

Figure C58: Site 28, Illinois River and S.H. 10 east of Tahlequah in Cherokee county, cross section A.

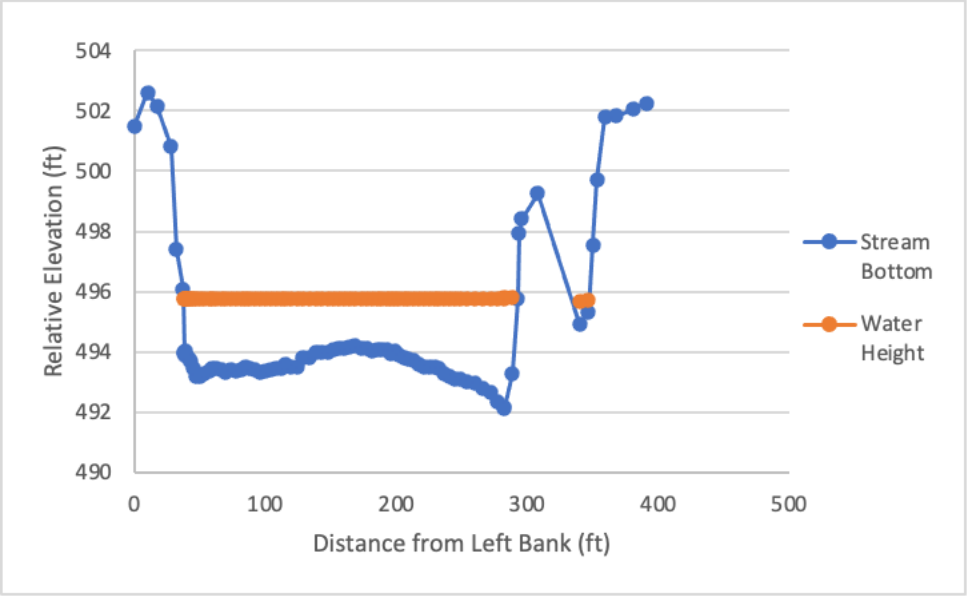

Figure C59: Site 28, Illinois River and S.H. 10 east of Tahlequah in Cherokee county, cross section B.

Site 29 - Washita River and S.H. 19 east of Lindsay in Garvin county

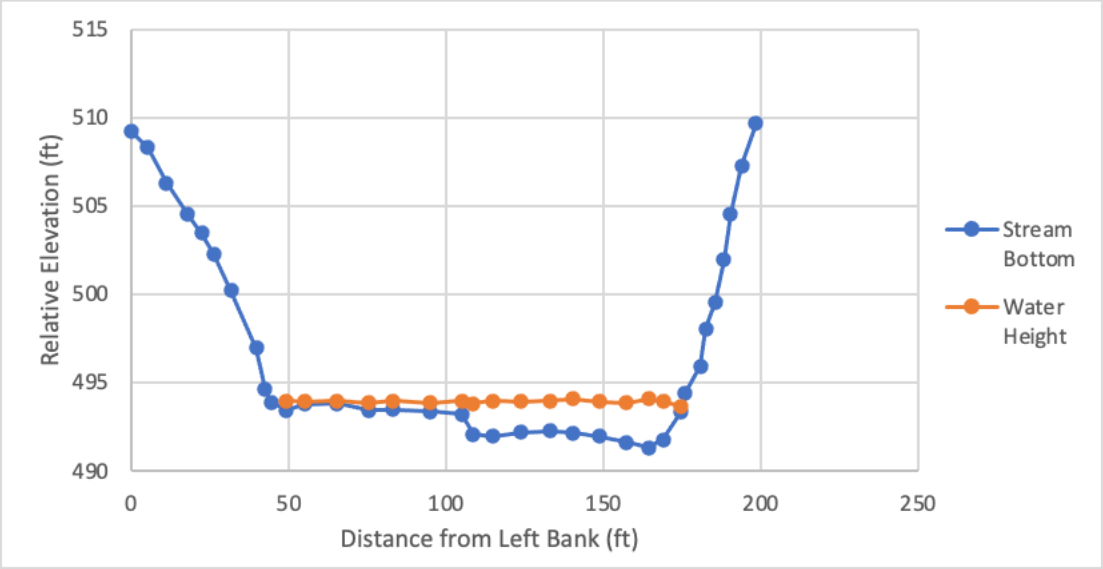

Figure C60: Site 29, Washita River and S.H. 19 east of Lindsay in Garvin county, cross section A.

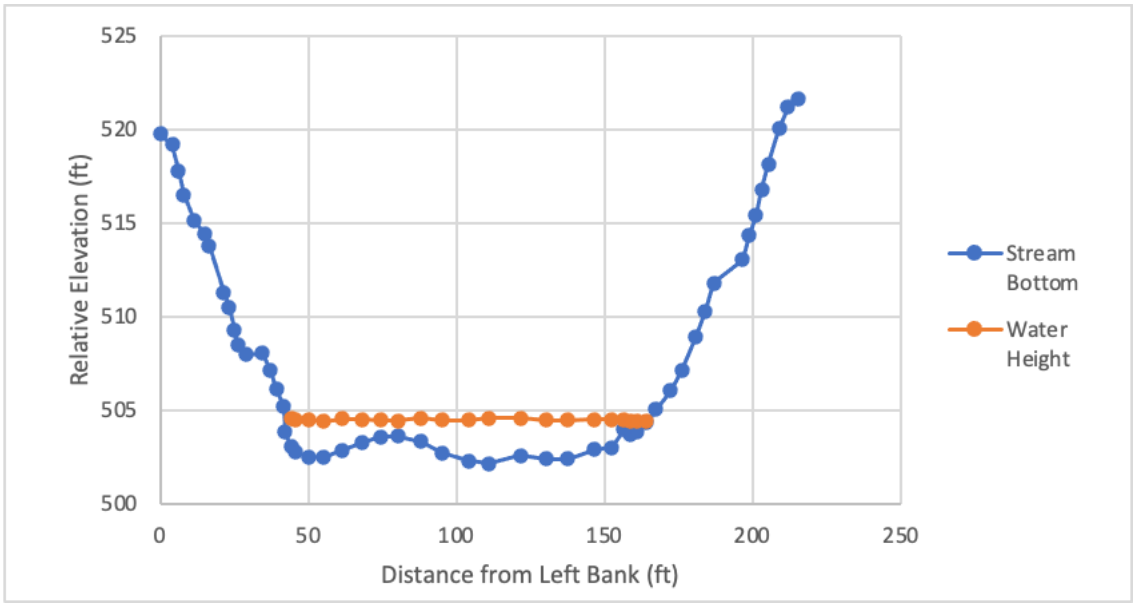

Figure C61: Site 29, Washita River and S.H. 19 east of Lindsay in Garvin county, cross section B.

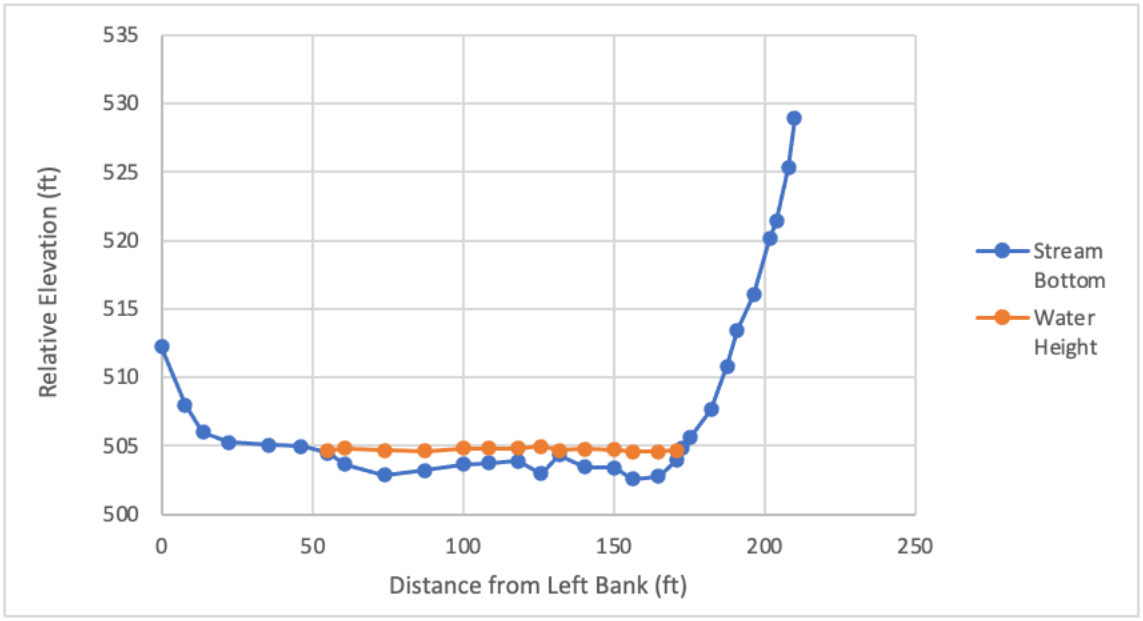

Figure C62: Site 29, Washita River and S.H. 19 east of Lindsay in Garvin county, cross section C.

Site 31 - Deer Creek Trib and U.S. 66 south of Hydro in Caddo county

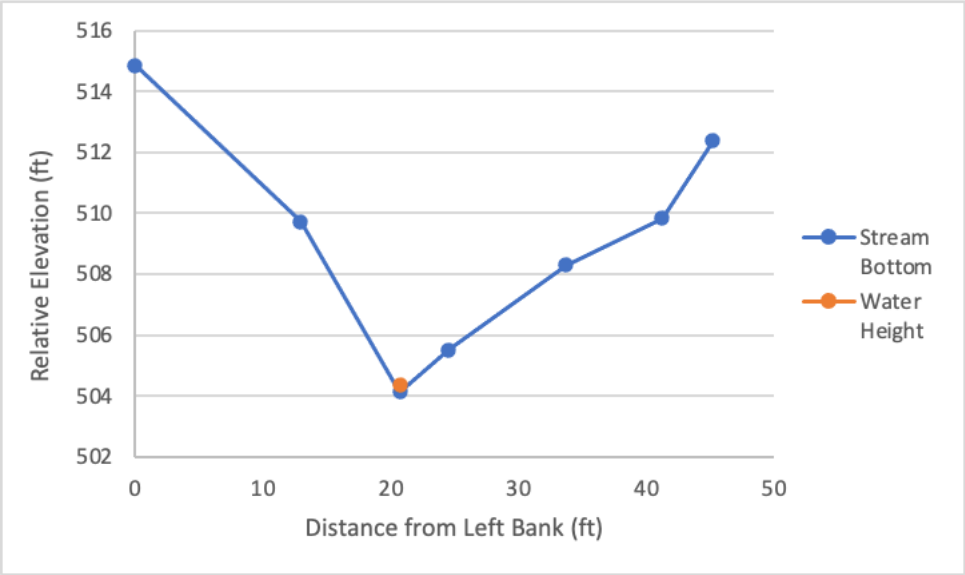

Figure C63: Site 31, Deer Creek Trib and U.S. 66 south of Hydro in Caddo county, cross section A.

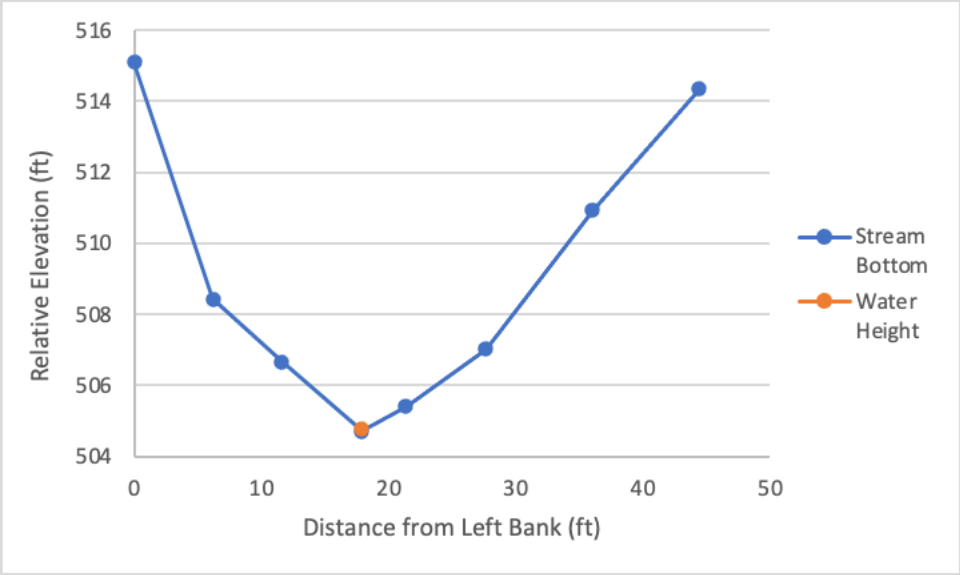

Figure C64: Site 31, Deer Creek Trib and U.S. 66 south of Hydro in Caddo county, cross section B.

Site 32 - Washita River and S.H. 7 west of Davis in Murray county

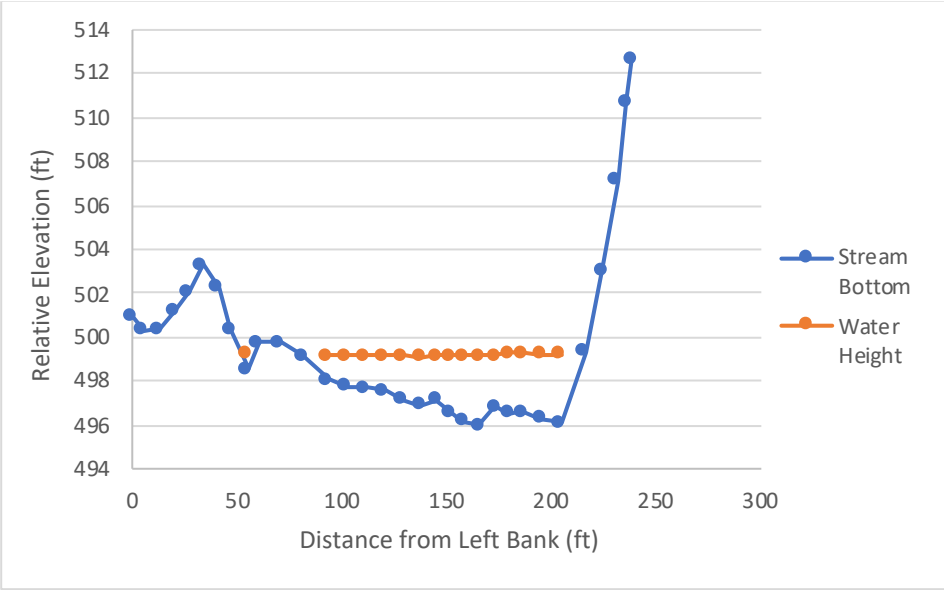

Figure C65: Site 32, Washita River and S.H. 7 west of Davis in Murray county, cross section A.

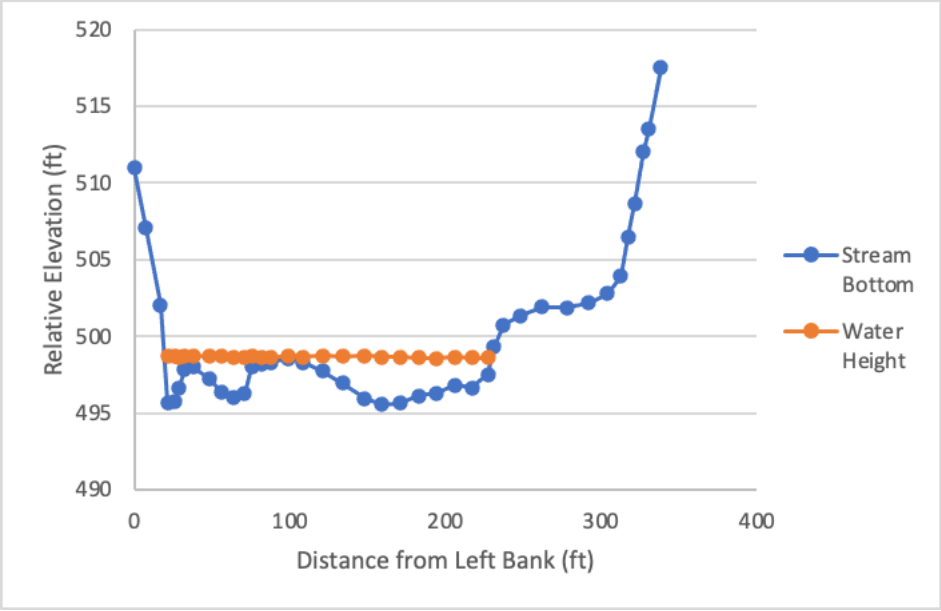

Figure C66: Site 32, Washita River and S.H. 7 west of Davis in Murray county, cross section B.

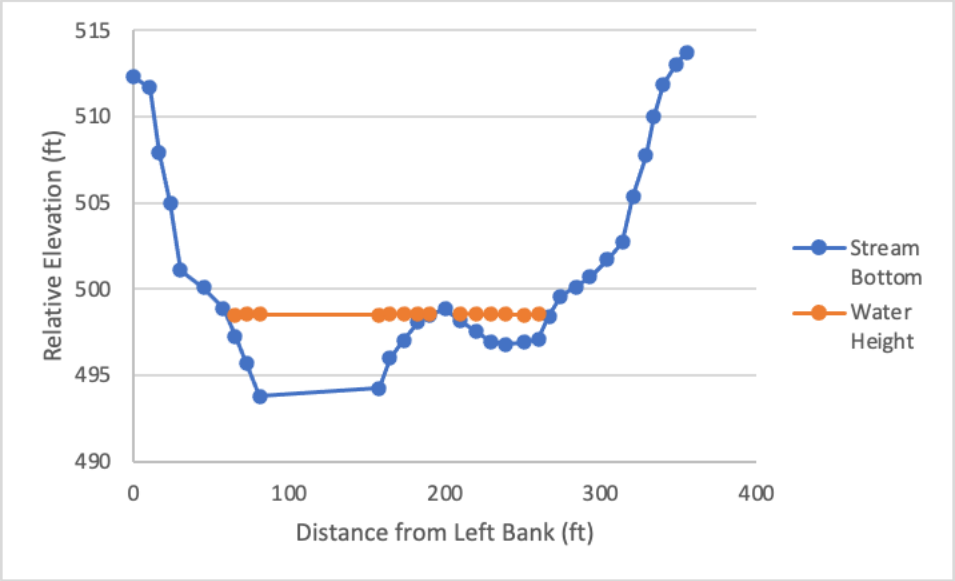

Figure C67: Site 32, Washita River and S.H. 7 west of Davis in Murray county, cross section C.

Site 33 - Salt Fork of the Arkansas River and S.H. 156 north of Marland in Kay county

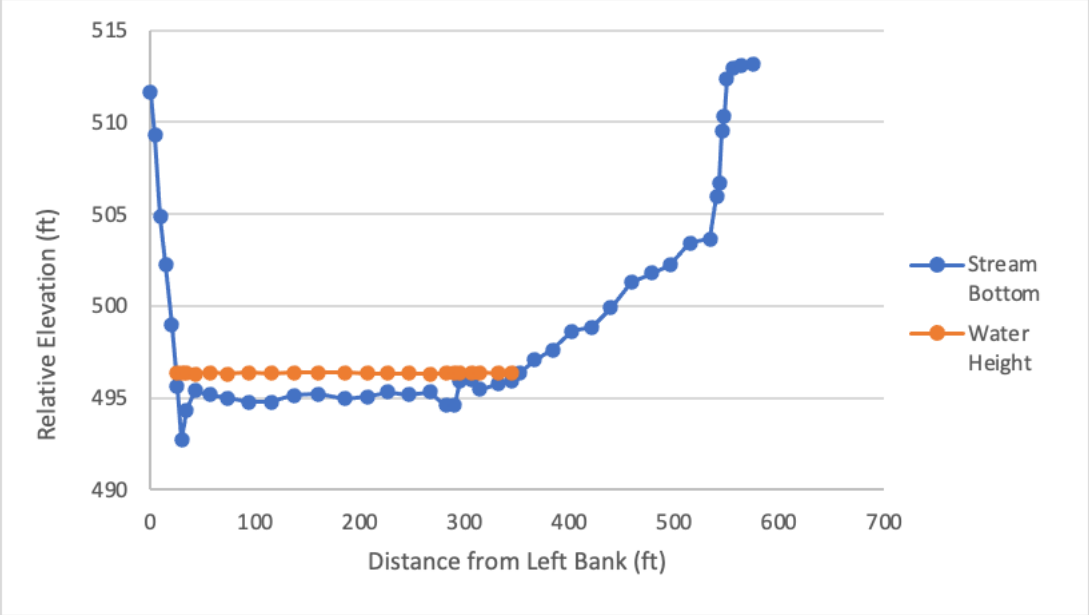

Figure C68: Site 33, Salt Fork of the Arkansas River and S.H. 156 north of Marland in Kay county, cross section A.

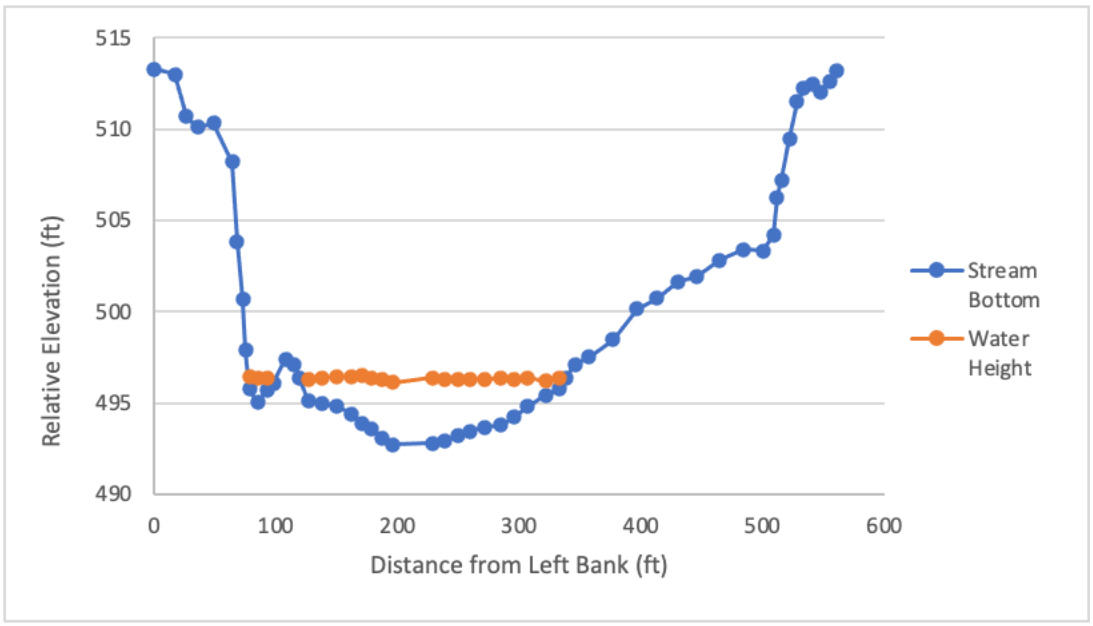

Figure C69: Site 33, Salt Fork of the Arkansas River and S.H. 156 north of Marland in Kay county, cross section B.

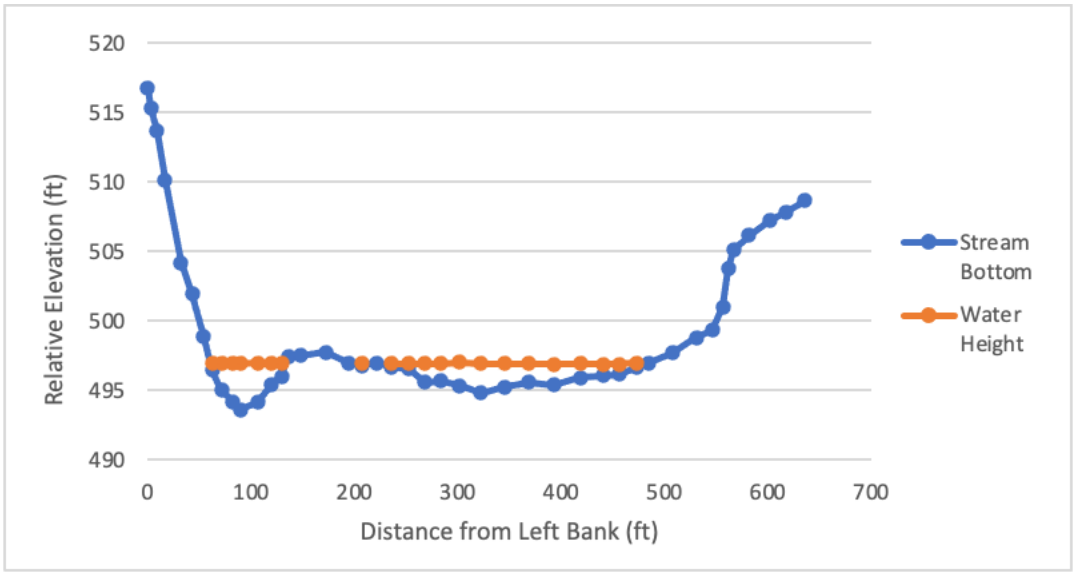

Figure C70: Site 33, Salt Fork of the Arkansas River and S.H. 156 north of Marland in Kay county, cross section C.

Appendix D – Velocity Profiles

Site 1 - Washita River and U.S. 77 north of Wynnewood in Garvin county

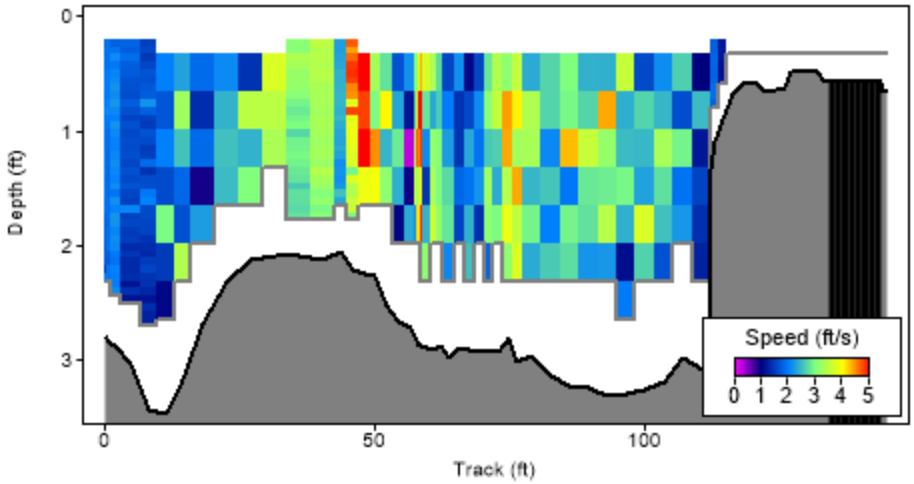

Figure D1: Site 1, Washita River and U.S. 77 north of Wynnewood in Garvin county, velocity profile A.

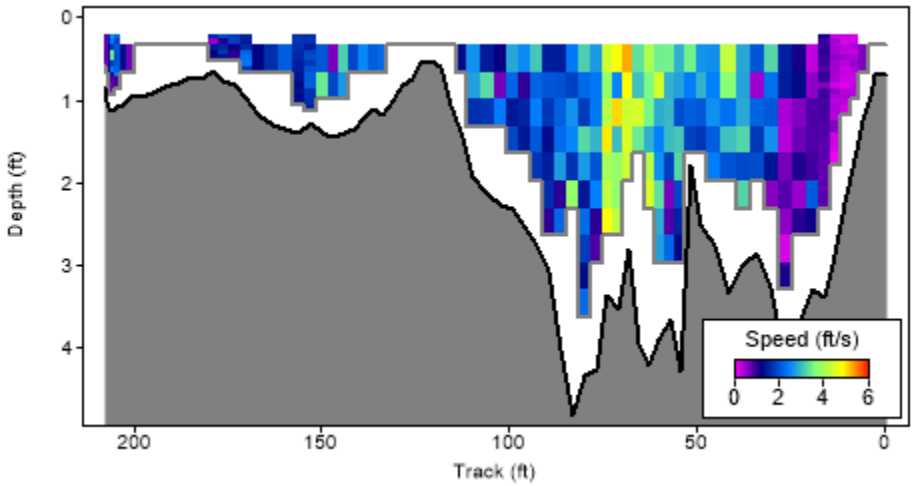

Figure D2: Site 1, Washita River and U.S. 77 north of Wynnewood in Garvin county, velocity profile B.

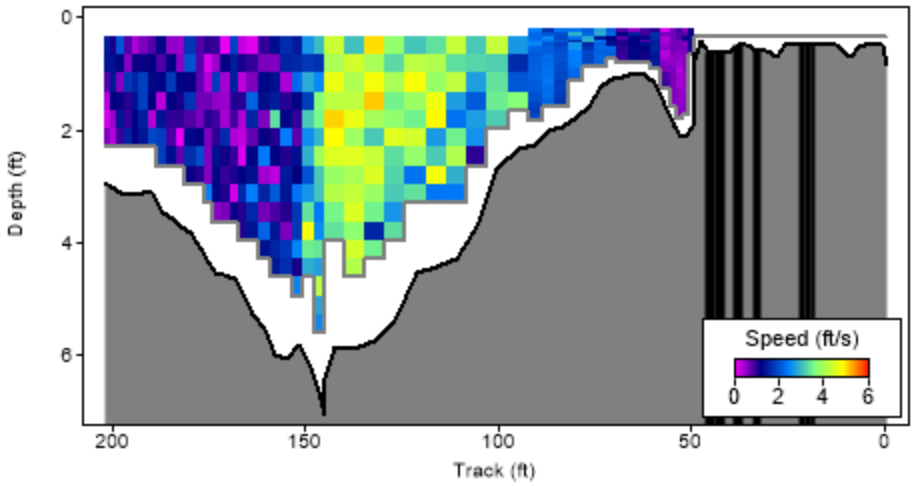

Figure D3: Site 1, Washita River and U.S. 77 north of Wynnewood in Garvin county, velocity profile C.

Site 2 - Cimarron River and U.S. 177 south of Perkins in Payne county

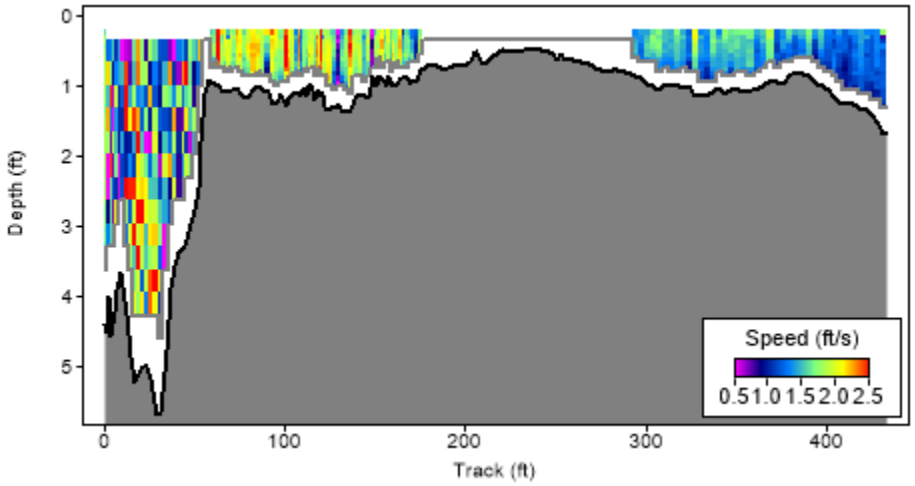

Figure D4: Site 2, Cimarron River and U.S. 177 south of Perkins in Payne county, velocity profile A.

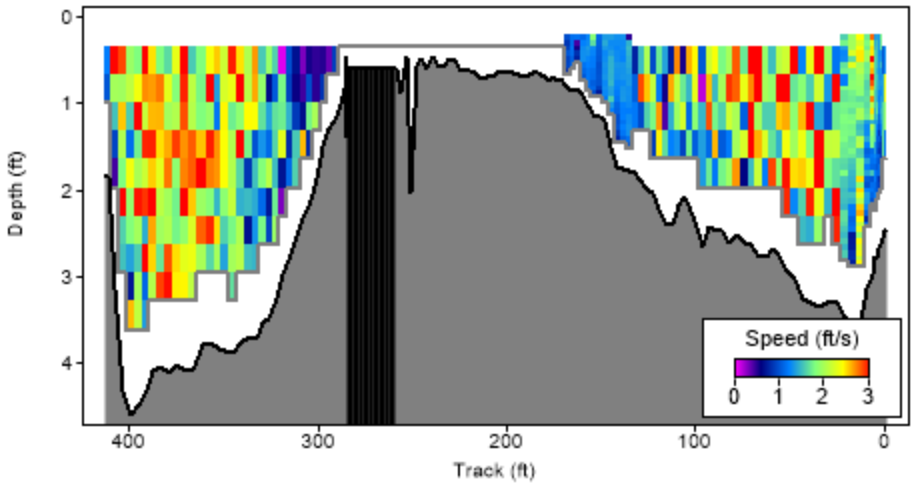

Figure D5: Site 2, Cimarron River and U.S. 177 south of Perkins in Payne county, velocity profile B.

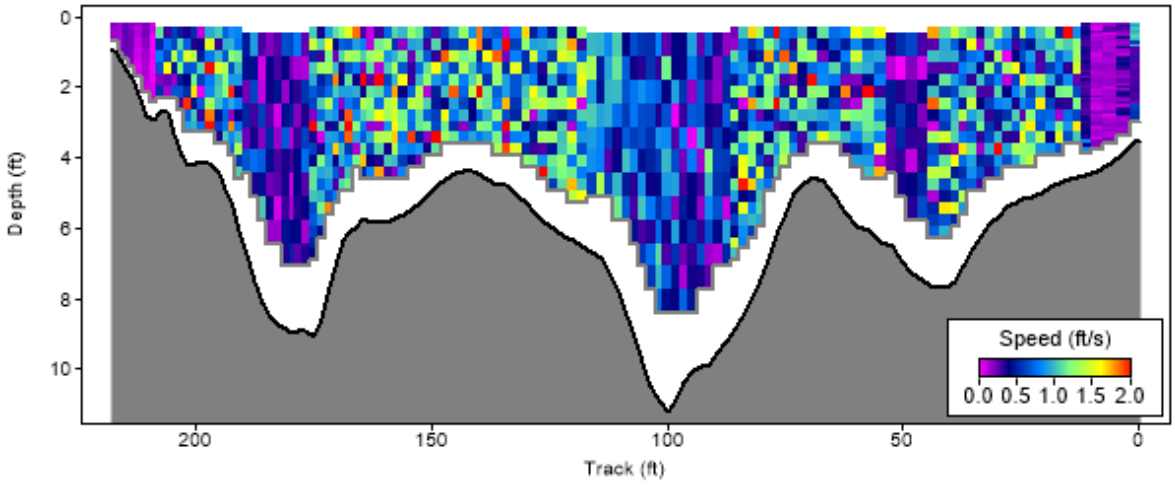

Figure D6: Site 2, Cimarron River and U.S. 177 south of Perkins in Payne county, velocity profile C.

Site 4 - Cimarron River and U.S. 281 south of Watonga in Blaine county

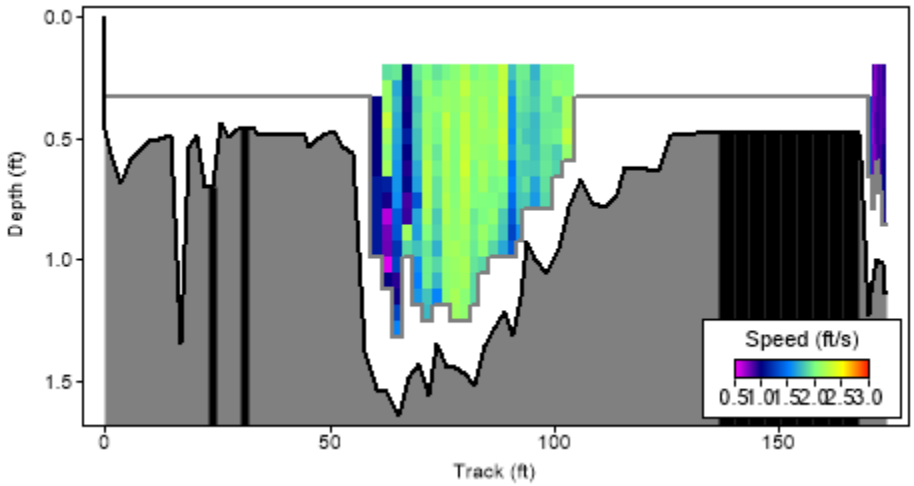

Figure D7: Site 4, Cimarron River and U.S. 281 south of Watonga in Blaine county, velocity profile A.

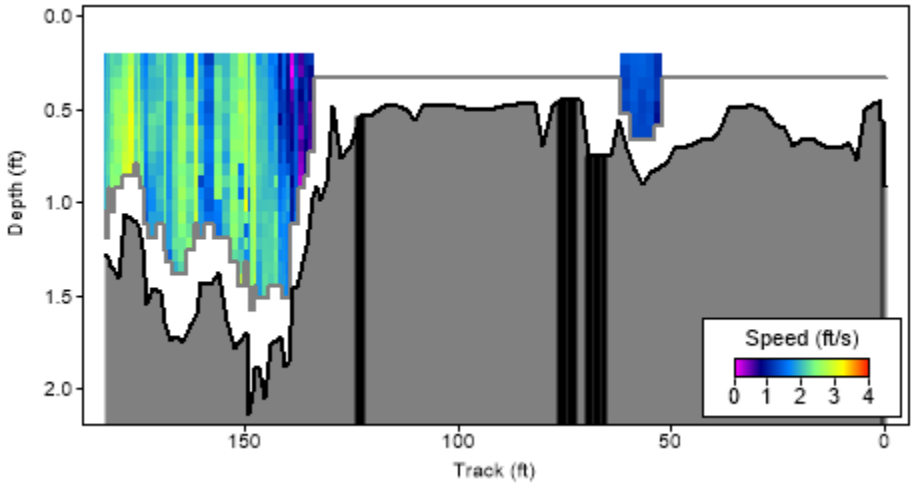

Figure D8: Site 4, Cimarron River and U.S. 281 south of Watonga in Blaine county, velocity profile B.

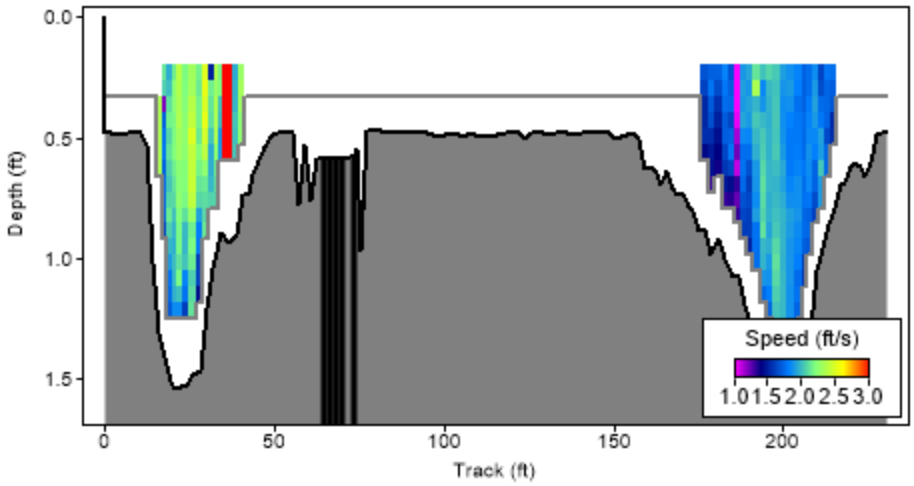

Figure D9: Site 4, Cimarron River and U.S. 281 south of Watonga in Blaine county, velocity profile C.

Site 6 - North Canadian River and U.S. 281 south Watonga in Blaine county

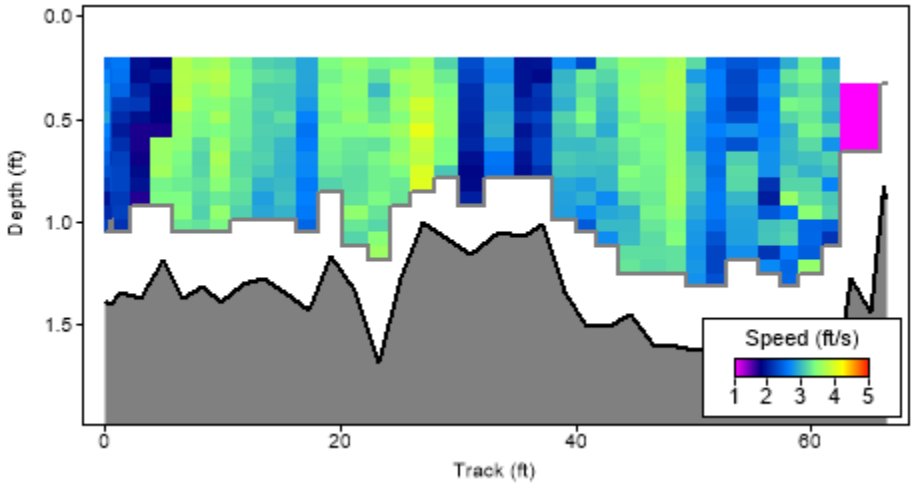

Figure D10: Site 6, North Canadian River and U.S. 281 south Watonga in Blaine county, velocity profile A.

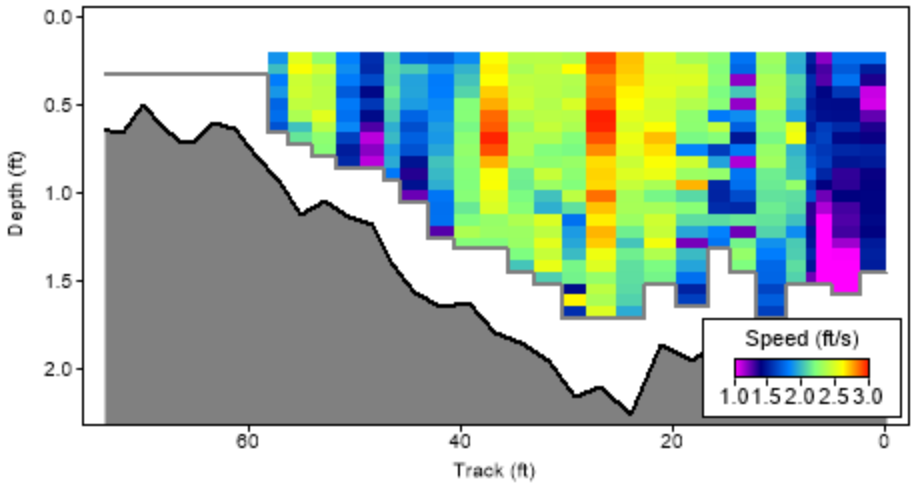

Figure D11: Site 6, North Canadian River and U.S. 281 south Watonga in Blaine county, velocity profile B.

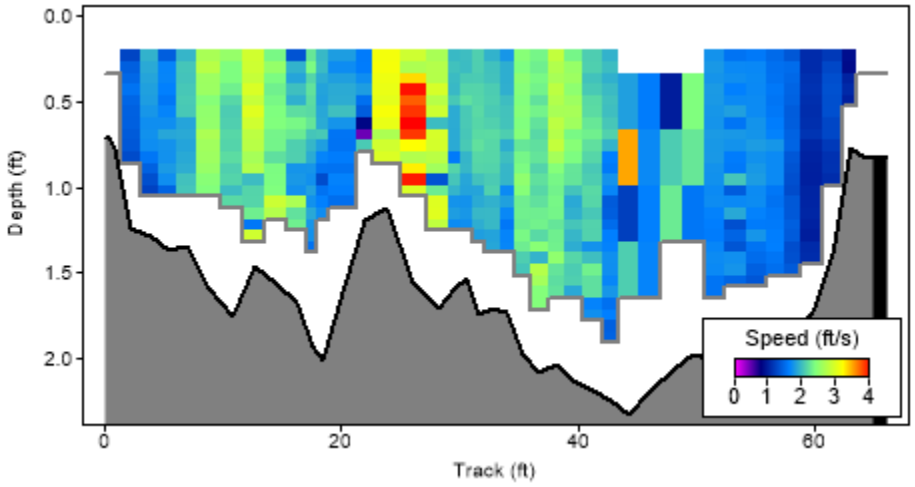

Figure D12: Site 6, North Canadian River and U.S. 281 south Watonga in Blaine county, velocity profile C.

Site 7 - Canadian River and U.S. 281 east of Bridgeport in Canadian county

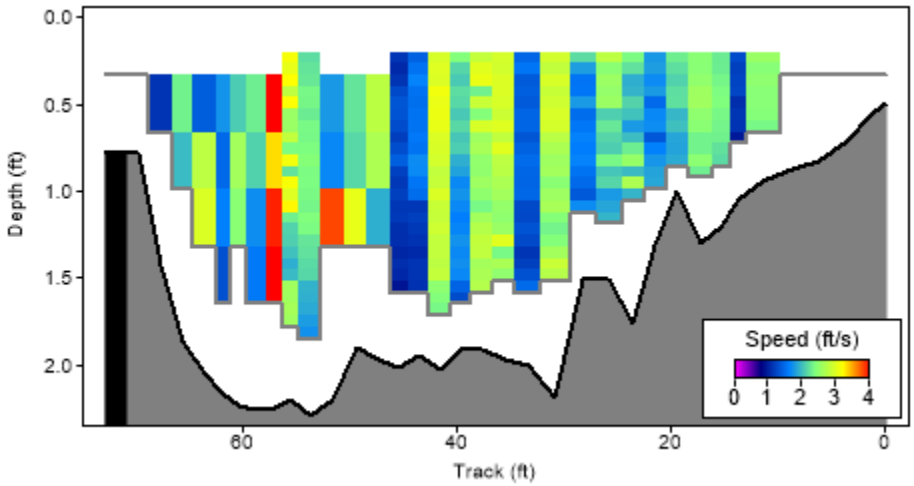

Figure D13: Site 7, Canadian River and U.S. 281 east of Bridgeport in Canadian county, velocity profile A.

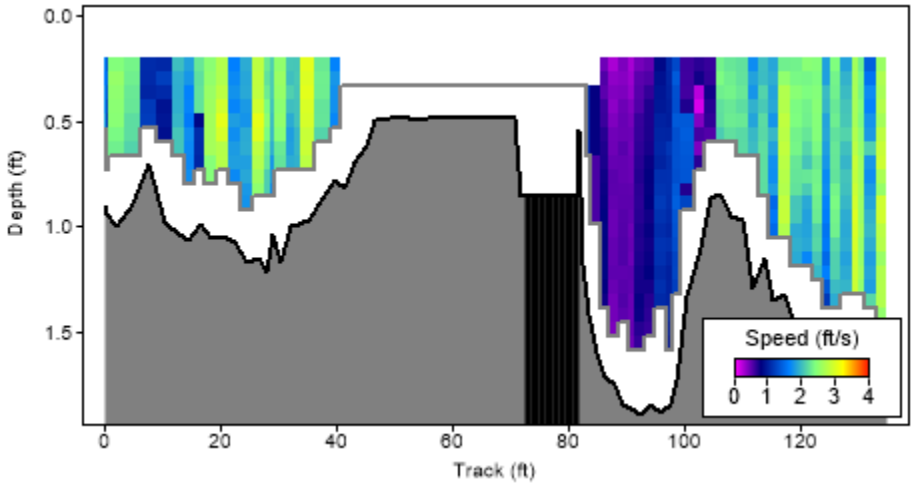

Figure D14: Site 7, Canadian River and U.S. 281 east of Bridgeport in Canadian county, velocity profile B.

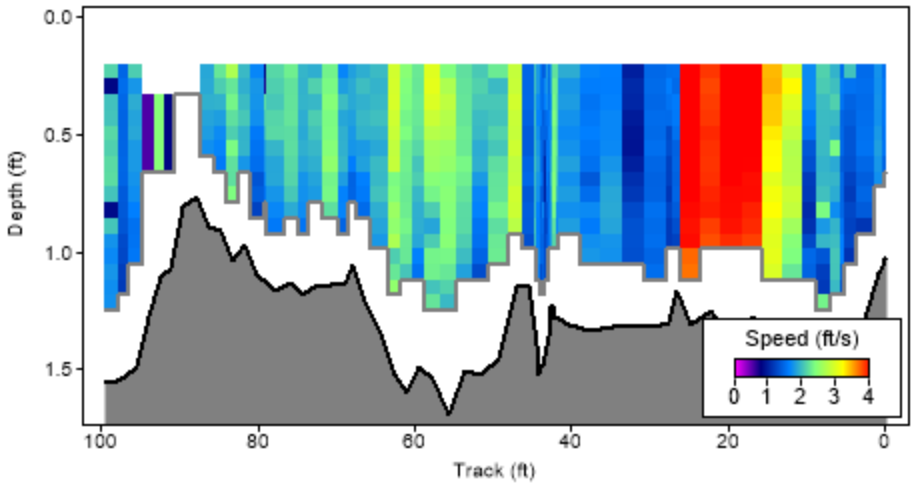

Figure D15: Site 7, Canadian River and U.S. 281 east of Bridgeport in Canadian county, velocity profile C.

Site 8 - Salt Fork of the Red River and U.S. 62 west of Altus in Jackson county

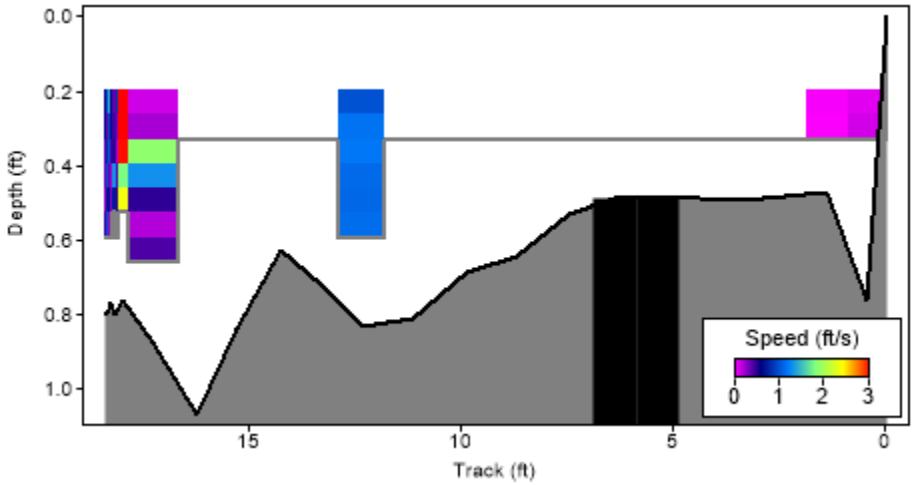

Figure D16: Site 8, Salt Fork of the Red River and U.S. 62 west of Altus in Jackson county, velocity profile A.

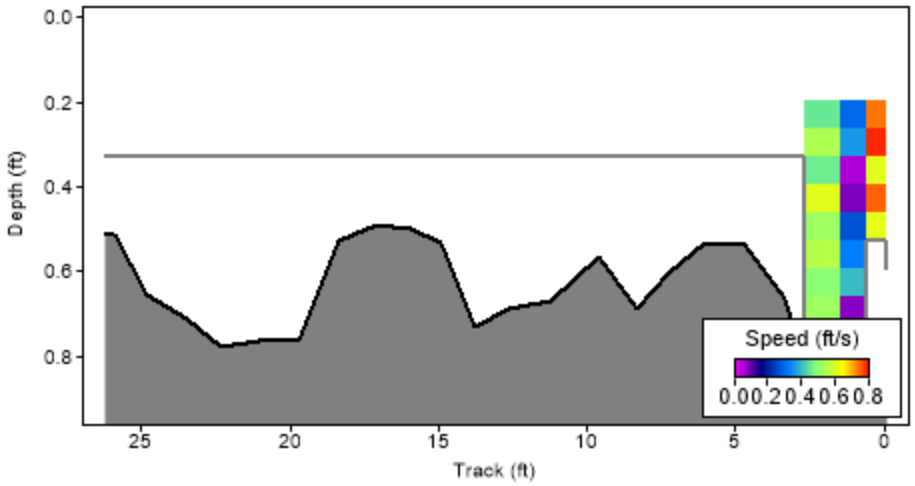

Figure D17: Site 8, Salt Fork of the Red River and U.S. 62 west of Altus in Jackson county, velocity profile B.

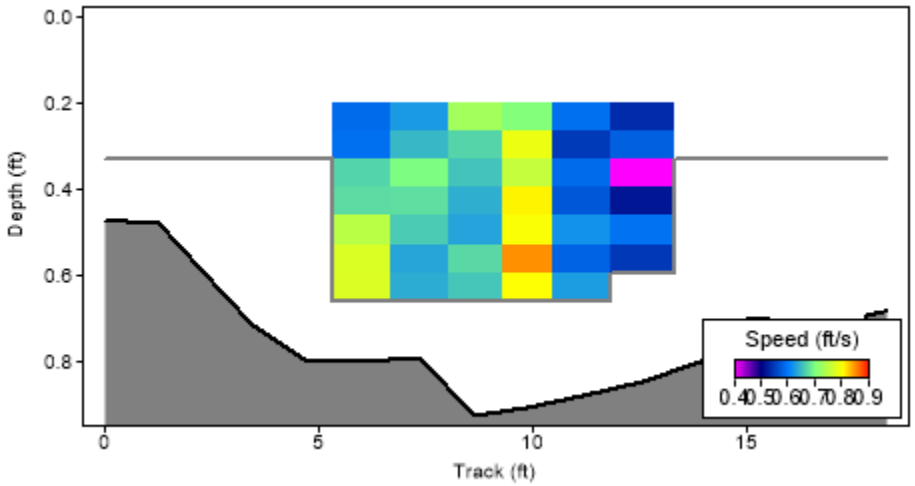

Figure D18: Site 8, Salt Fork of the Red River and U.S. 62 west of Altus in Jackson county, velocity profile C.

Site 10 - Washita River and S.H. 76 south of Lindsay in Garvin county

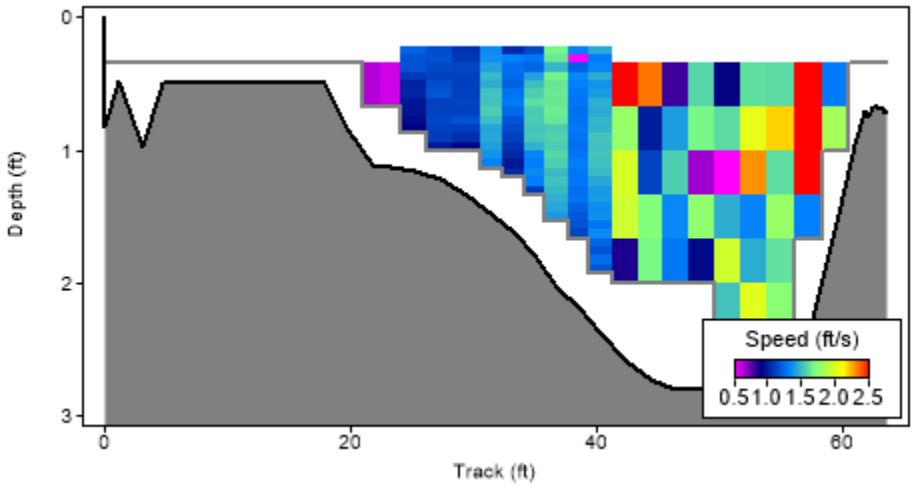

Figure D19: Site 10, Washita River and S.H. 76 south of Lindsay in Garvin county, velocity profile A.

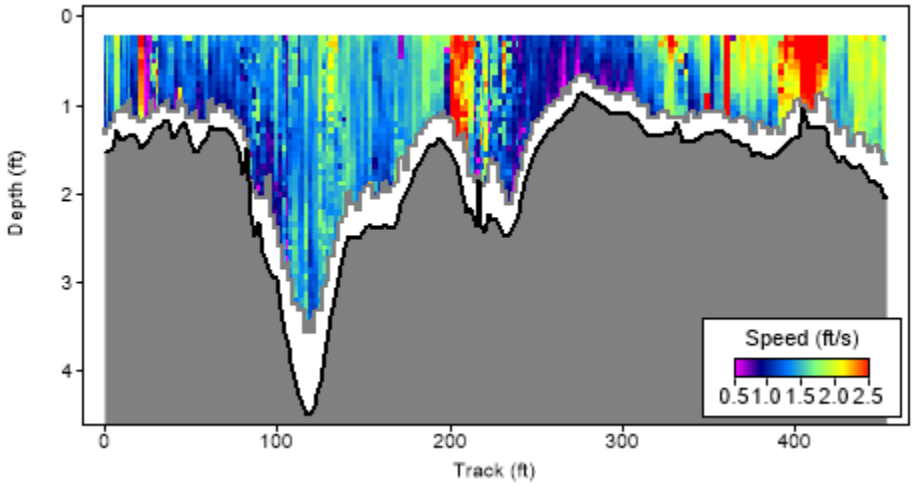

Figure D20: Site 10, Washita River and S.H. 76 south of Lindsay in Garvin county, velocity profile B.

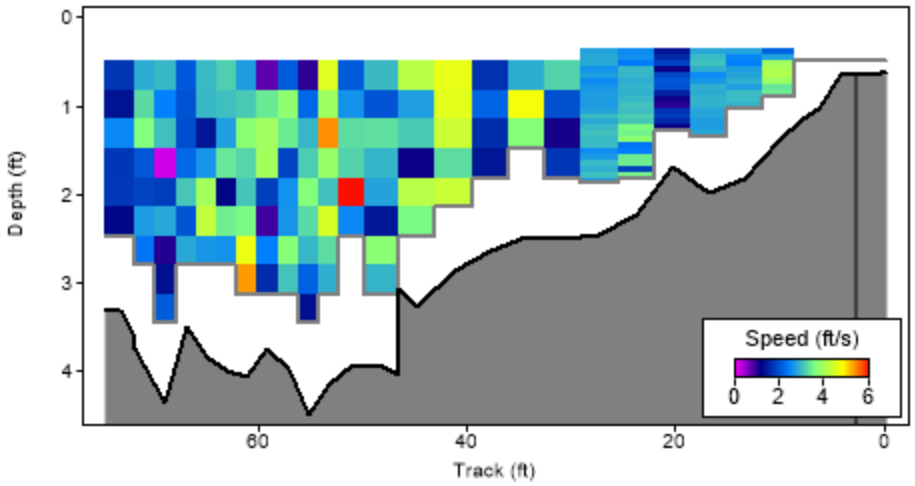

Figure D21: Site 10, Washita River and S.H. 76 south of Lindsay in Garvin county, velocity profile C.

Site 11 - Washita River and S.H. 74 north of Maysville in Garvin county

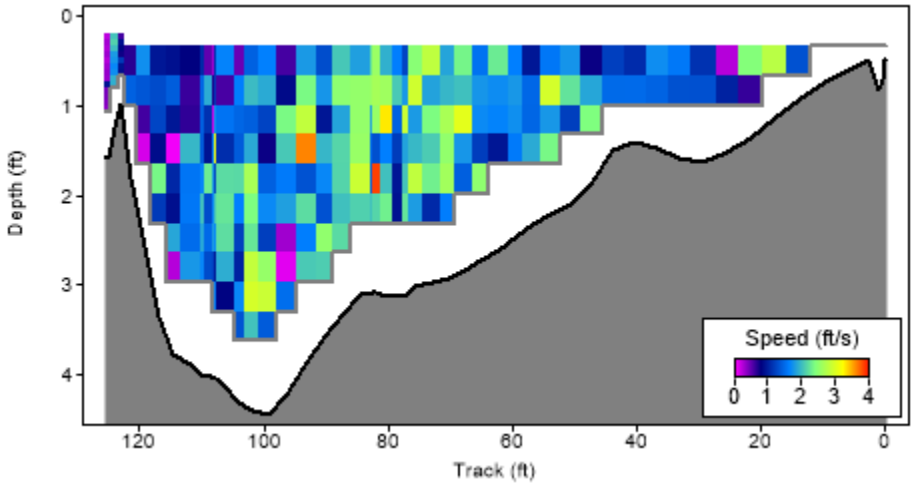

Figure D22: Site 11, Washita River and S.H. 74 north of Maysville in Garvin county, velocity profile A.

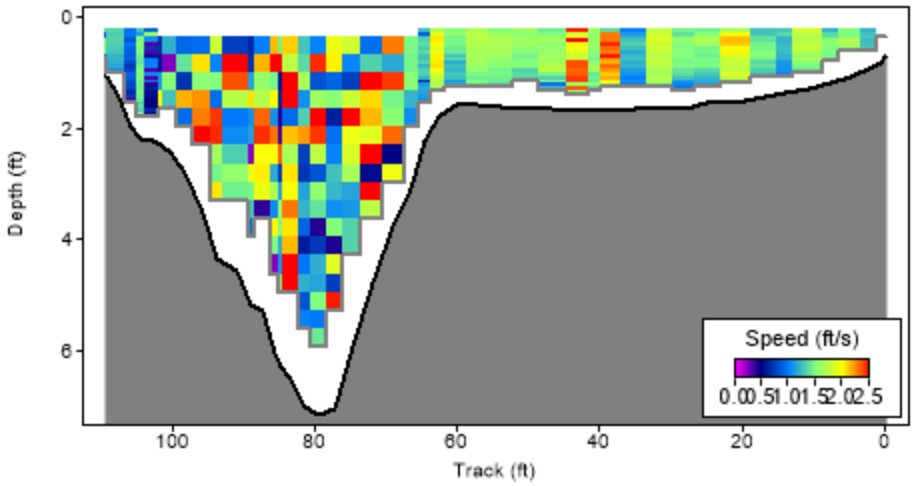

Figure D23: Site 11, Washita River and S.H. 74 north of Maysville in Garvin county, velocity profile B.

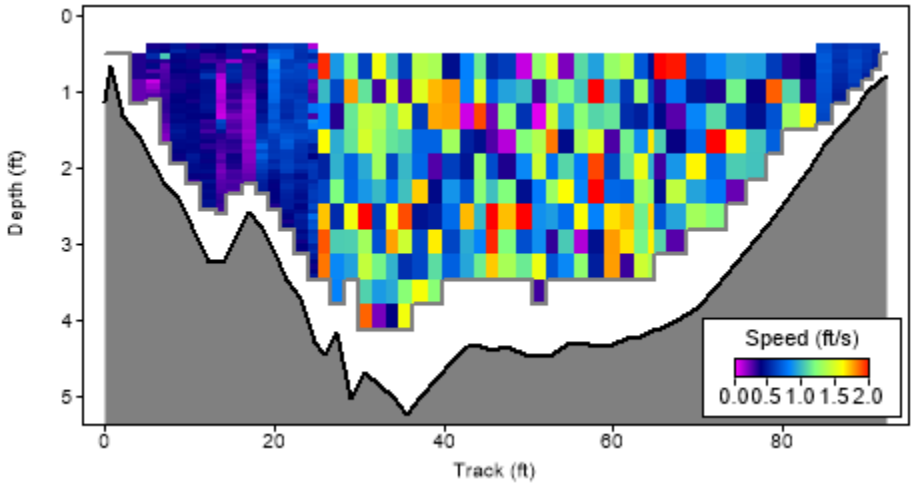

Figure D24: Site 11, Washita River and S.H. 74 north of Maysville in Garvin county, velocity profile C.

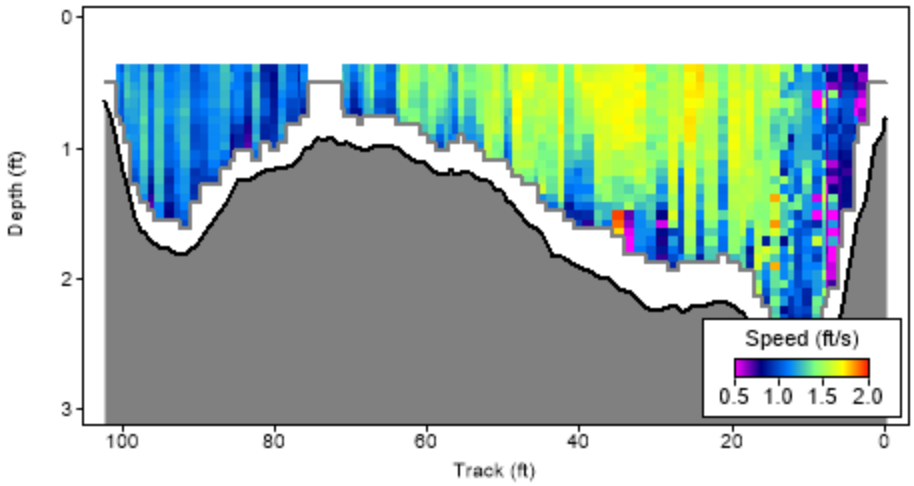

Figure D25: Site 11, Washita River and S.H. 74 north of Maysville in Garvin county velocity profile E.

Site 12 - Cimarron River and S.H. 33 north of Coyle in Logan county

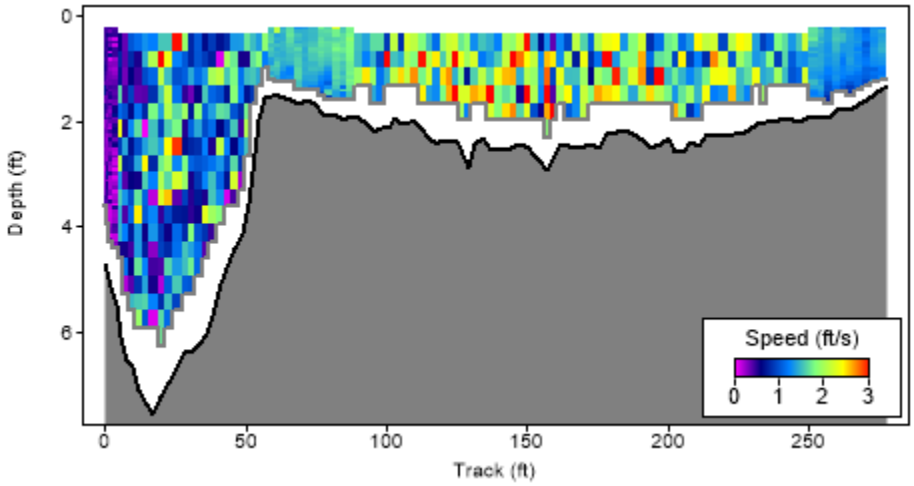

Figure D26: Site 12, Cimarron River and S.H. 33 north of Coyle in Logan county, velocity profile A.

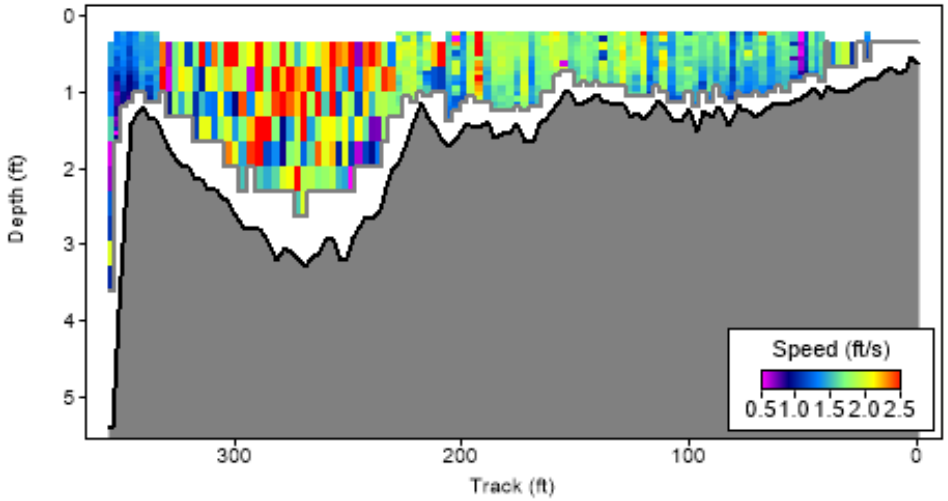

Figure D27: Site 12, Cimarron River and S.H. 33 north of Coyle in Logan county, velocity profile B.

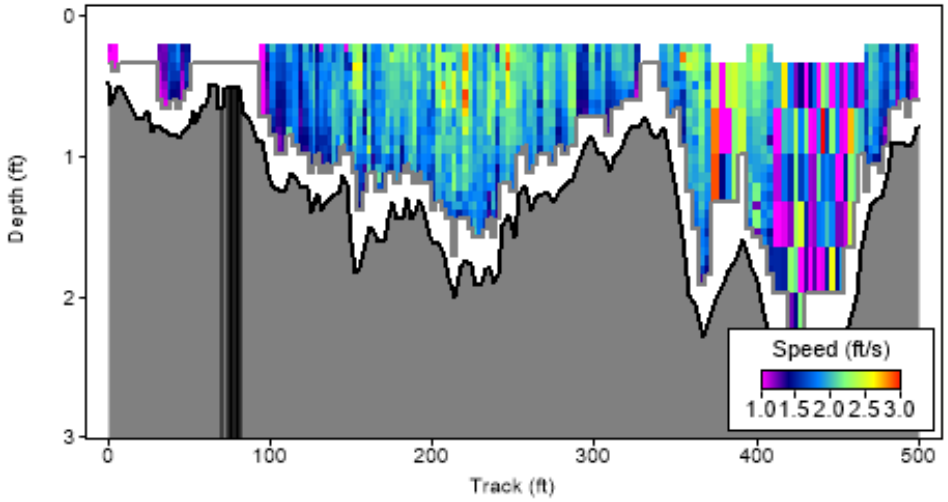

Figure D28: Site 12, Cimarron River and S.H. 33 north of Coyle in Logan county, velocity profile C.

Site 16 - North Canadian River and S.H. 3 east of Shawnee in Pottawatomie county

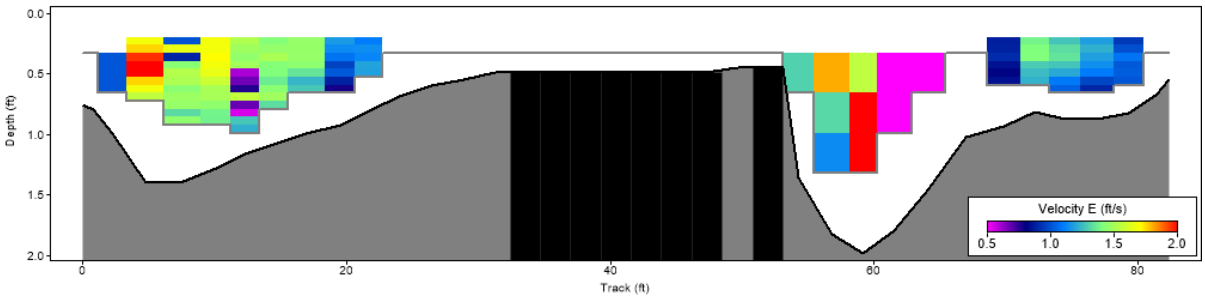

Figure D29: Site 16, North Canadian River and S.H. 3 east of Shawnee in Pottawatomie county, velocity profile A.

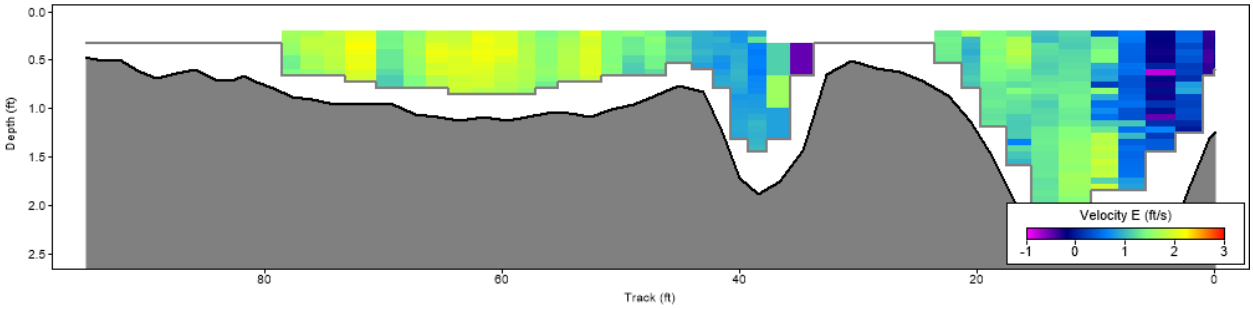

Figure D30: Site 16, North Canadian River and S.H. 3 east of Shawnee in Pottawatomie county, velocity profile B.

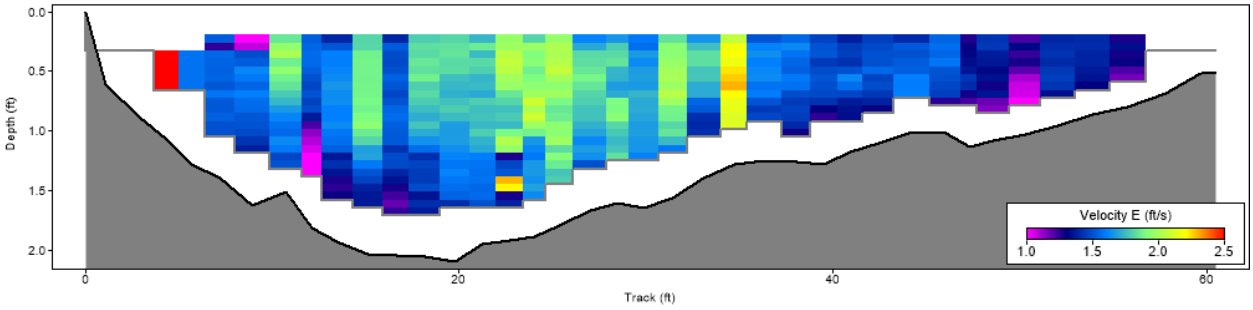

Figure D31: Site 16, North Canadian River and S.H. 3 east of Shawnee in Pottawatomie county, velocity profile C.

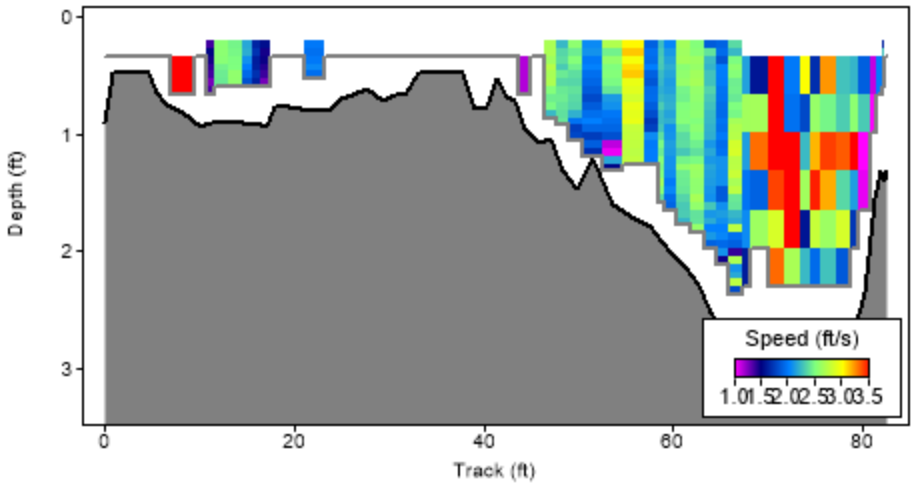

Figure D32: Site 16, North Canadian River and S.H. 3 east of Shawnee in Pottawatomie county, velocity profile D.

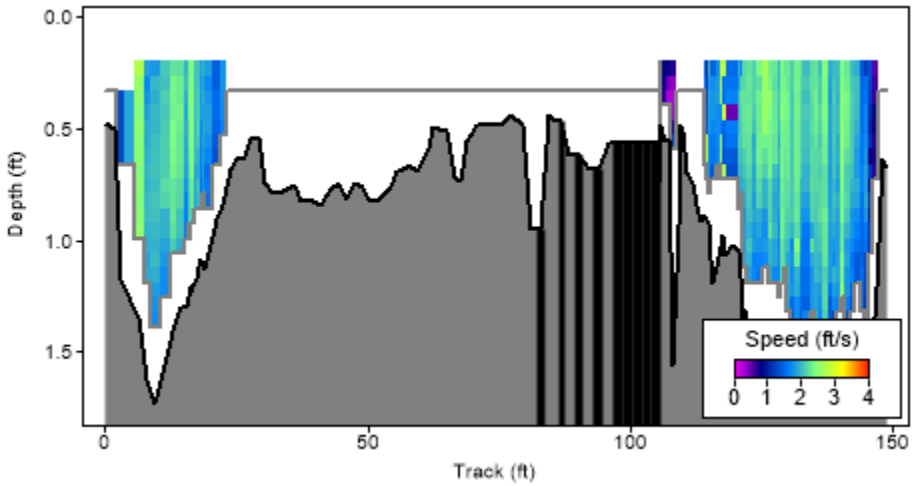

Figure D33: Site 16, North Canadian River and S.H. 3 east of Shawnee in Pottawatomie county, velocity profile E.

Site 17 - Cimarron River and S.H. 74 south of Crescent in Logan county

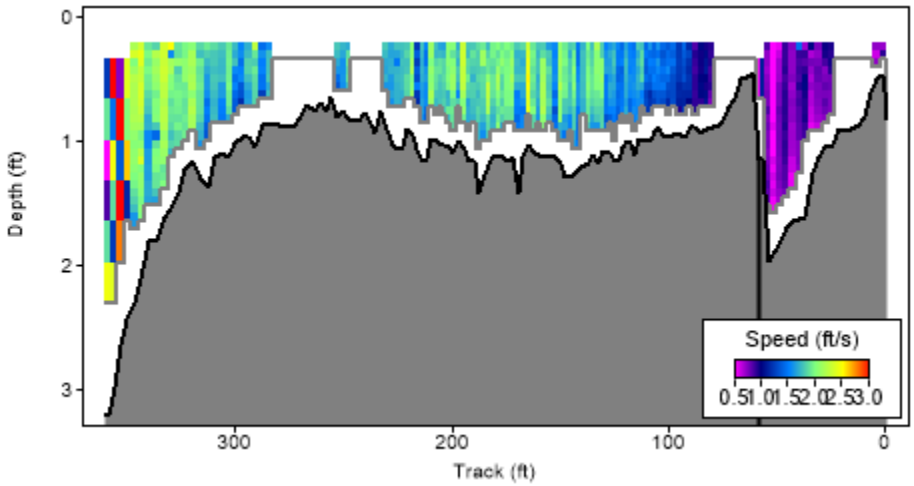

Figure D34: Site 17, Cimarron River and S.H. 74 south of Crescent in Logan county, velocity profile A.

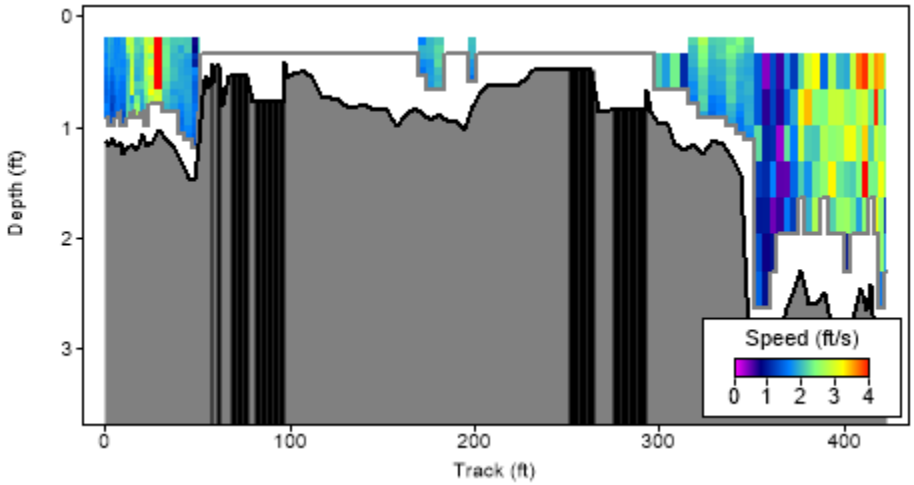

Figure D35: Site 17, Cimarron River and S.H. 74 south of Crescent in Logan county, velocity profile B.

Site 18 - Washita River and U.S. 77 south of Davis in Murray county

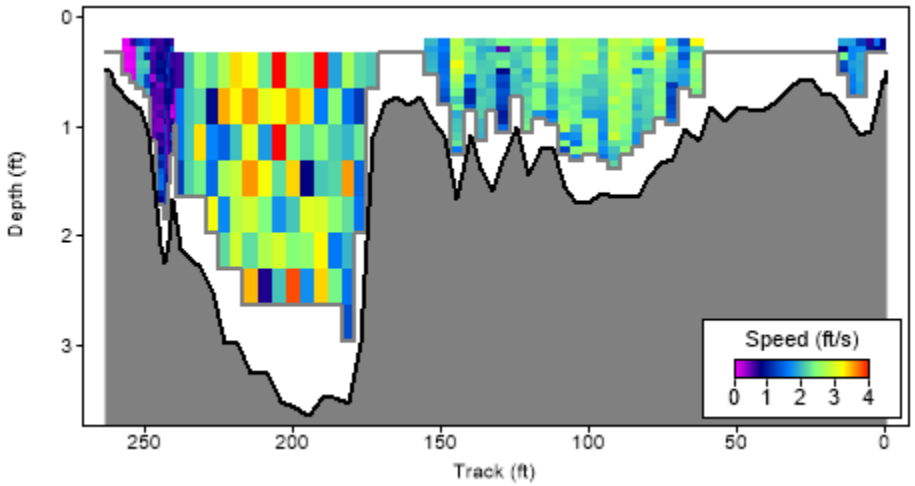

Figure D36: Site 18, Washita River and U.S. 77 south of Davis in Murray county, velocity profile A.

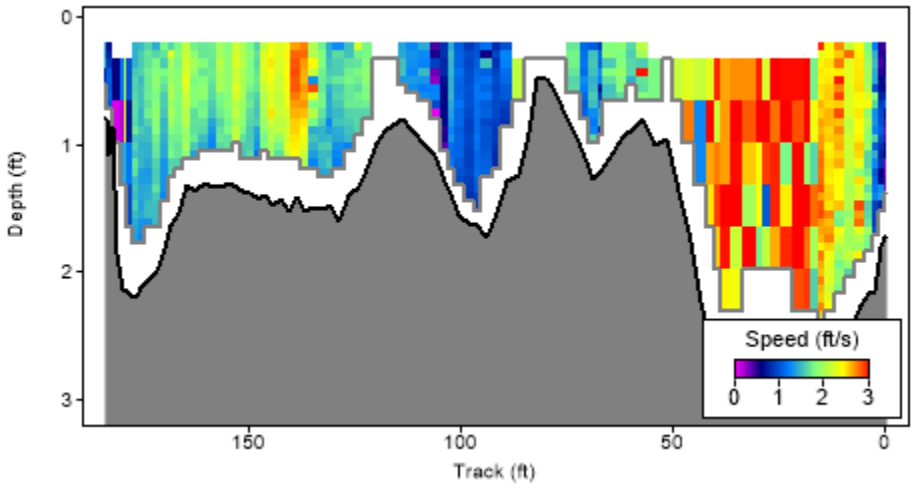

Figure D37: Site 18, Washita River and U.S. 77 south of Davis in Murray county, velocity profile B.

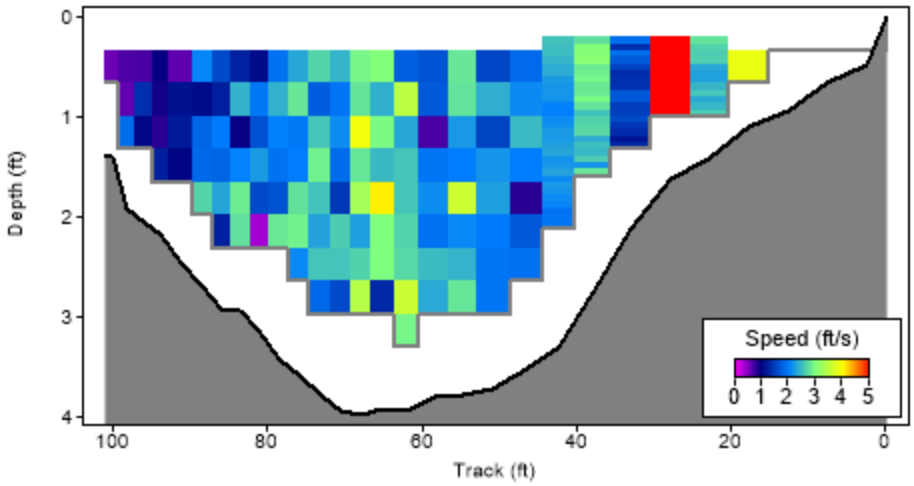

Figure D38: Site 18, Washita River and U.S. 77 south of Davis in Murray county, velocity profile C.

Site 20 - Washita River and I-35 southwest of Paoli in Garvin county

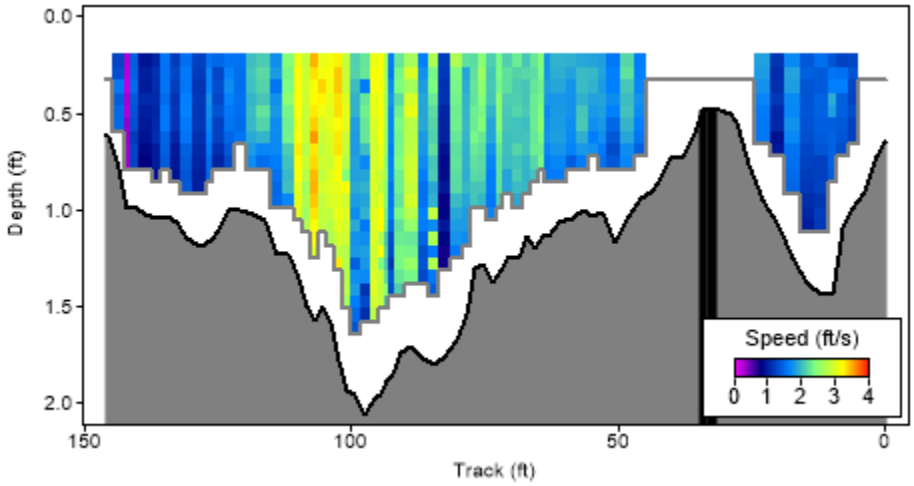

Figure D39: Site 20, Washita River and I-35 southwest of Paoli in Garvin county, velocity profile A.

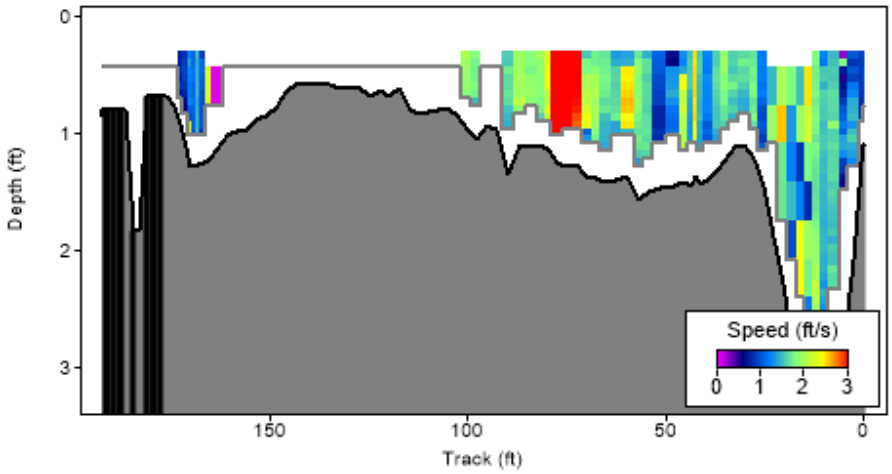

Figure D40: Site 20, Washita River and I-35 southwest of Paoli in Garvin county, velocity profile B.

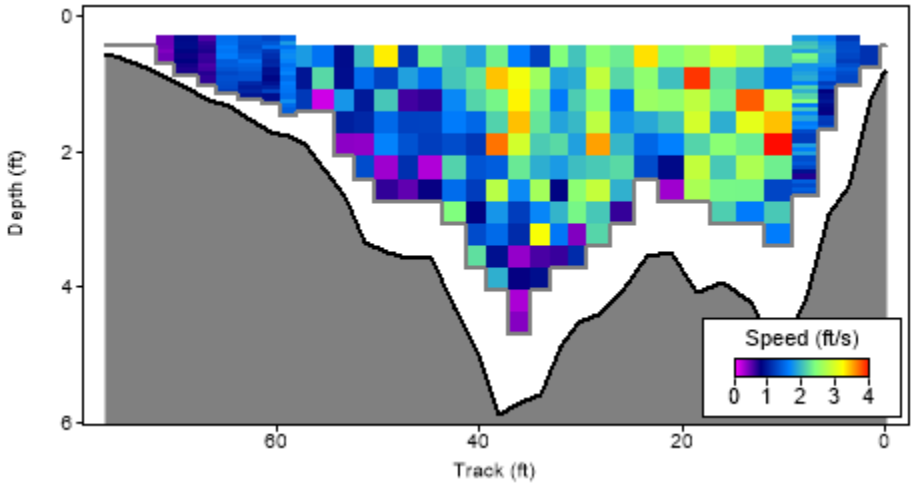

Figure D41: Site 20, Washita River and I-35 southwest of Paoli in Garvin county, velocity profile C.

Site 21 - Red River and S.H. 79 west of Waurika in Jefferson county

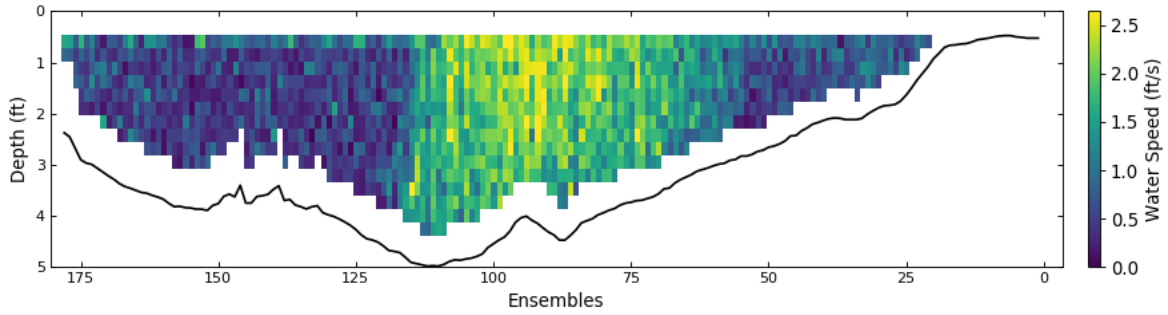

Figure D42: Site 21, Red River and S.H. 79 west of Waurika in Jefferson county, velocity profile A.

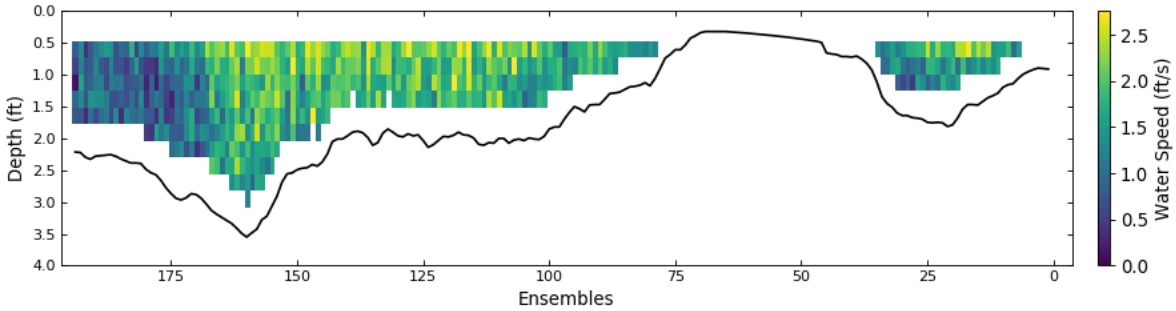

Figure D43: Site 21, Red River and S.H. 79 west of Waurika in Jefferson county, velocity profile B.

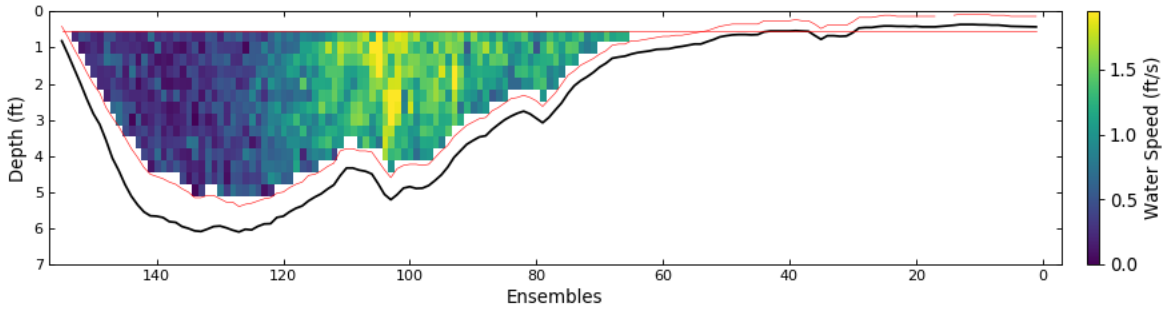

Figure D44: Site 21, Red River and S.H. 79 west of Waurika in Jefferson county, velocity profile C.

Site 22 - Washita River and S.H. 53 east of Gene Autry in Carter county

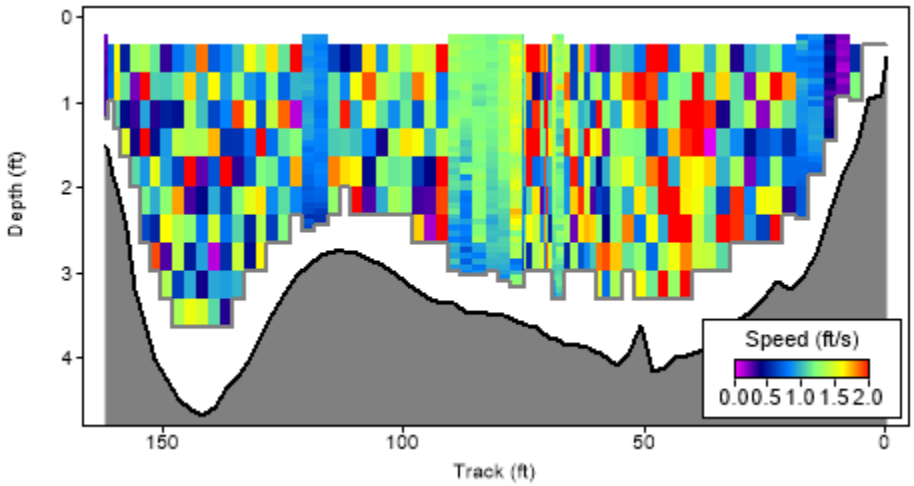

Figure D45: Site 22, Washita River and S.H. 53 east of Gene Autry in Carter county, velocity profile A.

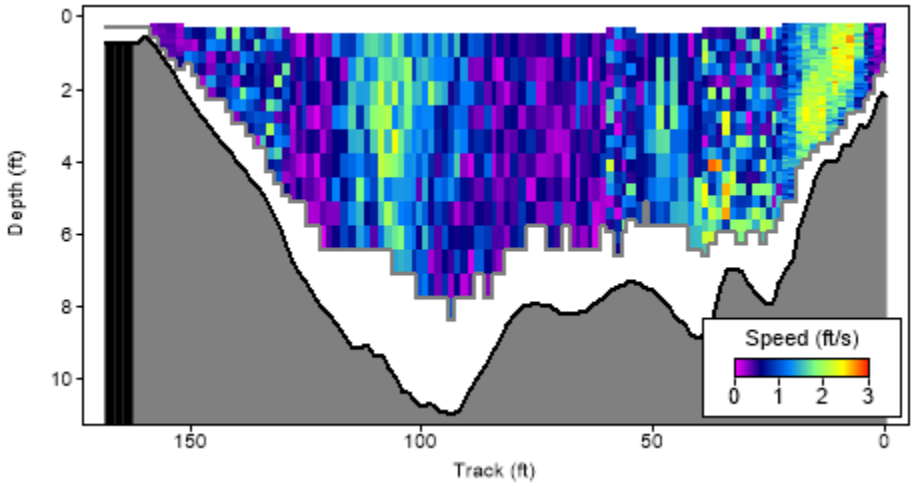

Figure D46: Site 22, Washita River and S.H. 53 east of Gene Autry in Carter county, velocity profile B.

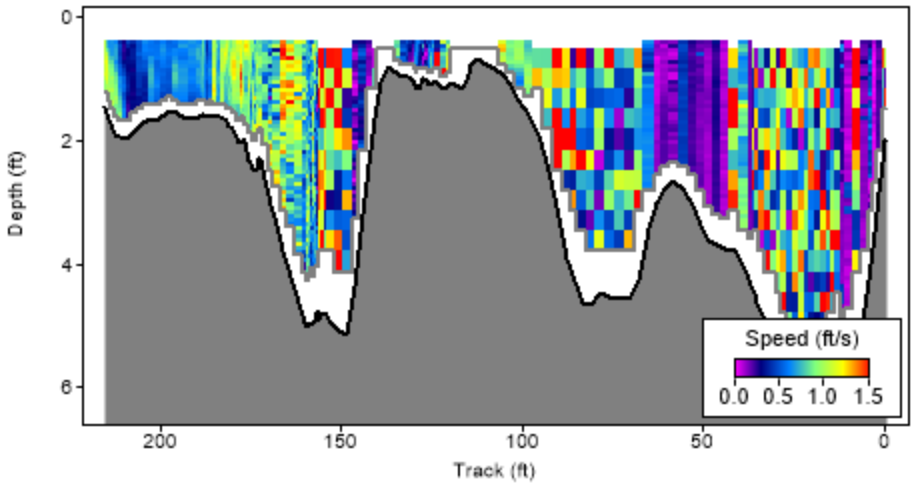

Figure D47: Site 22, Washita River and S.H. 53 east of Gene Autry in Carter county, velocity profile C.

Site 24 - Red River and U.S. 259 south of Harris in McCurtain county

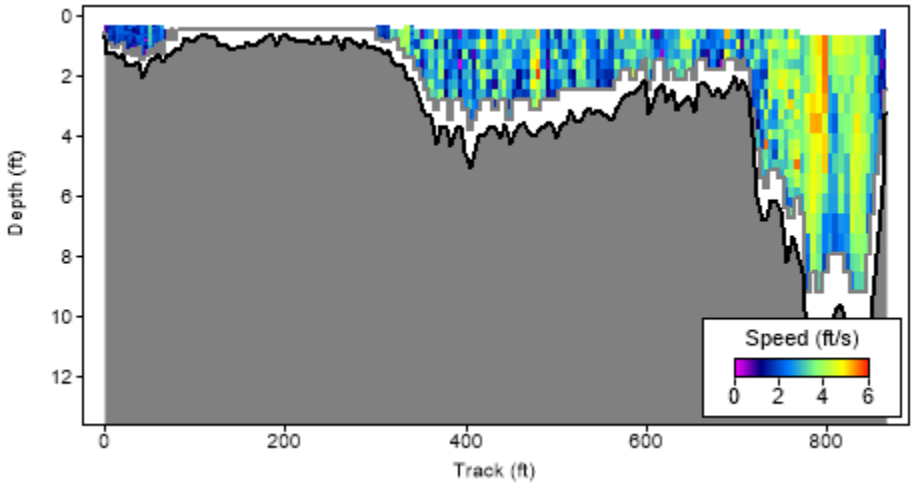

Figure D48: Site 24, Red River and U.S. 259 south of Harris in McCurtain county, velocity profile A.

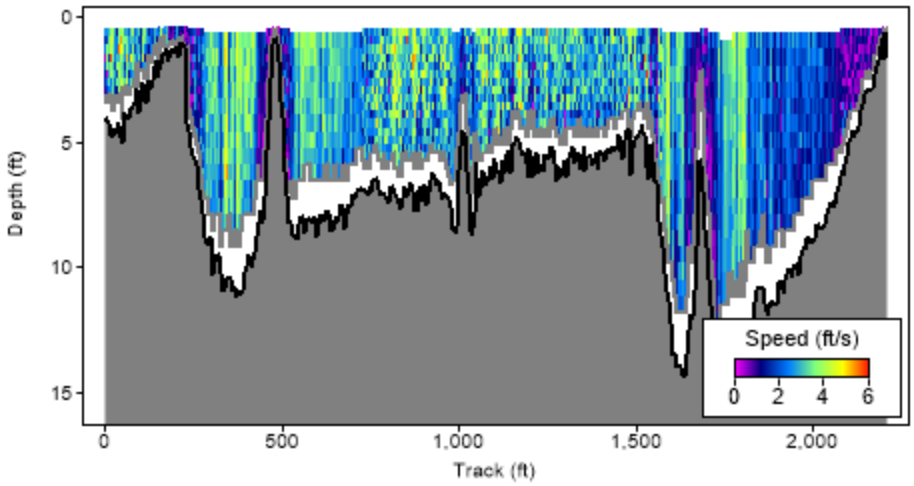

Figure D49: Site 24, Red River and U.S. 259 south of Harris in McCurtain county, velocity profile B.

Site 25 - North Canadian River and S.H. 48 north of Bearden in Okfuskee county

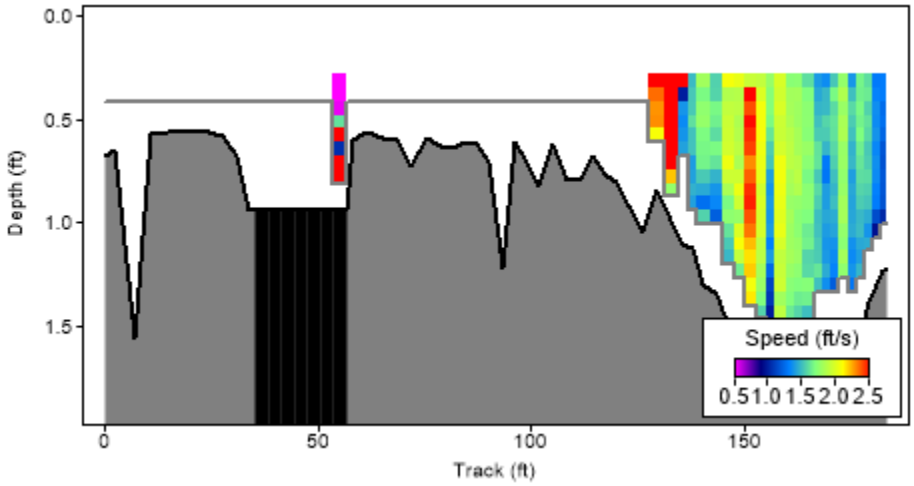

Figure D50: Site 25, North Canadian River and S.H. 48 north of Bearden in Okfuskee county, velocity profile A.

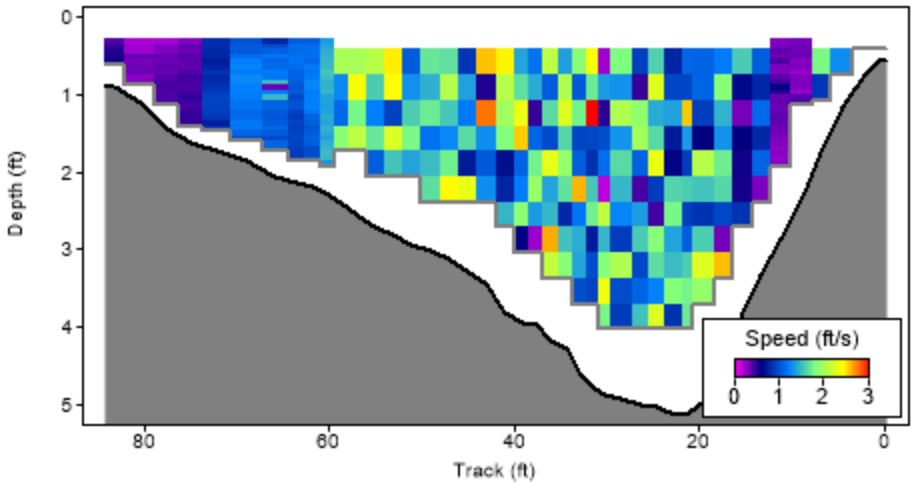

Figure D51: Site 25, North Canadian River and S.H. 48 north of Bearden in Okfuskee county, velocity profile B.

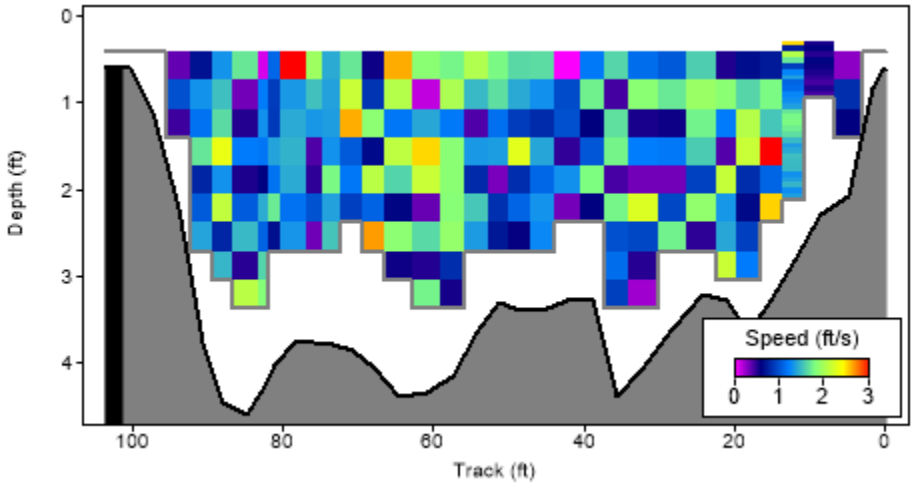

Figure D52: Site 25, North Canadian River and S.H. 48 north of Bearden in Okfuskee county, velocity profile C.

Site 26 - Sugar Creek and U.S. 281 south of Gracemont in Caddo county

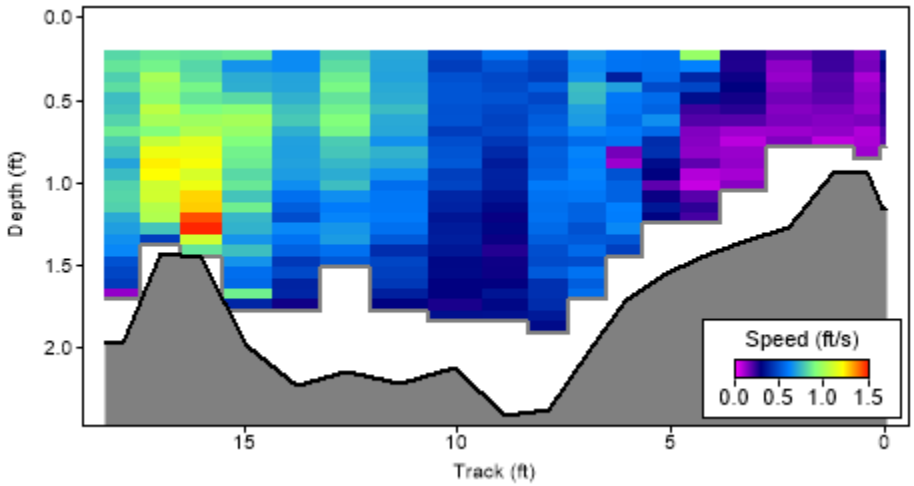

Figure D53: Site 26, Sugar Creek and U.S. 281 south of Gracemont in Caddo county, velocity profile A.

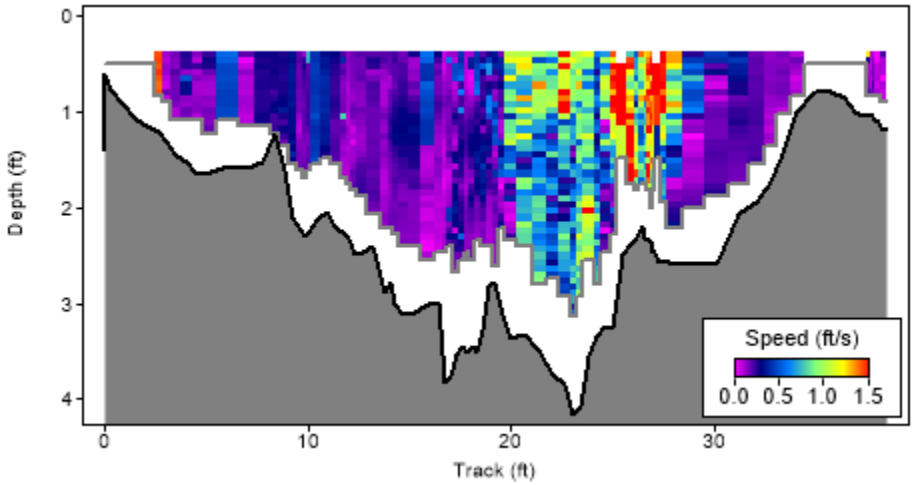

Figure D54: Site 26, Sugar Creek and U.S. 281 south of Gracemont in Caddo county, velocity profile B.

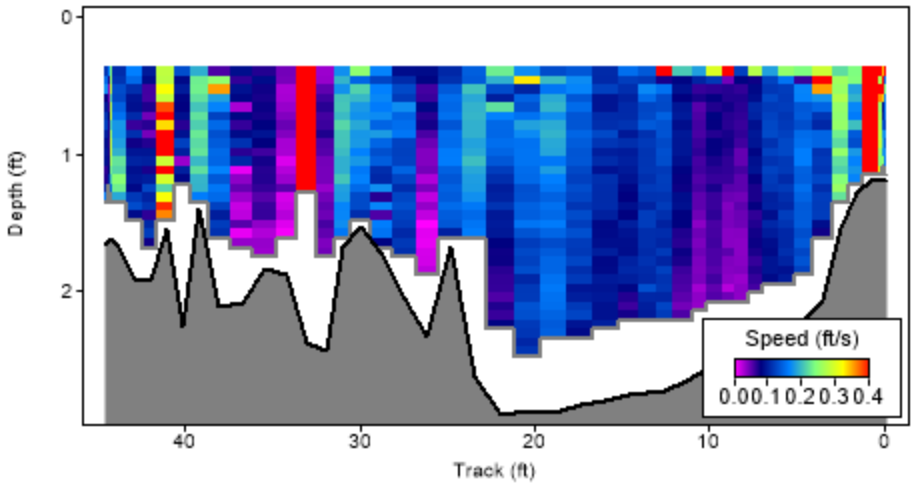

Figure D55: Site 26, Sugar Creek and U.S. 281 south of Gracemont in Caddo county, velocity profile C.

Site 27 - North Canadian River and S.H. 99 south of Prague in Seminole county

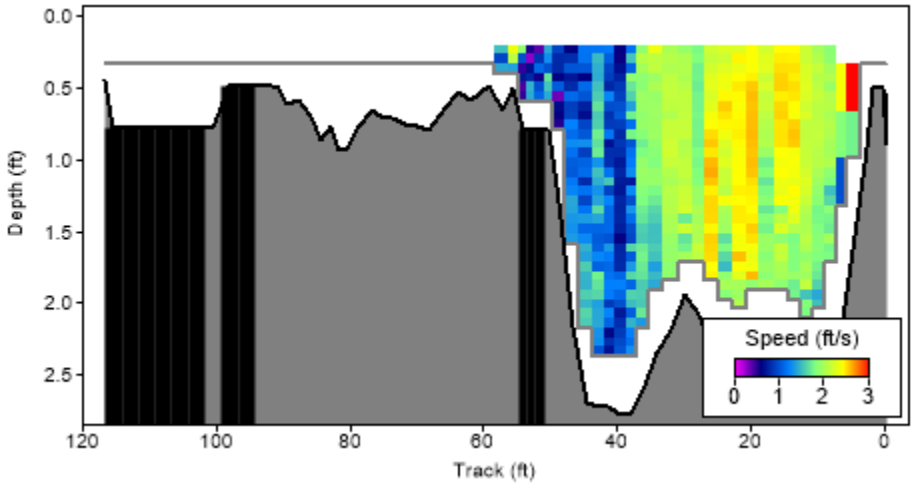

Figure D56: Site 27, North Canadian River and S.H. 99 south of Prague in Seminole county, velocity profile A.

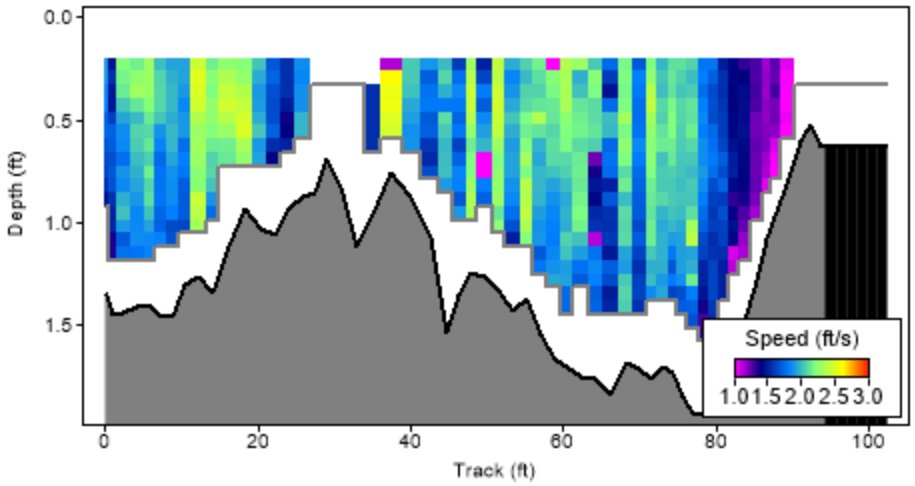

Figure D57: Site 27, North Canadian River and S.H. 99 south of Prague in Seminole county, velocity profile B.

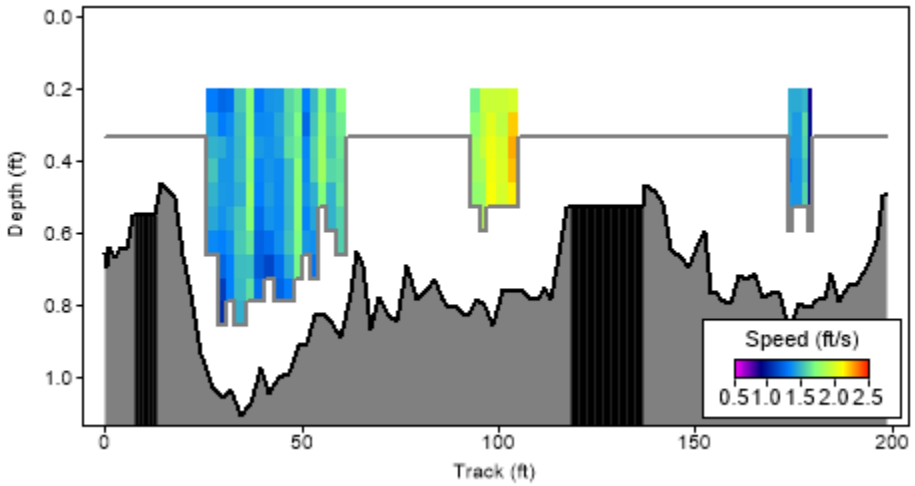

Figure D58: Site 27, North Canadian River and S.H. 99 south of Prague in Seminole county, velocity profile C.

Site 28 - Illinois River and S.H. 10 east of Tahlequah in Cherokee county

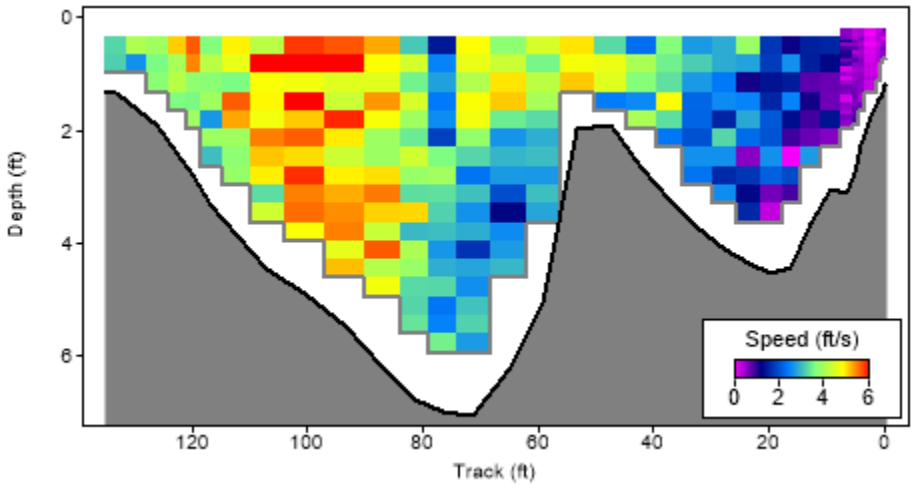

Figure D59: Site 28, Illinois River and S.H. 10 east of Tahlequah in Cherokee county, velocity profile A.

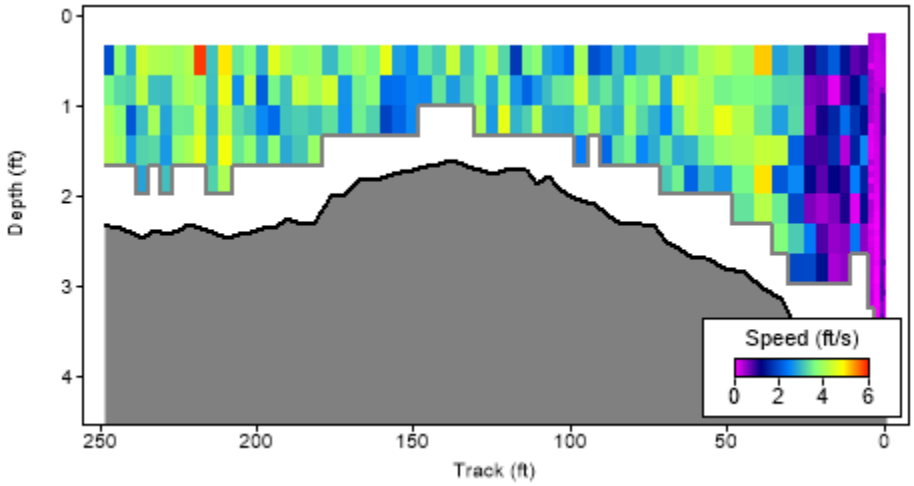

Figure D60: Site 28, Illinois River and S.H. 10 east of Tahlequah in Cherokee county, velocity profile B.

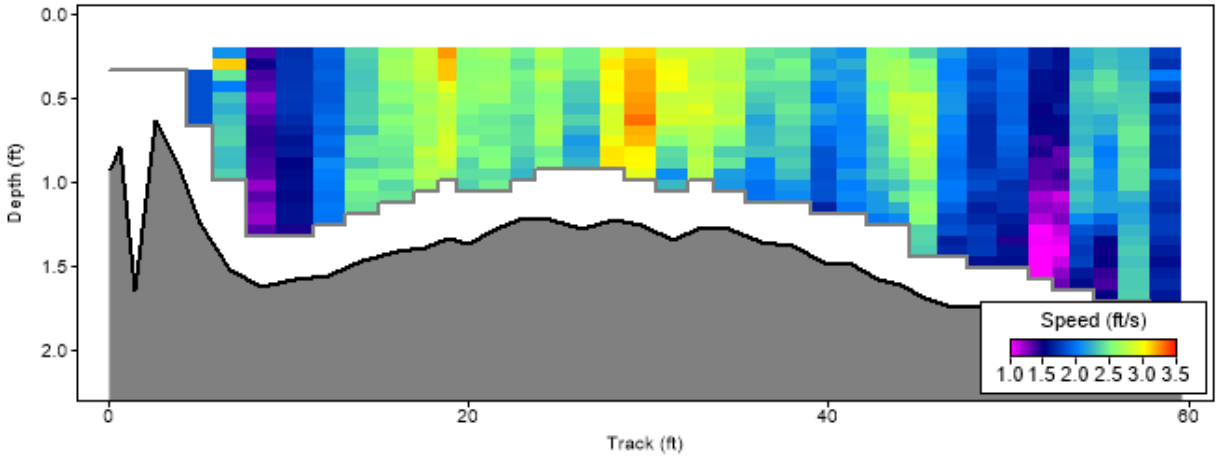

Figure D61: Site 28, Illinois River and S.H. 10 east of Tahlequah in Cherokee county, velocity profile C.

Site 29 - Washita River and S.H. 19 east of Lindsay in Garvin county

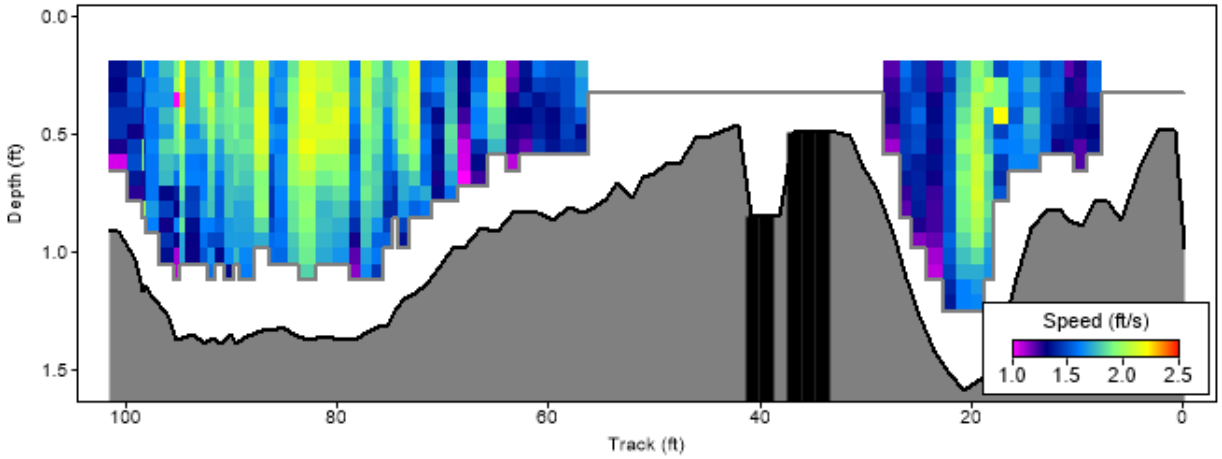

Figure D62: Site 29, Washita River and S.H. 19 east of Lindsay in Garvin county, velocity profile B.

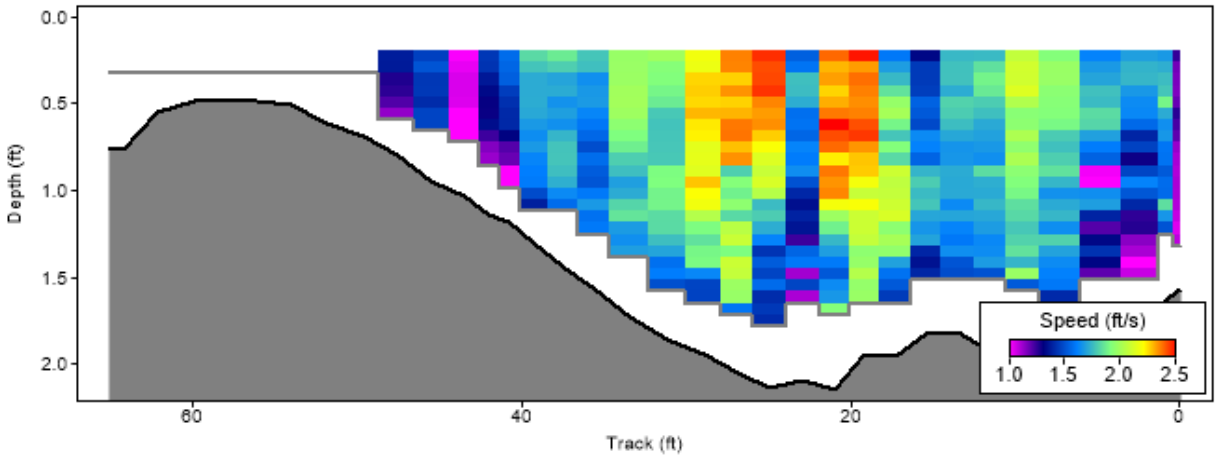

Figure D63: Site 29, Washita River and S.H. 19 east of Lindsay in Garvin county, velocity profile C.

Site 32 - Washita River and S.H. 7 west of Davis in Murray county

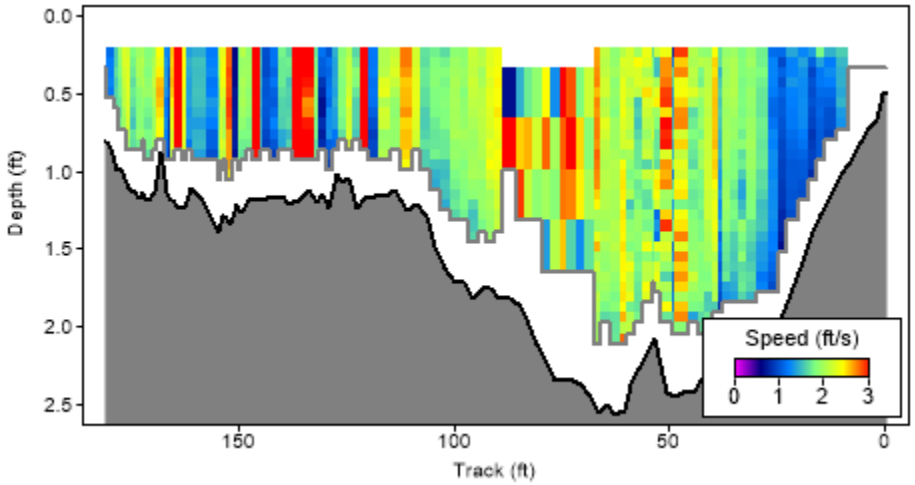

Figure D64: Site 32, Washita River and S.H. 7 west of Davis in Murray county, velocity profile A.

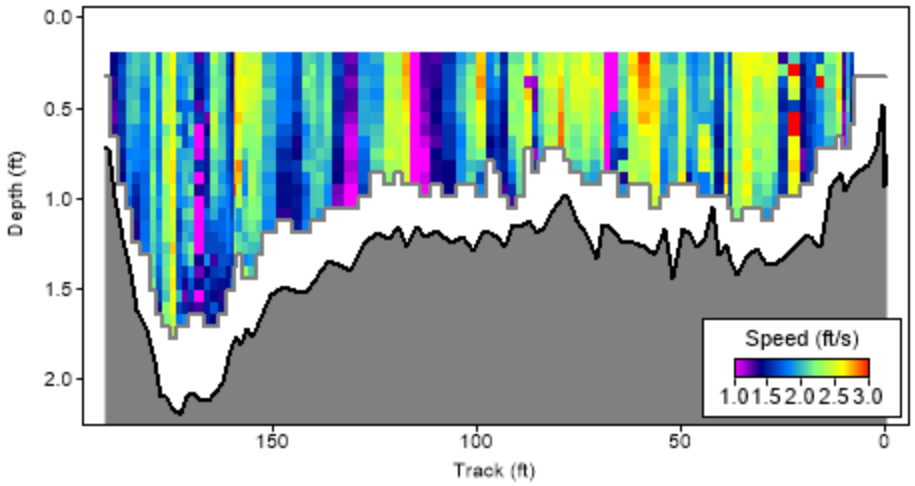

Figure D65: Site 32, Washita River and S.H. 7 west of Davis in Murray county, velocity profile B.

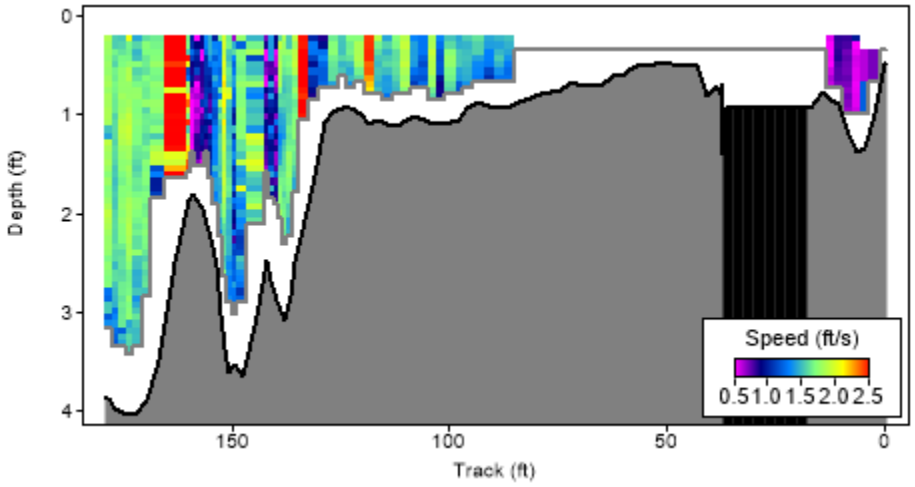

Figure D66: Site 32, Washita River and S.H. 7 west of Davis in Murray county, velocity profile C.

Site 33 - Salt Fork of the Arkansas River and S.H. 156 north of Marland in Kay county

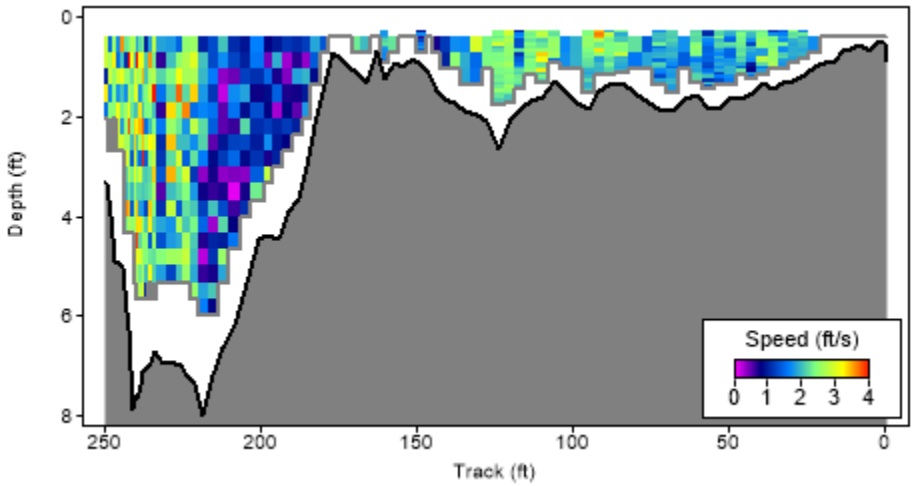

Figure D67: Site 33, Salt Fork of the Arkansas River and S.H. 156 north of Marland in Kay county, velocity profile A.

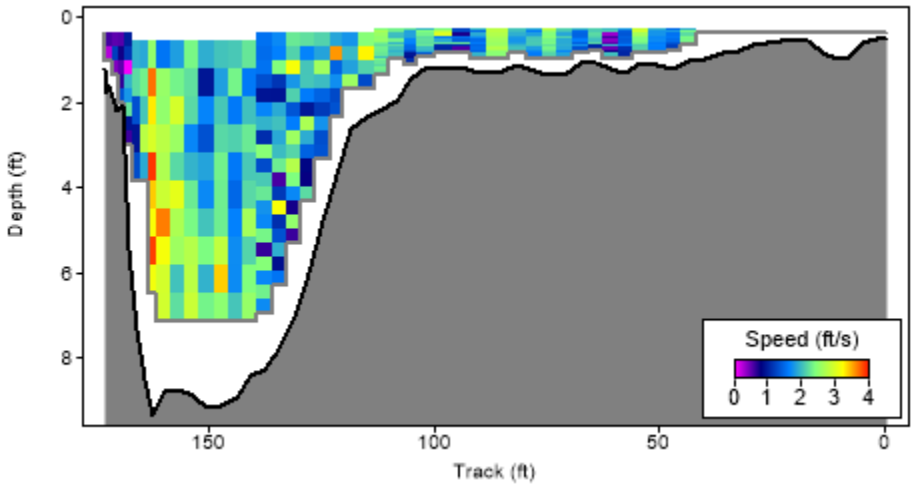

Figure D68: Site 33, Salt Fork of the Arkansas River and S.H. 156 north of Marland in Kay county, velocity profile between A and B.

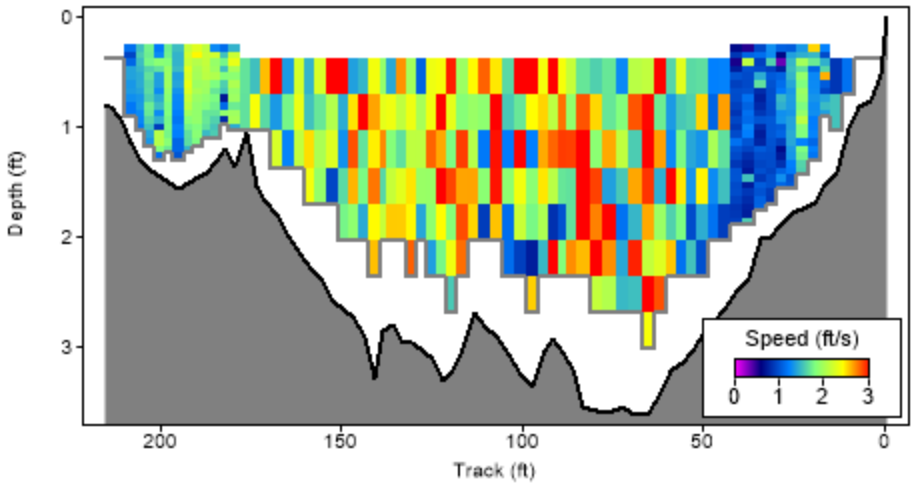

Figure D69: Site 33, Salt Fork of the Arkansas River and S.H. 156 north of Marland in Kay county, velocity profile B.

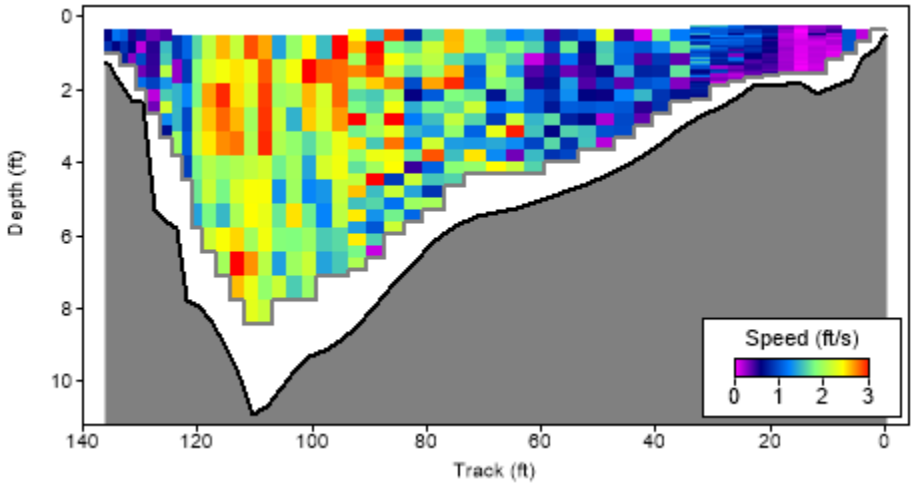

Figure D70: Site 33, Salt Fork of the Arkansas River and S.H. 156 north of Marland in Kay county, velocity profile between B and C.

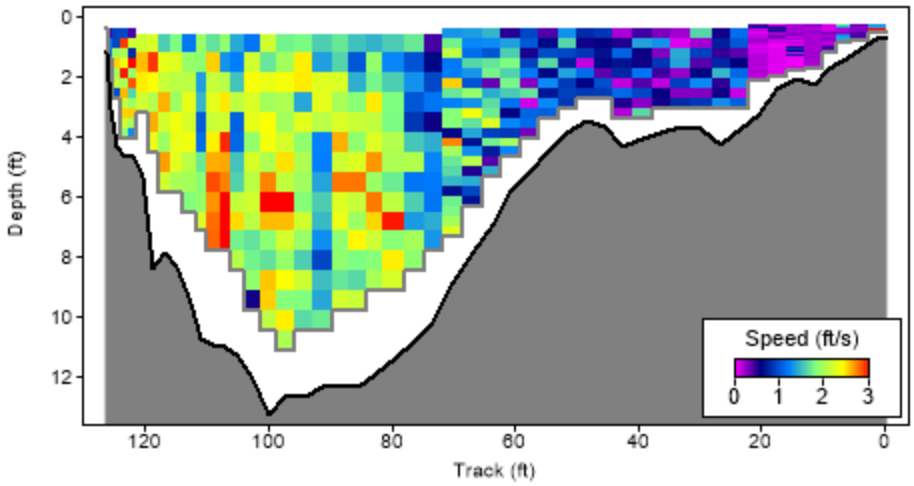

Figure D71: Site 33, Salt Fork of the Arkansas River and S.H. 156 north of Marland in Kay county, velocity profile C.

Site 34 - Sugar Creek and U.S. 281 east of Binger in Caddo county

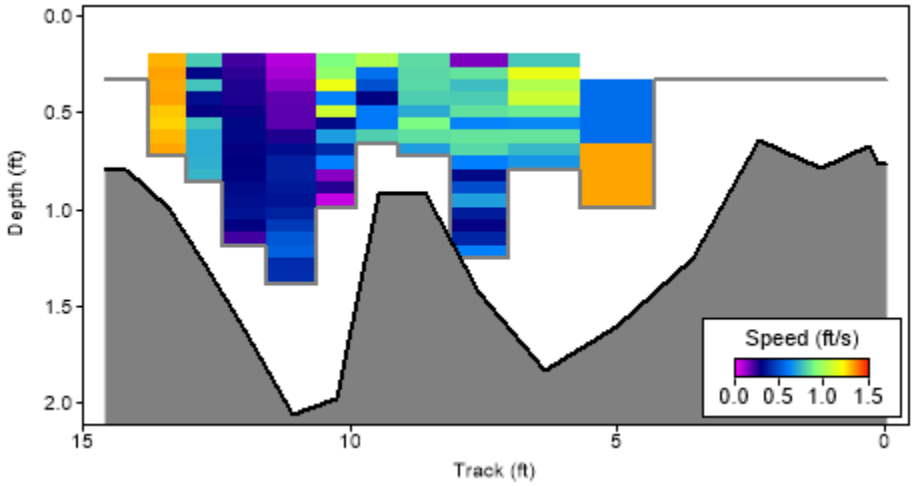

Figure D72: Site 34, Sugar Creek and U.S. 281 east of Binger in Caddo county, velocity profile A.

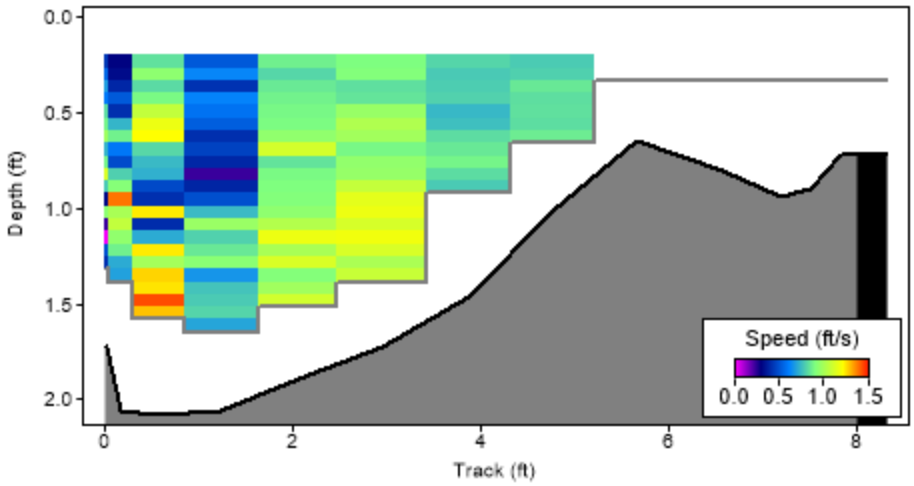

Figure D73: Site 34, Sugar Creek and U.S. 281 east of Binger in Caddo county, velocity profile B.

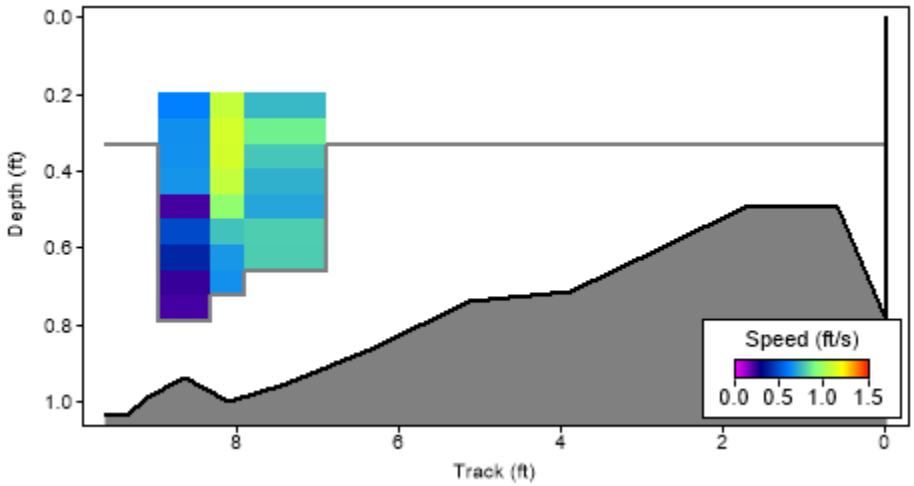

Figure D74: Site 34, Sugar Creek and U.S. 281 east of Binger in Caddo county, velocity profile C.

Appendix E – Bank Material Particle Size Distributions

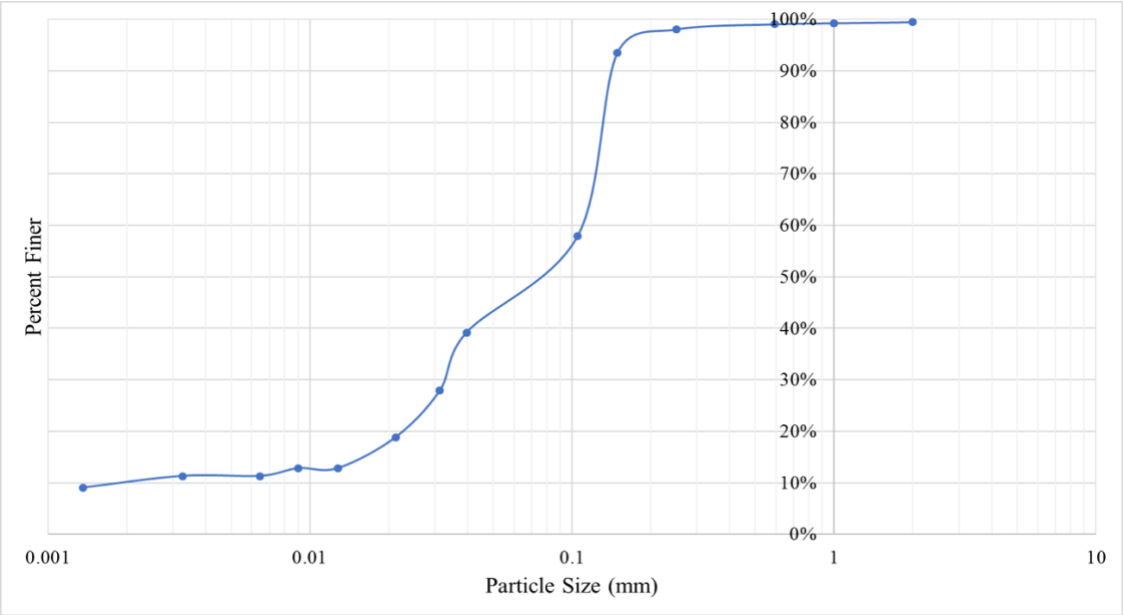

Figure E1: Site 1, Washita River and U.S. 77 north of Wynnewood in Garvin county, particle size distribution.

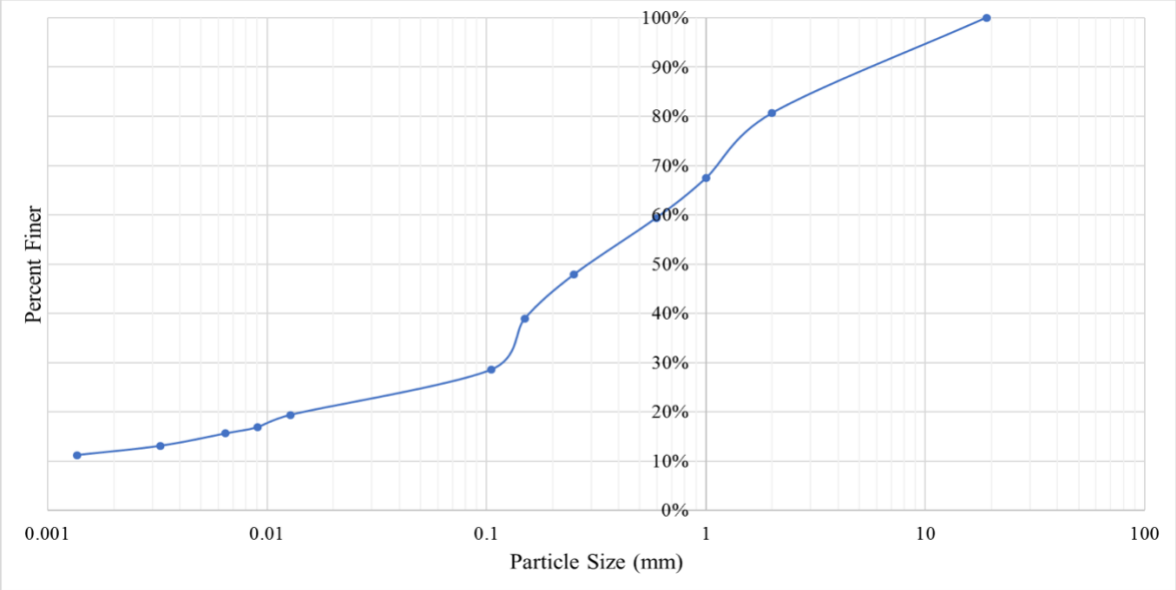

Figure E2: Site 2, Cimarron River and U.S. 177 south of Perkins in Payne county, particle size distribution.

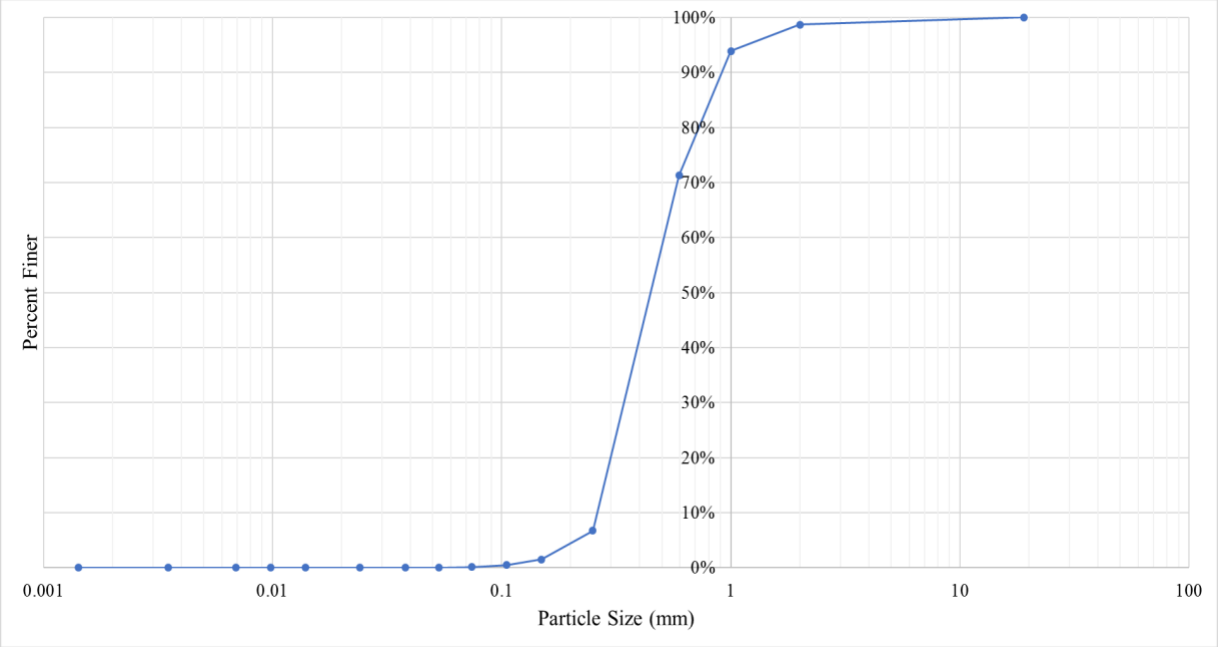

Figure E3: Site 4, Cimarron River and U.S. 281 south of Watonga in Blaine county, particle size distribution.

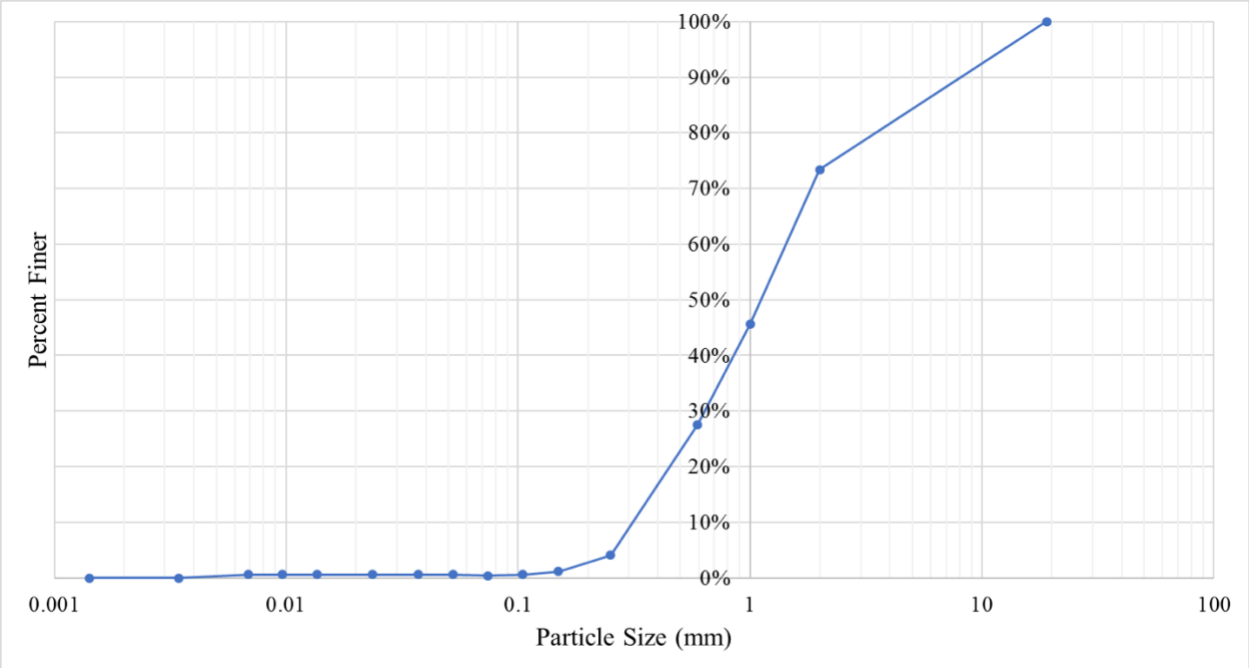

Figure E4: Site 5, Arkansas River and U.S. 64 north of Bixby in Tulsa county, particle size distribution.

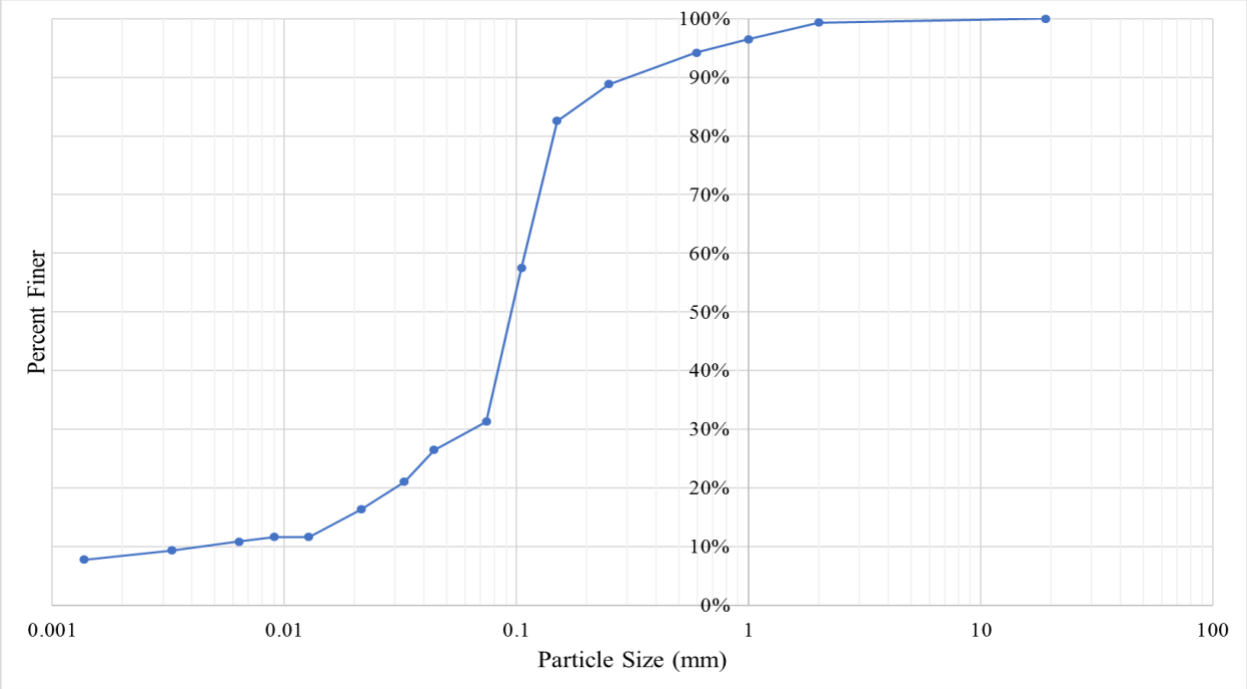

Figure E5: Site 6, North Canadian River and U.S. 281 south Watonga in Blaine county, particle size distribution.

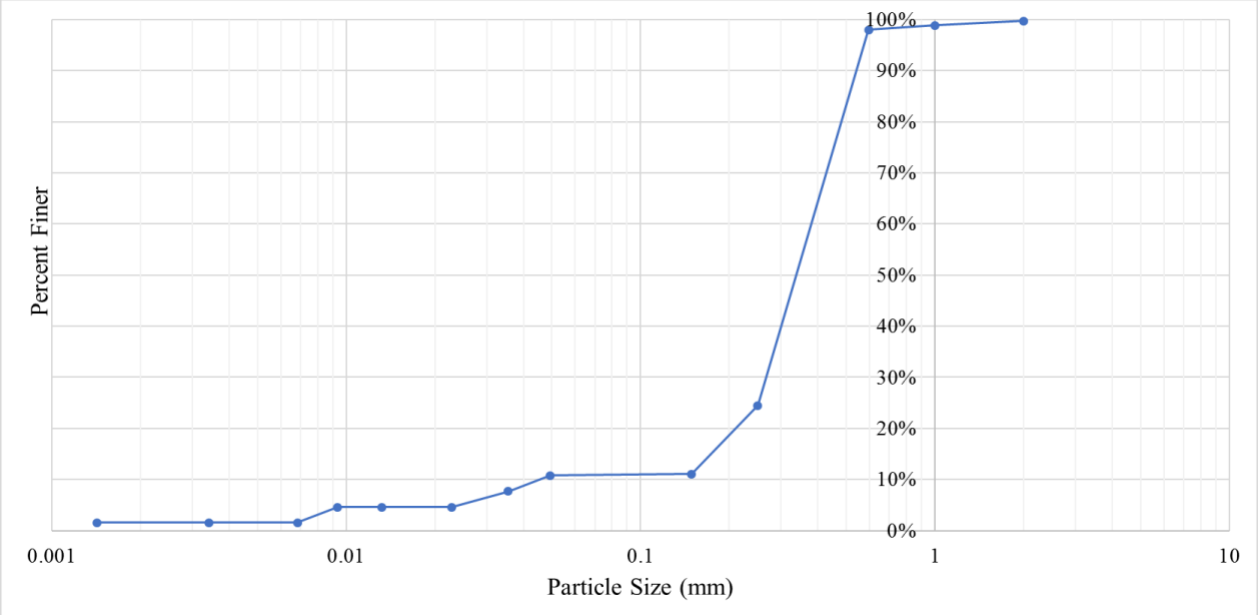

Figure E6: Site 7, Canadian River and U.S. 281 east of Bridgeport in Canadian county, particle size distribution.

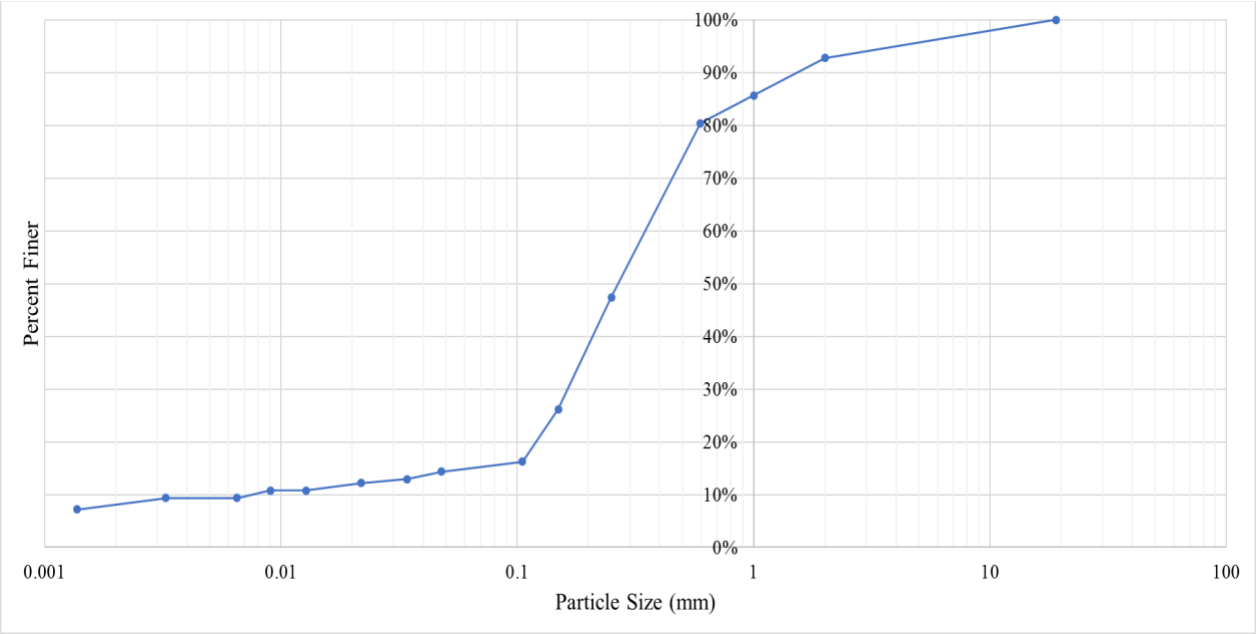

Figure E7: Site 8, Salt Fork of the Red River and U.S. 62 west of Altus in Jackson county, particle size distribution.

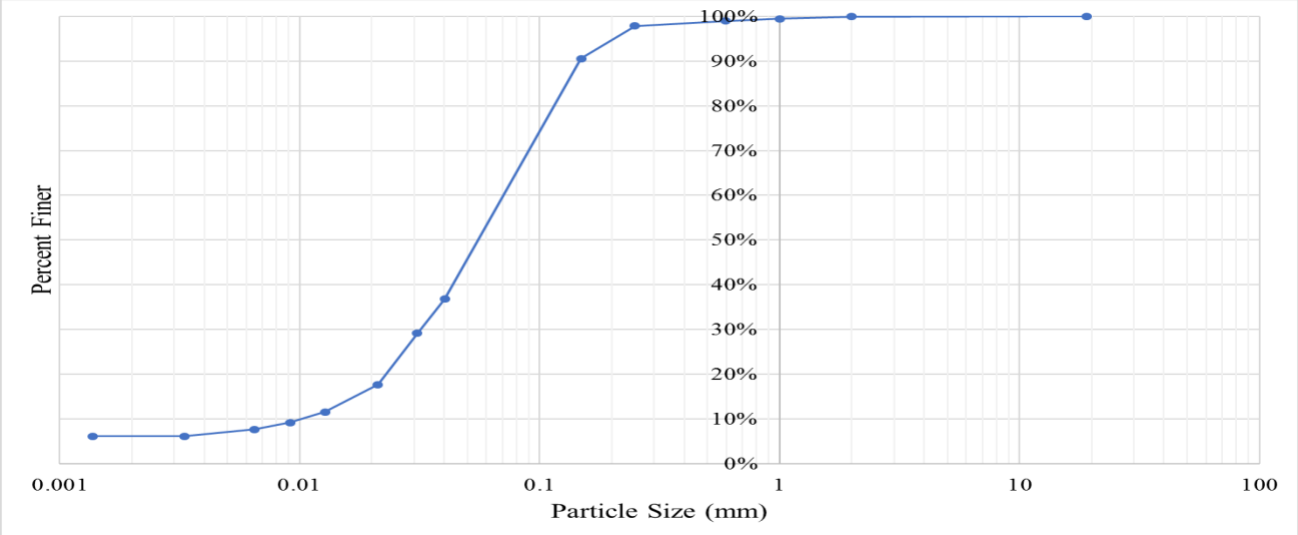

Figure E8: Site 10, Washita River and S.H. 76 south of Lindsay in Garvin county, particle size distribution.

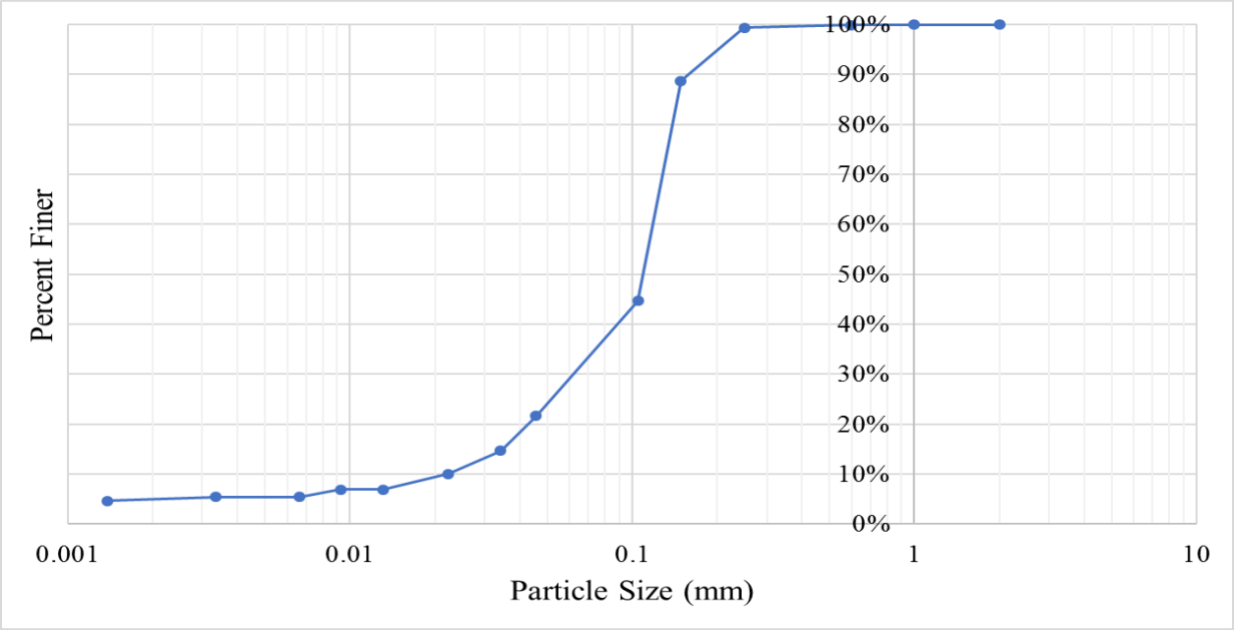

Figure E9: Site 11, Washita River and S.H. 74 north of Maysville in Garvin county, particle size distribution.

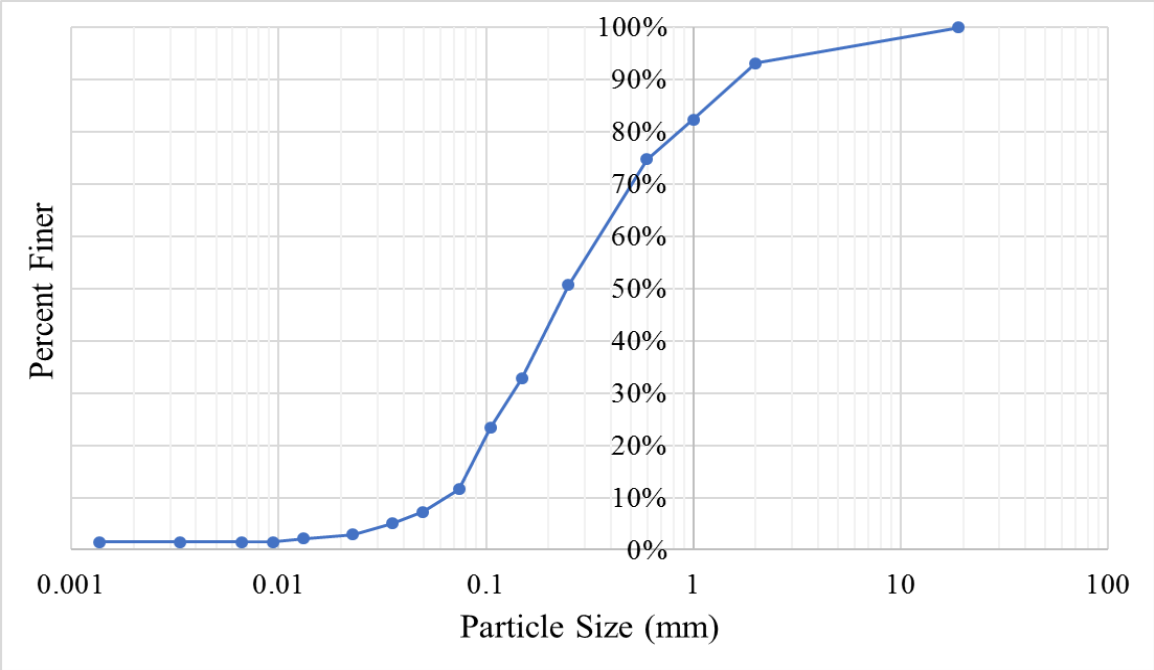

Figure E10: Site 12, Cimarron River and S.H. 33 north of Coyle in Logan county, particle size distribution.

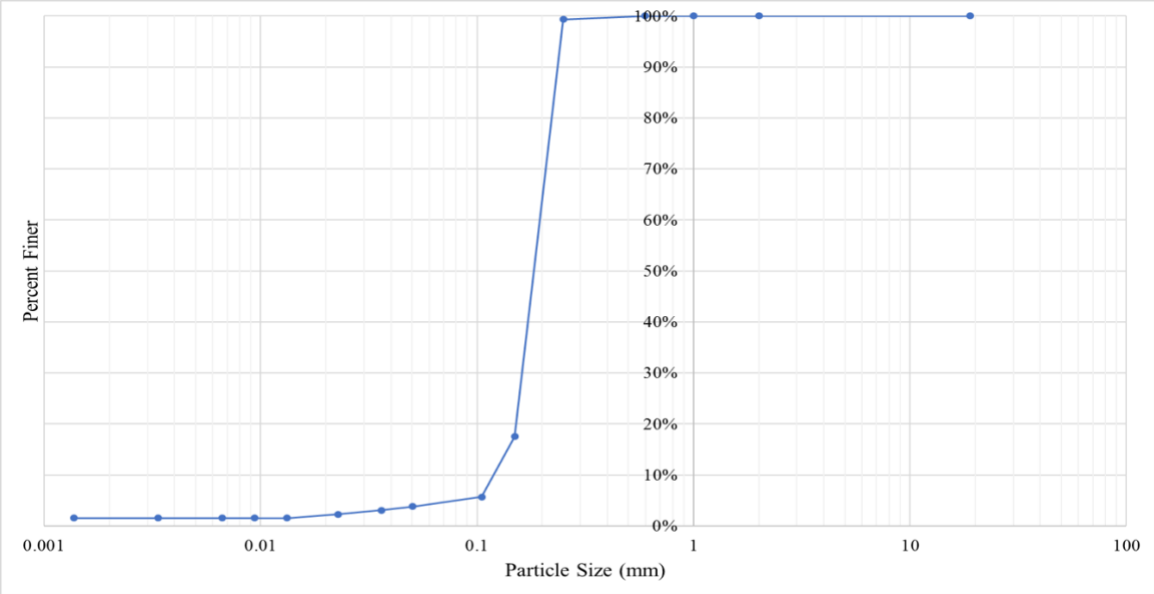

Figure E11: Size 13, Canadian River and S.H. 48 north of Atwood in Cotton county, particle size distribution.

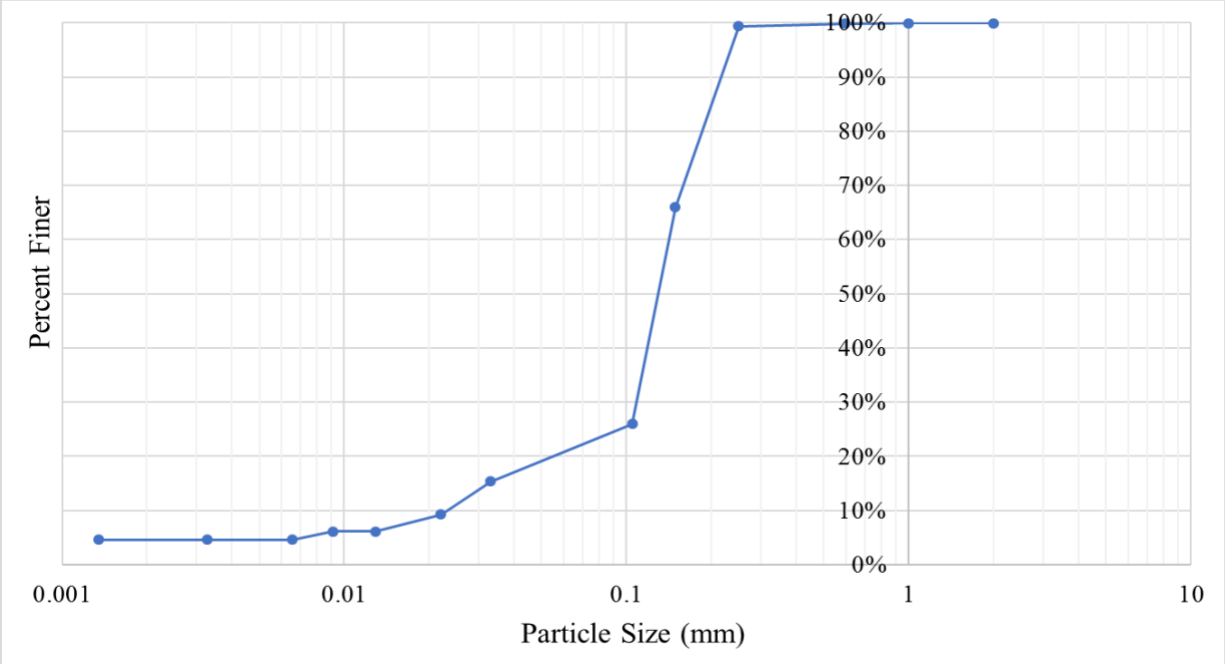

Figure E12: Site 14, North Canadian River and S.H. 84 north of Dustin in Okfuskee county, particle size distribution.

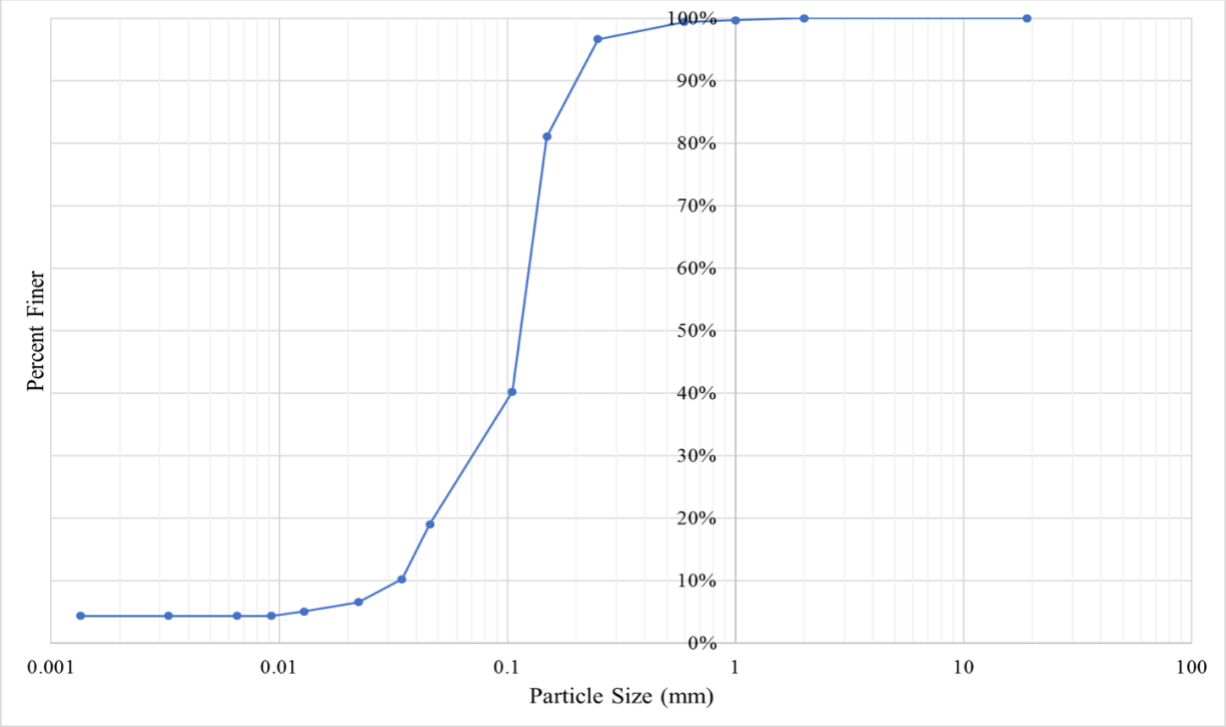

Figure E13: Site 16, North Canadian River and S.H. 3 east of Shawnee in Pottawatomie county, particle size distribution.

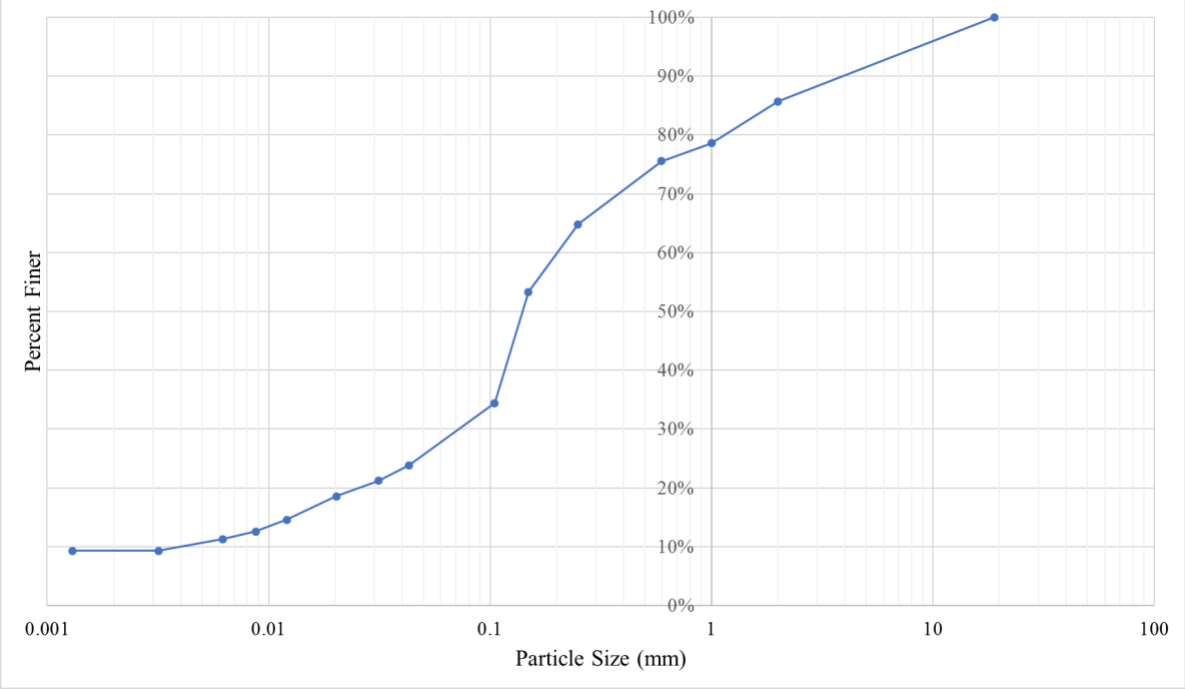

Figure E14: Site 17, Cimarron River and S.H. 74 south of Crescent in Logan county, particle size distribution.

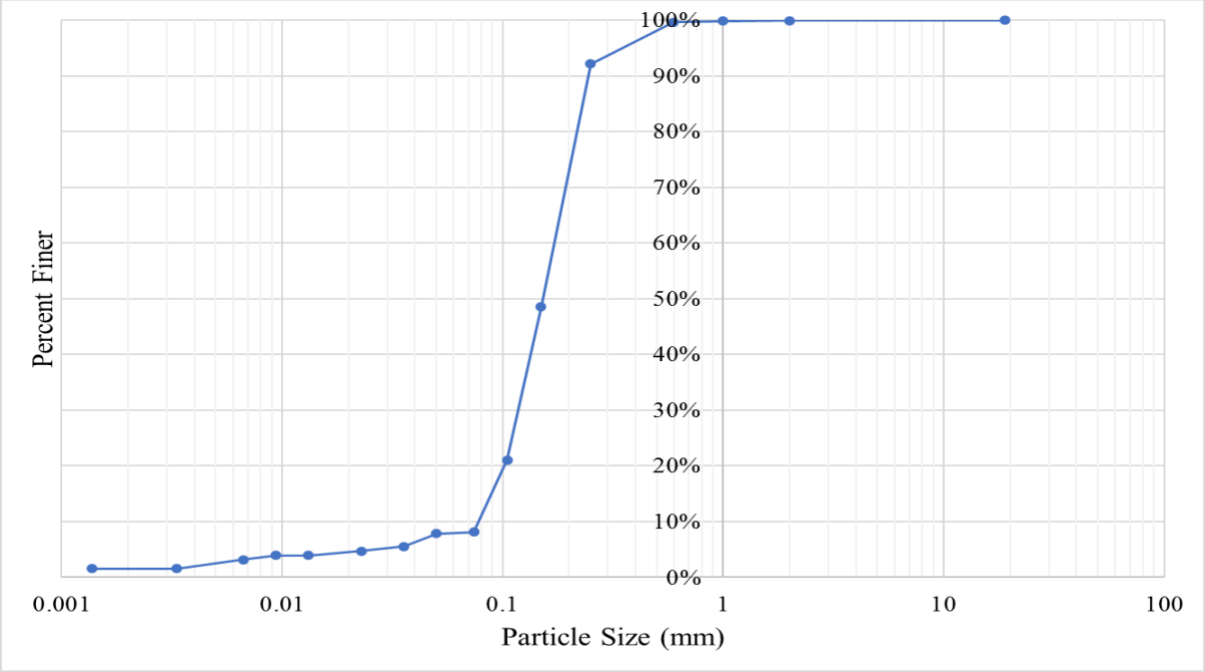

Figure E15: Site 18, Washita River and U.S. 77 south of Davis in Murray county, particle size distribution.

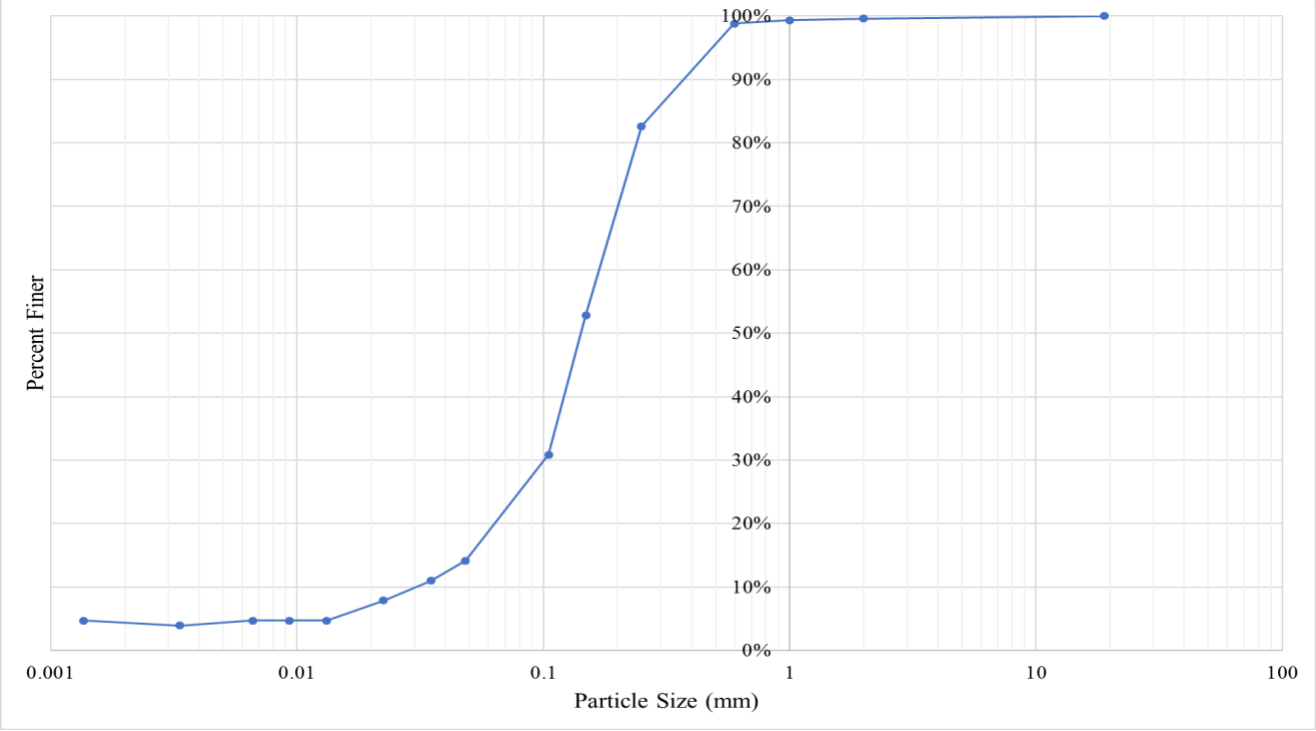

Figure E16: Site 19, Beaver River and U.S. 283 north of Laverne in Harper county, particle size distribution.

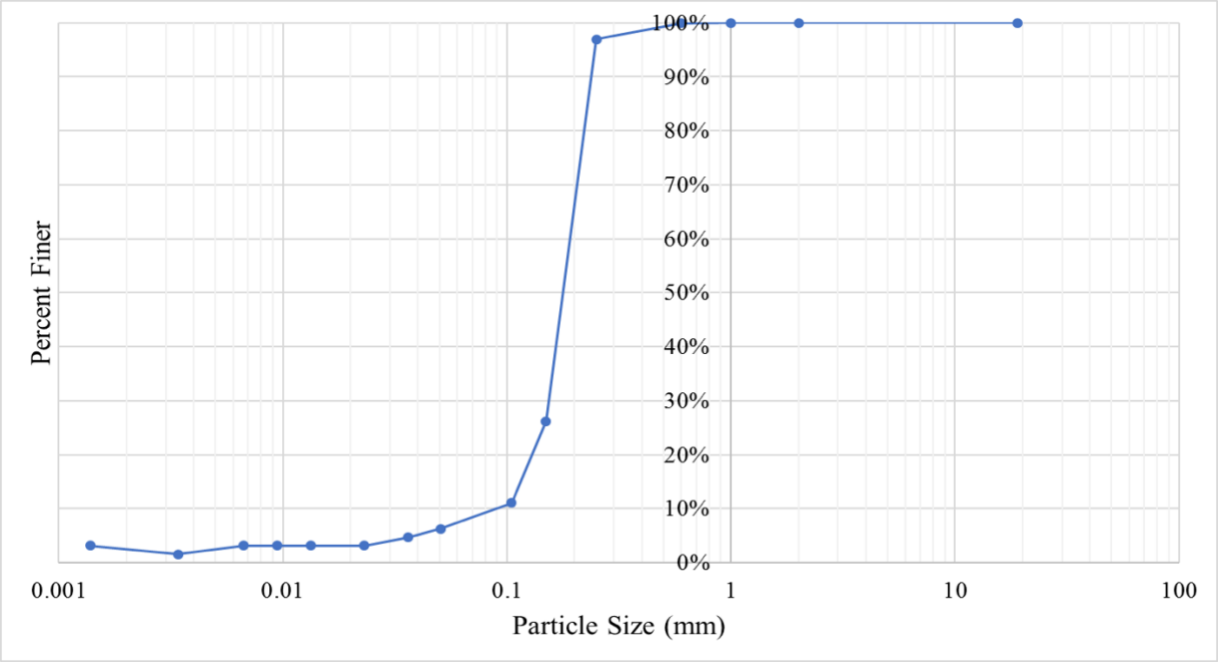

Figure E17: Site 20, Washita River and I-35 southwest of Paoli in Garvin county, particle size distribution.

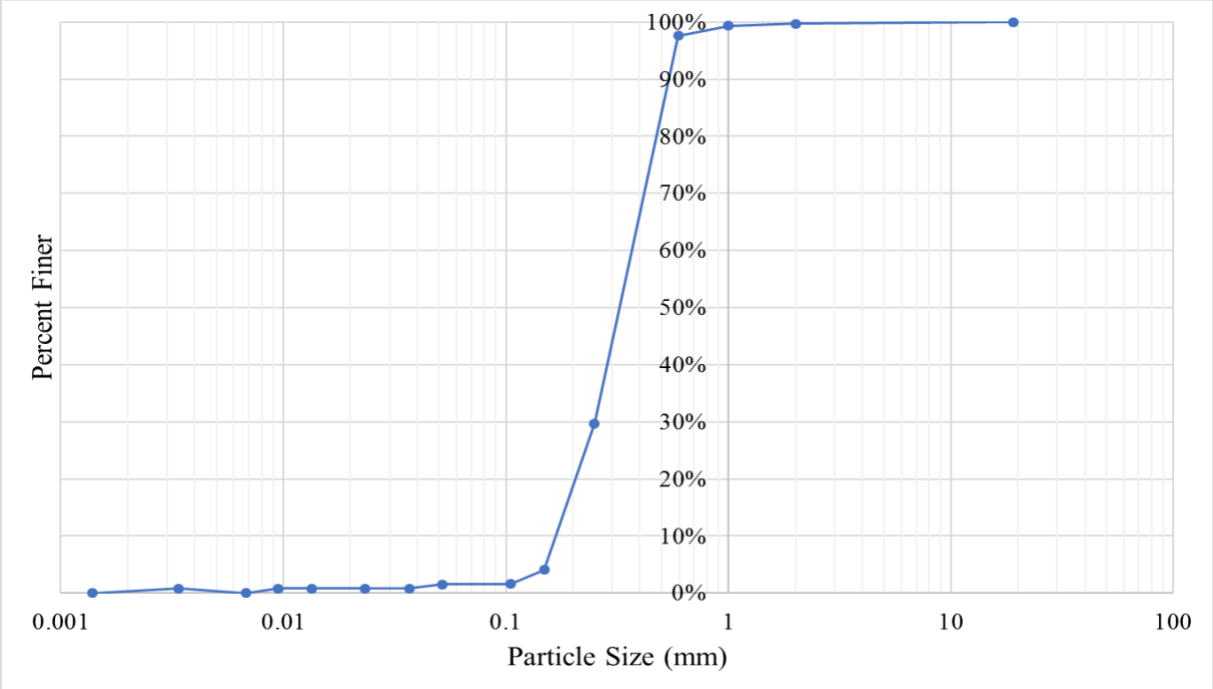

Figure E18: Site 21, Red River and S.H. 79 west of Waurika in Jefferson county, particle size distribution.

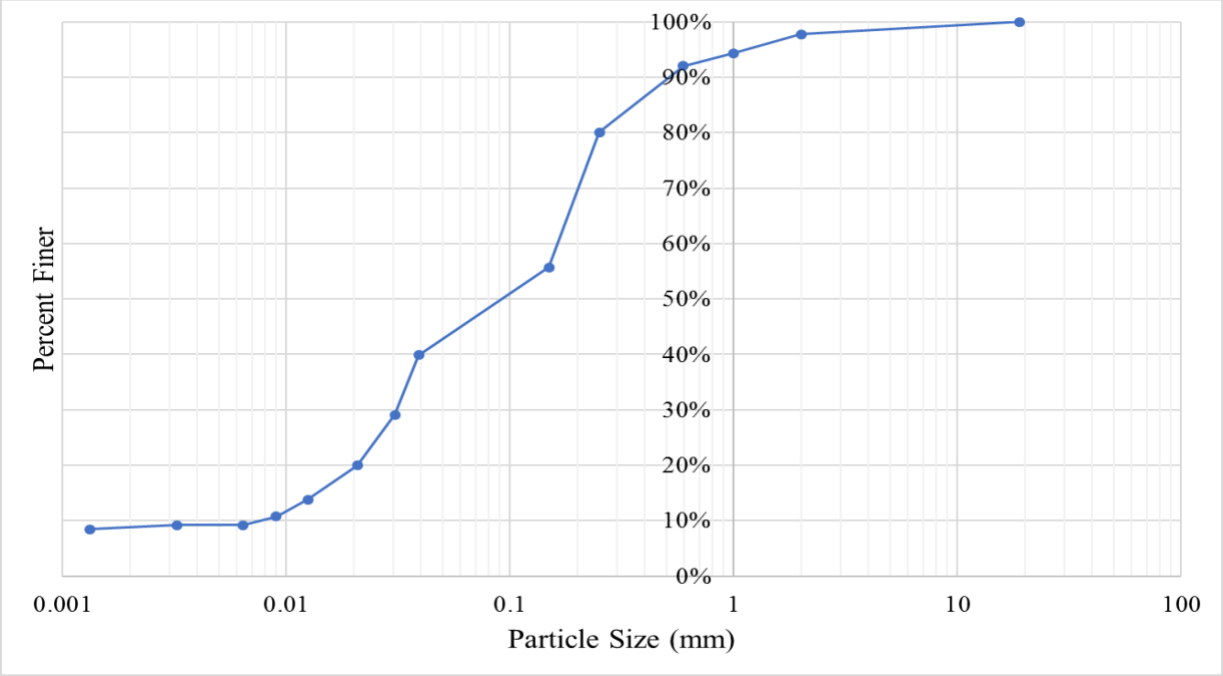

Figure E19: Site 22, Washita River and S.H. 53 east of Gene Autry in Carter county, particle size distribution.

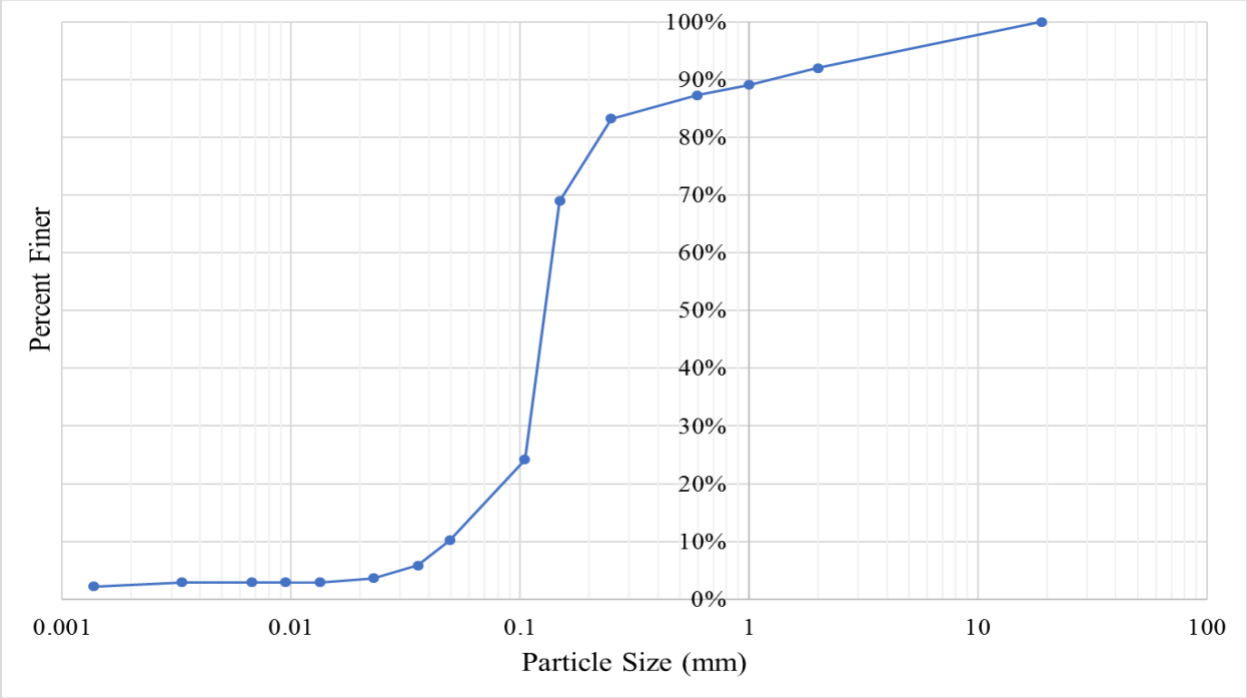

Figure E20: Site 24, Red River and U.S. 259 south of Harris in McCurtain county, particle size distribution.

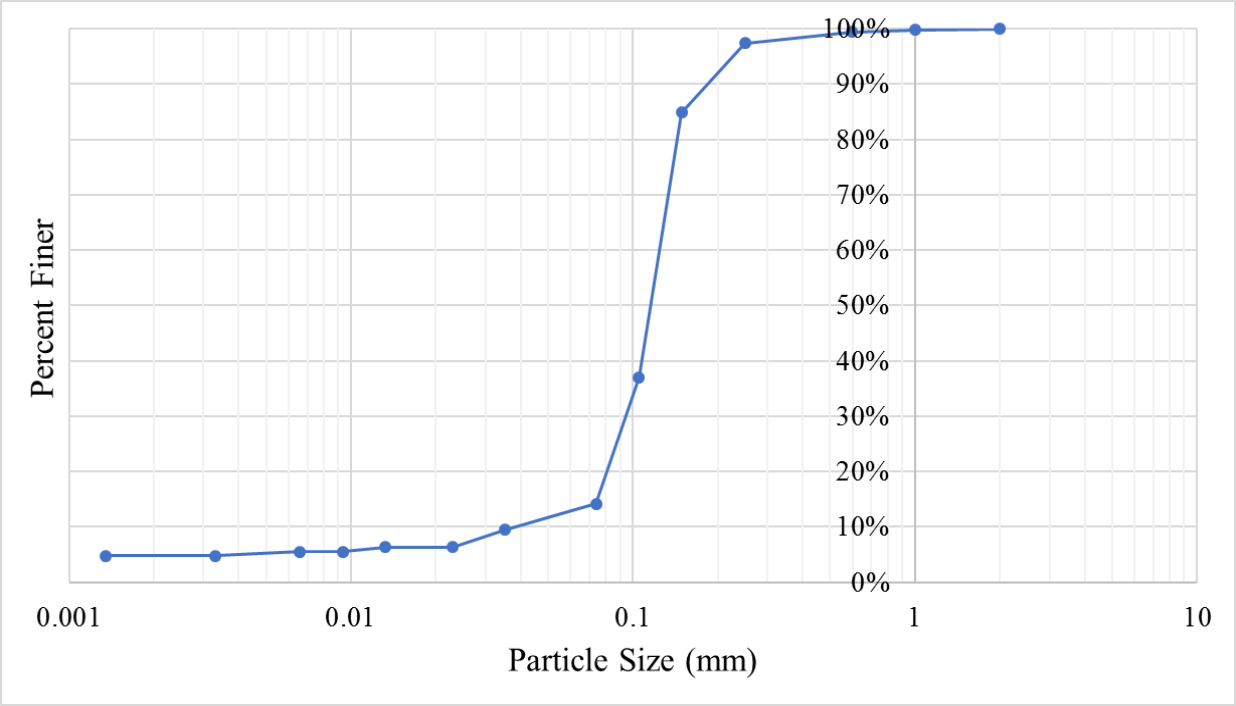

Figure E21: Site 25, North Canadian River and S.H. 48 north of Bearden in Okfuskee, particle size distribution.

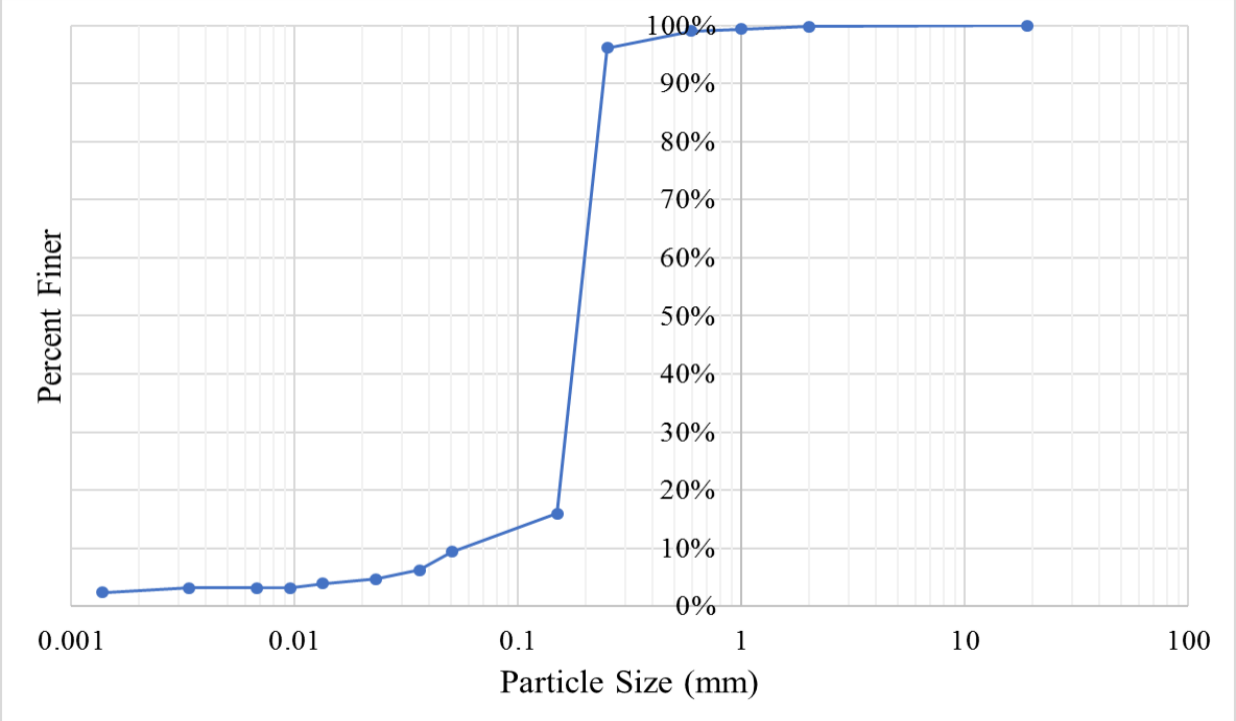

Figure E22: Site 26, Sugar Creek and U.S. 281 south of Gracemont in Caddo county, particle size distribution.

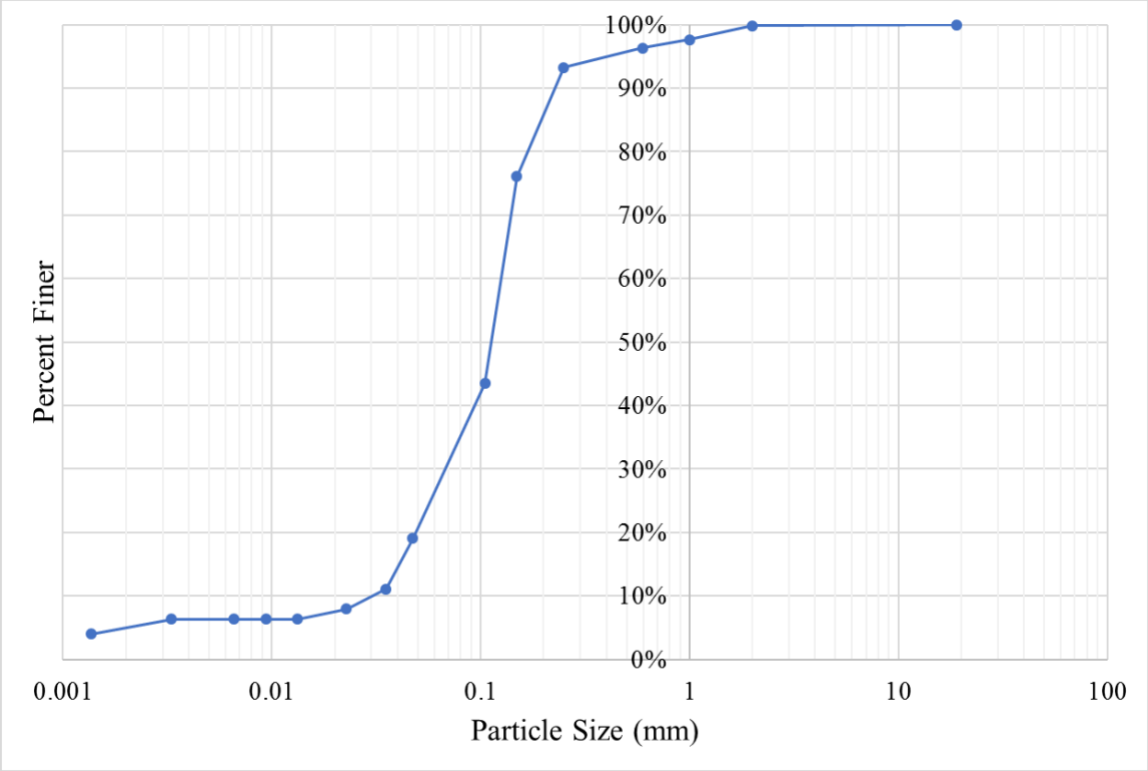

Figure E23: Site 27, North Canadian River and S.H. 99 south of Prague in Seminole county, particle size distribution.

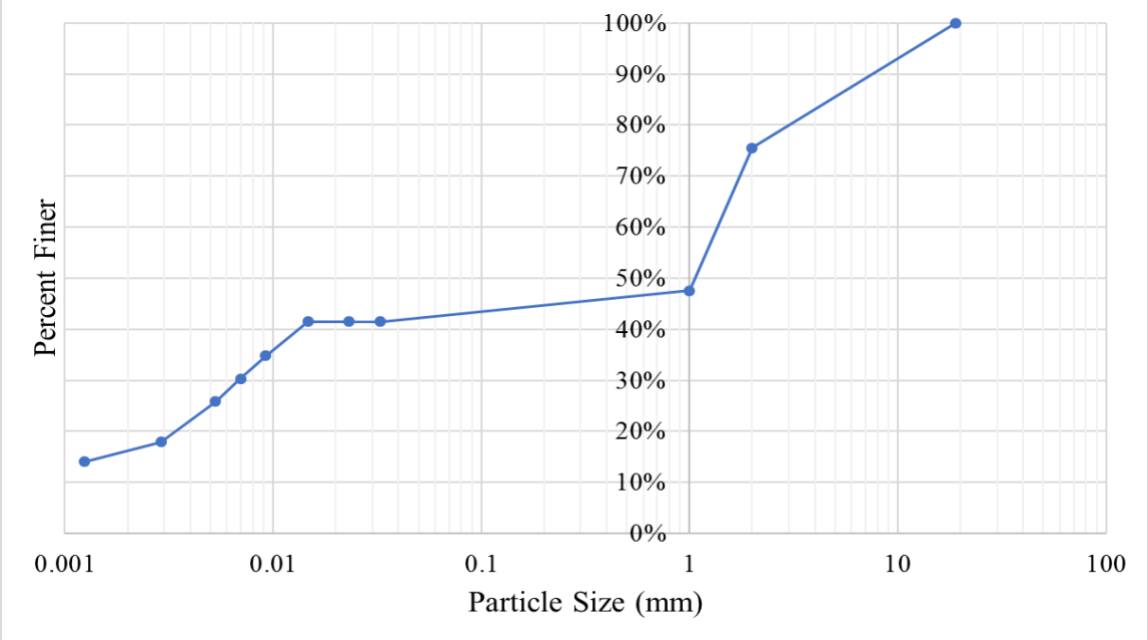

Figure E24: Site 28, Illinois River and S.H. 10 east of Tahlequah in Cherokee county, particle size distribution.

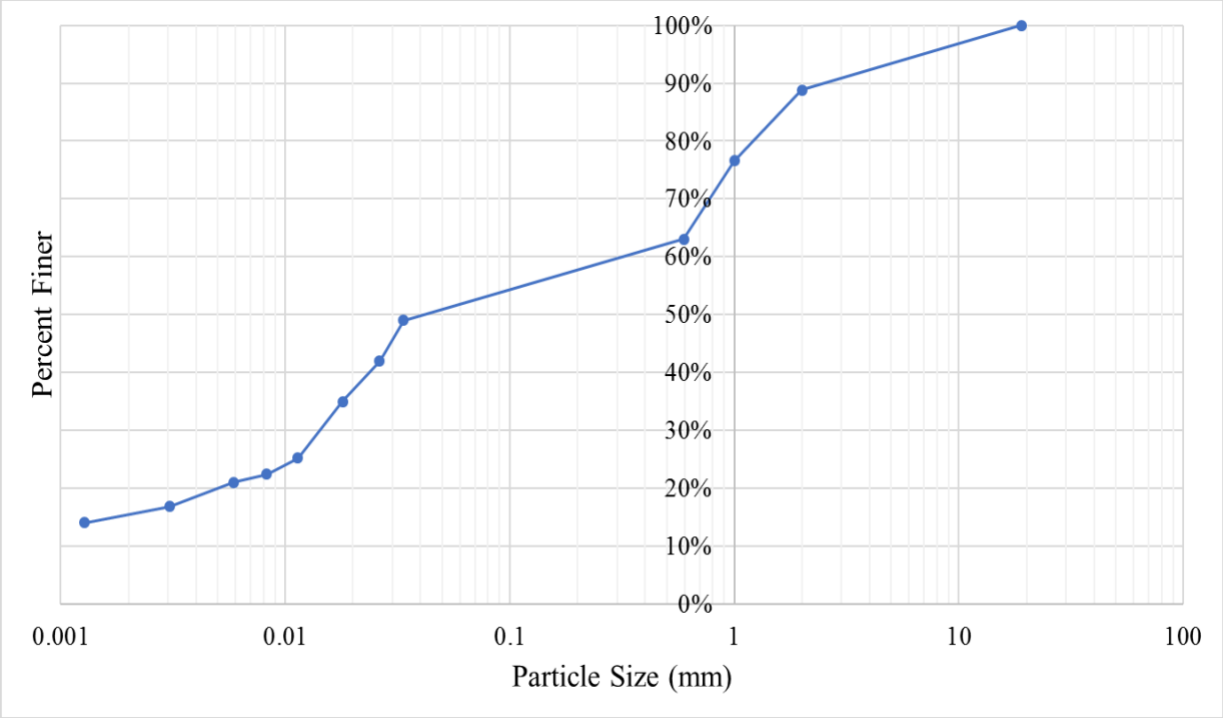

Figure E25: Site 29, Washita River and S.H. 19 east of Lindsay in Garvin county, particle size distribution.

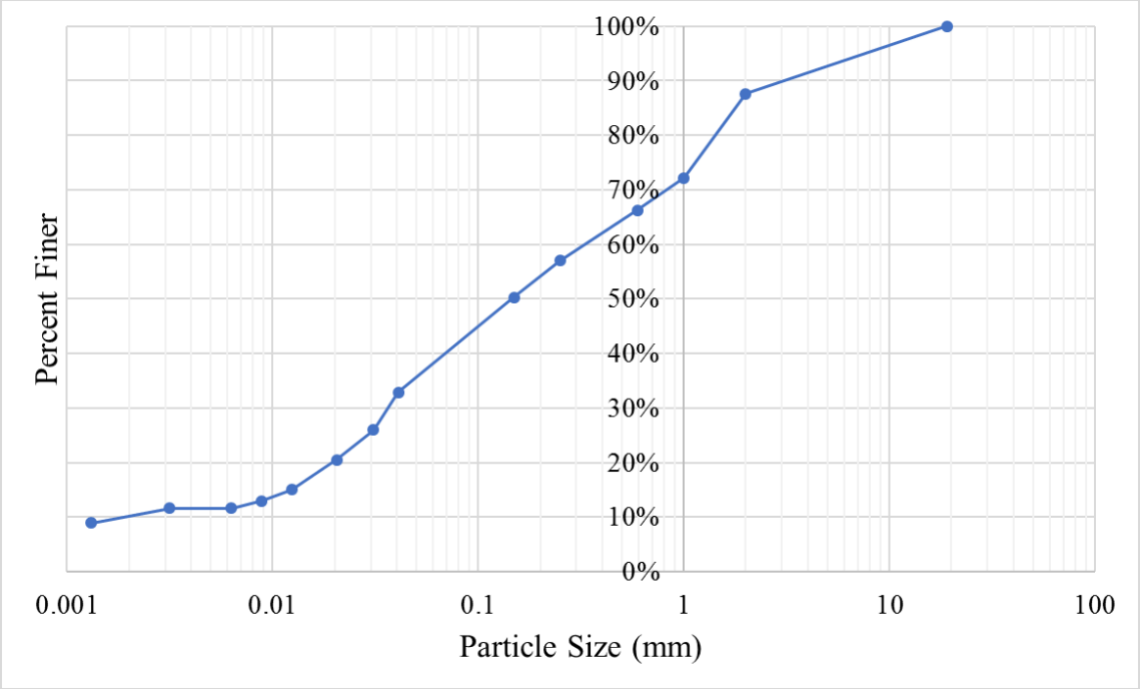

Figure E26: Site 31, Deer Creek Trib and U.S. 66 south of Hydro in Caddo county, particle size distribution.

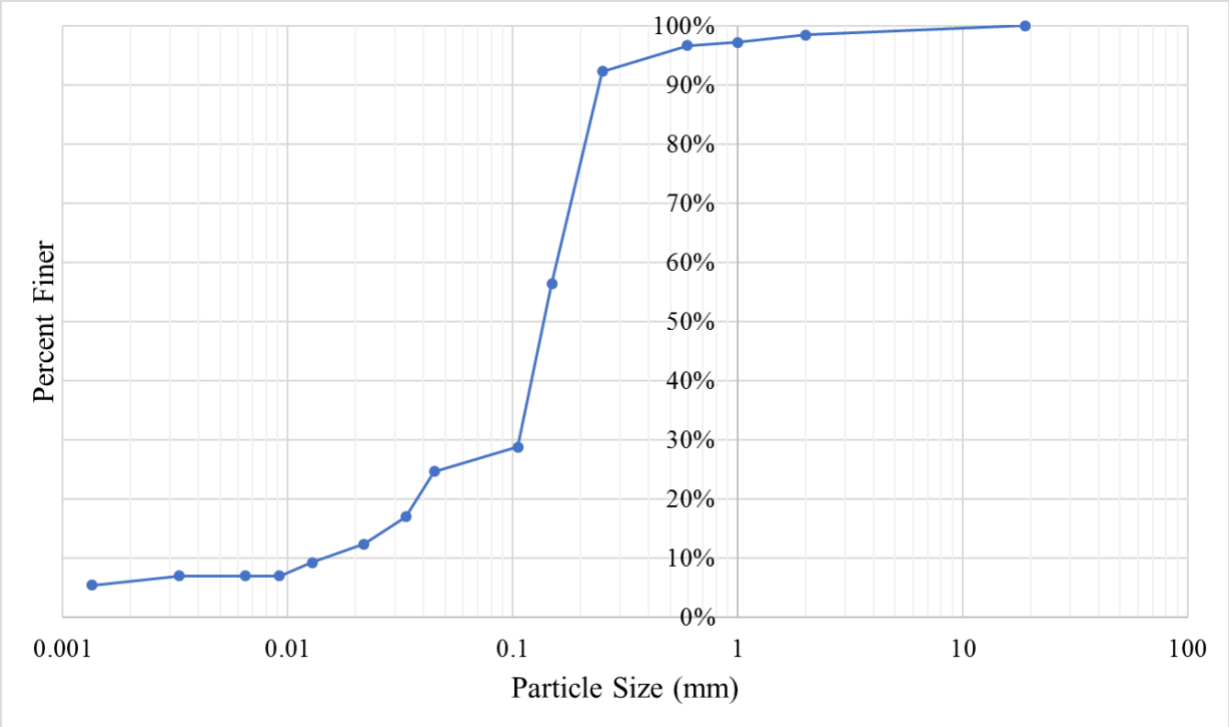

Figure E27: Site 32, Washita River and S.H. 7 west of Davis in Murray county, particle size distribution.

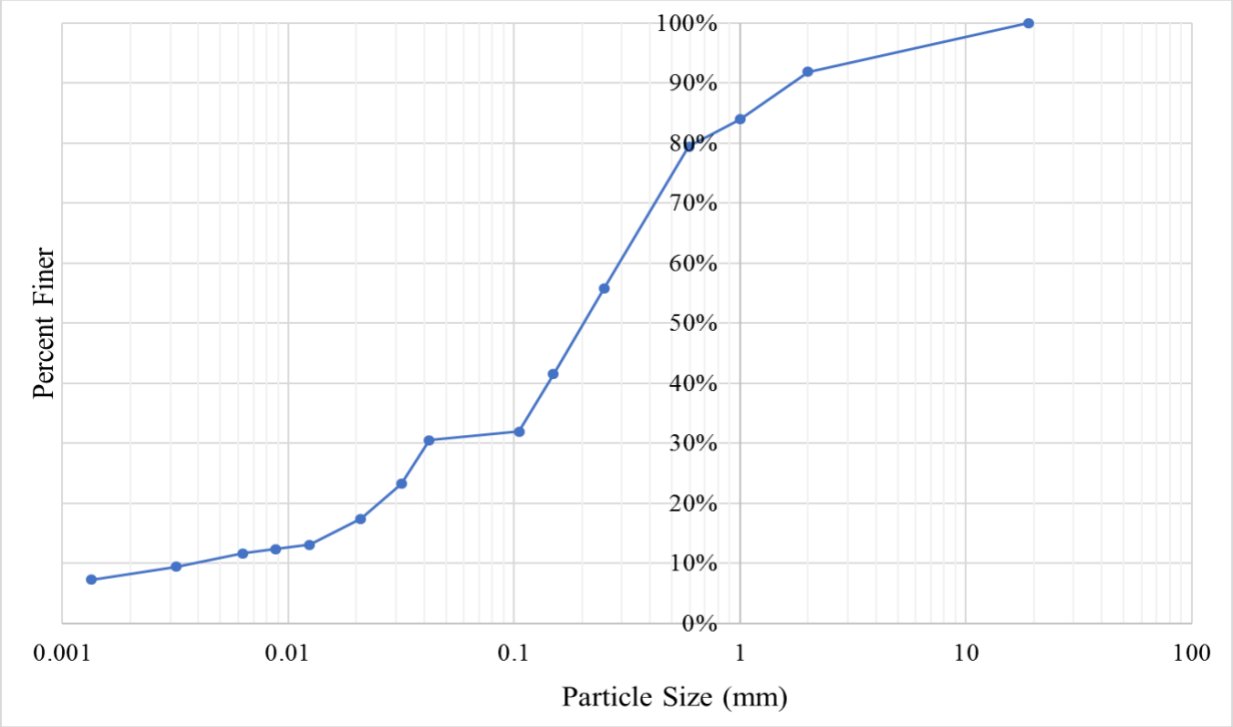

Figure E28: Site 33, Salt Fork of the Arkansas River and S.H. 156 north of Marland in Kay county, particle size distribution.

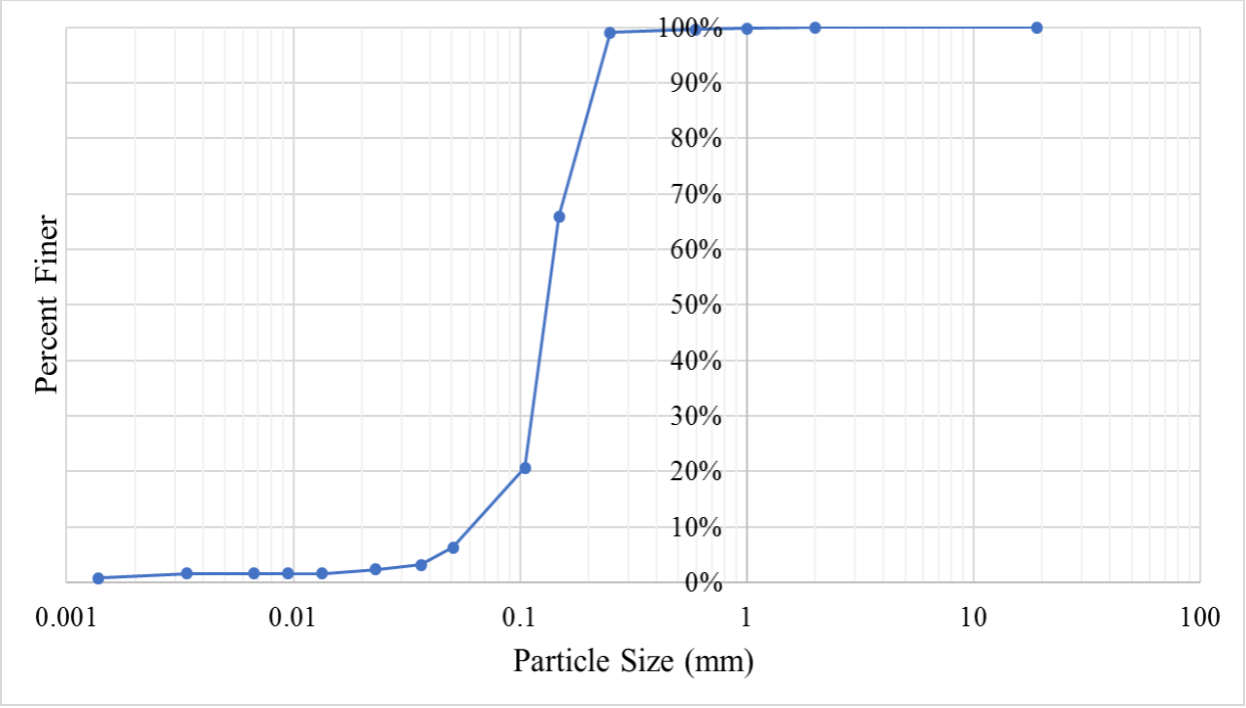

Figure E29: Site 34, Sugar Creek and U.S. 281 east of Binger in Caddo county, particle size distribution.

Appendix F – Historical Aerial Images

Figure F1: Site 1, Washita River and U.S. 77 north of Wynnewood in Garvin county, in 1956 (left) and 2019 (right).

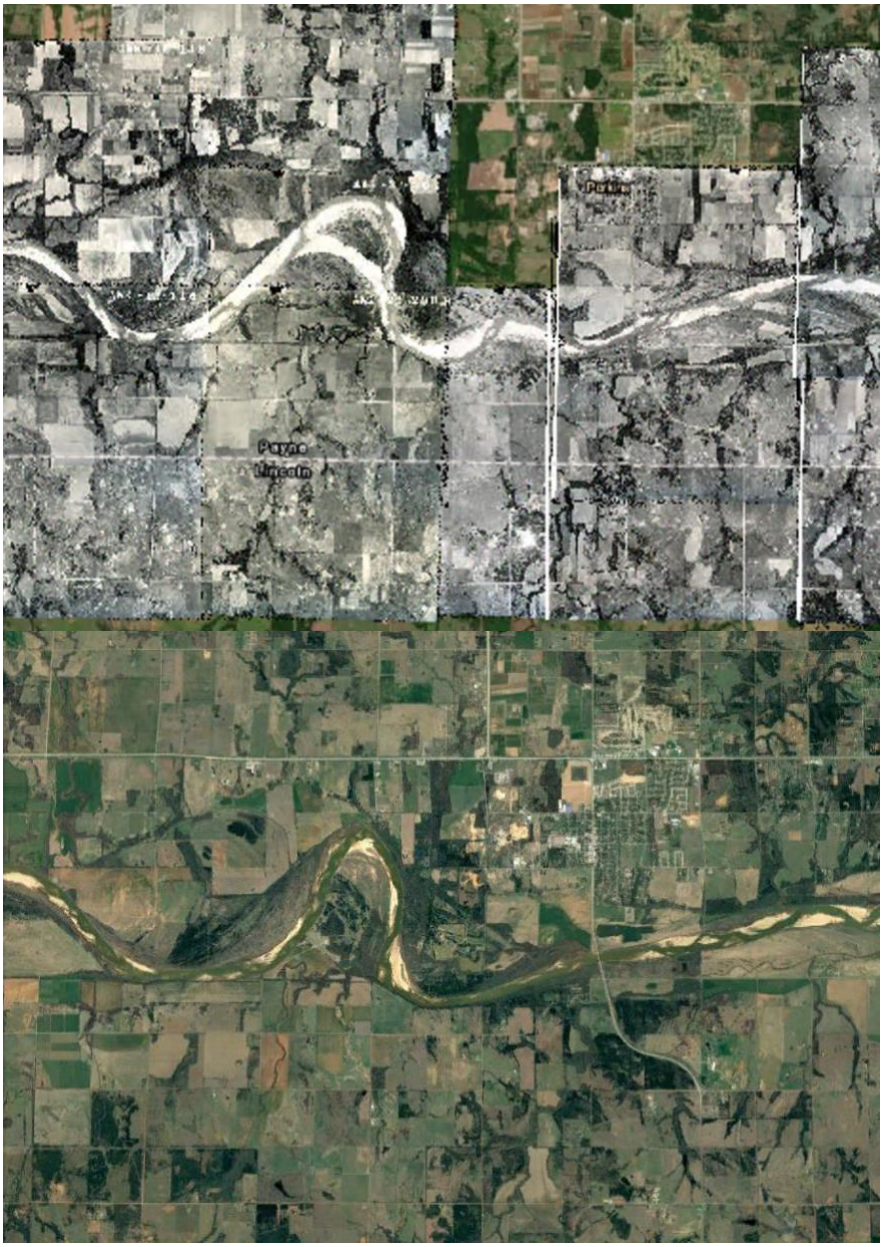

Figure F2: Site 2, Cimarron River and U.S. 177 south of Perkins in Payne county, in 1956 (top) and 2020 (bottom).

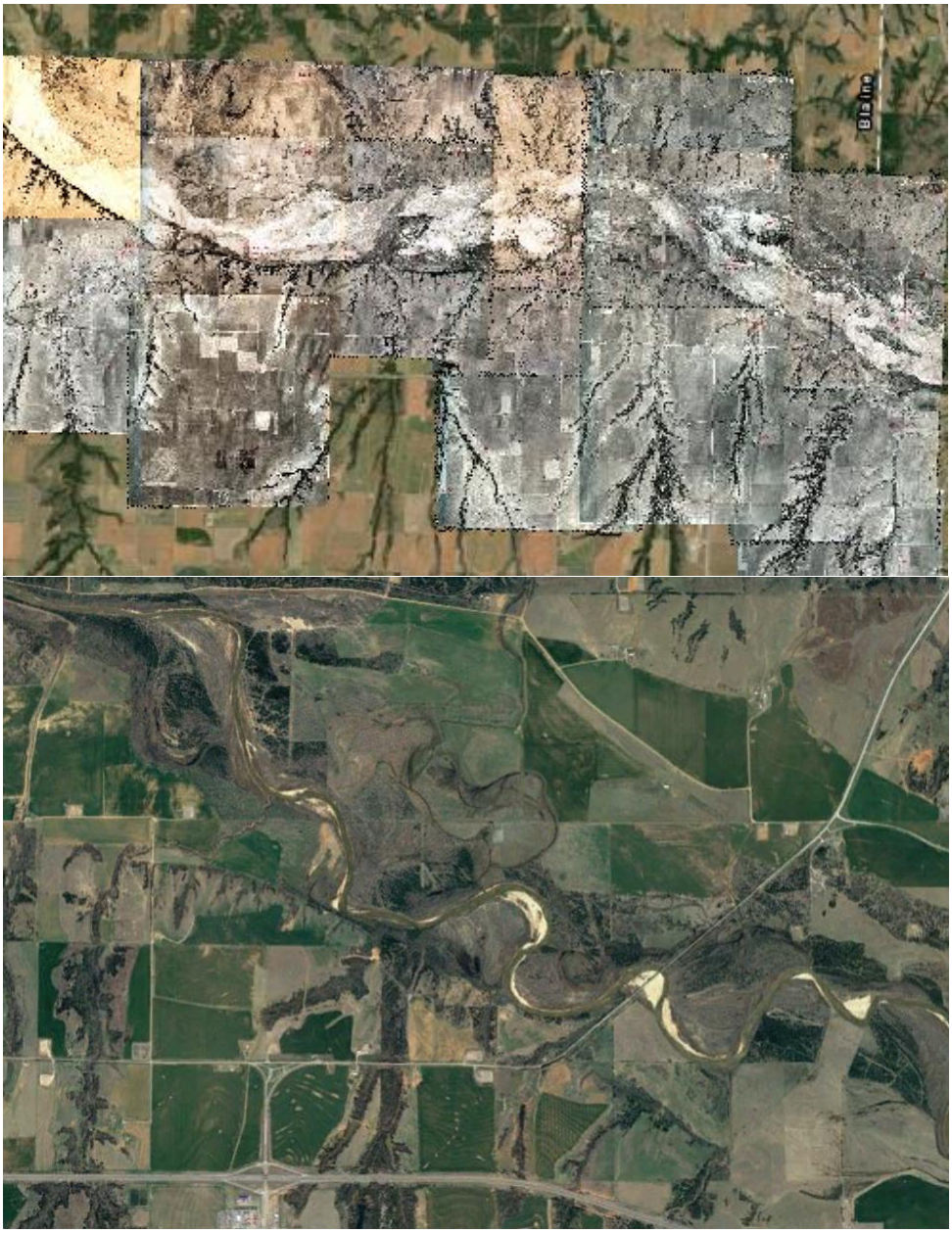

Figure F3: Site 7, Canadian River and U.S. 281 east of Bridgeport in Canadian county, in 1948 (top) and 2020 (bottom).

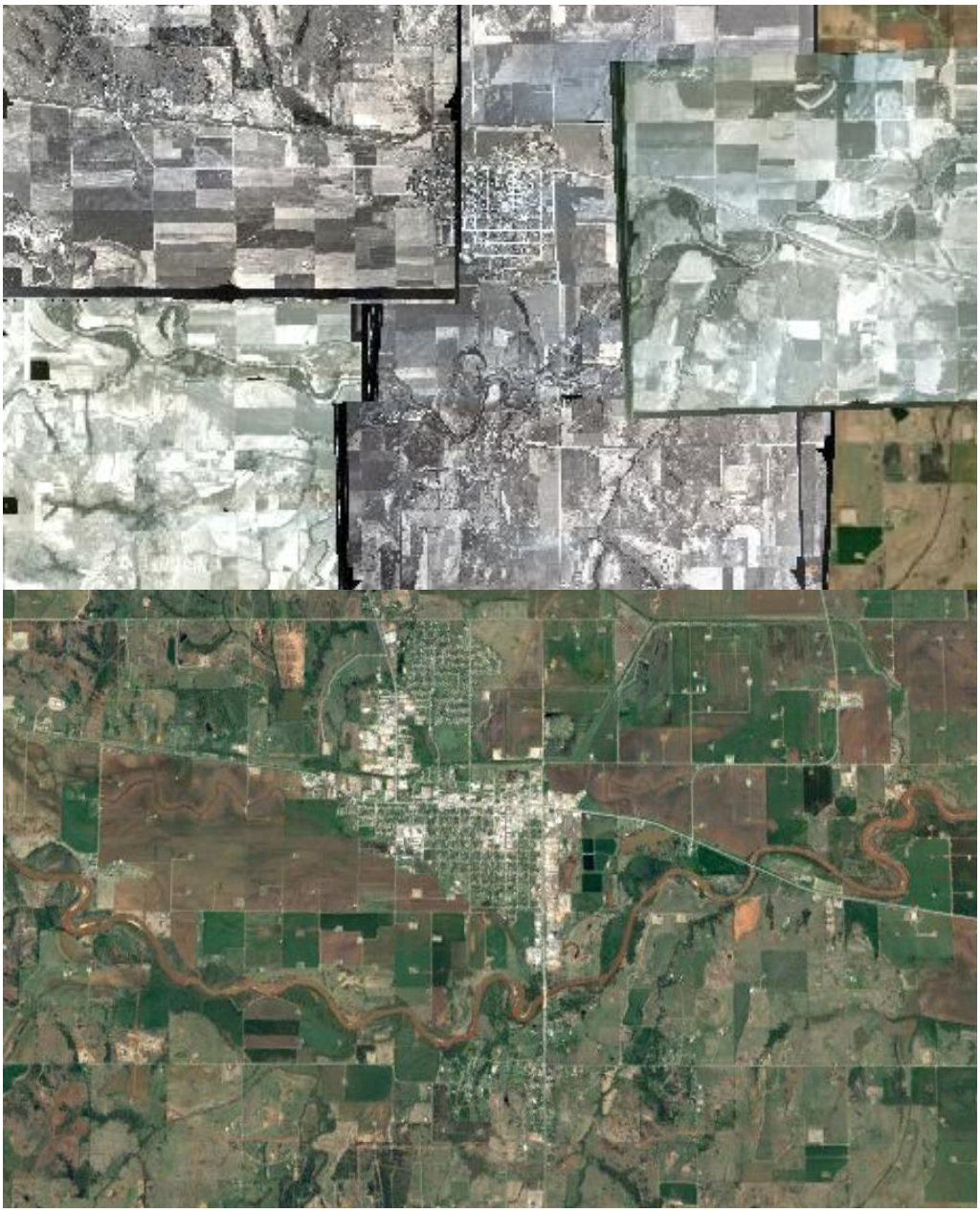

Figure F4: Site 10, Washita River and S.H. 76 South of Lindsay in Garvin county, in 1949 (top) and 2020 (bottom).

Figure F5: Site 11, Washita River and S.H. 74 north of Maysville in Garvin county, in 1956 (top) and 2020 (bottom).

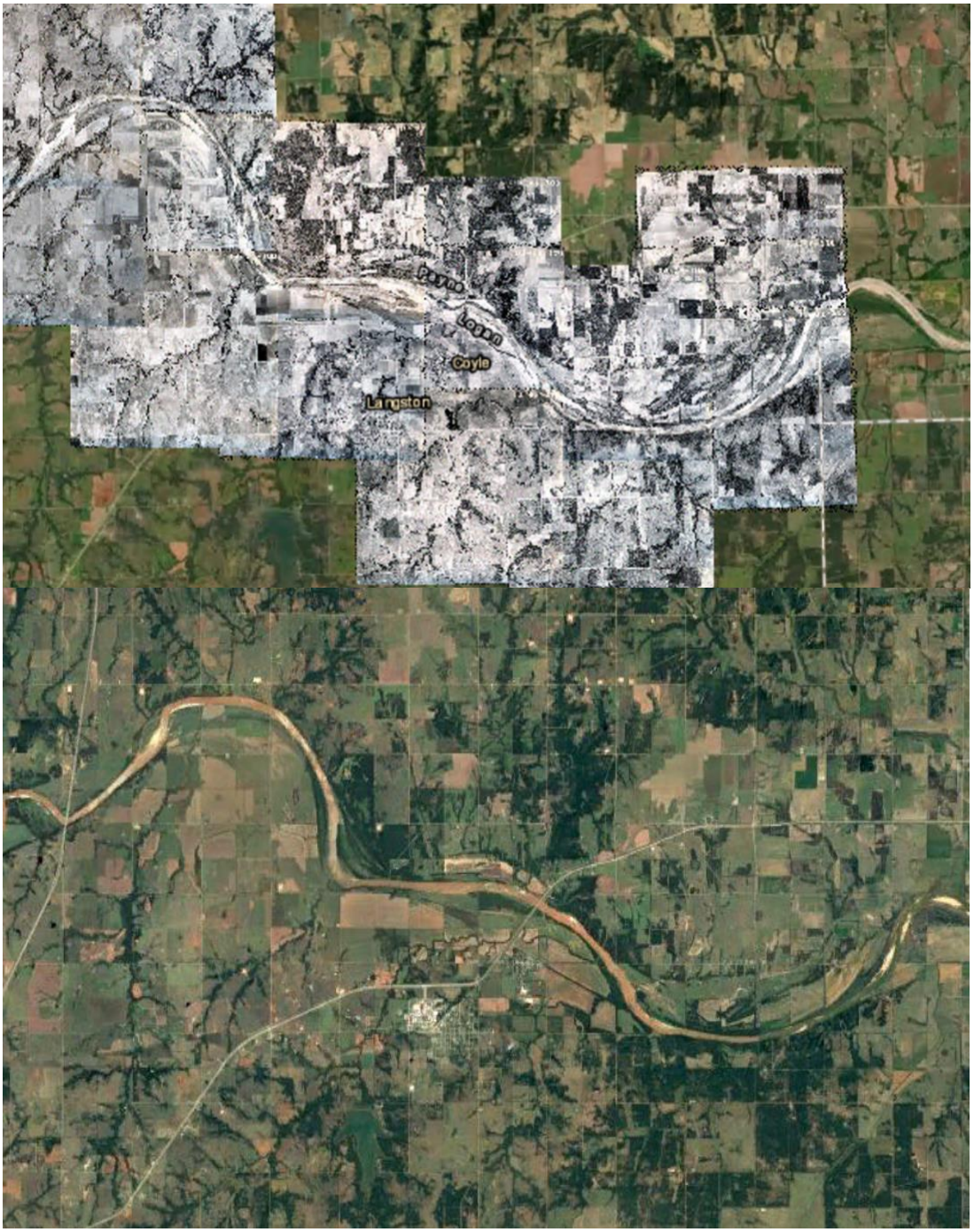

Figure F6: Site 12, Cimarron River and S.H. 33 north of Coyle in Logan county, in 1951 (top) and 2020 (bottom).

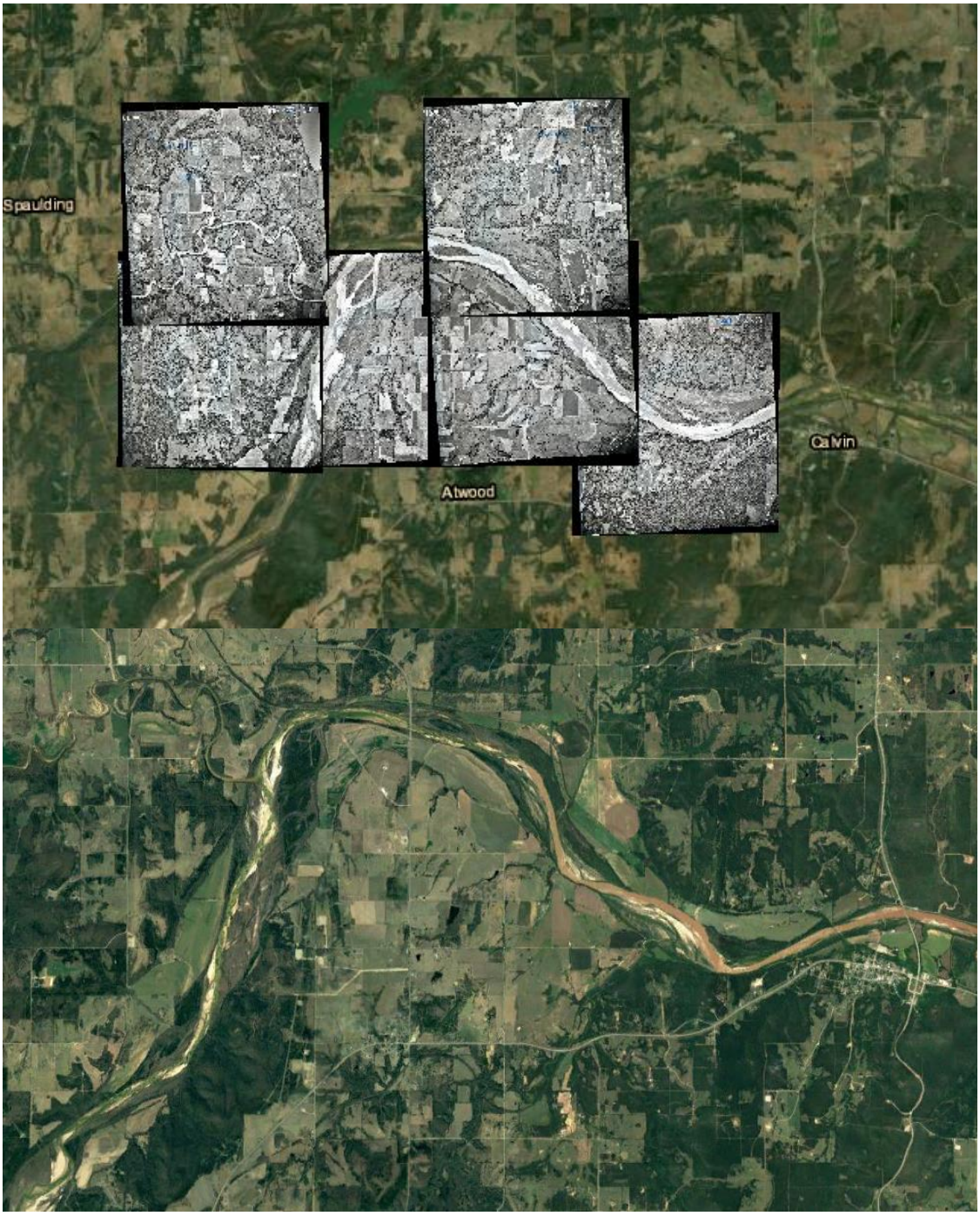

Figure F7: *Site 13, Canadian River and S.H. 48 north of Atwood in Cotton county, in 1968 (top) and 2020 (bottom).*

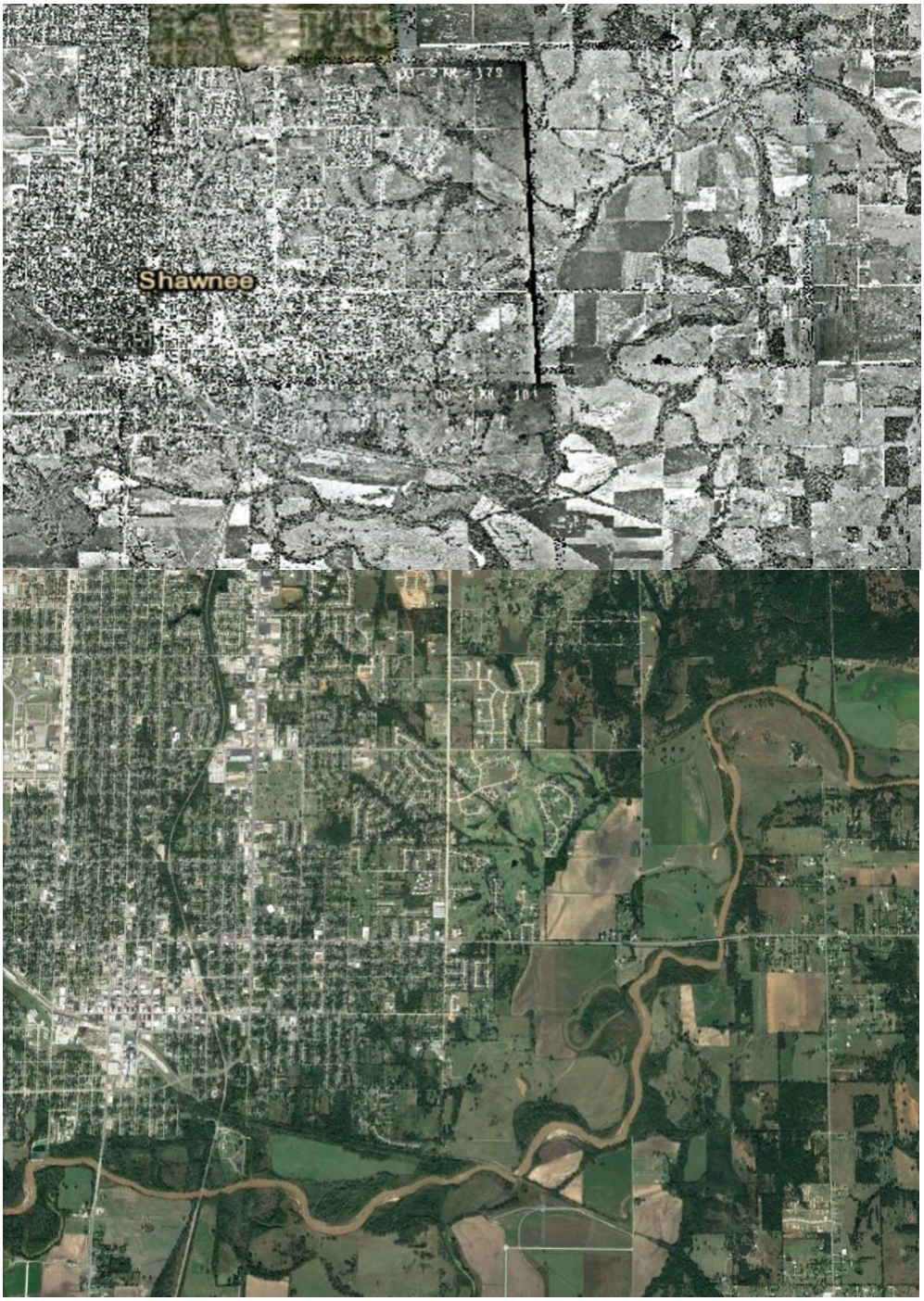

Figure F8: Site 16, North Canadian River and S.H. 3 east of Shawnee in Pottawatomie county, in 1961 (top) and 2020 (bottom).

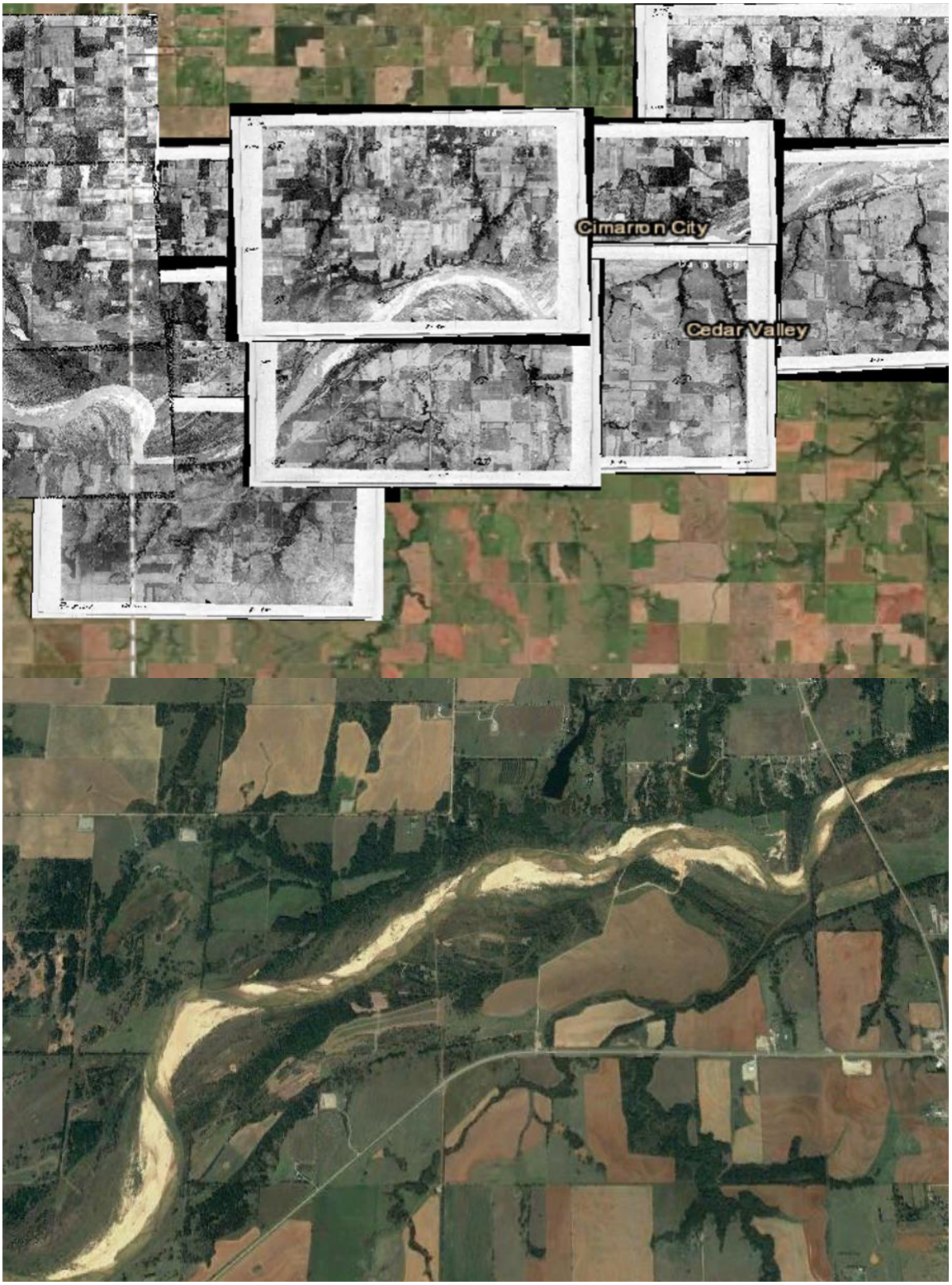

Figure F9: Site 17, Cimarron River and S.H. 74 south of Crescent in Logan county, in 1937 (top) and 2020 (bottom).

Figure F10: Site 20, Washita River and I-35 southwest of Paoli in Garvin county, in 1956 (top) and 2020 (bottom).

Figure F11: Site 21, Red River and S.H. 79 west of Waurika in Jefferson county, in 1940 (left) and 2020 (right).

Figure F12: Site 25, North Canadian River and S.H. 48 north of Bearden in Okfuskee county in 1961 (left), 1995 (middle), and 2019 (right).

Figure F13: Site 27, North Canadian River and S.H. 99 south of Prague in Seminole county in 1995 (top) and 2019 (bottom).

Figure F14: Site 29, Washita River and S.H. 19 east of Lindsay in Garvin county, in 1969 (top) and 2020 (bottom).

Appendix G – Bank Erosion Hazard Index (BEHI)

Table G1: Site 1, Washita River and U.S. 77 north of Wynnewood in Garvin count, left bank (LB) erosion hazard index scoring breakdown.

Site 1 (LB)	Sediment Adjustment	Root Depth/Bank Height (%)	Root Density (%)	Surface Protection (%)	Bank Angle (Degrees)	Total
	Loam	32	50	65	13	
BEHI Score	0	5	5	3	1	14

Table G2: Site 1, Washita River and U.S. 77 north of Wynnewood in Garvin county, right bank (RB) erosion hazard index scoring breakdown.

Site 1 (RB)	Sediment Adjustment	Root Depth/Bank Height (%)	Root Density (%)	Surface Protection (%)	Bank Angle (Degrees)	Total
	Loam	20	65	70	20	
BEHI Score	0	7	3	3	1	14

Table G3: Site 2, Cimarron River and U.S. 177 south of Perkins in Payne county, left bank (LB) erosion hazard index scoring breakdown.

Site 2 (LB)	Sediment Adjustment	Root Depth/Bank Height (%)	Root Density (%)	Surface Protection (%)	Bank Angle (Degrees)	Total
	Sand	67	60	65	29	
BEHI Score	Sand	67	60	65	29	14

Table G4: Site 2, Cimarron River and U.S. 177 south of Perkins in Payne county, right bank (RB) erosion hazard index scoring breakdown.

Site 2 (RB)	Sediment Adjustment	Root Depth/Bank Height (%)	Root Density (%)	Surface Protection (%)	Bank Angle (Degrees)	Total
	Sand	38	75	75	29	
BEHI Score	10	5	3	3	3	24

Table G5: Site 4, Cimarron River and U.S. 281 south of Watonga in Blaine county, left bank (LB) erosion hazard index scoring breakdown.

Site 4 (LB)	Sediment Adjustment	Root Depth/Bank Height (%)	Root Density (%)	Surface Protection (%)	Bank Angle (Degrees)	Total
	Sand	67	90	90	15	
BEHI Score	10	3	1	1	1	16

Table G6: Site 5, Arkansas River and U.S. 64 north of Bixby in Tulsa county, left bank (LB) erosion hazard index scoring breakdown.

Site 5 (LB)	Sediment Adjustment	Root Depth/Bank Height (%)	Root Density (%)	Surface Protection (%)	Bank Angle (Degrees)	Total
	Gravel	100	75	75	27	
BEHI Score	5	1	3	3	3	15

Table G7: Site 5, Arkansas River and U.S. 64 north of Bixby in Tulsa county, right bank (RB) erosion hazard index scoring breakdown.

Site 5 (RB)	Sediment Adjustment	Root Depth/Bank Height (%)	Root Density (%)	Surface Protection (%)	Bank Angle (Degrees)	Total
	Gravel	20	75	75	25	
BEHI Score	5	7	3	3	3	21

Table G8: Site 6, North Canadian River and U.S. 281 south Watonga in Blaine county, right bank (RB) erosion hazard index scoring breakdown.

Site 6 (RB)	Sediment Adjustment	Root Depth/Bank Height (%)	Root Density (%)	Surface Protection (%)	Bank Angle (Degrees)	Total
	Loam	19	60	65	64	
BEHI Score	0	7	3	3	5	18

Table G9: Site 7, Canadian River and U.S. 281 east of Bridgeport in Canadian county, right bank (RB) erosion hazard index scoring breakdown.

Site 7 (RB)	Sediment Adjustment	Root Depth/Bank Height (%)	Root Density (%)	Surface Protection (%)	Bank Angle (Degrees)	Total
	Sand	38	90	90	51	
BEHI Score	10	5	1	1	3	20

Table G10: Site 8, Salt Fork of the Red River and U.S. 62 west of Altus in Jackson county, left bank (LB) erosion hazard index scoring breakdown.

Site 8 (LB)	Sediment Adjustment	Root Depth/Bank Height (%)	Root Density (%)	Surface Protection (%)	Bank Angle (Degrees)	Total
	Sand	57	90	90	8	
BEHI Score	10	3	1	1	1	16

Table G11: Site 8, Salt Fork of the Red River and U.S. 62 west of Altus in Jackson county, right bank (RB) erosion hazard index scoring breakdown.

Site 8 (RB)	Sediment Adjustment	Root Depth/Bank Height (%)	Root Density (%)	Surface Protection (%)	Bank Angle (Degrees)	Total
	Sand	67	90	90	5	
BEHI Score	10	3	1	1	1	16

Table G12: Site 10, Washita River and S.H. 76 south of Lindsay in Garvin county, left bank (LB) erosion hazard index scoring breakdown.

Site 10 (LB)	Sediment Adjustment	Root Depth/Bank Height (%)	Root Density (%)	Surface Protection (%)	Bank Angle (Degrees)	Total
	Sand	30	50	60	40	
BEHI Score	10	5	5	3	3	26

Table G13: Site 10, Washita River and S.H. 76 south of Lindsay in Garvin county, right bank (RB) erosion hazard index scoring breakdown.

Site 10 (RB)	Sediment Adjustment	Root Depth/Bank Height (%)	Root Density (%)	Surface Protection (%)	Bank Angle (Degrees)	Total
	Sand	30	50	60	40	
BEHI Score	10	5	5	3	3	26

Table G14: Site 11, Washita River and S.H. 74 north of Maysville in Garvin county, left bank (LB) erosion hazard index scoring breakdown.

Site 11 (LB)	Sediment Adjustment	Root Depth/Bank Height (%)	Root Density (%)	Surface Protection (%)	Bank Angle (Degrees)	Total
	Sand	25	70	75	29	
BEHI Score	10	7	3	3	3	26

Table G15: Site 11, Washita River and S.H. 74 north of Maysville in Garvin county, upstream left bank (LB) erosion hazard index scoring breakdown.

Site 11 (US LB)	Sediment Adjustment	Root Depth/Bank Height (%)	Root Density (%)	Surface Protection (%)	Bank Angle (Degrees)	Total
	Cobble	13	70	100	31	
BEHI Score	-10	8.5	3	1	3	5.5

Table G16: Site 11, Washita River and S.H. 74 north of Maysville in Garvin county, right bank (RB) erosion hazard index scoring breakdown.

Site 11 (RB)	Sediment Adjustment	Root Depth/Bank Height (%)	Root Density (%)	Surface Protection (%)	Bank Angle (Degrees)	Total
	Sand	25	65	70	62	
BEHI Score	10	7	3	3	5	28

Table G17: Site 12, Cimarron River and S.H. 33 north of Coyle in Logan county, left bank (LB) erosion hazard index scoring breakdown.

Site 12 (LB)	Sediment Adjustment	Root Depth/Bank Height (%)	Root Density (%)	Surface Protection (%)	Bank Angle (Degrees)	Total
	Sand	40	80	80	10	
BEHI Score	10	7	3	3	5	28

Table G18: Site 12, Cimarron River and S.H. 33 north of Coyle in Logan county, right bank (RB) erosion hazard index scoring breakdown.

Site 12 (RB)	Sediment Adjustment	Root Depth/Bank Height (%)	Root Density (%)	Surface Protection (%)	Bank Angle (Degrees)	Total
	Sand	40	80	80	10	
BEHI Score	10	5	1	1	1	18

Table G19: Site 13, Canadian River and S.H. 48 north of Atwood in Cotton county, left bank (LB) erosion hazard index scoring breakdown.

Site 13 (LB)	Sediment Adjustment	Root Depth/Bank Height (%)	Root Density (%)	Surface Protection (%)	Bank Angle (Degrees)	Total
	Sand	40	80	80	20	
BEHI Score	10	5	1	1	1	18

Table G20: Site 14, North Canadian River and S.H. 84 north of Dustin in Okfuskee county, right bank (RB) erosion hazard index scoring breakdown.

Site 14 (RB)	Sediment Adjustment	Root Depth/Bank Height (%)	Root Density (%)	Surface Protection (%)	Bank Angle (Degrees)	Total
	Sand	27	30	40	65	
BEHI Score	10	7	5	5	5	32

Table G21: Site 16, North Canadian River and S.H. 3 east of Shawnee in Pottawatomie county, right bank (RB) erosion hazard index scoring breakdown.

Site 16 (RB)	Sediment Adjustment	Root Depth/Bank Height (%)	Root Density (%)	Surface Protection (%)	Bank Angle (Degrees)	Total
	Sand	33	75	75	20	
BEHI Score	10	5	3	3	1	22

Table G22: Site 16, North Canadian River and S.H. 3 east of Shawnee in Pottawatomie county, upstream left bank (LB) erosion hazard index scoring breakdown.

Site 16 (US LB)	Sediment Adjustment	Root Depth/Bank Height (%)	Root Density (%)	Surface Protection (%)	Bank Angle (Degrees)	Total
	Sand	33	70	80	20	
BEHI Score	10	5	3	1	1	20

Table G23: Site 17, Cimarron River and S.H. 74 south of Crescent in Logan county. right bank (RB) erosion hazard index scoring breakdown.

Site 17 (RB)	Sediment Adjustment	Root Depth/Bank Height (%)	Root Density (%)	Surface Protection (%)	Bank Angle (Degrees)	Total
	Sand	19	60	65	64	
BEHI Score	10	7	3	3	5	28

Table G24: Site 18, Washita River and U.S. 77 south of Davis in Murray county, left bank (LB) erosion hazard index scoring breakdown.

Site 18 (LB)	Sediment Adjustment	Root Depth/Bank Height (%)	Root Density (%)	Surface Protection (%)	Bank Angle (Degrees)	Total
	Sand	20	50	50	40	
BEHI Score	10	7	5	5	3	30

Table G25: Site 18, Washita River and U.S. 77 south of Davis in Murray county, right bank (RB) erosion hazard index scoring breakdown.

Site 18 (RB)	Sediment Adjustment	Root Depth/Bank Height (%)	Root Density (%)	Surface Protection (%)	Bank Angle (Degrees)	Total
	Sand	67	80	80	20	
BEHI Score	10	3	1	1	1	16

Table G26: Site 19, Beaver River and U.S. 283 north of Laverne in Harper county, right bank (RB) erosion hazard index scoring breakdown.

Site 19 (RB)	Sediment Adjustment	Root Depth/Bank Height (%)	Root Density (%)	Surface Protection (%)	Bank Angle (Degrees)	Total
	Sand	30	90	90	15	
BEHI Score	10	5	1	1	1	18

Table G27: Site 20, Washita River and I-35 southwest of Paoli in Garvin county, right bank (RB) erosion hazard index scoring breakdown.

Site 20 (RB)	Sediment Adjustment	Root Depth/Bank Height (%)	Root Density (%)	Surface Protection (%)	Bank Angle (Degrees)	Total
	Sand	25	50	60	50	
BEHI Score	10	7	5	3	5	30

Table G28: Site 21, Red River and S.H. 79 west of Waurika in Jefferson county, right bank (RB) erosion hazard index scoring breakdown.

Site 21 (RB)	Sediment Adjustment	Root Depth/Bank Height (%)	Root Density (%)	Surface Protection (%)	Bank Angle (Degrees)	Total
	Sand	67	90	90	10	
BEHI Score	10	3	1	1	1	16

Table G29: Site 22, Washita River and S.H. 53 east of Gene Autry in Carter county, left bank (LB) erosion hazard index scoring breakdown.

Site 22 (LB)	Sediment Adjustment	Root Depth/Bank Height (%)	Root Density (%)	Surface Protection (%)	Bank Angle (Degrees)	Total
	Loam	31	60	65	11	
BEHI Score	0	5	3	3	1	12

Table G30: Site 24, Red River and U.S. 259 south of Harris in McCurtain county, left bank (LB) erosion hazard index scoring breakdown.

Site 24 (LB)	Sediment Adjustment	Root Depth/Bank Height (%)	Root Density (%)	Surface Protection (%)	Bank Angle (Degrees)	Total
	Sand	60	90	90	15	
BEHI Score	10	3	1	1	1	16

Table G31: Site 25, North Canadian River and S.H. 48 north of Bearden in Okfuskee county, left bank (LB) erosion hazard index scoring breakdown.

Site 25 (LB)	Sediment Adjustment	Root Depth/Bank Height (%)	Root Density (%)	Surface Protection (%)	Bank Angle (Degrees)	Total
	Sand	33	75	80	30	
BEHI Score	10	5	3	1	3	22

Table G32: Site 25, North Canadian River and S.H. 48 north of Bearden in Okfuskee county, right bank (RB) erosion hazard index scoring breakdown.

Site 25 (RB)	Sediment Adjustment	Root Depth/Bank Height (%)	Root Density (%)	Surface Protection (%)	Bank Angle (Degrees)	Total
	Sand	50	75	80	20	
BEHI Score	10	3	3	1	1	18

Table G33: Site 26, Sugar Creek and U.S. 281 south of Gracemont in Caddo county, left bank (LB) erosion hazard index scoring breakdown.

Site 26 (LB)	Sediment Adjustment	Root Depth/Bank Height (%)	Root Density (%)	Surface Protection (%)	Bank Angle (Degrees)	Total
	Sand	15	95	95	55	
BEHI Score	10	7	1	1	3	22

Table G34: Site 27, North Canadian River and S.H. 99 south of Prague in Seminole county, right bank (RB) erosion hazard index scoring breakdown.

Site 27 (RB)	Sediment Adjustment	Root Depth/Bank Height (%)	Root Density (%)	Surface Protection (%)	Bank Angle (Degrees)	Total
	Sand	30	75	80	20	
BEHI Score	10	5	3	1	1	20

Table G35: Site 28, Illinois River and S.H. 10 east of Tahlequah in Cherokee county, right bank (RB) erosion hazard index scoring breakdown.

Site 28 (RB)	Sediment Adjustment	Root Depth/Bank Height (%)	Root Density (%)	Surface Protection (%)	Bank Angle (Degrees)	Total
	Gravel	38	80	85	15	
BEHI Score	5	5	1	1	1	13

Table G36: Site 29, Washita River and S.H. 19 east of Lindsay in Garvin county, right bank (RB) erosion hazard index scoring breakdown.

Site 29 (RB)	Sediment Adjustment	Root Depth/Bank Height (%)	Root Density (%)	Surface Protection (%)	Bank Angle (Degrees)	Total
	Sand	50	50	60	30	
BEHI Score	10	3	5	3	3	24

Table G37: Site 31, Deer Creek Trib and U.S. 66 south of Hydro in Caddo county, left bank (LB) erosion hazard index scoring breakdown.

Site 31 (LB)	Sediment Adjustment	Root Depth/Bank Height (%)	Root Density (%)	Surface Protection (%)	Bank Angle (Degrees)	Total
	Sand	50	70	90	25	
BEHI Score	10	3	3	1	3	20

Table G38: Site 31, Deer Creek Trib and U.S. 66 south of Hydro in Caddo county, right bank (RB) erosion hazard index scoring breakdown.

Site 31 (RB)	Sediment Adjustment	Root Depth/Bank Height (%)	Root Density (%)	Surface Protection (%)	Bank Angle (Degrees)	Total
	Sand	50	70	90	25	
BEHI Score	10	3	3	1	3	20

Table G39: Site 32, Washita River and S.H. 7 west of Davis in Murray county, left bank (LB) erosion hazard index scoring breakdown.

Site 32 (LB)	Sediment Adjustment	Root Depth/Bank Height (%)	Root Density (%)	Surface Protection (%)	Bank Angle (Degrees)	Total
	Sand	20	40	50	65	
BEHI Score	10	7	5	5	5	32

Table G40: Site 33, Salt Fork of the Arkansas River and S.H. 156 north of Marland in Kay county, left bank (LB) erosion hazard index scoring breakdown.

Site 33 (LB)	Sediment Adjustment	Root Depth/Bank Height (%)	Root Density (%)	Surface Protection (%)	Bank Angle (Degrees)	Total
	Sand	25	75	85	30	
BEHI Score	10	7	3	1	3	24

Table G41: Site 34, Sugar Creek and U.S. 281 east of Binger in Caddo county, left bank (LB) erosion hazard index scoring breakdown.

Site 34 (LB)	Sediment Adjustment	Root Depth/Bank Height (%)	Root Density (%)	Surface Protection (%)	Bank Angle (Degrees)	Total
	Sand	15	95	95	55	
BEHI Score	10	7	1	1	3	22